THE UNIVERSITY OF CALGARY

Optimal Design of Precast I-Girder Bridges Made with High-Performance Concrete

by

Mostafa Ahmed Hassanain

A DISSERTATION
SUBMITTED TO THE FACULTY OF GRADUATE STUDIES
IN PARTIAL FULFILMENT OF THE REQUIREMENTS FOR THE
DEGREE OF DOCTOR OF PHILOSOPHY

DEPARTMENT OF CIVIL ENGINEERING

CALGARY, ALBERTA

MARCH, 1998

ABSTRACT

For several years, the most common application of high-performance concrete (HPC) has been in the building industry where concrete strengths of 100 MPa and more have been frequently used in the lower columns of high-rise buildings. In comparison, strengths of about 60 MPa have been considered the maximum achievable in the precast, prestressed concrete industry; this appears to be very timid especially considering that several research studies have indicated that the potential advantages from the utilization of HPC with its increased strength and improved durability for precast, prestressed concrete highway bridges are quite promising. In spite of this, there is still some disagreement within the industry that HPC is beneficial. The misconception that the benefits of the material do not justify its higher cost and the increased quality control requirements associated with its production seems to deter most designers and precast concrete producers from exploiting it. The use of HPC in bridges is unlikely to advance quickly without a clear economic incentive for precasters to utilize the material widely. This study is intended to help provide such an incentive.

The overall objective of the study is to assess the potential economic benefits from the utilization of concretes with compressive strengths of up to about 100 MPa for continuous, precast, pretensioned I-girder highway bridges. These were chosen because they represent the most common type of precast, prestressed concrete bridges constructed in North America. The problem is formulated as an optimal design problem. Refined computer-oriented structural analysis methods combined with modern computational design optimization techniques are used to develop an optimization system that is utilized to perform extensive economic studies on this type of bridges. The results of these studies are presented, interpreted and discussed. It is shown that the cost savings with HPC can far outweigh its additional material and production costs, particularly for the longer span bridges. Sensitivity analyses of the obtained results with respect to the major assumptions made in developing the optimization system are performed. These analyses suggest that the findings of this study are applicable to a wide range of practical values surrounding those assumed.

ACKNOWLEDGEMENTS

First and foremost, praise and thanks be to Almighty Allah, the Most Gracious, the Most Merciful, and peace be upon His Prophet.

I would like to express my deepest gratitude and appreciation to my supervisor, Dr. Robert E. Loov for his invaluable guidance, support and encouragement, and for his profound patience throughout all the stages of this study. I also greatly appreciate the help and encouragement provided by Dr. Walter H. Dilger and Dr. Marc A. Maes.

The financial support received from Concrete Canada (The Network of Centres of Excellence on High-Performance Concrete), Alberta Economic Development and Tourism, and the Department of Civil Engineering is gratefully acknowledged.

Last, but never least, I would like to express my heartfelt appreciation to my dear parents for thirty years of support, encouragement and love.

To my parents

TABLE OF CONTENTS

LIST OF TABLES

LIST OF FIGURES

LIST OF SYMBOLS

a	Amplitude of the vertical deflection of a girder
a	Restraint moment coefficient for prestressing effects
a	Depth of the equivalent rectangular compressive stress block
A	Girder cross-sectional area
[A]	Matrix that defines the geometry of a bridge
A_p	Area of the prestressing tendons in a girder
A_s	Cross-sectional area of the deck slab
A_s^+	Area of the positive moment reinforcing steel bars in a girder
A_s^-	Area of the negative moment reinforcing steel bars over a pier
A_{spn}	Area of the positive moment steel at support n
b	Restraint moment coefficient for dead load effects
b_1	Width of a girder's top flange
b_2	Width of a girder's bottom flange
b_3	Width of a girder's web
b_e	Effective flange width of the composite section
b_f	Width of a girder's bottom flange
b_i^l	Lower bound on the ith design variable
b_i^u	Upper bound on the ith design variable
{b}	Vector of design variables
c	Distance of a point load from the left support of a beam
c	Restraint moment coefficient for shrinkage effects
c	Depth of the neutral axis
c_r	Stiffness of a spring representing the transverse torsional stiffness of the deck slab panel r
C	Total compression force
C_c	Cost of concrete in the deck slab per unit volume
C_f	A fixed cost representing the mobilization, setup and dismantling charges of the crane
C_g	Cost of one girder, including cost of materials, production, transportation and erection
C_s	Cost of non-prestressing steel per unit mass
C_{te}	Girder transportation and erection costs
C.G.C	Centre of gravity of a concrete section
C.G.S	Centre of gravity of prestressing steel
CMCR	Concrete mix cost ratio
Cost	Minimum initial superstructure cost / deck area
d_1	Depth of the vertical portion of a girder's top flange
d_2	Depth of the sloped portion of a girder's top flange
d_3	Depth of a girder's web
d_4	Depth of the sloped portion of a girder's bottom flange
d_5	Depth of the vertical portion of a girder's bottom flange
$(d_c)_{min}$	Minimum feasible value of concrete cover measured from the bottom fibre to the

centroid of the strands

d_p Effective depth of the composite section with respect to the prestressing tendons

d_s Effective depth of the composite section with respect to the reinforcing bars

D_y Transverse flexural stiffness of the transverse medium

D_{yx} Transverse torsional stiffness of the transverse medium

DLA Dynamic load allowance

e Tendon eccentricity

e_c Tendon eccentricity at and near girder mid-span

e_e Tendon eccentricity over the piers

e_{max} Maximum practical tendon eccentricity

E_c Elastic modulus of concrete

E_{cg} Elastic modulus of the precast girder concrete

E_{cs} Elastic modulus of the cast-in-place deck slab concrete

E_s Elastic modulus of the deck slab concrete

$E_c(t_0)$ Elastic modulus of concrete at age t_0

$\overline{E_c}(t,t_0)$ Age-adjusted effective modulus of concrete

EI Flexural stiffness of a beam

f_c Concrete stress

f'_c Girder concrete compressive strength at 28 days

f'_{ci} Girder concrete compressive strength at the time of prestress transfer

f_{cr} Cracking strength of concrete

f'_{cs} Deck slab concrete compressive strength at 28 days

f_{pe} Effective stress in the prestressing tendons

f_{pr} Stress in the prestressing tendons at factored flexural resistance

f_{pu} Ultimate strength of the prestressing tendons

f_{py} Yield strength of the prestressing tendons

f_s Tensile stress in the reinforcing steel bars

f_y Yield strength of the reinforcing steel bars

$f(\{b\})$ Objective function to be minimized

$f(l_g)$ A transportation cost function of the girder span length

$f(m_g)$ An erection cost function of the girder mass

$g_i(\{b\})$ Inequality constraint function

GJ Torsional stiffness of a girder

$h_i(\{b\})$ Equality constraint function

I First moment of inertia of a girder

I A specified number of consecutive iterations that signifies convergence in IDESIGN

jd_s Moment arm

J Saint-Venant torsional constant of a precast concrete girder

k Number of equality constraints

k_b Distance from centroid of the girder cross section to the lower limit of the central kern area

k_r Stiffness of a spring representing the flexural stiffness of girder r

k_t Distance from centroid of the girder cross section to the upper limit of the central kern area

kd_s A fraction of d_s which locates the neutral axis

l Span length of a girder

L Total length of a bridge

m Girder number

m Number of inequality constraints

m_p Mass of positive moment steel in the girders

m_r Stiffness of a spring representing the torsional stiffness of girder r

m_s Mass on non-prestressing steel in the deck slab

m_{sn} Mass of negative moment steel in the deck slab at each pier

m_{sp} Mass of positive moment connection steel at each pier

M_{cr} Cracking moment of the composite section

M_{csn} Final moment at support n due to the combined effect of creep and shrinkage

M_{da} Moment caused by the additional dead load applied after the deck slab hardens and continuity is achieved

M_{dg} Moment due to a girder's own wight

M_{dn} Restraint moment at support n due to dead load

M_{ds} Moment caused by the dead load of the deck slab concrete

M_f Factored load moment

M_l Live load moment

M_{ln} Live load moment at support n

M_n Elastic restraint moment at support n

$M_n(t)$ Moment induced by creep at support n

M_{pn} Restraint moment at support n due to prestressing

M_{sh} Restraint moment over a pier due to shrinkage

M_{shn} Restraint moment at support n due to shrinkage

M_{sn} Service moment at support n provided by the composite section

M_{SLSn} Moment at support n at serviceability limit states

M_r Factored flexural resistance

M_x Bending moment at point x

n Harmonic number

n Support number

n Number of design variables

n_g Number of girders

n_p Number of positive moment connections at the piers

n_r Modular ratio between the reinforcing steel and the girder concrete

N Number of girders

N.A. Neutral axis

p_x Intensity of a continuous load function

P Point load

P_e Final effective prestressing force after losses

P_i Initial prestressing force at the time of transfer

q Intensity of a uniformly distributed load

r Girder number

R Downward loading

R Ratio of the effective prestressing force to the prestressing force at transfer

$\{R\}$ Vector that defines the loading on a bridge

R_f Ratio of the girder concrete compressive strength at transfer to the 28-day strength

S Centre-to-centre spacing of girders

S' Length of the slab overhang

S_b Girder cross section modulus with respect to the bottom surface

S_{bc} Section modulus of the composite transformed section with respect to the bottom face of the composite girder

S_{ic} Section modulus of the composite transformed section at the interface of the cast-in-place and precast concretes

S_t Girder cross section modulus with respect to the top surface

S_{tc} Section modulus of the composite transformed section

t Age of concrete when the strain is considered

t Thickness of the deck slab

t_0 Age of concrete when the initial stress is applied

t_1 Some time between t_0 and t

t_x Twisting moment

T Total tension force at serviceability limit states

T_p Total tension force in prestressing steel at ultimate limit states

T_s Total tension force in non-prestressing steel at ultimate limit states

u A portion of the span length of a beam

V_c Volume of concrete in the deck slab

V_x Shear force at point x

w_d Dead load

W Width of a bridge

x Distance along the span length of a beam

y_b Distance from centroid of the girder cross section to the extreme bottom fibre

y_s Distance between centroid of the slab to centroid of the composite section

α_1 $0.85 - 0.0015\, f'_c \geq 0.67$

β_1 $0.97 - 0.0025\, f'_c \geq 0.67$

γ_c Correction factor in creep theory

γ_c Mass density of concrete

δ Rotation from the initially vertical position of a girder

δ A parameter used in IDESIGN for calculation of gradients of various functions by the finite difference method

$\Delta\sigma_c(t)$ Final value at age t of a stress increment increasing gradually from magnitude zero at t_o

$\Delta\sigma_c(t_0)$ A stress increment (or decrement) applied at age t_0

ε_1 A specified parameter used in IDESIGN to decide if a certain "percent" violation of a constraint is acceptable

ε_2 A specified parameter used in IDESIGN to decide if a certain convergence parameter is acceptable

ε_3 A specified parameter used in IDESIGN to decide if a certain percentage change in the cost function is acceptable

ε_c Maximum strain in concrete at the extreme compression fibre = -0.0035

$\varepsilon_c(t)$ Total strain (instantaneous plus creep) at time t under sustained stress

ε_p Strain in prestressing steel at ultimate limit states

ε_s Strain in non-prestressing steel at ultimate limit states

ε_{sh} Differential shrinkage strain of concrete = 100×10^{-6}

θ_x Slope at point x

ρ Reinforcement ratio

$\{\rho\}$ Vector that contains the distribution coefficients for a bridge

ρ_b Balanced reinforcement ratio

σ Normal stress

σ_a Allowable normal stress

$\sigma_c(t_0)$ A stress introduced at age t_0 and sustained during the period t_0 to t

υ Amplitude of the rotation of a girder

φ_u Ultimate creep coefficient of concrete

$\varphi(t,t_0)$ Creep coefficient of concrete = ratio of creep to the instantaneous strain due to a stress applied at time t_0 and sustained to time t

ϕ_c Material resistance factor for concrete = 0.75

ϕ_p Material resistance factor for prestressing steel = 0.95

ϕ_s Material resistance factor for reinforcing steel bars = 0.90

$\Phi(t,t_0)$ Creep function

$\chi(t,t_0)$ Aging coefficient of concrete = χ

ω Vertical deflection of a girder

Of all the structures that man builds, none are more noble, truthful, enduring and beautiful than great bridges.

Noble because a bridge stands in simple dignity, spanning space decisively from one point to another as it soars over some obstruction in service to society.

Truthful because a bridge stands exposed to the world revealing its from, its material, and its function for all to see.

Enduring because bridges are constructed to span generations, centuries, millennia or more.

Beautiful because.... well, most bridges ARE beautiful!

C. Seim and T. Y. Lin,
Esthetics in Concrete Bridge Design,
ACI MP-1, 1990.

CHAPTER 1

INTRODUCTION

1.1 GENERAL

In 1950, the first precast, prestressed concrete bridge to be built in North America was completed in the United States. It was a small highway girder bridge in Madison County, Tennessee [1,2]. The superstructure consisted of precast girders placed longitudinally side by side under a cast-in-place concrete deck slab. The girders were 8-inch blocks made in a block machine and strung on a seven-wire strand "like a string of beads" [1]. This bridge was followed shortly thereafter by the justly more famous cast-in-place, post-tensioned Walnut Lane Memorial Bridge in Philadelphia, Pennsylvania, and soon by many other structures. During that period, post-tensioning received most of the attention. It was not until the manufacturers of precast concrete products had the equipment, knowledge and experience to produce acceptable precast, pretensioned concrete girders, that the use of prestressed concrete in bridge construction started to grow rapidly. The introduction of standard girder cross sections in general and of I-girders in particular has helped this growth significantly. In an exhaustive survey [3] on the performance of highway bridges in the United States published in 1992, it is indicated that the percentage of the total population of bridges which are constructed of prestressed concrete has increased steadily from almost 0% in 1950 to about 50% in 1989. It is also noted that, during that period, the most common type of prestressed concrete bridges used nationally was I-girder bridges, also known as slab-on-girder bridges (see Fig. 1.1). More than 35,000 bridges constructed, or about half of all prestressed concrete bridges, were of this type (42.1% simple and 6.0% continuous I-girders). The survey also indicates that, during the ten-year period prior to its publishing, slab-on-girder bridges have covered more than one-third of the prestressed concrete bridge market.

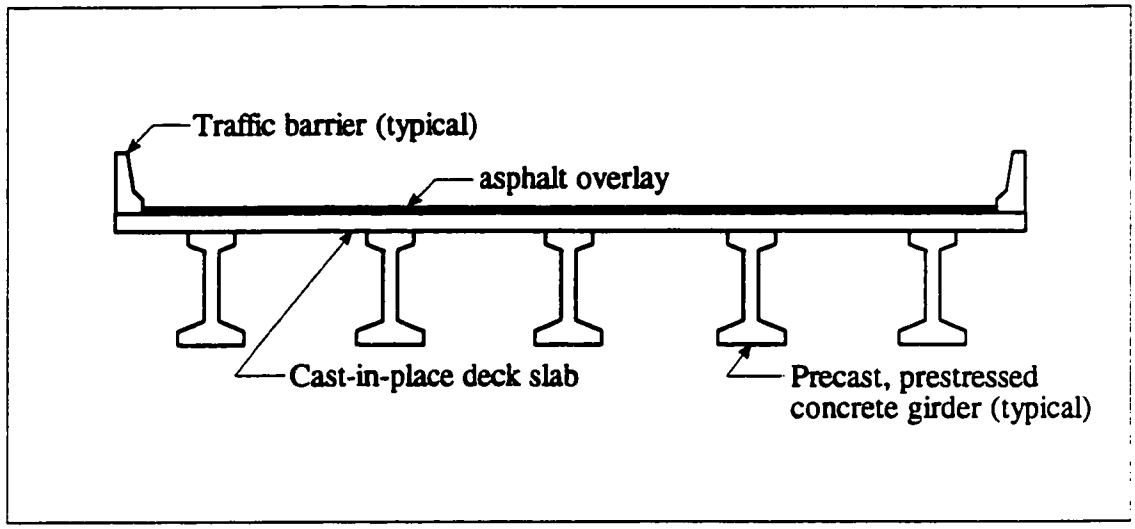

Figure 1.1 Typical slab-on-girder bridge cross section

There are no indications that these patterns have changed since then. Similar trends have been observed in Canada [4]. At comparable ages and spans, smaller percentages of prestressed concrete bridges were classified "structurally deficient" than steel or timber bridges [3,5]. Most of the early prestressed concrete bridges, while approaching the end of their planned fifty-year service life, are still in use. Based on some inspection [6] and testing [7] results, a large number of these bridges may last for many years beyond their planned service life.

Along with these developments in the area of precast, prestressed concrete bridge engineering, there came another important development in the broader area of structural engineering. For at least the past three decades, the trend in structural design has been towards improving the final design to the maximum degree possible without impairing the functional purposes the structure is supposed to serve. This trend in the design process can be attributed to several reasons. Firstly, the advent of relatively low-cost, high-power computers, and the developments in structural analysis methods and mathematical programming techniques have made both the analysis and design processes, regardless of complexity, manageable with relative ease. Secondly, the practical attainment of improved construction materials, such as high-strength / high-performance concrete, and thirdly,

scarcity of resources and the need for efficiency in today's competitive world have contributed to design progress. It is safe to say that, until very recently, most bridge designers have kept their distance from those significant innovations in computer-oriented analysis and design methods, and in construction materials. And yet, as was mentioned earlier, the majority of those early bridges have performed, and are still performing very well after about fifty years of service. One may wonder though about the impact such innovations would have on bridge engineering, particularly with regard to the economy of bridge design and construction.

1.2 OBJECTIVE

The overall objective of this study is to assess the potential economic benefits from the utilization of concretes with compressive strengths of up to about 100 MPa for continuous, precast, pretensioned slab-on-girder highway bridges. These were chosen because they represent the most common type of prestressed concrete bridges constructed in North America, as was mentioned in the previous section. To reach the above objective, computer-oriented structural analysis methods combined with computational design optimization techniques are used to develop an optimization system that can be utilized to perform economic studies on the type of bridges investigated.

1.3 SCOPE

The intent of this study is to look beyond current precast concrete production capabilities, and bridge analysis, design and construction methods. Although current practice is considered as the basis for the assumptions made in developing the optimization system, it is not used as a means to restrict potential applications of high-strength / high-performance concrete in precast, prestressed concrete slab-on-girder bridges.

For engineers, the central problem in design optimization is the formulation and execution of problems rather than the mathematical techniques themselves. This is the central

theme of the approach used in this study. In this approach, optimization is considered as a new perspective to the process of design, and one that gives considerable insight into the engineering design process. Mathematical techniques are not treated in detail.

The findings of this study are based on a slab-on-girder bridge of a configuration typical or representative of the majority of existing bridges of this type. It is outside the scope of this study to consider every possible variation in bridge geometry or layout. The results obtained, however, are general enough to apply for all bridges of this kind.

1.4 ORGANIZATION

This thesis is divided into eight chapters and two appendices. Chapter 2 contains the portion of the literature review dealing with the development and applications of high-strength / high-performance concrete in the precast, prestressed concrete industry. The potential advantages from the use of the material for highway bridges are outlined. Then, some of the challenges causing opposition to the widespread utilization of the material in the precast concrete industry are discussed. Chapter 3 presents the part of the literature review related to design economics of precast, prestressed concrete slab-on-girder bridges. Different previous approaches to solving the optimal design problem of this type of bridges are critically reviewed. Then, the latest significant developments in optimizing girder shapes for optimal utilization of high-strength / high-performance concrete are discussed. In Chapter 4, the bases of a highly efficient refined method of live load analysis for continuous slab-on-girder bridges are described. Next, an approach for determining creep and shrinkage effects in continuous bridges is explained. The behaviour of deck slabs is then discussed, and an empirical method for slab design that is not based on conventional analysis is presented. Chapter 5 describes the formulation of the optimal design problem of slab-on-girder bridges. A standard design optimization mathematical model is presented. Then, a design optimization software package is introduced to solve the optimal design problem. The information provided in Chapters 4 and 5 are used to develop the optimization system. The application

of this system is illustrated, and its validity is tested in Chapter 6 through a numerical design example. The system is then used to perform economic studies on a slab-on-girder bridge of a configuration typical of most existing bridges of this type. The findings of these economic studies are interpreted and discussed. In Chapter 7, the governing design criteria of the problem under consideration are identified and their significance studied. Then, sensitivities of the obtained results with respect to the different assumptions made in developing the optimization system are investigated. The conclusions of this study along with the recommendations for further research are listed in Chapter 8.

Appendix A contains the input data file required by the design optimization program to solve the numerical design example of Chapter 6. In Appendix B, the output data file generated by the program for the design example is given.

CHAPTER 2

HIGH-PERFORMANCE CONCRETE FOR BRIDGES

2.1 INTRODUCTION

For several years, the most common application of high-strength / high-performance concrete has been in the building industry. Concrete strengths of 100 MPa and more have been frequently used in the lower columns of high-rise buildings. In comparison, strengths of about 60 MPa have been considered the maximum achievable in the precast, prestressed concrete industry; this appears to be very timid especially in the light of the potential advantages of the material that have been indicated in several research studies.

This chapter deals with the utilization of high-strength / high-performance concrete in highway bridges. An historical account of the development of concrete strength since the beginning of this century is first presented. The distinction between *high-strength* and *high-performance* concretes is later made. Then, applications of the material in the building industry and, to a larger extent, in the precast, prestressed concrete industry are discussed. The potential advantages from the use of the material for slab-on-girder bridges are then presented. Finally, some of the challenges causing opposition to the widespread utilization of the material in the precast industry are discussed.

2.2 HISTORICAL DEVELOPMENT OF CONCRETE STRENGTH

Since the time structural concrete was introduced as a construction material, it has been characterized mainly by its strength. This is because, compared to most other characteristics, testing of strength is relatively easy. Furthermore, strength is perhaps the most

important overall indicator of concrete quality because it is directly related to the structure of hardened cement paste. Although strength is not a direct measure of concrete durability, it has a strong relationship to the water / cementitious materials ratio of the concrete. This ratio, in turn, influences durability and other properties of the concrete by controlling porosity. Concrete compressive strength, in particular, has long been widely used in specifying, controlling and evaluating concrete quality [8].

At the turn of the twentieth century, when the most dramatic growth of knowledge relating to construction with concrete occurred, cube tests produced compressive strengths in the 12.5 to 18.2 MPa range [9]. Later on, attention was brought to the need for manufacturing concrete of strengths very much in excess of those commonly produced then. In 1932, Towles [10] discussed the possible benefits of using concrete with strength of 48 MPa as compared to the maximum practical strength, at that time, of about 35 MPa. He stated that "the subject is not one of merely speculative interest, but of an immediate practical importance," and recommended that more work be done to develop methods for practical production of much stronger concretes in order to make the way clear to raise the strength standards of that time. Apparently, however, not much was done for a long time after that since more than forty years later, there was still an urgent need for research in this field [11]. By that time, concrete strengths around 55 MPa were achievable in building construction, not much more than what Towles [10] had hoped for. Additionally, there was little information in the literature concerning the properties of stronger concretes making it difficult to extend the codes and specifications that cover design and construction using such concretes.

Figure 2.1, which is adopted from Ref. [12], shows typical stress-strain curves for a range of concrete strengths under uniaxial compression. An equation developed by Loov [12] was used to fit actual experimental values from published stress-strain curves in order to produce the curves shown in the figure. It can be readily appreciated that the stress-strain curves, and thus the physical properties, of concretes of higher strength differ significantly from those of normal-strength concretes. The shape of the ascending part of the curves

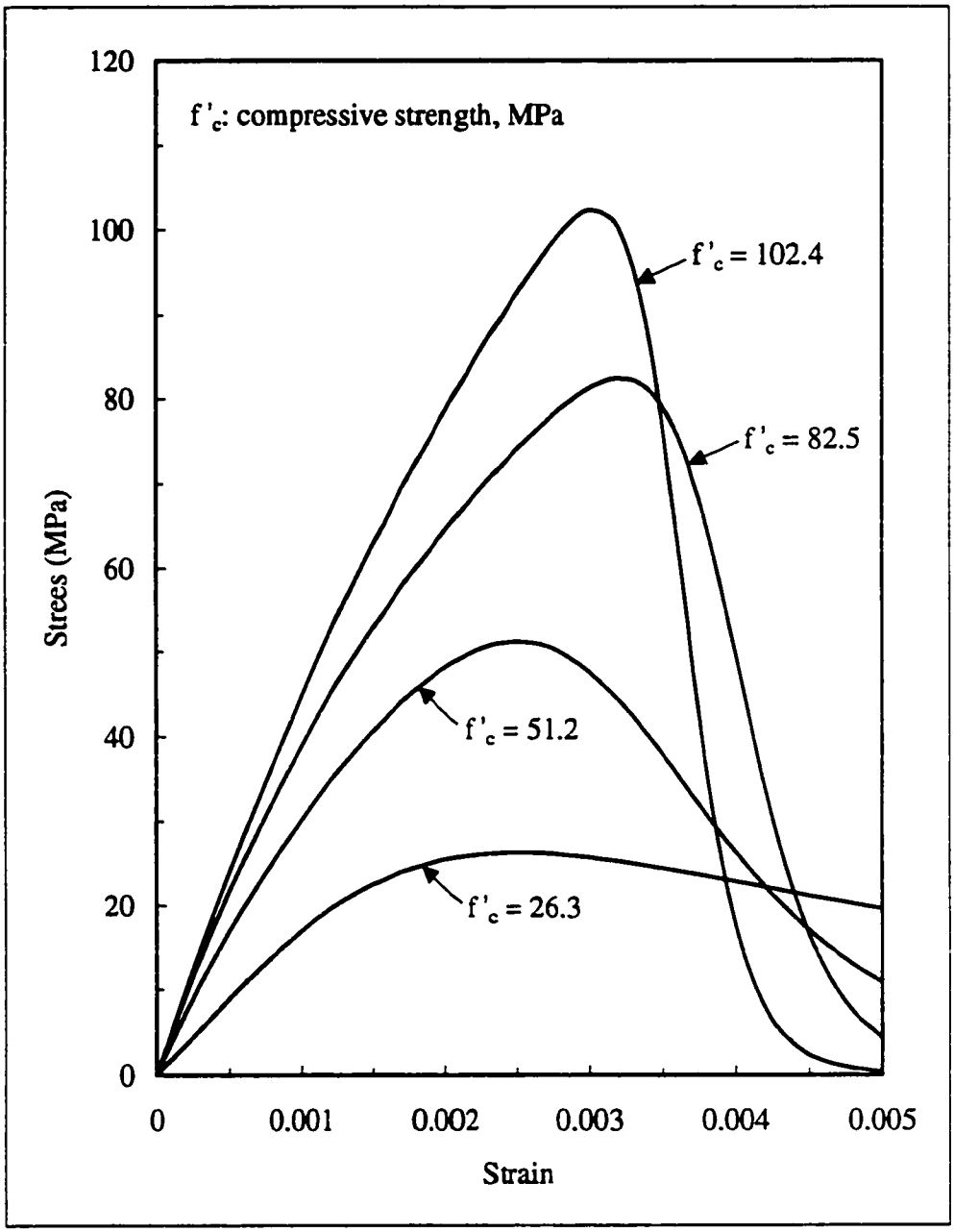

Figure 2.1 Stress-strain curves for various concrete strengths

becomes steeper with increasing compressive strength, and thus the modulus of elasticity increases. Moreover, the strain at maximum stress usually tends to increase slightly with increasing strength. Also, the slope of the descending part becomes steeper for the high-strength concretes than for normal-strength concretes, so the former in effect are more brittle than the latter. These differences make it essential that the properties of high-strength concrete be clearly understood and incorporated into design codes before the material can be widely used.

Considerable research has been carried out in many countries on high-strength concrete over the past twenty years or so, primarily dealing with the selection and proportioning of materials, and determination of physical characteristics of the concrete. A recent report from the American Concrete Institute (ACI) Committee 363 on High-Strength Concrete [13] has cited over 390 references covering all aspects of the topic. These and other efforts have brought about much better understanding of the material and its properties. With the advent of chemical admixtures (superplasticizers) and mineral admixtures (pozzolanic materials), and better quality control, concretes of strengths of 100 MPa and more have been produced consistently and used on a routine basis particularly in high-rise buildings [14]. While the use of high-strength concrete only a few years ago was an exclusive technology in a few developed countries, the recent profusion of literature reported in technical journals, and presentations made at national and international professional meetings on the topic clearly demonstrate that this material is in the process of being mature on all continents.

The most recent development in this field is the introduction of a new breed of concretes that is expected to revolutionize the way structures are built. French researchers have developed a Portland cement based material with 200-MPa compressive strength while maintaining good workability properties [15,16]. The material, known as reactive powder concrete, exhibits high ductility in addition to the ultra high strength. Such strength is achieved by improving the homogeneity of the mix through the elimination of coarse aggregates and careful selection of the grain size of different ground quartz powders.

Concrete is pressed before and after setting so that the entrapped air can be eliminated as well as most of the shrinkage accompanying hydration reactions. Furthermore, the microstructure is improved after setting through a heat treatment that changes the nature of the hydrates formed. The high ductility exhibited by the material is a result of the use of steel fibres. Work is currently in progress to enhance this material's performance characteristics leading to a material with a compressive strength of up to 800-MPa. Efforts are being made to introduce reactive powder concrete into the construction market in Canada [17,18] and the United States [19,20].

2.3 HIGH-STRENGTH vs. HIGH-PERFORMANCE CONCRETE

It is natural to refer to concrete that exhibits a higher strength than usual as high-strength concrete. However, in recent practical applications of this kind of concrete, the emphasis has in many cases gradually shifted from the compressive strength only to other characteristics of the material, such as a high modulus of elasticity, high density, low permeability and increased durability [21]. Therefore, it is logical to refer to such concrete by the more general term high-performance concrete (HPC).

HPC is not clearly defined for highway applications. Several definitions exist that are mostly dependent upon the production capacities and practices at different locations. The American Strategic Highway Research Program (SHRP) on High-Performance Concrete, for example, defines HPC for highway applications in terms of strength, durability attributes and water/cementitious materials ratio as follows [22]:

- It shall have one of the following strength characteristics:
  4-hour compressive strength $\geq$ 21 MPa termed as very early strength concrete,
  24-hour compressive strength $\geq$ 34 MPa termed as high early strength concrete, or
  28-day compressive strength $\geq$ 69 MPa termed as very high strength concrete.
- It shall have a durability factor $\geq$ 80% after 300 cycles of freezing and thawing.
- It shall have a water/cementitious materials ratio $\leq$ 0.35.

Another definition of HPC for highway structures has been proposed by the Federal Highway Administration (FHWA) [23]. The definition consists of four durability and four strength parameters. Associated with each definition parameter are performance criteria, testing procedures to measure performance, and recommendations to relate performance to adverse field conditions. To specify an HPC concrete mixture using the FHWA definition of the material, a user states the level of performance desired for each performance characteristic, based on field conditions. Updates will be required to keep the definition current with improvements in technology and with field experience.

A more generic definition has been recently proposed in a special report from the ACI High-Performance Concrete Committee [24]. HPC is defined in this report as concrete that meets special performance and uniformity requirements that cannot always be achieved routinely by using conventional ingredients, normal mixing and placing procedures, and typical curing practices. These requirements may involve enhancements of placement and compaction without segregation, long-term mechanical properties, early-age strength, toughness, volume stability, or service life in severe environments. This was a general definition to cover all structures as there was a strong feeling within the Committee that to define HPC more precisely would be restrictive.

All of the above definitions and several others [25,26] are attempts to establish a clear understanding of HPC, and to stimulate and standardize its utilization. However, they basically remain as guides for bridge designers, and they identify areas in which additional research is needed.

2.4 APPLICATIONS OF HPC

2.4.1 HPC in the Building Industry

The most common application of HPC has been in the lower columns of high-rise buildings where conventional concrete would make those unacceptably large. Since the

columns in high-rise buildings are likely to be located in prime retail rentable floor space, minimization of the size of these columns is advantageous for the architect's layout as well as for the owner who wants to maximize rentable floor space.

An outstanding example of the use of HPC in a major construction project is Seattle's Two Union Square building which was completed in 1988. Concrete with a compressive strength of 97 MPa was originally specified to construct all 18 columns of the 62-storey building. However, the designer also wished to achieve a modulus of elasticity of 50 GPa in order to meet the occupant-comfort criterion for the completed building. To achieve the modulus of elasticity, testing showed that it was necessary to use a concrete compressive strength of 131 MPa. This has been the highest strength used so far in an actual construction project [27]. Among other more recent examples are the Pacific First Center, also in Seattle (124-MPa concrete) [28], and the 31-storey building at 225 W. Wacker Drive in Chicago (97-MPa concrete) [29]; both were completed in 1989. In Canada, HPC has been utilized in the construction of several high-rise buildings. However, the maximum concrete strengths achieved have been usually less than those achieved in the United States. Examples include La Laurentienne Building in Montréal which was built in 1984. Concrete with a compressive strength of 90 MPa was used to construct an experimental column that carried through the four sub-basement floors of the 26-storey building [30]. In 1990, 80 MPa and 100 MPa concretes were utilized to cast the basement columns of the new library of Concordia University in Montréal [31]. There exist many other examples of the use of HPC in building applications in Canada [32] and the United States [33].

2.4.2 HPC in the Precast, Prestressed Concrete Industry

2.4.2.1 General:

In a relatively recent survey conducted by the Precast/Prestressed Concrete Institute (PCI) High-Strength Concrete Committee, the average 28-day concrete strength used in the American precast, prestressed concrete industry was found to be 41 MPa [34]. The maximum

strength that producers felt they can reliably supply was 59 MPa. Strengths in the same order of magnitude represent the norm in the Canadian industry. These strengths are much less than those in the 100 MPa range that have been achieved for many buildings. A number of obstacles to the use of higher-strength concretes were identified in the PCI survey by the producers; they included the increased material cost and additional quality control required to produce such concretes, and the claim that engineers do not specify higher strengths.

Aïtcin and Neville [21] have explained that in many locations the use of HPC is precluded by its unavailability. At the same time, the unavailability is often a reflection of the lack of demand. It is just possible that both the designers and the producers are reluctant to depart from the familiar; they cannot be blamed. Conversely, in those areas where there are designers keen on exploiting HPC, there is always a producer or two who can supply the material to the given specifications. This availability of HPC, in turn, encourages other designers to use it and consequently helps the spread of its utilization.

2.4.2.2 Examples of the Use of HPC in Precast Bridges:

Since the early nineties, some precast, prestressed concrete bridges, most of them experimental / demonstration bridges, have been constructed in North America and elsewhere in the world to showcase the advantages of HPC, and to provide the economic incentive for precast concrete producers to utilize the material. Designers of these bridges have utilized concrete strengths that are greater than those commonly used in the precast concrete industry. These strengths, however, have mostly remained well below those used in building construction practice.

It should be noted that the list of example bridges presented in this section is not inclusive of all HPC bridges; the purpose of this discussion is to illustrate the successful use of the material in some significant applications rather than listing every bridge project that has utilized HPC. In addition, emphasis is placed on HPC bridge projects in Canada since, in

general, there has been more acceptance of the material in this country compared to the United States and most other countries. This fact is evident from the 100 or so bridge projects that have used HPC in Canada since 1990 [35].

During 1990, a single-span, slab-on-girder highway bridge with an overall length of 52 m and a clear span of 50 m was constructed in British Columbia, approximately 700 km northwest of Vancouver [36]. The Esker Overhead was built to eliminate a level crossing of the Canadian National Railway in northwestern British Columbia. The remote location of this structure, combined with the high cost of transporting heavy girders, prompted designers to employ a single-span structure. Reducing the shipping weight of girders and lowering erection costs were achieved by precasting the span in three segments using 2300 mm deep I-girders and a 60-MPa concrete strength at 28 days. These segments were erected on falsework, closure diaphragms were cast, and the three segments were post-tensioned together.

In 1992, an experimental HPC bridge was constructed over the Portneuf river, approximately 60 km west of Québec City [37,38]. The structure was a portal frame bridge with an overall length of 27.1 m and a clear span of 24.8 m. The superstructure was built of five precast, post-tensioned, 60-MPa, air-entrained concrete rectangular beams with depths varying from 515 to 550 mm, on which a 170 mm thick concrete slab was poured to form a built-up T-beam section. After casting the slab, the bridge was post-tensioned longitudinally with external tendons running between the precast beams. At the ends of the deck, some transverse tendons were post-tensioned to counteract the anchorage stresses of the longitudinal prestress. An average 28-day compressive strength of 75.3 MPa was achieved for the precast beams. For the cast-in-place slab, the actual concrete strength was 70.7 MPa. Long-term behaviour of the bridge is currently being investigated through an extensive monitoring program [39].

In 1996, two HPC bridges, forming part of Ontario's Highway 407 Express Toll Route, were constructed as a demonstration project [40]. Both structures are single-span,

slab-on-girder bridges with spans of 34 m each. Concrete with a design compressive strength of 60 MPa at 28 days was utilized for the 235 mm thick, cast-in-place deck slabs and barrier walls of both bridges. Test results indicated that the actual 28-day concrete strength for both structures varied between 70 and 80 MPa. Relying on the low permeability of such concrete to provide corrosion protection for the reinforcement, uncoated reinforcing steel was used, and waterproofing membranes and asphalt paving on the decks were eliminated. Standard Canadian Prestressed Concrete Institute (CPCI) Type 1900 precast, pretensioned I-girders were used for both bridges. However, HPC (60-MPa concrete at transfer) was used for girders of only one of the bridges. The actual strength achieved at 28 days was about 80 MPa. The use of HPC instead of a 40-MPa concrete to manufacture the girders allowed a reduction in their number for that bridge from four girders to three. Long-term performance of the two bridges is currently being monitored.

HPC was used extensively throughout the design and construction process of the Confederation Bridge linking Prince Edward Island with New Brunswick [41,42]. The bridge, which was completed in May of 1997, has a total length of 12.9 km, and is designed as a series of distinct portal frames. The main bridge consists of 44 spans of 250 m each. The superstructure was constructed out of precast, post-tensioned box girder concrete segments using the balanced cantilever method. For this structure to have a 100-year service life in an aggressive marine environment, the designer specified HPC with a strength of 55 MPa at 28 days and 60 MPa at 91 days. The main agent of deterioration was expected to be that of chloride penetration and subsequent corrosion of the embedded reinforcing and post-tensioning steels. Other deteriorating agents included alkali-aggregate reaction, sulfate attack, freezing and thawing, and ice abrasion of the bridge pier shafts. Using HPC in combination with significant concrete cover was found to be the most effective way of protecting the structure against all these adverse agents. An average 28-day compressive strength of 81.9 MPa was achieved. The Confederation Bridge represents the largest usage of HPC in a prestressed concrete bridge in North America so far.

Several experimental / demonstration HPC bridges have been constructed in the United States over the past few years. The Braker Lane Bridge, for example, was built in 1990 to cross Interstate I-35 in Austin, Texas [43]. This slab-on-girder bridge consists of two, simply supported spans of 26 m each. It was constructed using 1016-mm deep Texas Type C precast, pretensioned I-girders fabricated with a concrete of 66-MPa design strength at 28 days. This allowed a design with increased transverse girder spacing and, consequently, fewer girders compared to a design with normal-strength concrete. For this bridge, eleven girders per span spaced at 2.6 m were used compared to seventeen or eighteen girders spaced at approximately 1.5 m if the girders were to be used with a 41-MPa concrete. Actual concrete compressive strengths at 28 days averaged 92.4 MPa. Another HPC structure, also in Texas, was built in 1997 to cross State Highway 249 in Houston [44,45,46]. The Louetta Road Overpass consists of two adjacent bridges. Each bridge consists of three, simply supported spans. The spans range in length from 37 to 41.3 m. These long spans were needed because of some roadway constraints underneath the structure. The superstructures consist of the newly developed precast, pretensioned, 1372-mm deep Texas U-beams with composite precast / cast-in-place concrete deck slabs. The U-beams are designed for concretes with specified 56-day design strengths varying between 69 and 90 MPa. Actual concrete strengths ranged from 90 to 110 MPa. This project involved a detailed instrumentation plan for monitoring long-term behaviour of the two bridges. In Nebraska, a HPC slab-on-girder bridge with an overall length of 68.6 m was constructed in 1996 at 120th Street and Giles Road in Omaha [47]. This bridge consists of three continuous spans of equal lengths. It was constructed using 1100-mm deep Nebraska Type NU1100 precast, pretensioned I-girders fabricated with a concrete of 82.7-MPa design strength at 56 days. This allowed a design with only seven lines of girders compared to eleven lines of Nebraska Type 3A girders, which are even deeper than Type NU1100, made with a 34.5-MPa concrete. Actual concrete compressive strength at 56 days was slightly more than 96 MPa. Long-term performance of the bridge is currently being monitored. In New Hampshire, another HPC slab-on-girder bridge was built in 1996 to carry State Route 104 over the Newfound River in Bristol [48]. The bridge is a 19.8-m, single-span structure. It was constructed using standard American

Association of State Highway and Transportation Officials (AASHTO) Type III precast, pretensioned girders fabricated with a concrete of 55.2-MPa design strength at 28 days. Two fewer girders were required for this bridge compared to a design with a 34.5-MPa concrete. The structure was instrumented to determine how well HPC aids the bridge's initial and long-term performance. Some other HPC bridges have been also built in Washington [49], North Carolina [50] and Virginia [51].

Apart from Canada and the United States, several HPC bridges have been constructed in a number of other countries over the past few years. France [52,53,54,55,56,57,58], Norway [59,60,61,62], Japan [63,64], the Netherlands [65], Denmark [66], Spain [67], India [68] and several other countries all have bridges built with HPC. Most of these bridges were constructed on experimental bases to establish the economical and structural feasibility of using HPC for prestressed concrete bridges.

2.5 IMPACT OF HPC ON THE PRECAST CONCRETE INDUSTRY

2.5.1 Advantages of HPC

2.5.1.1 General:

The potential advantages from the utilization of HPC for precast, prestressed concrete highway bridges have been indicated in several research studies [69,70,71,72,73,74,75]. Some of these advantages were mentioned briefly in the previous section. They are further discussed in this section.

2.5.1.2 Cost Effectiveness:

The main reason for considering the use of HPC especially for precast, prestressed concrete bridge I-girders is the possible reduction in overall costs leading consequently to less expensive bridges. This would help stretch out the services Federal and Provincial transportation authorities can provide with the funds available. The cost savings with HPC

may come from several areas. Although the basic concrete cost per cubic metre is obviously increased, primarily due to increased mix constituent and quality control costs, this may be partially or fully offset by the reduced quantities of concrete required in the form of fewer girders for a given span length as a result of the proportionate increase in girder capacity. One area of cost which may not change very much is the cost of prestressing strands. Typically, the total number of strands required for any bridge design decreases only slightly as the concrete strength increases. As the number of required girders decreases, the number of strands per girder increases, usually resulting in little net change in strand requirements. Consequently, the cost of prestressing strands may remain relatively unchanged. The most significant cost savings in using HPC may come from the reduction in non-material costs associated with the production of girders. These include the labour to produce the girders, the precaster's overhead allocated to each girder, transportation costs and erection costs. The amount of non-material costs associated with a HPC girder is the same as that for a normal-strength concrete girder; the cost savings come from the reduction in the number of girders [43]. Some earlier studies [76,77,78,79,80,81] have revealed that, for a given span, it is most economical to use as few girder lines as possible, i.e. to place girders at the largest practical transverse spacing, although the fact that this could be achieved through the use of HPC was not directly acknowledged in them.

Alternatively, for a given transverse girder spacing, the use of HPC may result in significant increases in girder span lengths [43,73,74,75]. When span lengths increase, the number of piers and foundations can be reduced for multi-span bridges, reducing in turn the cost of the substructure. If the bridge is crossing an existing roadway, a reduction in the number of piers and foundations would also ease traffic disruptions to the roadway underneath during construction of the bridge.

In 1990, Adelman and Cousins [82] reported the results of a study comparing the cost effectiveness of the use of HPC to normal-strength concrete for pretensioned AASHTO girders. Cost comparisons showed that the utilization of HPC, instead of normal-strength

concrete, to manufacture the girders could reduce the cost of a two-lane interstate bridge by as much as 17 US$/m^2, depending on the span length and transverse girder spacing. Considering a typical three-span bridge in Louisiana, the specification of 69-MPa concrete instead of 41-MPa concrete would reduce the superstructure cost by US$ 17,000, or approximately 5% of the total bridge construction cost. Even though the cost data used are not current, cost comparisons using this data are enlightening. In some recent actual bridge projects, however, it was found that the initial costs of HPC bridges can be sometimes higher than those of equivalent designs with normal-strength concrete [40,48]. This may be attributed to the fact that most precasters and contractors are still unfamiliar with HPC. Therefore, they assume higher risk levels and subsequently submit higher bids. Another possibility is that HPC requires additional mix development and testing under increased quality control requirements which increases the initial costs. If these costs are distributed over a small volume of concrete, such as the case in most experimental / demonstration bridge projects, this could inflate the cost of HPC. It is anticipated that initial costs associated with the use of HPC will diminish significantly with increased familiarity with the material, and increased frequency of applications since mix trial, testing and developmental premiums would be spread more proportionally.

2.5.1.3 Structural Advantages:

There are many structural advantages of using HPC for precast, prestressed concrete highway bridges. One advantage of HPC is its greater compressive strength, which can be evaluated in relation to unit cost, unit weight and unit volume. HPC, with its greater compressive strength per unit cost, is the least expensive means of carrying compressive force. In addition, the material's greater compressive strength per unit weight and unit volume allows lighter and more slender bridge members and piers to be used, leading consequently to improved horizontal clearance underneath the structure [70,71].

Other advantages of HPC include increased modulus of elasticity and increased

tensile strength. Increased modulus of elasticity gives smaller elastic shortening losses at the transfer of prestress in pretensioned girders. In addition, increased stiffness is advantageous when deflections or stability govern the design of the bridge. Increased tensile strength is advantageous in service load design of prestressed concrete because it increases the permissible stress range under service conditions [70,71].

Weerasekera [83] and Mitchell *et al.* [84] studied the influence of HPC on the transfer length and development length of pretensioning strands. They found that an increase in the concrete compressive strength results in a reduction of the transfer and development lengths. These improved bond characteristics permit the use of larger pretensioning strands which are required to effectively utilize HPC in precast bridge girders, as will be discussed in detail later in Sec. 2.5.2.2.

In general, HPC can decrease the effects of volume changes, such as creep and shrinkage. Based on an extensive review of the information available in the literature, Dilger and Wang [85] presented a detailed discussion on creep and shrinkage of HPC. They indicated that total creep of HPC is significantly lower than that of normal-strength concrete. In some cases, the ultimate creep coefficient of HPC can be as low as 50% or even 30% of the value observed for normal-strength concrete. Additionally, total shrinkage of HPC is also lower than, or similar to, that of normal-strength concrete. Reduced creep and shrinkage of HPC reduces, in turn, the long-term prestress losses [86].

2.5.1.4 Durability Aspects:

Several researchers [87,88] have found that primarily due to its low permeability, HPC exhibits excellent durability to various physical and chemical agents that are responsible for concrete deterioration. As was discussed in Sec. 2.4.2.2., in the case of the Confederation Bridge for example, using HPC can be a very effective way of protecting bridges against corrosion of the reinforcement, alkali-aggregate reaction, sulfate attack, freezing and thawing,

and abrasion. This is possible because of the low porosity, and more uniform and homogeneous microstructure of HPC compared to that of normal-strength concrete. Although the initial costs of HPC bridges may be sometimes higher than those of equivalent designs with normal-strength concrete, the increased durability of the former translates into longer service lives and fewer repairs, leading consequently to a reduction in the life-cycle costs.

2.5.2 Opposition to the Use of HPC

2.5.2.1 General:

From the above discussion, it is apparent that HPC should enable the design and construction of more economical, more structurally efficient and more durable precast, prestressed concrete highway bridges. However, as with every new concept introduced into any field, there is some opposition. According to the PCI High-Strength Concrete Committee survey discussed in Sec. 2.4.2.1, 10% of the responses indicated that there are absolutely no benefits gained from the utilization of HPC in the precast, prestressed concrete industry [34]. Some argue that as promising as HPC is, there is a price to pay. However, such argument stems primarily from the fact that there are still a number of gray areas when it comes to the utilization of HPC in the industry; some of these are discussed next.

2.5.2.2 Strength Limitations:

There is an argument that the benefits of HPC in precast, prestressed bridge girders diminish with increasing concrete compressive strengths, particularly at the wider girder spacings. At relatively lower concrete strengths, the increase in girder span length, as a result of strength increase, comes from an increase in the prestressing force at a large eccentricity and an increase in the allowable tensile strength of the concrete. However, at higher concrete strengths, the increase in span length is limited to the increase in the allowable tensile strength of the concrete because additional prestressing cannot be fitted into the girder cross section

below its neutral axis. Because the allowable tensile strength of concrete is usually taken as some factor of the square root of the concrete strength, the increase in span length becomes relatively small at the higher strengths, and thus HPC cannot be used efficiently [89,90].

To effectively utilize HPC, ways to apply additional prestressing force to the girder cross section are required. Using closer strand spacing or larger diameter strands can be one solution. In 1988, a FHWA memorandum prohibited the use of 15.2-mm-diameter strands in pretensioned concrete girders in the United States in favour of 12.7-mm-diameter strands at a centre-to-centre spacing of 50.8 mm [91]. This moratorium was ordered because of concerns related to the transfer and development of the larger strands with their greater prestressing force. Recent experimental investigations, however, have shown that 12.7-mm-diameter strands can be spaced at 44.5 mm centre-to-centre with no significant difference between the moment capacities of bridge girders with this spacing and those with 50.8 mm spacing [91]. In addition, it has been recommended that 15.2-mm-diameter strands should be allowed for use in pretensioned concrete girders at a centre-to-centre spacing of 50 mm [91,92,93]. Although 15.2-mm-diameter strands require longer transfer lengths in normal-strength concrete girders, their use in HPC girders is associated with a reduction of these lengths as was discussed in Sec. 2.5.1.3. These larger strands have been recently used in the Louetta Road Overpass project, described in Sec. 2.4.2.2. They were deemed necessary to fully utilize concrete strengths greater than 69 MPa. However, their use required a special approval from FHWA based on their performance results from experimental testing conducted on this project [44,45,46]. This and other projects have recently helped to lift the moratorium mentioned above. The current Ontario Highway Bridge Design Code (OHBDC) [94] does not explicitly prohibit the use of 15.2-mm-diameter strands in pretensioned concrete girders. However, their use is not common in Canada.

Another way of effectively utilizing HPC is to conduct optimization studies on precast, prestressed concrete girder shapes in order to develop new cross sections that will take full advantage of HPC. It is expected that enlarging the bottom flanges to accommodate

more strands may be the most effective solution to improve the efficiency of HPC girders.

2.5.2.3 Time-Dependent Deflections of Shallower Girder Sections:

As was discussed in Sec. 2.5.1.2, the use of HPC can result in significant increases in girder span lengths for a given transverse girder spacing. Some of these long spans may exceed the practical limit for highway transportation. For such cases, girder transportation requires detailed planning and cooperation from Federal and Provincial authorities. Because handling and transportation constraints may impose a limit on maximum span lengths, economies gained through the use of HPC may also be limited if one considers only increased span lengths. However, HPC may result in significant economies by allowing shallower girder sections to span longer lengths. In a recent study, Russell [89] considered a bridge span of 30.5 m, which is very common throughout the United States. He found out that using a 40-MPa concrete would require a 1371-mm deep AASHTO Type IV cross section to bridge the 30.5 m span. However, by using a 70-MPa concrete, that same bridge could be constructed from the 1016-mm deep Texas Type C cross section.

The observation that longer span lengths can be achieved using shallower girder cross sections can be very important if one considers the expense of bridge piers, abutments and approaches. The cost of these components will usually exceed the cost savings associated with the efficiency of deeper girders. If the elevation of a bridge can be reduced, the total cost of the bridge will decline. Therefore, the utilization of HPC would lead to potentially large savings [89].

In advocating shallower girder sections, some concern may be expressed regarding time-dependent deflections. The use of shallower sections may require more attention to detailing in order to reduce creep and shrinkage. For example, designers may incorporate mild steel reinforcement or other design features to negate time-dependent effects. Moreover, aggregates and other concrete constituents may require selection based on time-dependent

properties and not solely on strength [89]. Analytical and experimental studies on these aspects are needed. Long-term field measurements are also required in order to assess the accuracy of the research results.

2.5.2.4 Lateral Stability:

Another matter of controversy has to do with the lateral stability (roll equilibrium) of precast, prestressed HPC I-girders during lifting, transportation and erection. This is natural because these girders tend to be longer and more slender than normal-strength concrete girders. As the cross sectional areas reduce and masses decrease, there is the possibility of increased vulnerability to stability problems.

The lateral stability of long precast I-girders during lifting and erection can be improved by moving the lifting points inward away from the girder ends. Mast [95] reported that this is the most effective means of improving lateral stability. He found out that moving the lifting points a few percent of the span length may more than double the factor of safety against lateral instability. However, moving the lifting points towards midspan could increase the top fibre tensile stresses and the bottom fibre compressive stresses at transfer conditions. Imper and Laszlo [96] have suggested using temporary post-tensioning in the flanges where necessary to control stresses. Additionally, using HPC with its increased compressive strength to cast the girders can help to satisfy allowable stress criteria. Another way of improving the lateral stability during lifting and erection is to raise the girder's roll axis. This may be achieved by attaching a lifting frame to the girder that can maintain some kind of twist restraint on the girder's end, while at the same time raising the lifting point [89].

To improve the lateral stability of long precast I-girders during transportation, they are often braced using a king post truss system; steel posts are attached to the girder sides at midspan and several prestressing strands are partially tensioned over the posts and anchored in bearing plates near or at each end of the girder. Although such bracing has been used for

many years, recent studies [97,98] have revealed that this system has only minimal effects on the behaviour of girders when subjected to lateral loads. The steel area of the prestressing strands is usually too small to make a significant contribution to the lateral stiffness of the girder. The use of temporary post-tensioning of the top flange was reported to be more effective in this regard than lateral bracing.

While lateral stability cannot be overlooked when handling and shipping long precast, prestressed HPC I-girders, it should not become a limiting factor for handling common design cases, especially that there have been projects where such girders were lifted, transported and erected without any lateral stability problems. For example, in the Annacis Channel East Bridge in British Columbia, I-girders with a depth of 2300 mm and a top flange width of 1000 mm were successfully produced, transported and installed in single pieces of 51 m long [99]. Additional research studies may be needed to ascertain shipping and handling requirements for longer HPC I-girders.

2.6 SUMMARY

It has been shown in this chapter that the potential advantages from the utilization of HPC with its increased strength and improved durability for precast, prestressed concrete highway bridges are quite promising. Despite of this, there is still some disagreement in the precast industry that HPC is beneficial. This can be attributed to the fact that the benefits of the material are not fully understood within the industry due, in part, to the lack of research in this area. More significantly, the higher initial costs that have been reported recently for some HPC bridges seem to deter most designers and precast concrete producers from exploiting the material. The use of HPC is unlikely to advance quickly without a clear economic incentive for precasters to utilize the material widely. There lies the need for more extensive cost effectiveness analyses of the use of HPC for precast, prestressed highway bridges.

CHAPTER 3

DESIGN ECONOMICS OF PRECAST I-GIRDER BRIDGES

3.1 INTRODUCTION

A designer's cherished goal is to develop an optimal solution for the structural design under consideration. In prestressed concrete design, "optimal solution" normally implies the most economic structure. This chapter deals with design economics of precast, prestressed concrete slab-on-girder highway bridges. Different previous approaches to solving the optimal design problem of this type of bridges are reviewed. Then, the latest significant developments in optimizing girder shapes for optimal utilization of HPC are discussed.

3.2 DESIGN OPTIMIZATION OF PRECAST CONCRETE I-GIRDER BRIDGES

3.2.1 General

Traditionally, the process of design in structural engineering has relied solely on the designer's experience, intuition and ingenuity. Although this process has worked well as evidenced by the existence of many fine structures, it has led to a less than rigorous approach to design. Moreover, it has been quite labourious and time consuming, and has often led to conservative designs that were not the best (optimum). In structural engineering, "best" generally implies cost effective and durable structures. Scarcity of resources and the need for efficiency in today's competitive world force the designer to evince much greater interest in computational design optimization techniques. These have matured over the past four decades [100], and can be of significant aid to the designer not only in the creative process of finding the optimal design, but also in substantially reducing the amount of effort and time required to do so. Despite this, there has always been an obvious gap between the progress of the

optimization theory, and its application to the practice of structural engineering in general and bridge engineering in particular. In 1994, Cohn and Dinovitzer [101] estimated that the published record on structural optimization since 1960 can conservatively be placed at some 150 books and 2500 papers, the vast majority of which deals with the theoretical aspects of optimization. Documentation in a comprehensive catalogue of published examples [101] shows that, in practice, very little work has been done in the area of optimizing precast, prestressed concrete slab-on-girder highway bridges. Some of the results of this work are presented herein.

3.2.2 Previous Work on Optimizing Precast Concrete I-Girder Bridges

Lounis and Cohn [102] defined the optimal bridge superstructure as "one of minimum total cost, using standardized girder sections and traffic loading". In this context, they identified three levels of optimization and indicated that the overall economic impact increases with higher levels [102,103]. These three levels are discussed below.

Level 1: Component Optimization

This is the most widely reported optimization procedure due to its relative simplicity. It involves the optimization of the cross-sectional dimensions of the bridge superstructure's components (e.g. girders, deck slab), prestressing and non-prestressing reinforcements, and prestressing tendon profile, defined by its eccentricities at the critical sections. If standard precast I-girders are used, cross-sectional dimensions of the girders are known *a priori*, and are thus eliminated from the optimization procedure.

One of the earliest studies in this area was that reported in 1961 by Bonasia [104]. He developed a computer program which can be used to select and design post-tensioned standard AASHTO girders in simple-span highway bridges. The method used was essentially a trial-and-error method for which a computer was needed to carry out the repetitive calculations involved. Girders were tested for successively increasing span lengths until their

limiting values for each girder were found, for a given girder spacing and slab thickness. The program then calculated the required amount of prestressing steel and its eccentricity at mid-span. Using the computer program, some design charts were developed that could be utilized to determine the optimal girder size for any given span length, girder spacing and slab thickness; alternatively, they could be utilized to determine the maximum girder spacing and slab thickness for any girder given its span length. It is worth mentioning that the girders' concrete compressive strength in this study was fixed at a modest 34.5 MPa. This same concrete strength was used later in the development of another computer program by Naaman [105] for the selection and design of pretensioned AASHTO bridge girders. The program was used to produce design charts that could be used to select the best girder for a given span length and girder spacing. Using these charts also, the required prestressing force, number of strands and the most feasible mid-span eccentricity could be determined. It was indicated that the selection capability of the program, which was based on choosing the smallest suitable girder, may be extended in order to follow a minimum cost criterion based on given unit prices. Such extension, however, was not performed in this study. Jacques [77] utilized a minimum cost criterion to evaluate the economy of a proposed Colorado precast I-girder section that can be used to reach a simple span of 46 m. Computer programs were developed in order to perform cost effectiveness comparisons between the new section and several other I-girder sections commonly used in the United States. Girder concrete strengths were taken as 41.4 and 48.3 MPa. A similar approach was used later by Rabbat and Russell [79,80,81] to evaluate the cost effectiveness of a series of I-girder cross sections in order to determine which represented optimal designs that could be promoted as national or regional standards in the United States. The investigation was limited to pretensioned girders of simple spans in excess of 24.4 m and made with concretes having compressive strengths up to 48.3 MPa. More recently, Russell *et al.* [90] have utilized the same methods used by Rabbat and Russell [79,80,81] to study the applications and limitations of HPC in precast, prestressed bridge I-girders. They adopted a minimum cost criterion as a measure of comparison of the efficiency of the various girder cross sections investigated.

It can be noted that although minimum cost was used as a criterion for optimization in the majority of the studies reported in the previous paragraph, formal design optimization techniques were not utilized. The approach used was to "translate" the conventional design process of trail and error into computer code, and instruct the computer to carry out the substantial amount of repetitive calculations involved. This is only part of what formal design optimization techniques are intended for. They are also intended to transform the conventional design process of trial and error into a more formal and systematic procedure that is based on a clear and precise understanding of the design problem under consideration. This will be discussed further in Chapter 5. It suffices here to say that design optimization techniques force the designer to clearly and precisely identify a set of *design variables* that describe the design of the structure, an *objective function* that measures the relative merit of alternate acceptable (feasible) designs, and all *design constraints* on performance that the final design must satisfy [106,107]. Once these have been identified, it is said that the optimal design problem has been formulated. If both the objective function as well as the constraints are linear functions of the design variables, then the optimal design problem is called a linear programming problem. Conversely, if the objective function or any of the constraints are nonlinear functions of the design variables, then the problem is a nonlinear programming problem. In prestressed concrete design optimization, the problem is normally nonlinear, requiring nonlinear optimization procedures to be used. When these were in their infancy during the sixties, and even after they matured and became available through commercial software two decades later, it was more feasible, although more cumbersome and not very efficient, to reduce the nonlinear programming problem into a linear one because the software was expensive to obtain and to operate, and because linear programming methods were more well-developed. The reduction was mostly based on a transformation of the design variables leading to linear expressions for the objective function and the constraints; in other words, the problem could be linearized by representing curved boundaries in the nonlinear design space by a series of straight lines in a linear design space. Currently, however, design optimization software packages that can solve nonlinear programming problems are relatively inexpensive and easy to operate.

It would be more efficient, therefore, to utilize them for prestressed concrete design optimization.

Kirsch [108] used a linear programming approach to solve the nonlinear programming problem of optimizing general prestressed concrete continuous I-beams with prismatic cross sections. Cost of materials (concrete and prestressing steel) was selected as the objective function to be minimized. Optimal values of the cross-sectional dimensions, prestressing force and tendon layout coordinates were determined subject to a set of constraints on the design variables and allowable working stresses. A similar approach was utilized later to determine the optimal values of the prestressing force and tendon layout coordinates for a prestressed concrete continuous I-beam with prescribed, non-prismatic cross section [109]. Linear programming methods were also used more recently by Kirsch [110] to optimize indeterminate prestressed concrete flexural systems with uniform concrete dimensions through what was called a "bounding procedure". To simplify the optimal design problem, a two-level formulation was proposed that could reduce the problem size, and eliminate potential numerical difficulties encountered due to the fundamentally different nature of the design variables; the concrete dimensions were optimized in the second level and the tendon variables (prestressing force and layout coordinates) were determined in the first level. As a first step, a lower bound on the concrete volume was established without evaluating the tendon variables. The corresponding minimum prestressing force, calculated by linear programming, was an upper bound. Similarly, a lower bound on the prestressing force was determined by assuming the maximum concrete dimensions. Based on the two bounding solutions, a lower bound on the objective function was evaluated. The best of the bounding solutions was first checked for optimality. If necessary, the search for the optimum was then continued in the reduced space of the concrete variables using a feasible directions technique. For any assumed concrete dimensions, a reduced linear programming problem was solved. The process was repeated until the optimum was reached. Although this bounding procedure is interesting and potentially helpful for effectively optimizing large structures, such as slab-on-girder bridges, the efficiency and relative ease of use of the nonlinear-programming-based

design optimization software packages currently available makes them more effective than such procedures. Among others who have utilized linear programming methods for prestressed concrete design optimization was Morris [111]. He linearized the problem to determine the adequacy of a given concrete trial section, the minimum necessary prestressing force and the permissible prestressing zone. The study was performed on precast, pretensioned, simply supported beams. Allowable working stress as well as ultimate strength constraints were considered. Based on the work done by Morris [111], Fereig [112] developed preliminary design charts that could be used to determine the required prestressing force for a given pretensioned, simply supported CPCI bridge girder, for any given span length and girder spacing. The girders' concrete strength used to develop these charts was 34.5 MPa at 28 days. Similar charts were later developed for some of the commonly used bridge I-girder sections in the United States [113,114]. For these more recent charts, the girders' concrete strength was taken as 41.4 MPa.

Goble and Lapay [115] seem to have been the first to attempt optimizing prestressed concrete beams using nonlinear programming techniques. They considered simply supported precast, pretensioned beams having rather general I-shaped cross sections. Minimum material (concrete, prestressing and non-prestressing steel, and formwork) cost was selected as a criterion for optimality subject to multiple design constraints. Optimal concrete cross-sectional dimensions, and prestressing and non-prestressing reinforcement requirements were determined. Bandyopadhyay and Kapoor [116] utilized nonlinear programming methods to minimize the cost of simply supported, prestressed concrete bridge I-girders for three different design philosophies: working stress design, ultimate strength design and reliability-based design. They concluded that reliability-based design optimization gives more economical cross sections than the other two design philosophies. Desayi and Ali [117] optimized simply supported, post-tensioned concrete I-girders using minimum cost as a criterion for optimization. The problem was formulated as a nonlinear programming problem, and was solved to determine the optimal cross-sectional dimensions as well as prestressing requirements. Similar approaches were utilized by Cohn and MacRae [118,119] for fully

prstressed (pretensioned and post-tensioned), and partially prestressed concrete I-beams. Few attempts have been reported on optimizing continuous prestressed concrete girders using nonlinear programming methods [e.g. 120,121]. It is worth mentioning that the concrete compressive strength used in the studies reported in this paragraph was in the vicinity of 40 MPa at 28 days.

Level 2: Configuration or Layout Optimization

This is concerned with finding the optimal combination of longitudinal and transverse component arrangement within a given bridge system. Specific items considered include the number of spans, the position of intermediate supports, the restraint conditions (simply supported or continuous), the number of girders, etc. Relatively much less work has been reported on this type of optimization than on component optimization.

Torres *et al.* [122] utilized linear programming methods to develop a computer program for the optimal design of single-span, precast, prestressed concrete AASHTO girder bridges. Minimum cost of the superstructure for a given bridge span and width was adopted as a criterion for optimization. The program was utilized to produce a series of design charts that could be used to obtain the optimal number of girders and their types for a range of bridge span lengths and widths, and live load specifications. These charts were based on a girder concrete strength of 34.5 MPa.

Aguilar *et al.* [123] developed a computer program that could be used to evaluate a multitude of preliminary designs and select the most economical configuration of a multi-span, simply supported slab-on-girder bridge. This included the number of spans and their lengths as well as the number of girders and their types chosen from the AASHTO cross sections. The criterion used for optimization was the minimum total cost of the bridge including superstructure and substructure. The program could handle any constraints that could be imposed upon the configuration of the bridge such as terrain geometry and soil profiles. Two design examples were presented to illustrate the application and capabilities of the program.

Level 3: System Optimization

This involves the optimization of the overall features of the bridge structural system, including material(s), structural type and configuration as well as component sizes. This is the most complex optimal design problem and very few attempts to solve it are known.

Kulka and Lin [4] performed a comparative economic study on four precast, prestressed concrete bridge systems that have been proven to be conducive to medium-span bridge structures. They were segmental box sections, AASHTO I-girders, T-girders and wing sections. The structural system selected was continuous for two spans of lengths varying between 15 and 46 m. The objective of the study was to find the optimal bridge system for medium-span construction. The comparisons were made on a material-use basis first, to show the material (concrete, prestressing and non-prestressing reinforcements) efficiency of the systems; costs were later assessed to the materials to show a material-cost efficiency. Formal design optimization techniques were not utilized. Results showed that the T-girder system was the lowest in material consumption and the highest in material cost effectiveness, while the wing section system was the highest in material consumption and the lowest in material cost effectiveness. It should be mentioned, however, that T-girders were considered in this study for span lengths of up to 31 m only. The I-girder system was more efficient in material use than the box girder system until a span length of about 31 m, after which the latter became more efficient. With regard to cost effectiveness, the I-girder system remained the most economical until a span length of about 43 m. This is due to the higher cost of concrete for box girders than for I-girders. It is worth mentioning that the concrete strength in this study was fixed at 34.5 MPa.

Lounis and Cohn [102] optimized short and medium-span precast, pretensioned concrete slab-on-girder bridge systems. Simply supported I-girder bridges (with one, two and three equal spans) and continuous I-girder bridges (with two and three equal spans) were considered. Span lengths were varied between 10 and 30 m. Continuity was achieved

by mild steel reinforcement in the deck slab. Some of the standard CPCI and AASHTO cross sections were used. Nonlinear programming methods were utilized to obtain the minimum superstructure cost, as a criterion for optimization, for the different bridge configurations investigated. Based on the resulting optimal solutions, some standards were developed for selecting optimal I-girder bridge systems for various ranges of geometry. For example, it was found that the optimal longitudinal configuration for bridge lengths not exceeding 27 m was a single span. For bridge lengths over 27m, the optimal superstructure system was, in general, a two-span continuous system. Such standards could serve both as guidelines for preliminary designs and also as yardsticks against which final bridge designs could be evaluated. However, the optimal solutions presented in this study were based on a girder concrete compressive strength of 40 MPa; their validity for higher strengths may be questionable.

3.3 RECENT SIGNIFICANT DEVELOPMENTS

3.3.1 General

It was mentioned in Sec. 2.5.2.2 that one way of effectively utilizing HPC in precast, prestressed bridge girders is to conduct optimization studies on girder shapes in order to develop new cross sections that will take full advantage of higher concrete strengths. It was also indicated that enlarging the bottom flanges to accommodate more prestressing strands may be a very effective solution to improve the efficiency of HPC girders.

During the past decade, several attempts have been made toward developing new girder sections, but for reasons not directly related to improving the girders' performance when made with HPC. Optimization studies have been conducted to produce new girder shapes that are structurally more efficient in continuous-span bridges, economically more competitive with structural steel, and aesthetically more pleasing than the older girder shapes. It can be noted, however, that most of these studies have resulted in girder cross sections with enlarged bottom flanges; thus, the need for girders that are expected to utilize higher concrete

strengths more efficiently was satisfied, although in an indirect way. It is, therefore, relevant here to discuss the results of some of those studies.

3.3.2 Florida Bulb-Tee Girders

Bulb-tee girders have the same general shape of I-girders, but they are generally characterized by a wide, flat top flange, a narrow web, and a large, compact bottom flange that looks like a bulb. The bulb-tee shape was first developed in Washington State by Arthur R. Anderson in 1959 [124]. This shape was adopted, with slight modifications, as the AASHTO / PCI bulb-tee standard shape in 1988 to be used as a national standard in the United States. Some states modified the standard for their own needs and production capabilities. For example, the thin webs of some of the Colorado shapes, which can be as thin as 127 mm in some cases [125], can be attributed to the availability of aggregates that allow easy production of higher strength concretes and to the technology developed by the local precasters that allows excellent consolidation of concrete. In eastern states, such as Pennsylvania, relatively shallow girders with depths ranging from 762 to 1600 mm [125] were necessary to compete economically with structural steel in areas where vertical under-clearance was a critical concern. In Florida, the need for continuous, long span bridges to satisfy stringent ship impact requirements has prompted the development of a series of bulb-tee girders primarily intended for use in continuous bridges [126,127]. Continuity over piers is one of the changes that are currently taking place in bridge design philosophy. It allows for longer span lengths with fewer piers, and improves the durability of the bridge by eliminating deck joints and thereby preventing water, deicing salts and debris from penetrating leaking joints and damaging the structure. Advantages of continuity will be discussed further in the next chapter.

There are three designated variations to the Florida bulb-tee. Shape and size of both flanges and the web width are constant; only the depth of the section is variable (1372, 1600 and 1829 mm). The 165-mm web permits use as either a fully prestressed simply

supported girder or a combined pretensioned and post-tensioned continuous girder. The 1219-mm wide top flange reduces the amount of formwork required for the cast-in-place deck slab, and assures composite action with the slab both longitudinally and transversely. The relatively large 762-mm wide, 191-mm thick bottom flange provides for a well-balanced cross section that has its neutral axis close to mid-height of the section. This wide bottom flange can house strands prestressed to approximately 9.0 MN, and it assures adequate compressive strength for negative moments developed over the bridge piers in continuous construction [126].

Bridge aesthetics is in revival as evidenced by the many recent publications on the topic [e.g. 128,129,130]. Many designers consider I-girders to be less attractive than box girders. This could be due to the fact that the sharp angles where flanges join the web and on the outside edge of flanges are considered unsightly, especially when viewed under bright sunlight. In an effort to improve its appearance, the Florida bulb-tee girder series was designed with circular curves, rather than sharp angles, at the points where the flanges join the web (but not at the edges of the flanges). Another important benefit of the circular curve between the web and the bottom flange is that it facilitates placement and consolidation of concrete by eliminating air pockets and thus reducing honeycombing [127].

The Florida bulb-tee girders were first used to construct the Eau Gallie Bridge which carries State Road 518 over the Indian River near Melbourne, Florida. The bridge is subdivided into five independent structures, each continuous over four spans. Each span is 44.2 m in length. For this span length, a conventional design would have required twelve AASHTO Type VI simply supported girders. The effectiveness of the 1829-mm deep bulb-tee girder and the continuous construction permitted a reduction in the number of girders to nine. Calculated savings were 39% in girder concrete and 45% in prestressing strands. It is worth mentioning that the girders were fabricated with a concrete of only 41.4-MPa design strength. Actual strength though was close to 70 MPa at six months [126]. Several other bridges in Florida, either built or under construction, have utilized the bulb-tee girders.

3.3.3 Nebraska University Girder Series

Recently, researchers at the University of Nebraska-Lincoln have proposed a series of optimized precast, prestressed concrete bulb-tee girders, called the Nebraska University (NU) girder series [131,132]. The girders were developed in "hard" metic units for optimal performance in a continuous bridge of two equal spans with full-length continuity post-tensioning. However, they should also perform well in pretensioned bridges with continuity achieved by mild steel reinforcement in the deck slab, and in simply supported bridges as well.

The NU girder series comprises eight sections designated according to their depths in mm as NU750, 900, 1100, 1350, 1600, 1800, 2000 and 2400. This wide range of depths was considered to provide flexibility for bridge designers because of the smaller increments between depths, and because of the close match with existing I-girder depths that are used by most other states. Two sets of relatively thin web widths exist; 150 mm for pretensioned girders and 175 mm for post-tensioned girders. Shape and size of both flanges are identical for the entire series. This allows the use of only one set of forms with web extension panels. For the pretensioned girders, the top flange is 1225-mm wide and the bottom flange is 975-mm wide. For the post-tensioned girders, width of the top flange is 1250 mm and that of the bottom flange is 1000 mm. The bottom flanges were made as wide as can be accommodated in existing precast concrete plants because it was found that, for a given total cross-sectional area and a given bottom flange area, the girder with the wider bottom flange has better structural efficiency. This is due to the fact that a greater number of prestressing strands can be fitted in the bottom row of the wider flanged section and thus at the greatest eccentricity from the centroid of the concrete section. This allows the wider flanged section a greater positive moment resistance for a given area of strands, and thus increases the maximum achievable span length of a given girder. One potential problem, however, with the bottom flanges of this girder series may be their relatively narrow edge thickness; with only 135 mm of edge thickness, most precasters may have difficulty getting the concrete properly placed in the corners of the bulb. It is worth mentioning that although the Nebraska researchers

recognized the drive towards the increased use of HPC, they based their optimum section on a concrete of only 41.4-MPa strength at 28 days [132].

Aesthetic aspects were considered in the development of the NU girder series. Similar to the Florida bulb-tee girders, the NU girder series was designed with circular curves, rather than sharp angles, at the points where the flanges join the web. In addition, sharp angles were eliminated on the outside edge of the flanges in favour of circular curves [132].

Some economic studies were performed by the Nebraska researchers to compare the cost effectiveness of the NU1800 girder relative to some of the commonly used girders in the United States and Canada. It was found that the NU girder was slightly better than the other girders at longer span lengths [132].

3.3.4 Texas U-Beam

Aesthetics and economy were the primary design considerations for this precast, prestressed concrete open-top trapezoidal girder with sloping webs, developed at the Texas Department of Transportation [133]. The emphasis on aesthetics came from the perception that I-shaped girders are unattractive. The girders are spaced relatively close together with many visual break lines along the side face of the bridge. To some observers, this is considered to be unsightly. I-shaped girder bridges are very common in Texas, and are both durable and economical. However, something common may eventually be considered unattractive even though still functional.

To achieve the desired aesthetics, yet maintain the economy of precast, prestressed concrete girders manufactured under controlled plant conditions, two new metric cross sections of the U-beam were developed such that the number of girders and the number of visual break lines are reduced by replacing the I-shaped girders with more widely-spaced girders having smoother lines. The Texas Type U40 girder, having a depth of 1016 mm, was

proposed as an aesthetic alternative to the 1016-mm deep Texas Type C girder. Likewise, the Texas Type U54 girder, having a depth of 1372 mm, was proposed as an aesthetically pleasing alternative to the 1372-mm deep AASHTO Type IV girder. The Texas Type C girder and, to a larger extent, the AASHTO Type IV girder constitute most of the prestressed concrete bridge girders used in Texas. Depths of the new sections were maintained approximately the same as existing girder sections, primarily to facilitate widening of existing bridges. Both U-beam types have web widths of 126 mm, two top flange widths of 400 mm each, and a bottom flange width of 1400 mm [133]. The U-beam sections were designed for use in pretensioned, simply supported bridges to span lengths comparable to those spanned by the I-girder sections. Type U54, for example, was designed to span 35.1 m if manufactured with a concrete of 55-MPa strength at 28 days, which is the maximum strength typically used in Texas. This is comparable to the 36.6 m preferred maximum length of the equally deep AASHTO Type IV girder.

Construction cost comparisons between I-girders and U-beams were performed [133]. It was found that the price per unit length of the latter was higher than that for the former because I-girders have lighter sections. It was argued, however, that bridges constructed with U-beams should be economically competitive with bridges constructed with I-girders; because I-girders are usually more closely spaced than U-beams, 1.7 to 2.0 times as many I-girders are typically required per span. Therefore, the total weight of a U-beam span is usually less because the reduced number of U-beams more than offsets the additional girder weight, particularly with Type U54 girders. Reduced superstructure dead weight leads to a reduction in substructure, with fewer and/or smaller piers required, and consequently a reduction in cost. The foundation requirements for the overall structure are likewise reduced. It is important to remember though that these economic advantages in favour of U-beams over I-girders are based on the utilization of normal-strength concretes to manufacture the girders, and on the relatively narrow I-girder spacings that are typical of current slab-on-girder bridge construction. Using HPC to fabricate the girders would allow for wider girder spacings, and may consequently reduce any economical gap in favour of U-beams over I-girders

significantly, or even eliminate it altogether. The U-beam transportation cost was found to be a higher percentage of the total cost per unit length than that for I-girders because special transport equipment is typically required. I-girders can usually be transported with 5- to 7-axle pole-type rigs, while the heavier U-beams may require 8- to 10-axle rigs, which may possibly include additional jeep or dolly units.

Although the U-beam was proposed as an aesthetic and economical alternative to I-girders, its developers anticipated that the majority of Texas bridge construction will continue using I-girders, and that U-beam bridges will be constructed at the more visible and/or urban locations where aesthetic structures are more appropriate [133]. As was mentioned in Sec. 2.4.2.2, Type U54 girders have been recently used successfully for the superstructure of the Louetta Road Overpass in Houston [44,45,46].

3.3.5 New England Bulb-Tee Girders

The most recent development in this field is the introduction of a new precast, prestressed concrete bulb-tee bridge girder series in the New England region which comprise six states [134]. For several years, the New England standard has been the AASHTO girders. These, however, were beginning to suffer limitations in their range of applicability in this region because precasters did not have the forms needed to fabricate the deeper sections that were required for the longer spans which have been increasingly called for in bridge design practice in recent years. This added to the fact that structural steel was already a strong economic competitor with a solid foothold in the New England market, has prompted the development of a new precast girder standard for the region that would be competitive with steel and would meet the often conflicting requirements posed by the New England environment: on the one hand, the depth, shipping length and weight of the girders have to be kept to a minimum due to the limitations of existing roads, particularly in rural areas; on the other hand, highway design considerations are pushing designers to use longer spans in order to improve safety on roadways under bridges by providing greater side clearances, and

also to minimize the impact on environmentally sensitive areas such as wetlands.

The general features of the bulb-tee shapes developed in Florida and Nebraska, and described in Secs 3.3.2 and 3.3.3, respectively, were adopted for the New England bulb-tee (NEBT) girder series. The NEBT girder series was developed in hard metric units. It comprises five sections designated according to their depths in mm as NEBT1000, 1200, 1400, 1600 and 1800. The relatively thick 180-mm wide web in intended to be accommodative of both pretensioning and post-tensioning. Shape and size of both flanges are identical for the entire series. The top flange is 1200-mm wide and the bottom flange is 810-mm wide. The depth of the bottom flange is 220 mm, allowing the bottom bulb to house up to 52 straight 12.7-mm-diameter prestressing strands at a large eccentricity. In order to be practical in New England, the NEBT girder series was designed to achieve a simple span of 38.1 m, the typical maximum shipping length that most New England states can normally accommodate. Other girder parameters included a typical girder spacing of 2.44 to 2.74 m. Similar to the NU girder series, the NEBT series was designed with circular curves, rather than sharp angles, to enhance its appearance [134].

The first application of the new NEBT girders in an actual bridge project was in the Summer Street Bridge over the West Service Road Extension in Boston, Massachusetts. The bridge, which was completed in August 1997, is an 18.6-m, single-span structure. The NEBT1200 section was chosen for the superstructure. Girders were cast with a 41.4-MPa concrete. Several other bridges all over the New England region are currently under construction [134].

3.4 SUMMARY

In spite of the significant aid that computational design optimization techniques can provide to the designer, there has always been an obvious gap between the progress of the optimization theory and its application to the practice of structural engineering in general and

bridge engineering in particular. Very little work has been done in the area of optimizing precast, prestressed concrete slab-on-girder highway bridges. Most of this work has dealt with simple-span bridges using linear programming methods that are not very efficient for the type of problem considered. It has been indicated that the overall economic impact increases with higher levels of optimization, from component optimization to configuration or layout optimization to the overall bridge system optimization. Yet, most of the reported work in this area have dealt with the first level only. The overwhelming majority of previous studies have utilized concretes with compressive strengths in the vicinity of only 40 MPa or even less. It is apparent, therefore, that there is a need for more extensive economic studies to evaluate the effectiveness of using HPC in continuous slab-on-girder bridges which are increasingly called for in bridge design practice. These studies should make use of the more efficient nonlinear programming techniques, and should move toward higher levels of optimization.

CHAPTER 4

ANALYSIS OF CONTINUOUS SLAB-ON-GIRDER BRIDGES

4.1 INTRODUCTION

The word *analysis* implies the conceptual break up of a whole into parts so that one can have an insight into the complete entity. In the context of structural engineering, analysis usually refers to *load (force) analysis*, a process in which one determines the distribution of load effects, such as bending moments, shear forces and deflections, in the various components of a structure. Final design of the structural components is based on such effects. Another less commonly used term in structural engineering is *strength analysis*, which refers to the process of determining the strength of the whole structure or its components. The term *analysis* is used in this chapter only in the meaning of load analysis. In the context of bridge engineering, the term *load distribution* is often used instead of analysis.

This chapter deals with the analysis of continuous slab-on-girder highway bridges. Advantages and methods of achieving continuity in this type of bridges are first discussed. Then, a highly efficient refined method of live load analysis to determine longitudinal moments, shears and deflections in girders is described. Creep and shrinkage effects in continuous bridges are then dealt with. Finally, the behaviour of deck slabs is discussed and an empirical method for slab design that is not based on conventional analysis is presented.

4.2 CONTINUITY IN SLAB-ON-GIRDER BRIDGES

4.2.1 General

During the late fifties and early sixties, most multi-span slab-on-girder bridges

constructed in North America consisted of a series of simple spans. Extensive experimental and analytical investigations directed toward improving the design and construction of this type of bridges were conducted at the Portland Cement Association in the early sixties [135]. One of the areas studied concerned the feasibility of establishing live-load continuity between the precast girders. It was found that there are several reasons that should encourage designers to utilize such continuity.

4.2.2 Advantages of Continuity

The most important reason for introducing continuity in bridges is the desire to eliminate joints at the piers. Joints can be eliminated also between the deck slab and the abutments in what is called an *integral bridge* [136,137]. This provides a continuous road surface from one approach embankment to the other. However, it presents a challenge to engineers because the design involves structure-soil interaction and structure-pavement interaction, and so requires the combined skills of structural engineering, geotechnical engineering and highway engineering. Moreover, there are many uncertainties associated with the behaviour and design of such a bridge [138]. Currently, there is no design guidance available for integral bridges, and therefore they are not considered in the present study. The elimination of many or even all deck joints improves the durability of the bridge by preventing water, deicing salts and debris from penetrating leaking joints and damaging the structure. Thus, initial and maintenance costs are reduced, both for the joints and the bridge, and the life of the structure is extended. Another reason for the introduction of continuity in bridges is the desire for longer spans; continuity allows a given girder to span greater lengths than if it were simply supported [139]. Mid-span bending moments and deflections are reduced when continuity is established, permitting the use of more slender girder sections. When a standard section is used, continuity will permit a reduction in positive moment reinforcement and prestressing force. Either alternative can lead to reduced costs if the means used to achieve continuity are not too costly [135].

The most widely used method to establish continuity is to place conventional reinforcing bars in the cast-in-place concrete deck slab over the piers to resist the negative moments there. This method is explained in detail in the following section. Other methods for achieving continuity also exist [140,141,142]. However, they are more expensive, and require speciality contractors.

4.2.3 Construction Method for Continuous Slab-on-Girder Bridges

Figure 4.1 illustrates the construction sequence for a two-span continuous slab-on-girder bridge. The procedure is identical for bridges with a greater number of spans. Initially, the precast, prestressed concrete girders are erected between piers as if they were going to

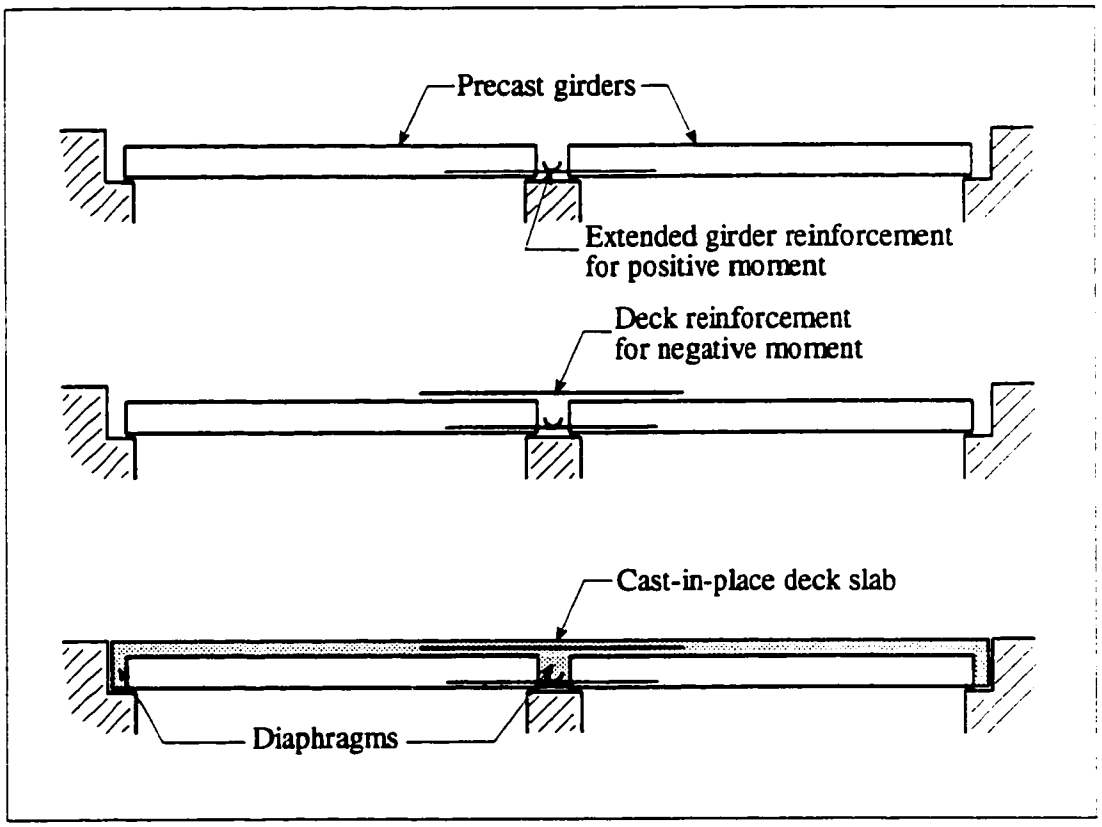

Figure 4.1 Construction sequence for a two-span bridge with precast, prestressed concrete girders made continuous

be simply supported in the final structure. Then, reinforcing bars are embedded in the cast-in-place deck slab across the piers to resist the negative bending moments induced by live loads. Continuity or closure diaphragms are then cast between the ends of adjacent girders at interior supports. These diaphragms, which are usually cast before the deck is placed, connect the girders so that the bridge becomes continuous for any loads applied to the composite structure. In many cases, reinforcing bars or prestressing strands are extended from the ends of the girders into the continuity diaphragms to provide connections for positive moment transfer between girders. Bridges constructed in this manner are often referred to as being *continuous for live load.*

4.3 LIVE LOAD ANALYSIS FOR SLAB-ON-GIRDER BRIDGES

4.3.1 General

In order to account properly for the construction sequence of slab-on-girder bridges, the moments at different cross sections are computed as follows: initially, when the girders are placed simply supported on the substructure, the analysis under the girder and slab self-weight is carried out as for simple beams. At this stage, the stresses are determined using the girder section only. Subsequently, when continuity is established, the analysis for live load, and traffic barrier and pavement weights is carried out as for continuous beams. Composite action of the precast girders and cast-in-place slab must be considered in evaluating the stresses produced by these loads.

4.3.2 Methods of Analysis

Dead load effects are often obtained using methods of statics such as the beam analogy method. Live load effects, on the other hand, are not so easily determined because of the wide variety of parameters (from the structure's geometry to its components' material properties) that influence exactly how live loads are distributed, especially in continuous bridges. Methods of live load distribution analysis range in sophistication from the overly

simplified AASHTO method [143] to the highly complex *refined* finite element method. The former, because of being too simple, is excessively conservative, and the latter, which requires fairly large standard computer programs, is prone to common errors of idealization and interpretation of results as well as being relatively costly.

Other refined methods which are frequently used for live load analysis of bridge superstructures, especially in Europe, include the grillage analogy method and the orthotropic plate theory method. Both of them are computer-based, but they differ in the way they mathematically idealize the structure. The grillage analogy method uses a discrete idealization in which the flexural and torsional stiffnesses of the actual structure in both longitudinal and transverse directions are concentrated in discrete beams of the grillage [144]. The orthotropic plate theory method, on the other hand, utilizes a continuous idealization in which stiffnesses are uniformly distributed in both the longitudinal and transverse directions [145].

In a third type of idealization, the longitudinal flexural and torsional stiffnesses of a slab-on-girder bridge are concentrated in a number of discrete longitudinal girders while the transverse flexural and torsional stiffnesses are uniformly distributed along the length in the form of an infinite number of transverse beams, which thereby constitute a transverse medium. This idealization is shown schematically in Fig. 4.2, and is considered a closer representation of a slab-on-girder type of bridge than the other two idealizations. Because the properties of the bridge are represented discretely insofar as longitudinal stiffness is concerned and continuously insofar as transverse stiffness is concerned, this representation is referred to as the *semicontinuum idealization.* In an early form of the semicontinuum idealization developed in the late fifties, the torsional stiffnesses of the longitudinal girders and the deck slab were either ignored completely or, in the case of longitudinal effects, were handled in an approximate manner [146]. During the early eighties, Jaeger and Bakht [147,148,149] formalized this idealization into a general method that can take proper account of torsional stiffnesses in both the longitudinal and transverse directions; it was appropriately referred to as the *semicontinuum method.*

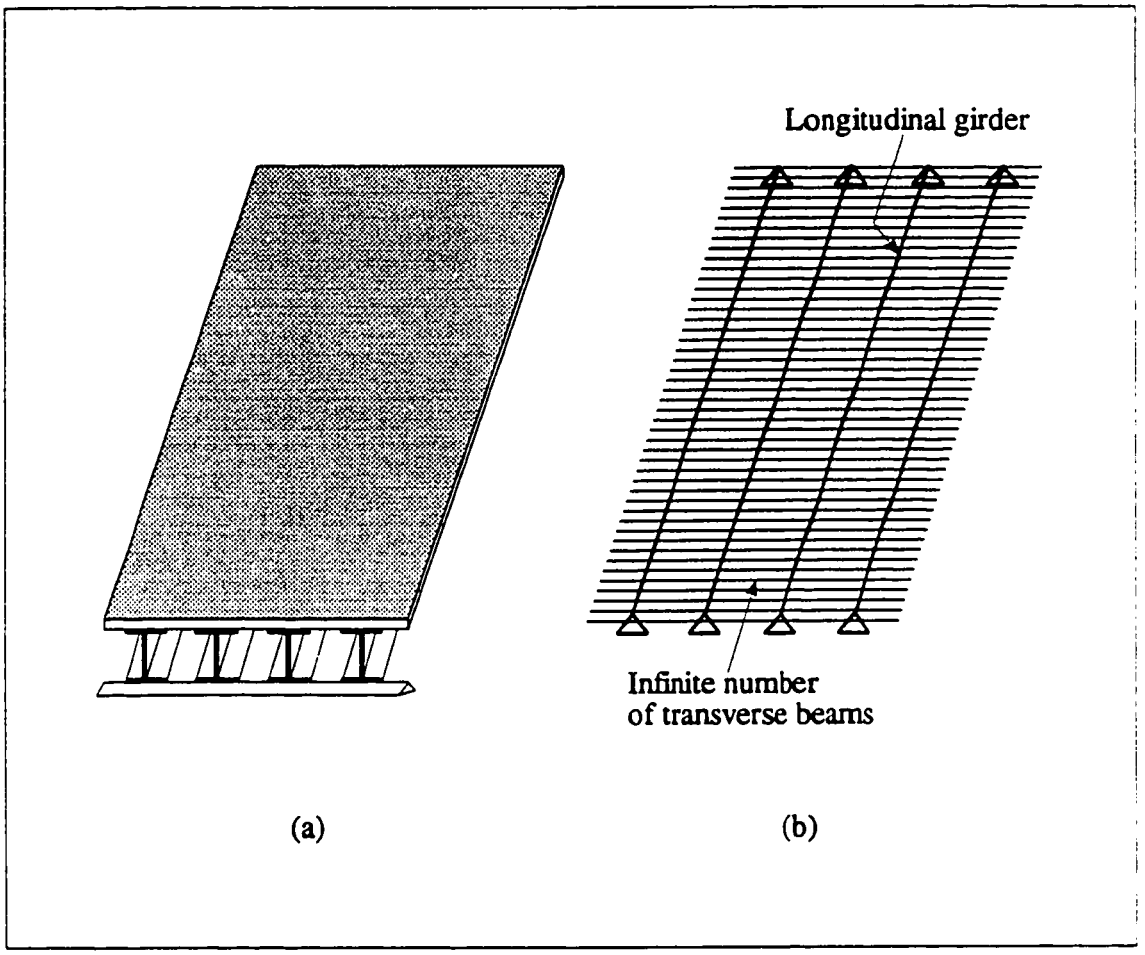

Figure 4.2 Idealization by a semicontinuum
(a) Actual bridge
(b) Semicontinuum idealization

The current OHBDC [94] permits a simplified method in determining the live load longitudinal moments in continuous-span I-girder bridges. According to this method, the positive and negative moment portions of a bridge girder can be idealized separately for purposes of live load distribution as simply supported girders having equivalent spans that are based on points of contra flexure in the corresponding continuous girder. Recently, Jaeger *et al.* [150] have reported that this method is valid for the positive moment regions, but is inaccurate for negative moments. A revision of the OHBDC method was proposed to be included in the new Canadian Highway Bridge Design Code (CHBDC), but only for bridges with two equal spans. The validity of the revision still needs to be confirmed for bridges with more than two unequal spans.

Because of the uncertainties that are still associated with the OHBDC method, the semicontinuum method discussed earlier is used in this study for live load analysis. The method is approved by the OHBDC as a refined method of analysis. Moreover, it has been recently incorporated in the AASHTO LRFD Bridge Design Specifications [151]. The validity and accuracy of this method have been verified with respect to the grillage method, the accuracy of which is often taken for granted [152]. Very good correlation exists between the results of the semicontinuum method and the grillage method which requires much larger computer power. In the following section, the bases of the semicontinuum method are presented in detail since the method is still not widely known among most bridge engineers. Reference is extensively made to Refs [147,148,149,153]. In the interest of clarity, these references are usually not explicitly cited in the discussion since they are for the same authors.

4.4 THE GENERAL SEMICONTINUUM METHOD

4.4.1 Load Distribution

It has been mentioned previously that in the context of bridge engineering, the term *load distribution* is often used instead of analysis to refer to the distribution of load effects in the various components of a bridge. In order to establish the meaning of this term,

reference is made to Fig. 4.3 in which three simply supported longitudinal girders, of span L, are connected by a transverse beam at mid-span. This assembly represents a very simple idealization of a slab-on-girder bridge with the longitudinal girders representing the actual girders in the bridge and the transverse beam representing the deck slab. The middle girder carries a central point load, P.

In the absence of any connection between these girders, the entire load will, of course, be carried by the loaded girder and the bending moment diagram will be the familiar triangular one with a maximum value of PL/4; this diagram is often referred to as the *free bending moment diagram*. However, since the girders are connected, a portion of the load P will be taken by the outer girders, which do not themselves carry the external load. How much of P is distributed to the outer girders will depend upon the girder stiffnesses, and their spans and spacings. If the flexural stiffness of the transverse beam is a very small fraction of the stiffnesses of the longitudinal girders and the spacings of the latter are relatively large, then hardly any load will be transferred to the girders not carrying the direct load. On the other hand, an infinitely stiff transverse beam will compel the three girders to deflect equally, and in that case each girder will accept a load of P/3.

Assuming that the load sustained by each of the symmetrical outer girders is P_2, the bending moment diagrams for the three girders will be as shown in Fig. 4.3. Obviously, the transference of load from the externally loaded girder to the girders not carrying the load directly takes place because the loaded girder has a tendency to deflect more than its neighbours, and the tendency of the transverse beam is to reduce the differential deflection between adjacent girders. The process of load transference from the loaded girders to girders which are not directly loaded is often referred to as *load distribution*.

4.4.2 Distribution Factors and Coefficients

Distribution factors and distribution coefficients are non-dimensional measures of load

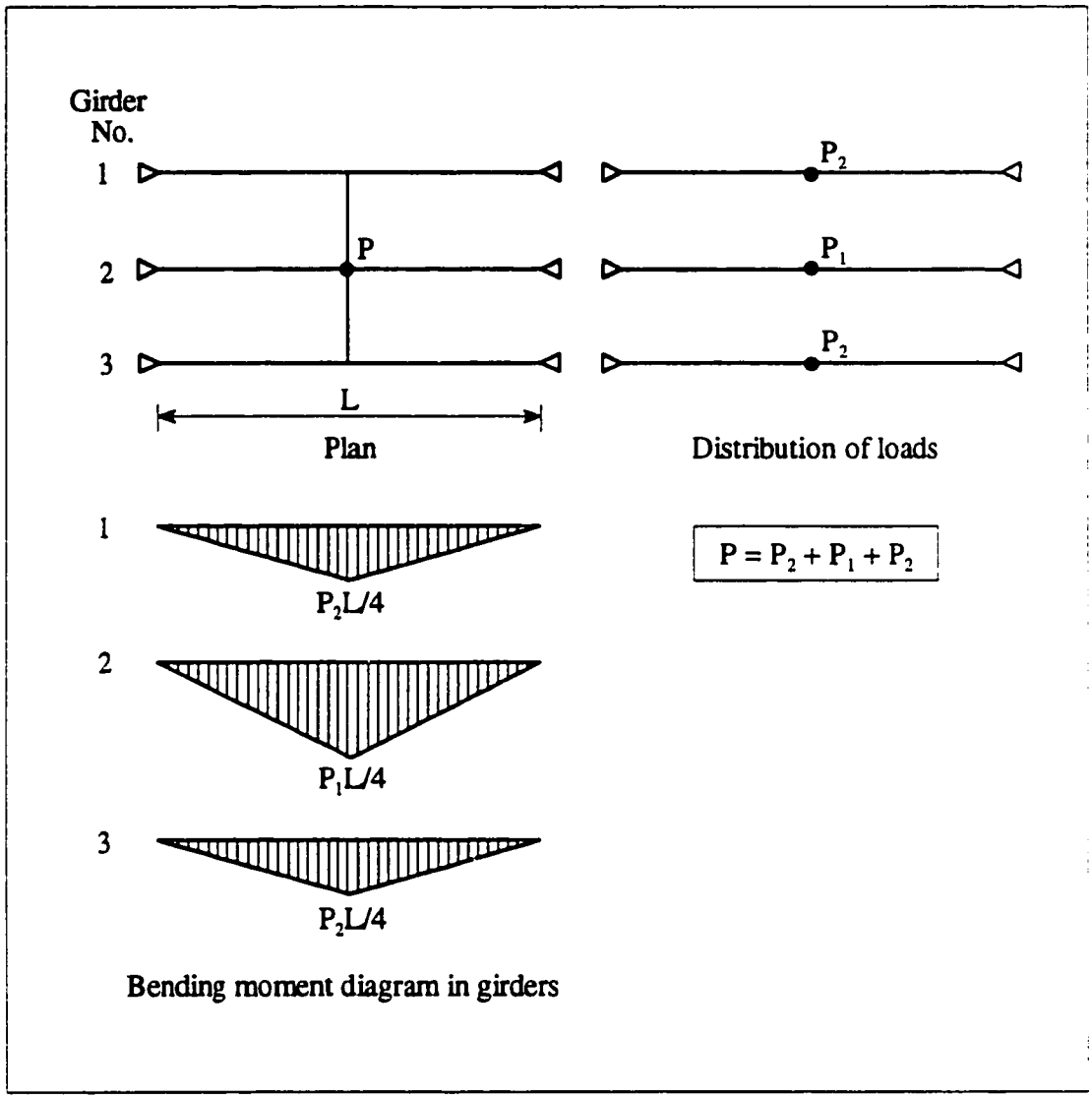

Figure 4.3 Load distribution in girders connected by one transverse beam

distribution in a bridge. At a given point of a transverse section, the distribution factor for a certain response is equal to the ratio of the response at that point to the average response at the cross section containing the point. For example, in the case shown in Fig. 4.3, the average moment in the three girders is PL/12, so that the distribution factor for longitudinal moment in the middle girder at mid-span is equal to $(P_1L/4)/(PL/12)$, or $3P_1/P$. It is noted that the terms *distribution factor* and *distribution coefficient* are interchangeable. The latter term is used in this discussion.

In the simple case shown in Fig. 4.3, the bending moment diagrams of the three girders are all of the same shape, being the familiar triangle. The bending moment diagram for any one girder can be regarded as the free bending moment diagram multiplied by a number which is called the *distribution coefficient.* Referring again to Fig. 4.3, the distribution coefficients are P_2/P, P_1/P and P_2/P.

4.4.3 Harmonic Analysis of Beams

4.4.3.1 General:

As was discussed in Sec. 4.3.2, for the purpose of analysis a bridge superstructure must usually be idealized as a mathematical model such as an assembly of finite elements, a grillage, an orthotropic plate or a semicontinuum. Similarly, applied loads also require appropriate mathematical idealization. For example, loads concentrated over relatively small lengths are often idealized as point loads for the purposes of beam analysis. These point loads, like the actual loads, are discontinuous functions with respect to the span of the beam. It is possible, and sometimes convenient for analysis, to represent a discontinuous load on a beam as a continuous function or a series of continuous functions by means of a harmonic series. For the method of analysis presented herein, the wheel loads of a design vehicle are represented by harmonic components as explained below. Only the final form of the harmonic series is given; derivation of the various expressions is given elsewhere [149].

4.4.3.2 Point Loads on Simply Supported Beams:

A point load P on a simply supported beam of span L can be represented as a continuous load of intensity given by the following expression:

$$p_x = \frac{2P}{L} \sum_{n=1}^{\infty} \sin\frac{n\pi c}{L} \sin\frac{n\pi x}{L} \qquad (4.1)$$

where c is the distance of the point load from the left support, and x is the distance along the span, also measured from the left support.

Therefore, according to Eq. (4.1), a point load is equivalent to the sum of an infinite number of distributed loads, each of which corresponds to a term of the series and is a continuous function of x. For example, if c equals L/4 in Eq. (4.1), one obtains the representation of a point load at the quarter-span point. This series is diagrammatically shown in Fig. 4.4. As shown in the figure, the load corresponding to the first term (or harmonic) has the shape of a half sine wave, and that corresponding to the second has the shape of two half sine waves, and so on. For this particular case, the contribution to the p_x series is zero for harmonic numbers that are divisible by 4. For other harmonics, the load consists of as many half sine waves as the harmonic number. It can be readily appreciated that when the harmonic number becomes sufficiently large, the harmonic load consists of a large number of small patches of loads acting alternately in upward and downward directions. When the effects of these upward and downward loads nearly cancel each other, the series can be regarded as having converged.

From elementary beam theory, it is known that the load intensity p_x, shear force V_x, bending moment M_x and slope θ_x of a beam of uniform flexural stiffness EI are related to its deflection ω by the following equations:

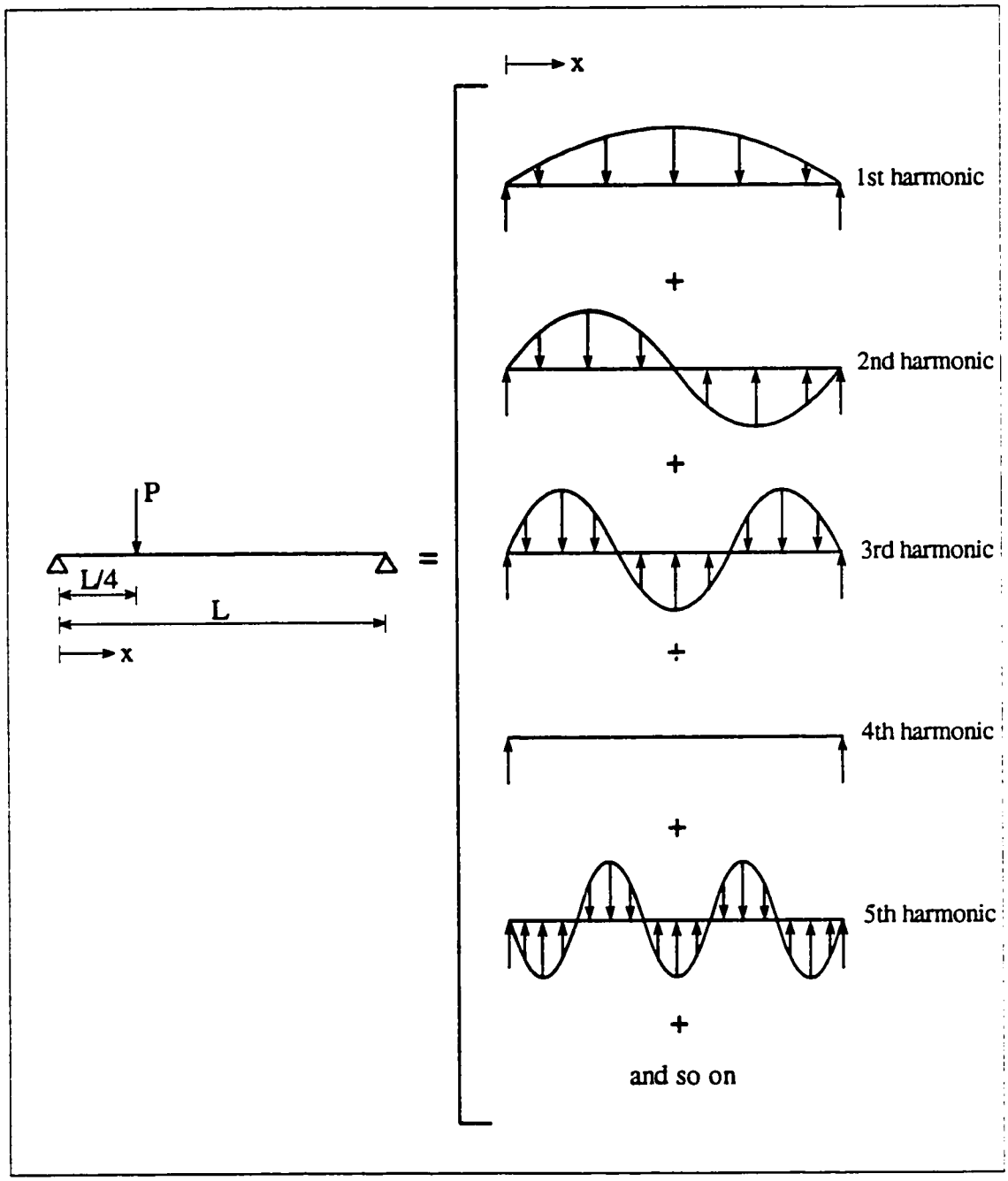

Figure 4.4 Representation of a point load by a harmonic series

$$p_x = EI \frac{d^4\omega}{dx^4} \tag{4.2a}$$

$$V_x = -EI \frac{d^3\omega}{dx^3} \tag{4.2b}$$

$$M_x = -EI \frac{d^2\omega}{dx^2} \tag{4.2c}$$

$$\theta_x = \frac{d\omega}{dx} \tag{4.2d}$$

Thus values of V_x, M_x, θ_x and ω can be obtained by successively integrating the right-hand side of Eq. (4.1) with respect to x. The end conditions of a simply supported beam are such that all constants of integration are equal to zero, and the following equations are obtained:

$$V_x = \frac{2P}{\pi} \sum_{n=1}^{\infty} \frac{1}{n} \sin\frac{n\pi c}{L} \cos\frac{n\pi x}{L} \tag{4.3a}$$

$$M_x = \frac{2PL}{\pi^2} \sum_{n=1}^{\infty} \frac{1}{n^2} \sin\frac{n\pi c}{L} \sin\frac{n\pi x}{L} \tag{4.3b}$$

$$\theta_x = \frac{2PL^2}{\pi^3 EI} \sum_{n=1}^{\infty} \frac{1}{n^3} \sin\frac{n\pi c}{L} \cos\frac{n\pi x}{L} \tag{4.3c}$$

$$\omega = \frac{2PL^3}{\pi^4 EI} \sum_{n=1}^{\infty} \frac{1}{n^4} \sin\frac{n\pi c}{L} \sin\frac{n\pi x}{L} \tag{4.3d}$$

4.4.3.3 Uniformly Distributed Loads on Simply Supported Beams:

A uniformly distributed load of intensity q on a simply supported beam of span L can be represented by the following expression:

$$p_x = \frac{4q}{\pi} \sum_{n=1,3,5}^{\infty} \frac{1}{n} \sin\frac{n\pi x}{L} \tag{4.4}$$

The equations for the various beam responses can then be obtained by successively integrating the right-hand side of Eq. (4.4) with respect to x. As was the case for the point load, the various constants of integration are all found to be equal to zero, and the following equations are obtained:

$$V_x = \frac{4qL}{\pi^2} \sum_{n=1,3,5}^{\infty} \frac{1}{n^2} \cos\frac{n\pi x}{L} \tag{4.5a}$$

$$M_x = \frac{4qL^2}{\pi^3} \sum_{n=1,3,5}^{\infty} \frac{1}{n^3} \sin\frac{n\pi x}{L} \tag{4.5b}$$

$$\theta_x = \frac{4qL^3}{\pi^4 EI} \sum_{n=1,3,5}^{\infty} \frac{1}{n^4} \cos\frac{n\pi x}{L} \tag{4.5c}$$

$$\omega = \frac{4qL^4}{\pi^5 EI} \sum_{n=1,3,5}^{\infty} \frac{1}{n^5} \sin\frac{n\pi x}{L} \tag{4.5d}$$

As mentioned previously, one of the reasons for representing discontinuous loads on a beam by a harmonic series is that this mathematical idealization provides a continuous load function with respect to the span. In the case of a uniformly distributed load covering the entire length of the span, the load is already a continuous function of the span, and it is therefore relevant to ask why such a load should be analyzed into a harmonic series. The reason is that each term of the harmonic series has the property that a load of that shape will produce a deflection of the same shape. This property is of indispensable importance in establishing the load distribution properties of bridges, as will be seen later. This behaviour is illustrated in Fig. 4.5. It can be readily seen that the deflected shape of a beam subjected to loading in the shape of two half sine waves is also in the shape of two half sine waves. Further, the bending moments also have the same shape as the loading.

For a load that is uniformly distributed over a length 2u (which is smaller than the span L) of a simply supported beam as shown in Fig. 4.6, the harmonic series representation is given as follows:

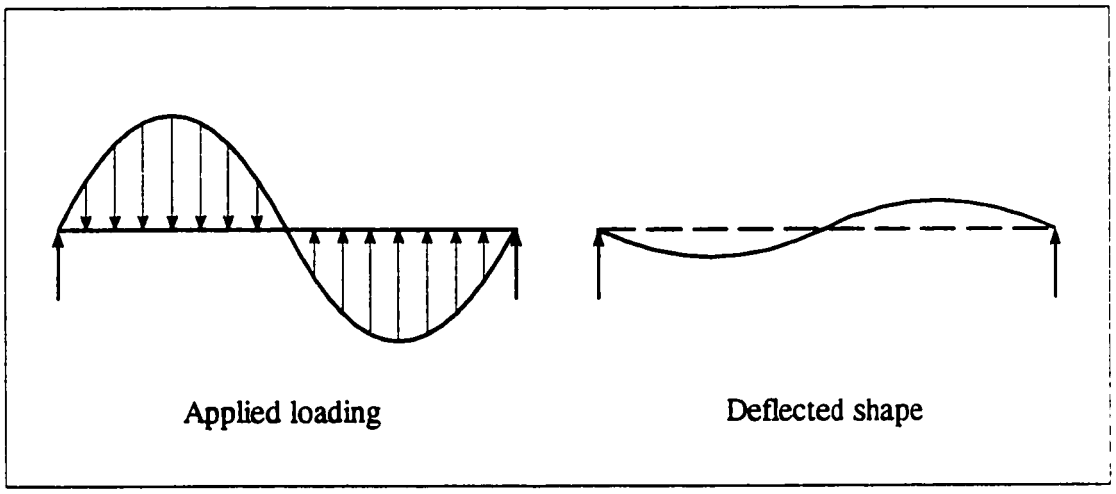

Figure 4.5 Deflection of a beam under sinusoidal loading

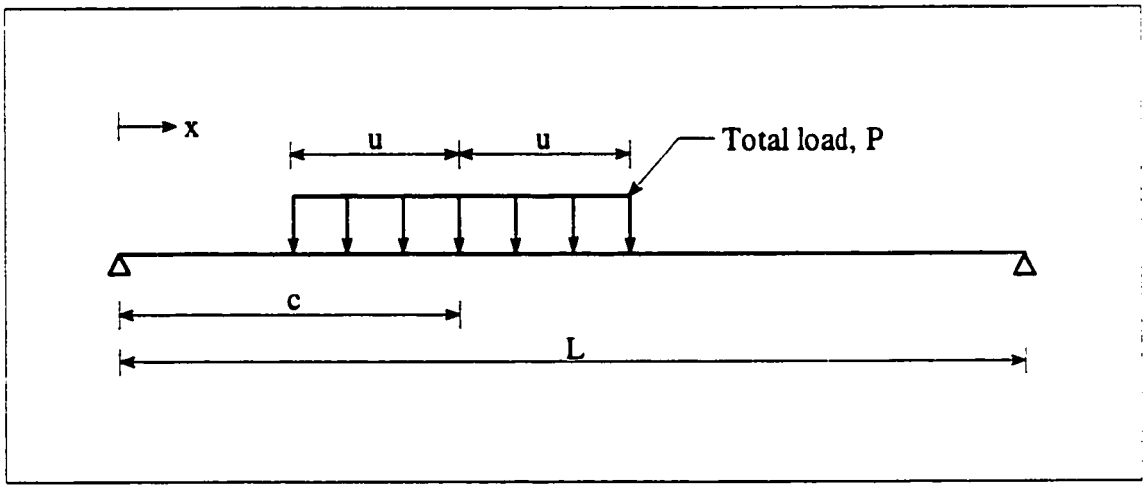

Figure 4.6 Load uniformly distributed over part of the span of a simply supported beam

$$p_x = \frac{2P}{\pi u} \sum_{n=1}^{\infty} \frac{1}{n} \sin\frac{n\pi c}{L} \sin\frac{n\pi u}{L} \sin\frac{n\pi x}{L} \tag{4.6}$$

where P is the total load, and c is the distance of the centre of gravity of the load from the same support from which x is measured. The other beam responses can be obtained in the manner discussed earlier

$$V_x = \frac{2PL}{\pi^2 u} \sum_{n=1}^{\infty} \frac{1}{n^2} \sin\frac{n\pi c}{L} \sin\frac{n\pi u}{L} \cos\frac{n\pi x}{L} \tag{4.7a}$$

$$M_x = \frac{2PL^2}{\pi^3 u} \sum_{n=1}^{\infty} \frac{1}{n^3} \sin\frac{n\pi c}{L} \sin\frac{n\pi u}{L} \sin\frac{n\pi x}{L} \tag{4.7b}$$

$$\theta_x = \frac{2PL^3}{\pi^4 uEI} \sum_{n=1}^{\infty} \frac{1}{n^4} \sin\frac{n\pi c}{L} \sin\frac{n\pi u}{L} \cos\frac{n\pi x}{L} \tag{4.7c}$$

$$\omega = \frac{2PL^4}{\pi^5 uEI} \sum_{n=1}^{\infty} \frac{1}{n^5} \sin\frac{n\pi c}{L} \sin\frac{n\pi u}{L} \sin\frac{n\pi x}{L} \tag{4.7d}$$

4.4.4 The Semicontinuum Method for Bridges

4.4.4.1 Significance of Harmonic Load Representation:

Similarly to the analysis of single beams, any loading along a longitudinal line of a bridge can be represented by a harmonic series. Figure 4.7 shows four simply supported longitudinal girders connected by three transverse beams with the second girder subjected to a point load at mid-span. The various girders will receive different patterns of loads. For example, as shown in the figure, girder 1 will accept loading in the form of three downward-acting point loads. Because of the different patterns of loading accepted by the various girders, their deflection patterns will differ from each other. The analysis of the problem shown in Fig. 4.7 will require the solution of 36 unknowns. If the number of transverse beams is increased to seven, as would be required for a realistic grillage idealization, the number of

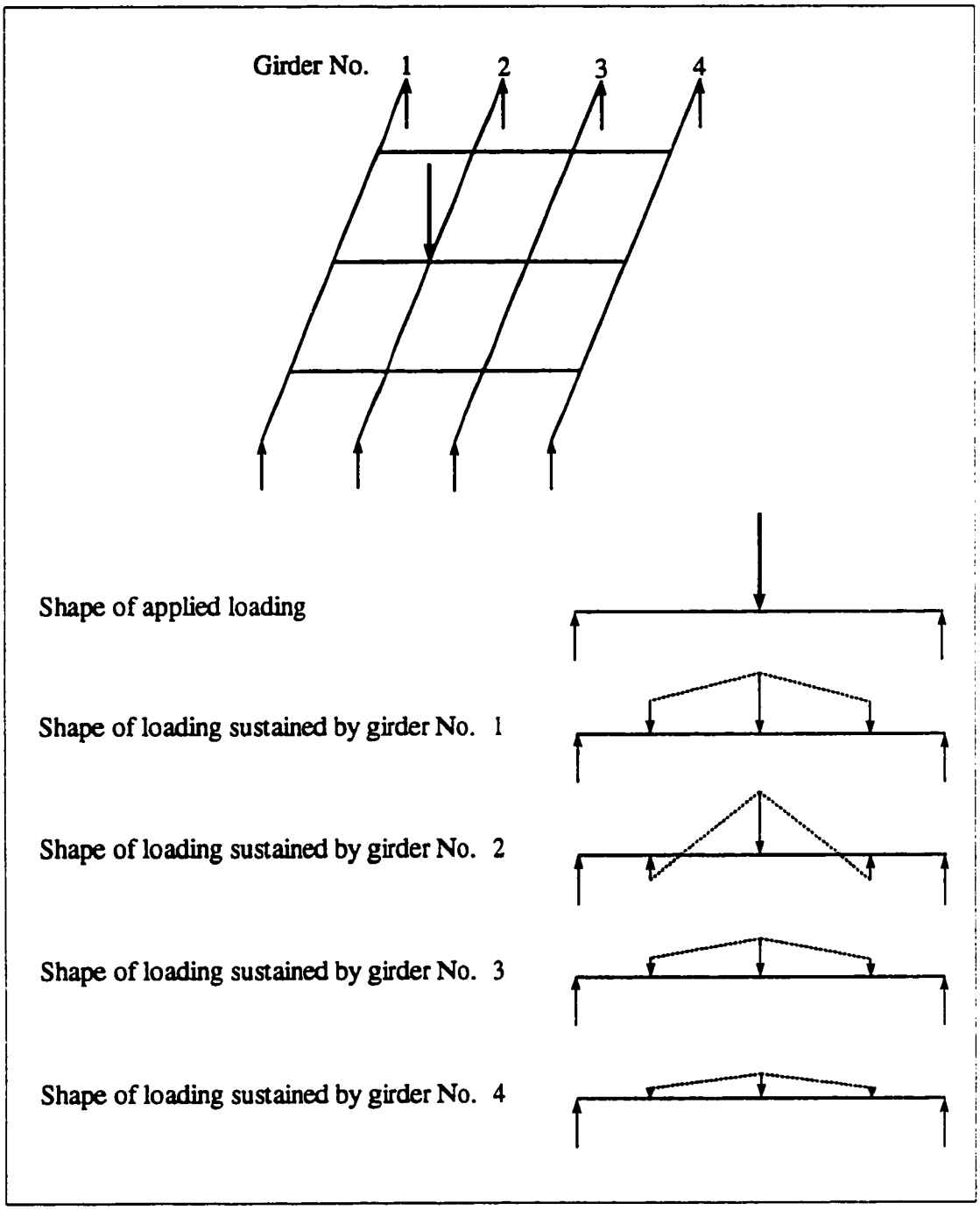

Figure 4.7 Distribution of loads in four girders connected by three transverse beams

unknowns will be increased to 84.

The number of transverse beams is now greatly increased and, as shown in Fig. 4.8, the second girder is subjected to a distributed load which is in the shape of a half sine wave. This loading, as discussed in Sec. 4.4.3.2, corresponds to the first term of a harmonic series representing a point load. For this case, all the loadings accepted by the various girders will have the same shape. Consequently, the deflection profiles of the girders will have the same shapes and will be related to each other by scalar multipliers. The implication of similar deflection patterns of the girders is that the assembly of beams can now be "exactly" analyzed by considering only a transverse slice of the structure. In this way, the number of unknowns for the four girders is reduced to eight without compromising accuracy. In fact, accuracy is enhanced with the seven (or some such small number) that are employed in the usual grillage idealization.

The distribution of loading represented by the second term of the harmonic series is shown in Fig. 4.9. As can be seen, the loads carried by the various girders in this case are also of similar shapes, with the result that the problem of distribution of this loading and those represented by higher harmonics can again be solved by determining only eight unknowns.

It can be noted that the various harmonics are distributed among the girders in different ways, with the result that when the distributed loads are added up, the total loads accepted by the girders are not, in general, similar to one another. This phenomenon is illustrated in Fig. 4.10 for a bridge with four girders carrying a point load at the mid-span of girder 2. For a point load at mid-span, the even-numbered harmonic terms of the series are all equal to zero, and the load is represented by only the odd-numbered terms. It can be seen in the figure that the sums of the loads accepted by the various girders do not have similar shapes. The key to the efficiency of the semicontinuum method lies in the separation of the dissimilar loads accepted by the various girders into components of similar shapes, as a result of which the number of unknowns is drastically reduced.

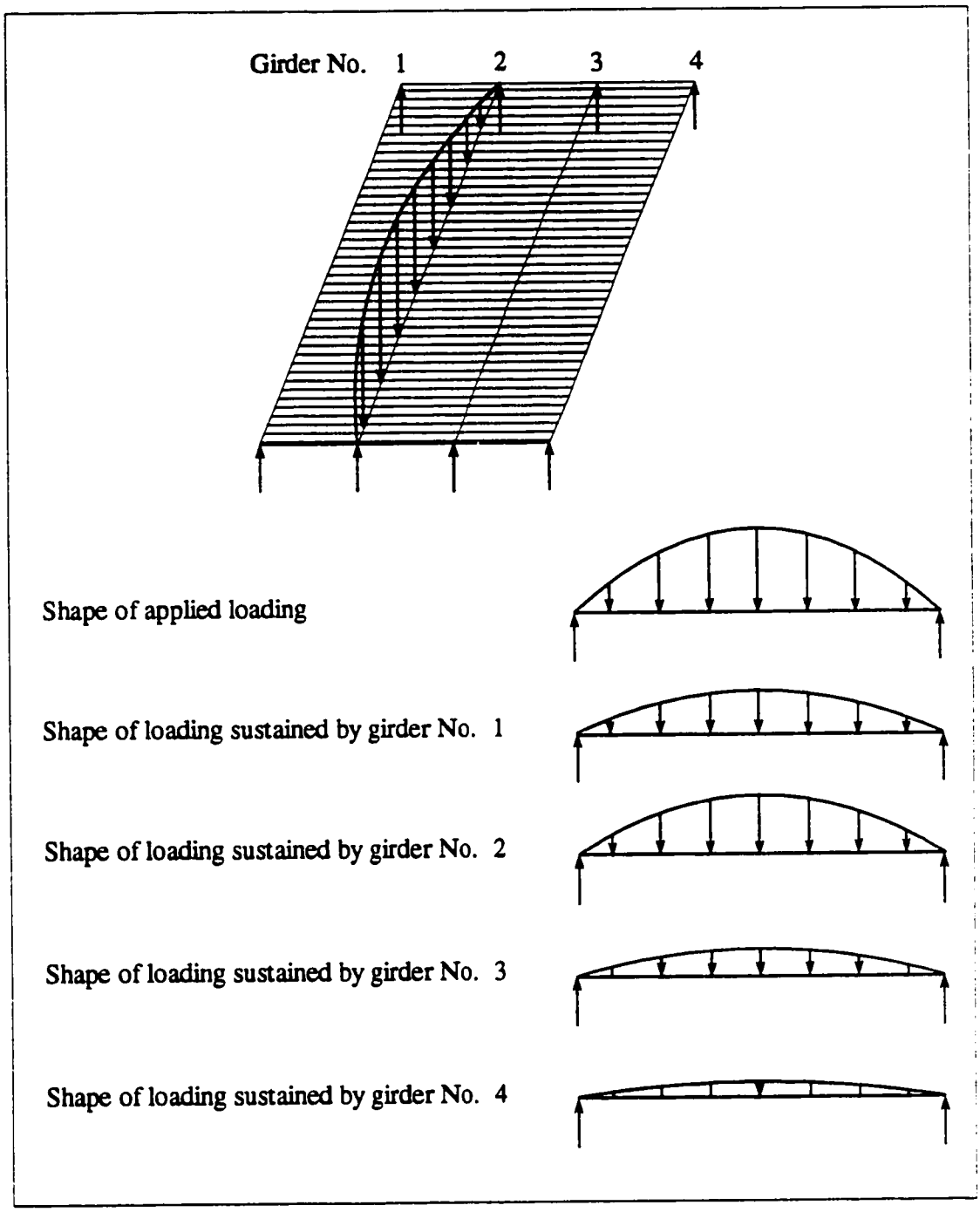

Figure 4.8 Distribution of first harmonic loading

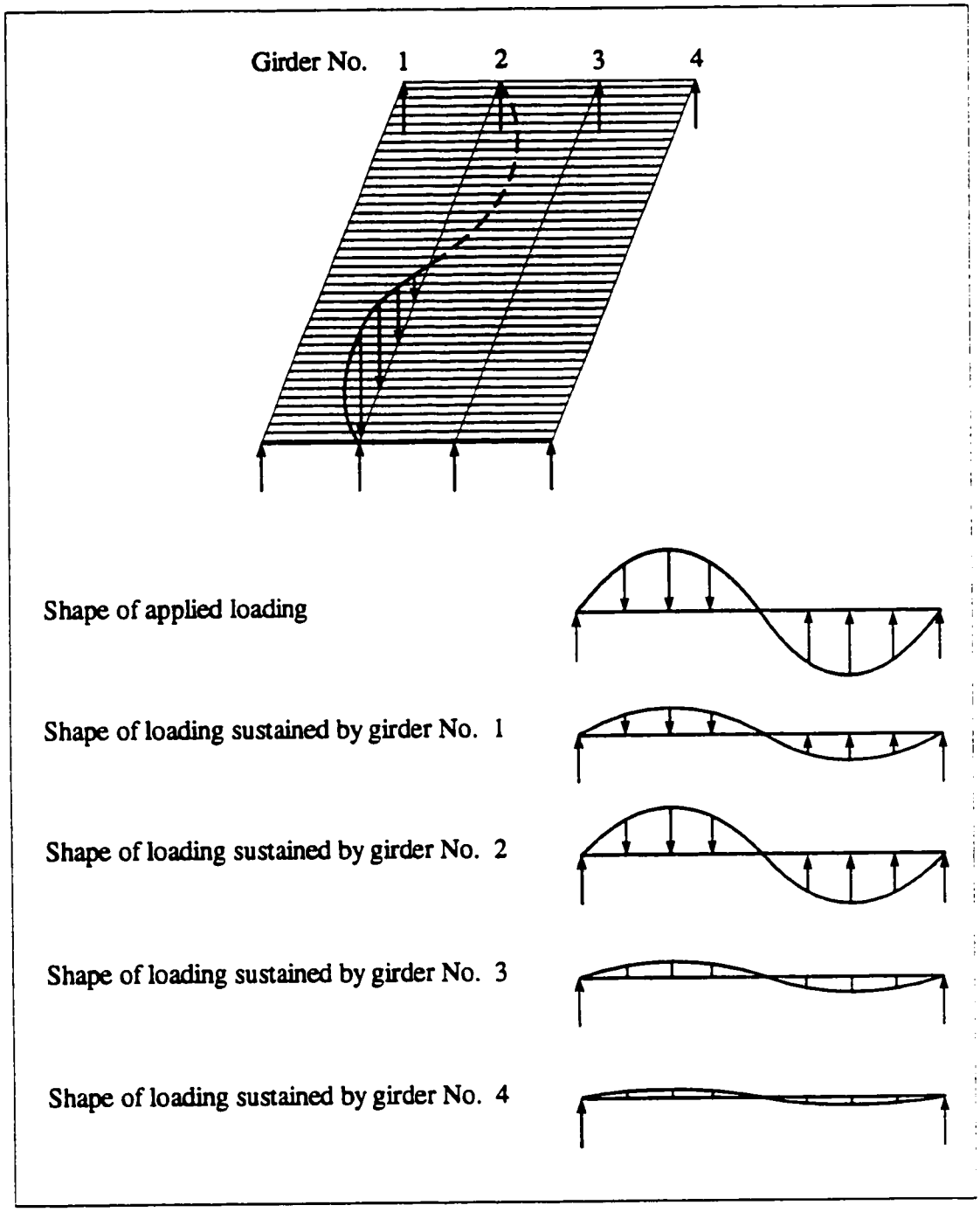

Figure 4.9 Distribution of second harmonic loading

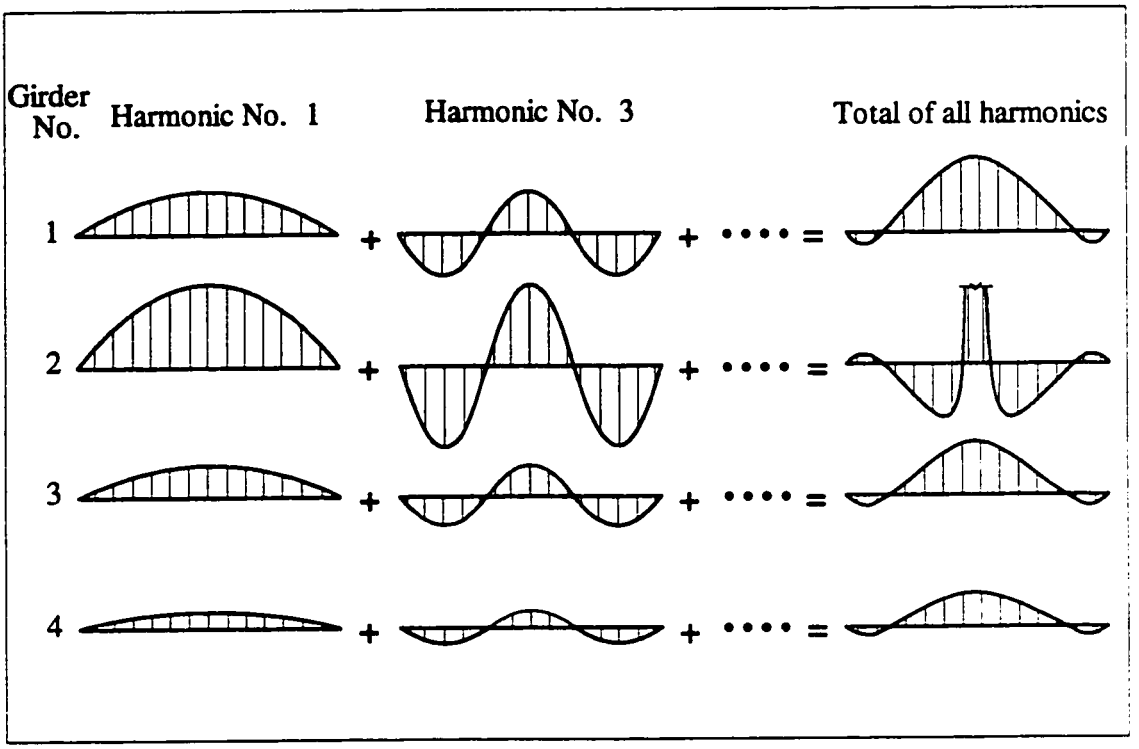

Figure 4.10 Loads accepted by the various girders of a bridge with four girders

4.4.4.2 First Harmonic Relationships:

A simply supported slab-on-girder bridge is shown in Fig. 4.11. The behaviour of this bridge is first examined under pure first harmonic conditions, i.e. an externally applied line load in the shape of a half sine wave is applied. It has been previously shown in Fig. 4.8 that the vertical loads accepted by all longitudinal girders have this same half sine wave shape. It can also be verified, as shown below, that the distribution of twisting moments along the girders (which are also the distributed bending moments in the transverse medium) have the same half sine wave shape as the applied loading.

Figure 4.12 shows girders 1 and 2 and the portion of transverse medium (deck slab) between them. The girders are all of length L and are a distance S_1 apart. A coordinate x is measured in the longitudinal direction of the bridge. The externally applied load is of intensity

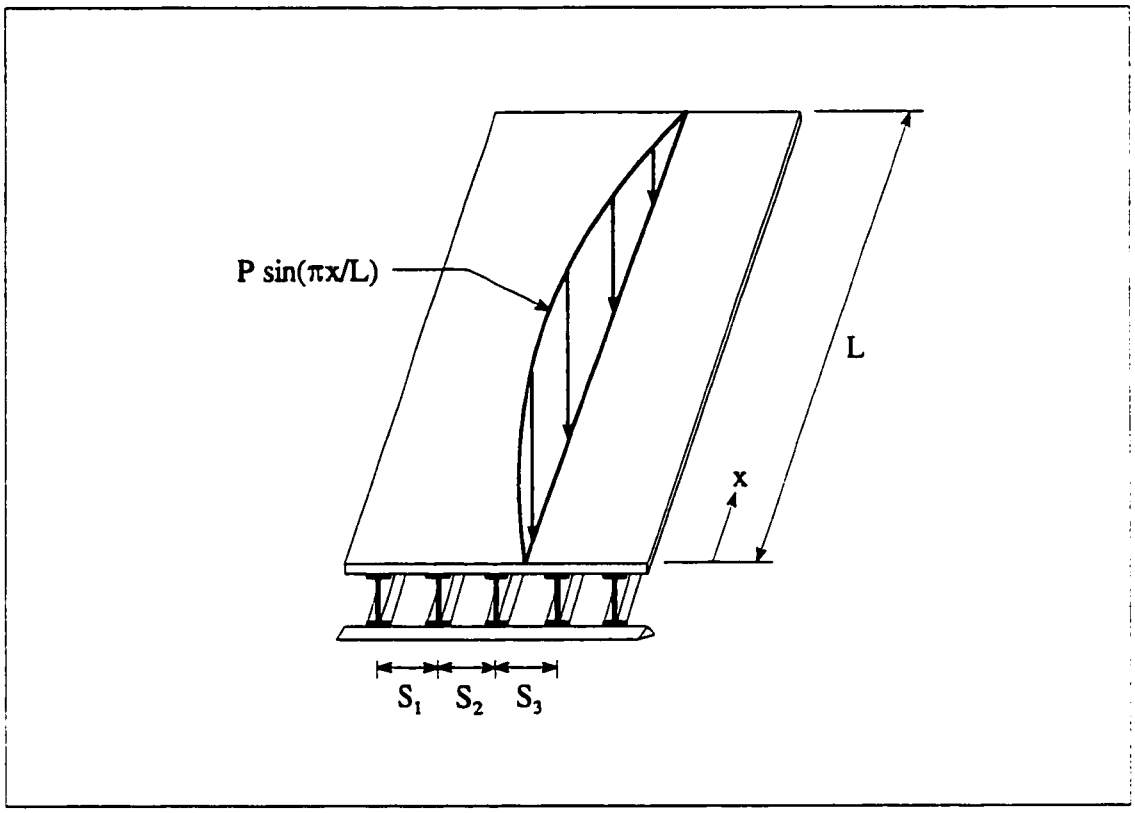

Figure 4.11 Bridge subjected to a sinusoidal load

P sin(πx/L) as shown in Fig. 4.11.

The interaction of force and moment between the girders and transverse medium is now examined. The girders may deflect into pure sine wave forms defined by the equations

$$\omega_1 = a_1 \sin\frac{\pi x}{L} \tag{4.8a}$$

$$\omega_2 = a_2 \sin\frac{\pi x}{L} \tag{4.8b}$$

where, as shown in Fig. 4.13, ω is the vertical deflection, a is its amplitude, and the subscripts 1 and 2 refer to the girder numbers. At the same time, the girders are permitted to rotate about their respective longitudinal centre lines through angles defined by the equations

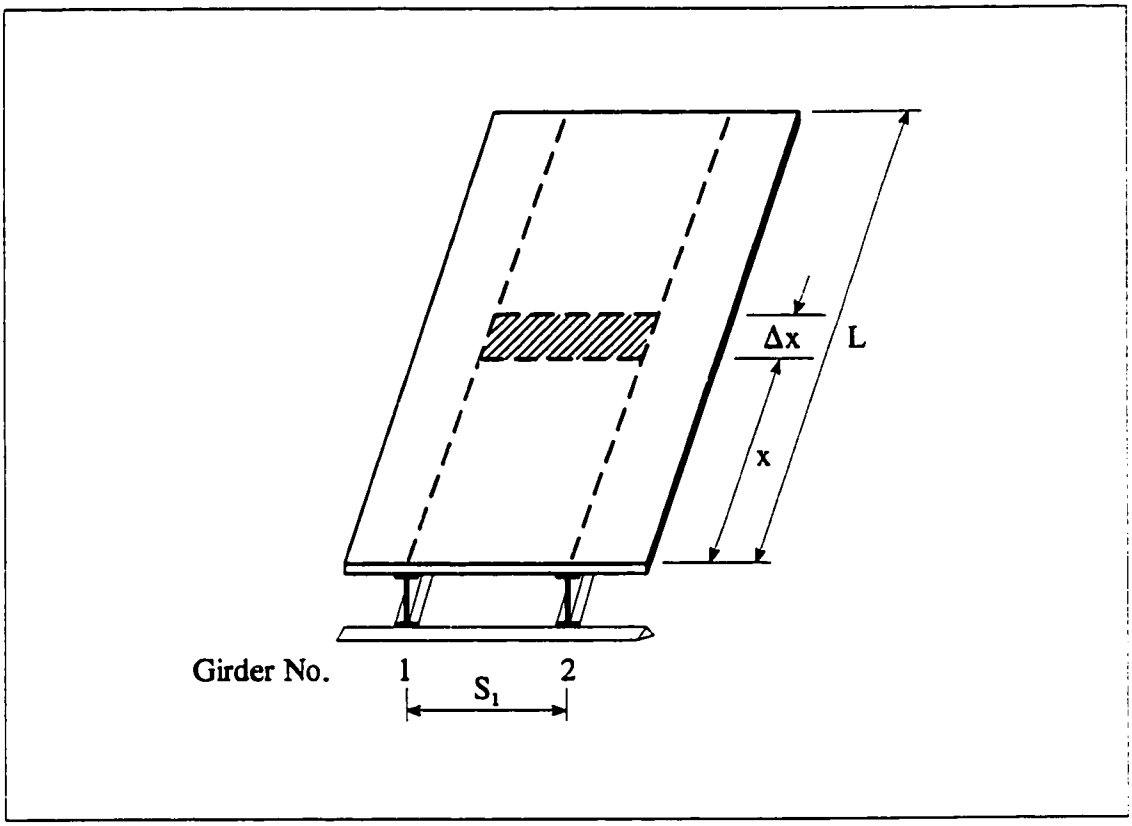

Figure 4.12 Segment of a bridge

$$\delta_1 = \upsilon_1 \sin\frac{\pi x}{L} \tag{4.9a}$$

$$\delta_2 = \upsilon_2 \sin\frac{\pi x}{L} \tag{4.9b}$$

where, as shown in Fig. 4.14, δ is the rotation from the initially vertical position of a girder, υ is its amplitude, and the subscripts refer to the girder numbers.

Figure 4.15 shows the combination of distributed vertical loading and distributed twisting moment that is needed to achieve the deflection $a_m \sin(\pi x/L)$ and the rotation $\upsilon_m \sin(\pi x/L)$ in girder m. The intensity of the vertical line load, p_x, is given by

$$p_x = \frac{(EI)_m \pi^4}{L^4} a_m \sin\frac{\pi x}{L} \tag{4.10}$$

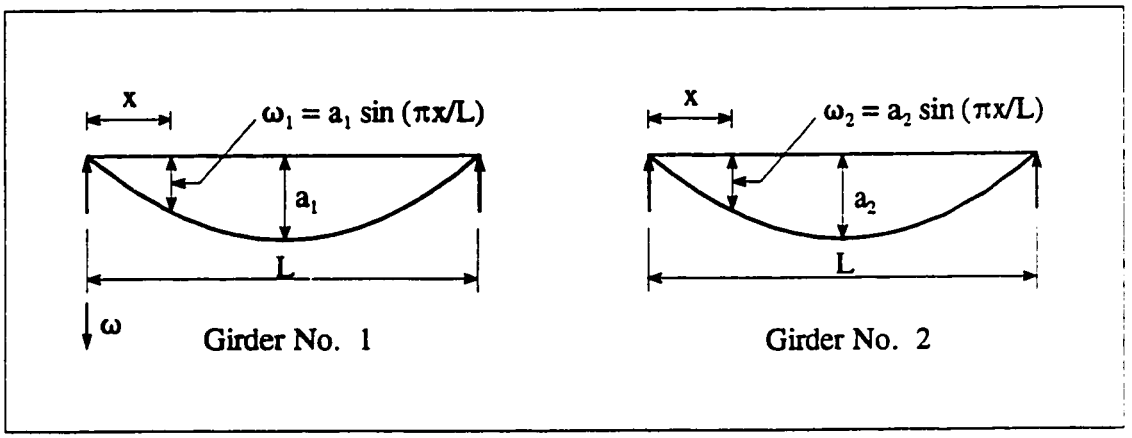

Figure 4.13 Girder deflections

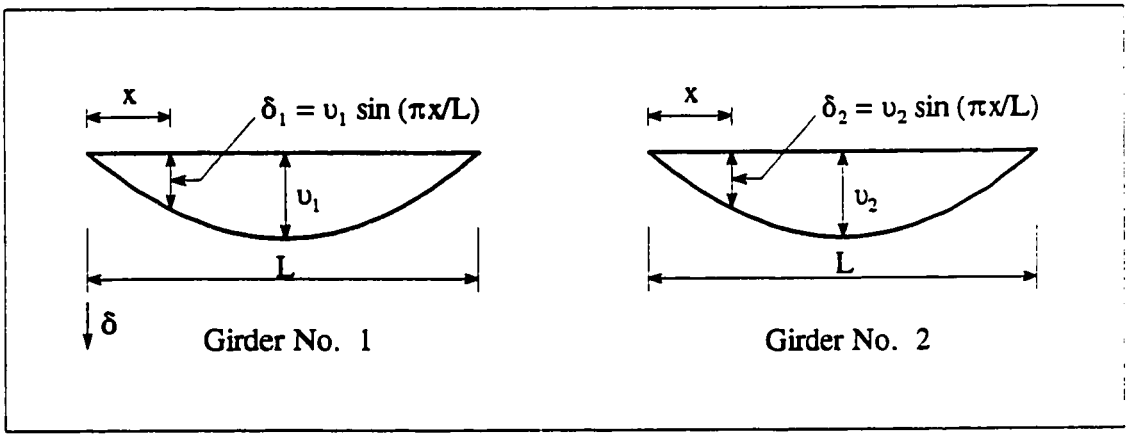

Figure 4.14 Girder rotations

This line load is supported by concentrated reactions at each end equal to $[(EI)_m \pi^3] a_m / L^3$.

The intensity of the twisting moment, t_x, is given by

$$t_x = \frac{(GJ)_m \pi^2}{L^2} \upsilon_m \sin\frac{\pi x}{L} \qquad (4.11)$$

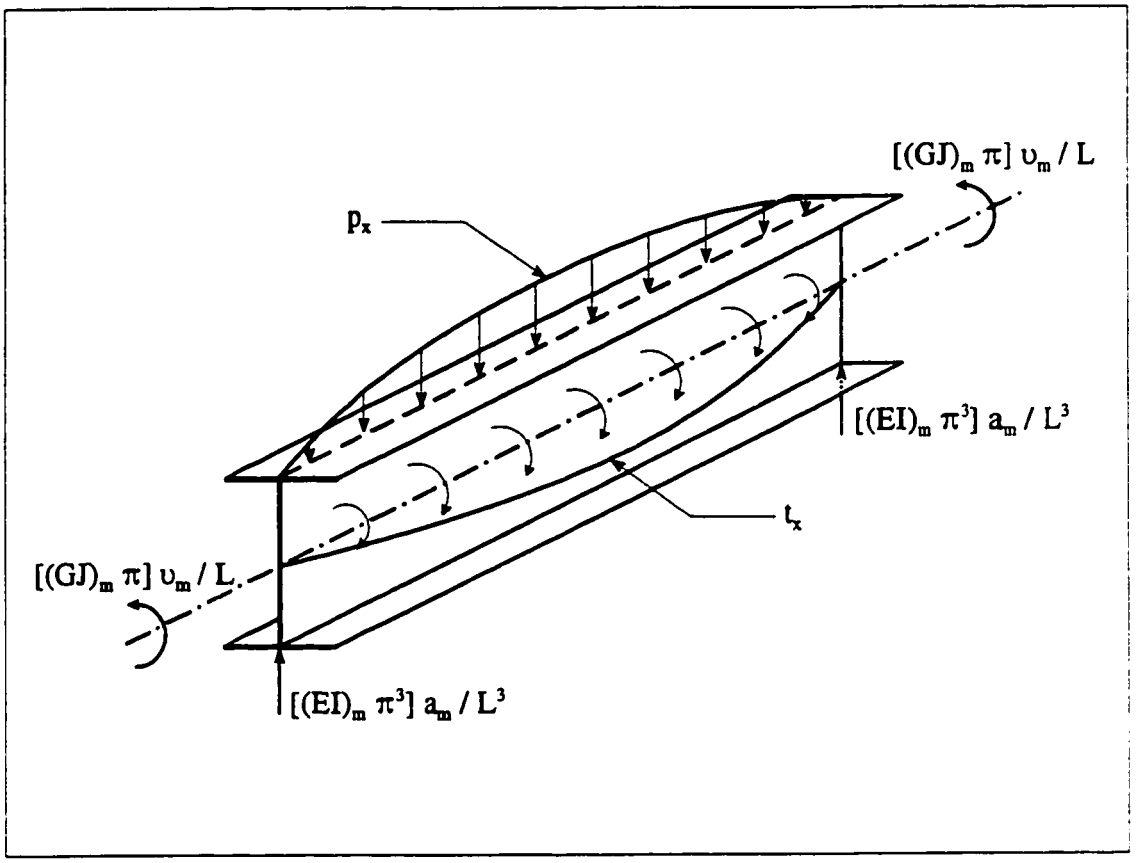

Figure 4.15 Forces on girder m due to first harmonic loading

where GJ is the torsional stiffness of the girder under consideration. This distribution of twisting moment is resisted by concentrated twisting moments $[(GJ)_m \pi]\ \upsilon_m / L$ at each end.

The next step is to consider how these distributions of vertical load and twisting moment come to be applied to the girders from the transverse medium. Figure 4.16 shows the strip of transverse medium of width Δx contained between values x and $(x+\Delta x)$ of the longitudinal coordinate. The slopes of girders 1 and 2 at the ends of this strip are $(\pi/L)\ a_1 \cos(\pi x/L)$ and $(\pi/L)a_2 \cos(\pi x/L)$, respectively. The transverse torsional stiffness of the transverse medium is represented by D_{yx}. Hence, the torsional stiffness of the strip is $D_{yx}\ \Delta x$, and therefore the equal and opposite twisting moments at the ends of the strip are of magnitude $(D_{yx}/S_1)(\pi/L)(a_2-a_1)\cos(\pi x/L)\ \Delta x$. These twisting moments can each be

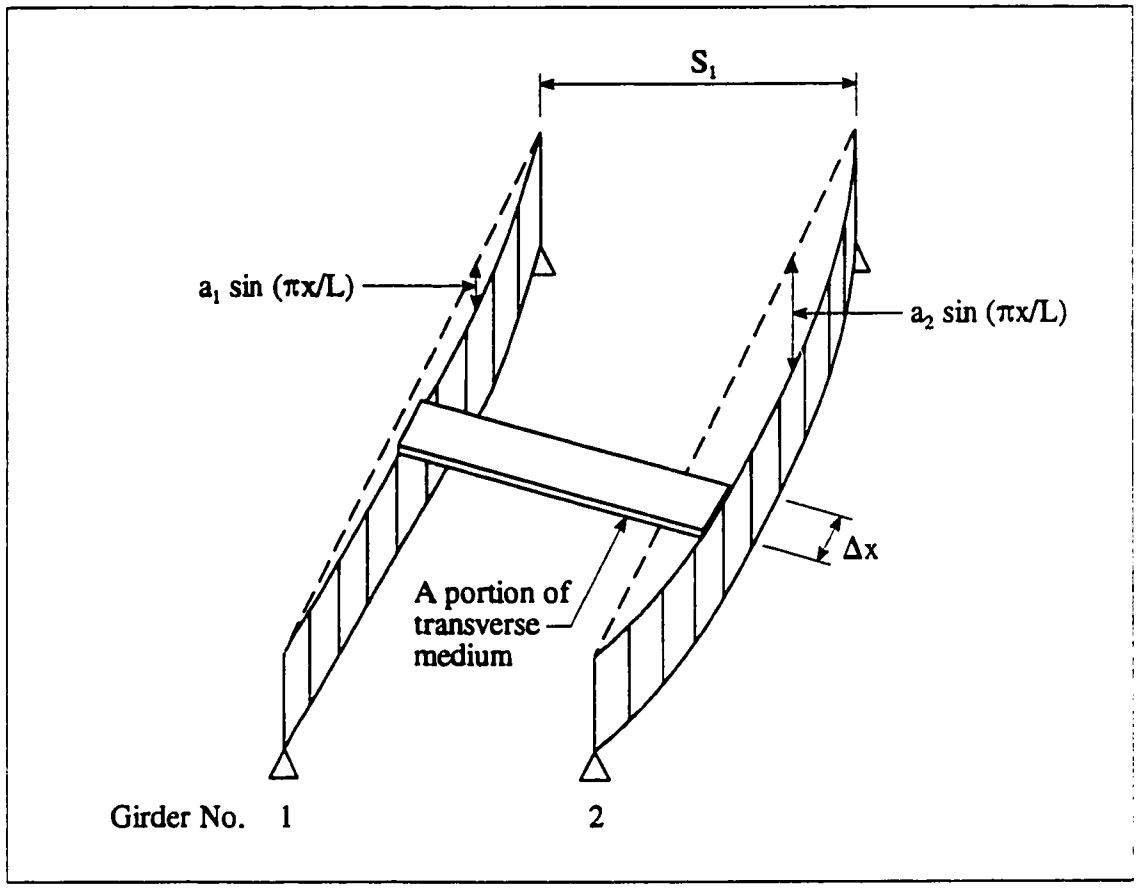

Figure 4.16 Segment of the transverse medium between two adjacent girders

represented as a pair of forces of magnitude $(D_{yx}/S_1)(\pi/L)(a_2-a_1)\cos(\pi x/L)$ parallel to one another, but in opposite senses, and a distance Δx apart as shown in Fig. 4.17. The twisting moments on all the strips of the transverse medium can now be replaced by such pairs of forces, the net result of which are downward loadings R_1 and R_2 on girders 1 and 2, respectively, as given by the following equations:

$$R_1 = \frac{D_{yx}}{S_1}\frac{\pi^2}{L^2}(a_2 - a_1)\sin\frac{\pi x}{L} \tag{4.12a}$$

$$R_2 = \frac{D_{yx}}{S_1}\frac{\pi^2}{L^2}(a_1 - a_2)\sin\frac{\pi x}{L} \tag{4.12b}$$

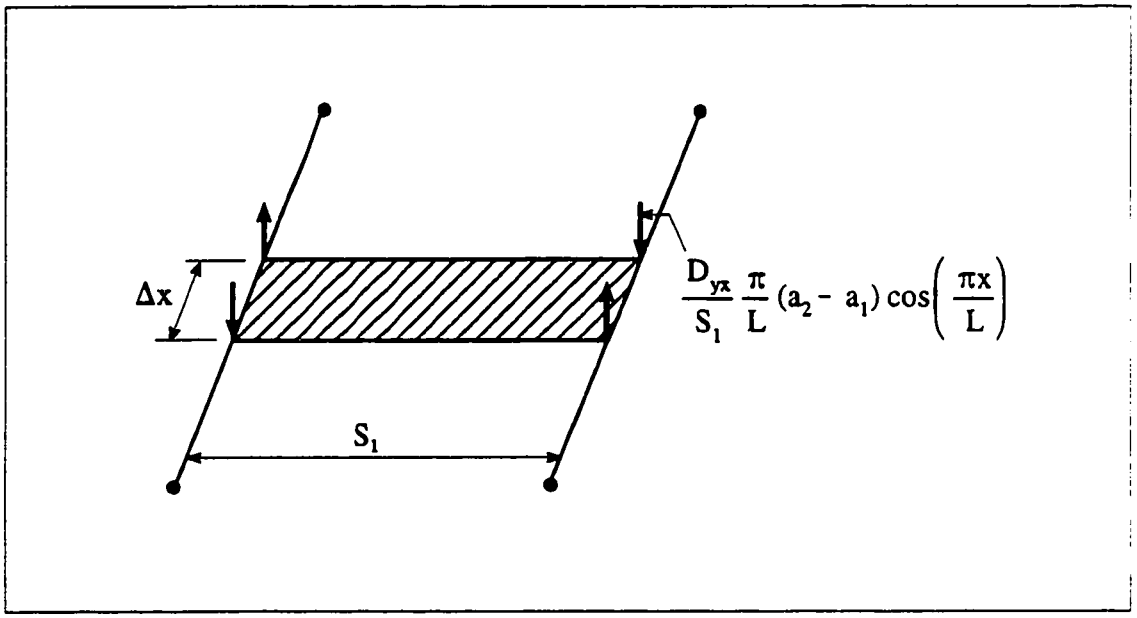

Figure 4.17 Forces on a segment of the transverse medium

If girder 1 is assumed to be an outer girder and girder 2 an inner one, then from Eqs (4.10) and (4.12a), the vertical interactive line force between girder 1 and the transverse medium is

$$P_1 \sin\frac{\pi x}{L} = \frac{(EI)_1 \pi^4}{L^4} a_1 \sin\frac{\pi x}{L} - \frac{D_{yx}}{S_1}\frac{\pi^2}{L^2}(a_2 - a_1)\sin\frac{\pi x}{L} \qquad (4.13a)$$

Therefore, the amplitude P_1 is given by

$$P_1 = \frac{(EI)_1 \pi^4}{L^4} a_1 - \frac{D_{yx}}{S_1}\frac{\pi^2}{L^2}(a_2 - a_1) \qquad (4.13b)$$

Insofar as girder 2 is concerned, there are twisting moments in the transverse medium on either side of it. Using the same procedure as above, the following equation is derived for the amplitude P_r for the interactive force between an inner girder r and the transverse medium:

$$P_r = \frac{(EI)_r \pi^4}{L^4} a_r + \frac{D_{yx}}{S_{r-1}} \frac{\pi^2}{L^2} (a_r - a_{r-1}) - \frac{D_{yx}}{S_r} \frac{\pi^2}{L^2} (a_{r+1} - a_r) \qquad (4.14)$$

The forces and moments applied to the strip of transverse medium between x and (x+Δx) are now considered together with the bending deflections that result. The transverse flexural stiffness of the transverse medium is denoted by D_y. Therefore, the flexural stiffness of the strip is $D_y \Delta x$.

At the position of girder 1, the strip experiences an upward force of magnitude $P_1 \sin(\pi x/L) \Delta x$, where P_1 is given by Eq. (4.13b), and a bending moment (which is positive counterclockwise if rotations are accounted positive clockwise) of magnitude $[(GJ)_1 \pi^2 \upsilon_1] / L^2 \sin(\pi x/L) \Delta x$ in accordance with Eq. (4.11). The deflection and rotation at the position of girder 1 are $a_1 \sin(\pi x/L)$ and $\upsilon_1 \sin(\pi x/L)$, respectively. The other girders give similar results.

For brevity, let

$$m_r = \frac{(GJ)_r \pi^2}{L^2} \qquad (4.15)$$

where the subscript r refers to the girder number. On canceling a common factor of $\sin(\pi x/L)$ between all forces, moments, deflections and rotations, and on canceling a common factor Δx between the applied forces and moments and the flexural stiffness of the strip, the reactive forces on a transverse slice of unit width at the mid-span are found to be as shown in Fig. 4.18. It is noted that this figure is representative of the behaviour per unit length of all strips of the transverse medium, on multiplying throughout by $\sin(\pi x/L)$.

The problem of distributing first harmonic effects in the bridge is thus reduced to solving the problem of the deflection of a beam supported by a system of linear springs. Specifically, with reference to Fig. 4.18, an external load of magnitude P is shared between

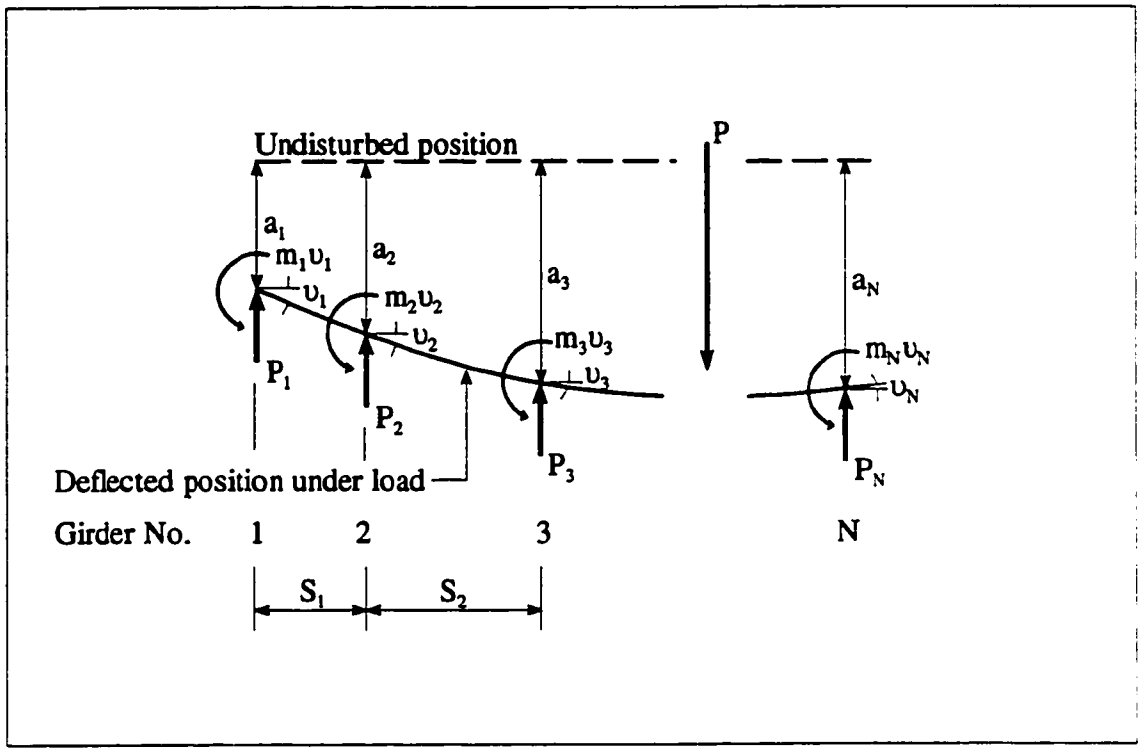

Figure 4.18 Responses at mid-span in a bridge with N girders

the girders as P_1, P_2, ..., P_N. Further, the beam has deflections a_1, a_2, ..., a_N and rotations υ_1, υ_2, ..., υ_N in response to (1) the external force P, (2) support forces P_1, P_2, ..., P_N, which are given by Eqs (4.13b) and (4.14), and (3) restraint moments $m_1\upsilon_1$, $m_2\upsilon_2$, ..., $m_N\upsilon_N$, where m_1, m_2, ..., m_N are given by Eq. (4.15).

As an example, the representation of a transverse strip of a five-girder bridge by a beam supported on a system of springs is shown in Fig. 4.19. The cross section of the bridge is shown in Fig. 4.19a. In Fig. 4.19b, the flexural and torsional stiffnesses of the girders are replaced by springs of stiffnesses k_r and m_r, respectively, with subscripts referring to girder numbers. The analogy is now a unit length of deck slab resting on elastic springs. For girder r, the expression for m_r is given by Eq. (4.15). The expression for k_r is given by

$$k_r = \frac{(EI)_r \pi^4}{L^4} \tag{4.16}$$

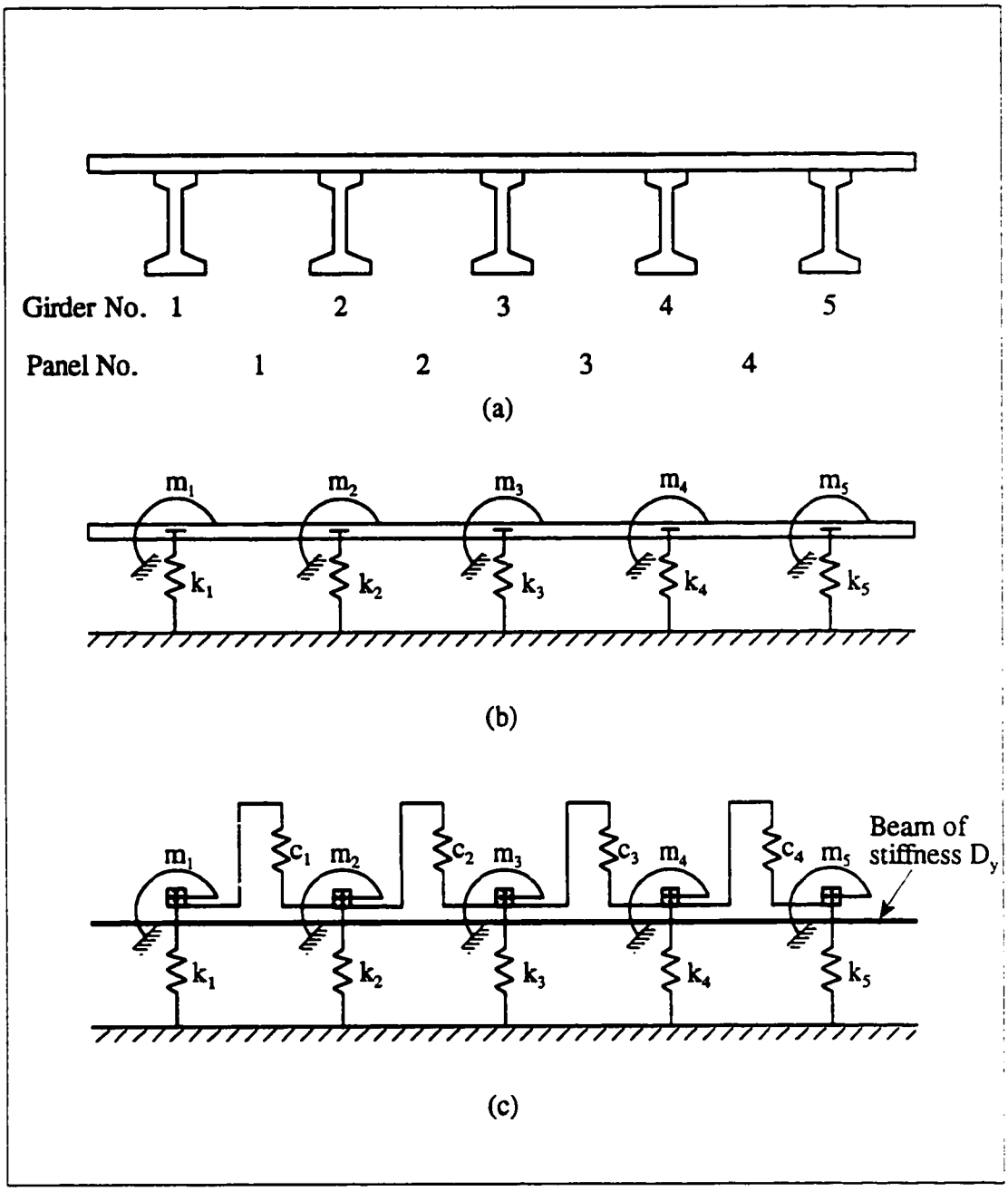

Figure 4.19 Transformation of a bridge into a system of springs
(a) Actual cross section
(b) Deck slab on springs
(c) A system of springs

The transverse torsional stiffness of the transverse medium (deck slab) is represented by springs of stiffness c_r with subscripts referring to the panel number identified in Fig. 4.19a. The expression for this spring stiffness for panel r is

$$c_r = \frac{D_{yx}}{S_r} \frac{\pi^2}{L^2} \tag{4.17}$$

The analogy now consists of a system of springs as shown in Fig. 4.19c. The same logic used for the first harmonic can now be used for higher harmonics.

4.4.4.3 Summary of the Steps in the Solution:

In the case of a bridge with N girders, there are N unknown deflections and N unknown rotations. The necessary 2N equations to solve for the 2N unknowns are developed as follows:

1. The first equation is for vertical equilibrium of the whole system.
2. The second equation is for moment equilibrium of the whole system.
3. The next (N-1) equations are for slope conditions for girders 2 to N, it being noted that the slope condition for girder 1 is used up in the form of a constant of integration.
4. The remaining (N-1) equations are for deflection conditions at girders 2 to N, it being similarly noted that the deflection condition for girder 1 is used up in the form of a constant of integration.

Derivation of these equations is given in Refs [147,149] and is not presented here. For the purposes of this discussion, it suffices to give the final form of the set of equations in matrix notation

$$[A]\{\rho\} = \{R\} \tag{4.18}$$

The vector $\{\rho\}$ contains the distribution coefficients for a bridge. The matrix [A] and vector $\{R\}$ define the geometry of a bridge and the loading, respectively.

4.4.5 The Case of Continuous Bridges

The semicontinuum method can also be used to analyze the general category of slab-on-girder bridges with simply supported ends and arbitrarily placed discrete intermediate supports, of which a continuous bridge is a particular case, as shown in Fig. 4.20. The force method can be used to determine the statically indeterminate reactions of the intermediate supports and thereby reduce the statically indeterminate problem into a determinate one. The following steps are required for the force method:

1. Remove all intermediate supports and, by treating the bridge as simply supported at its two ends, find deflections at the intermediate support locations due to the applied load, using the semicontinuum method of Sec. 4.4.4.
2. Again treating the bridge as simply supported at the two ends, find the (usually upward) forces at each of the intermediate support locations which would bring the bridge at these locations back to their respective original positions.
3. The bridge with intermediate supports can now be analyzed by the semicontinuum method of Sec. 4.4.4 as a simply supported bridge which is subjected to downward-applied loads and the (usually upward) reactions of the intermediate supports calculated above.

4.4.6 Evaluation of Saint-Venant Torsional Constant, J

Approximate methods are available to calculate the Saint-Venant torsional constant, J, of a precast concrete girder. According to such methods, the girder is divided into a number of rectangles. The torsional constant of the girder is then obtained by simply adding the torsional constants of the individual idealized rectangles [154]. These methods usually involve the use of charts. Besides the lack of accuracy that results, reading values out of charts poses a problem if one needs these values to be input into a computer program.

Refined methods of analysis require a more rational approach in determining J. One

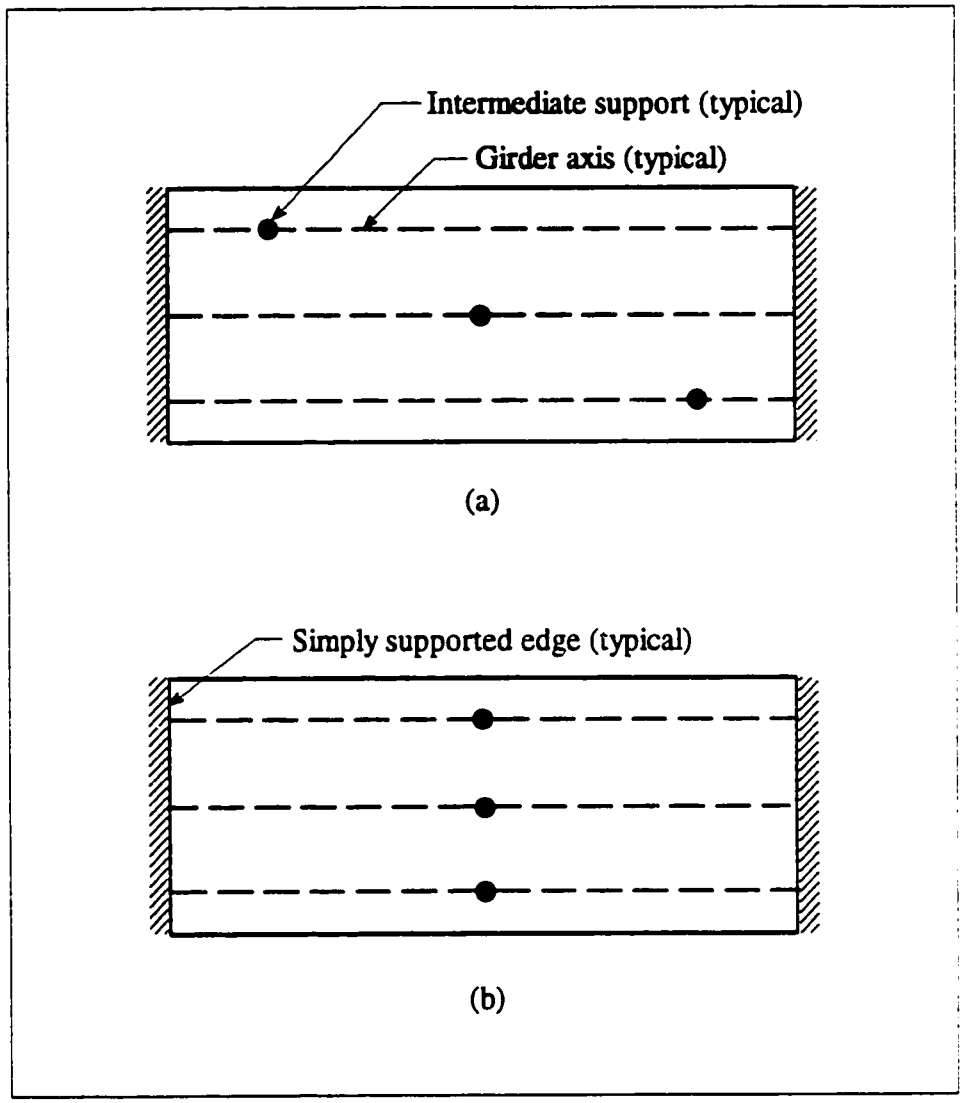

Figure 4.20 Plans of slab-on-girder bridges with intermediate supports
(a) General case with randomly spaced intermediate supports
(b) Particular case of a continuous-span bridge

such approach was presented by Eby *et al.* [155] in a comprehensive study of the various methods for evaluating J in the general case of precast concrete I-girders. Results obtained by a finite difference analysis were considered as an "exact" solution, and were compared to the results obtained using several approximate methods. An algebraic solution to the problem was then developed by modifying the method that showed the best correlation with the "exact" method. With reference to Fig. 4.21, the torsional constant of an I-girder can be obtained as follows:

$$J = 0.333 (b_1 t_1^3 + b_2 t_2^3 + d_3 b_3^3) + \alpha_1 D_1^4 + \alpha_2 D_2^4 - 0.21 (t_1^4 + t_2^4) \qquad (4.19)$$

where

$$t_1 = d_1 + \frac{d_2 (b_1 + b_3)}{2 b_1} \qquad (4.20a)$$

$$t_2 = d_5 + \frac{d_4 (b_3 + b_2)}{2 b_2} \qquad (4.20b)$$

$$\alpha_1 = - 0.042 + 0.2204 \frac{b_3}{t_1} - 0.0725 \left(\frac{b_3}{t_1} \right)^2 \qquad (4.21a)$$

$$\alpha_2 = - 0.042 + 0.2204 \frac{b_3}{t_2} - 0.0725 \left(\frac{b_3}{t_2} \right)^2 \qquad (4.21b)$$

$$D_1 = t_1 + \frac{b_3^2}{4 t_1} \qquad (4.22a)$$

$$D_2 = t_2 + \frac{b_3^2}{4 t_2} \qquad (4.22b)$$

For other precast I-girders that do not conform in shape to the girder shown in Fig. 4.21, such as CPCI 1600, 1900 and 2300 sections [156], their dimensions should be idealized to fit the basic I-shape shown in the figure. The results obtained for these sections should be considered as somewhat more approximate than those for the basic I-sections. Eby *et al.* [155] reported that the torsional constants computed using Eq. (4.19) were within ± 5% of their respective finite difference values.

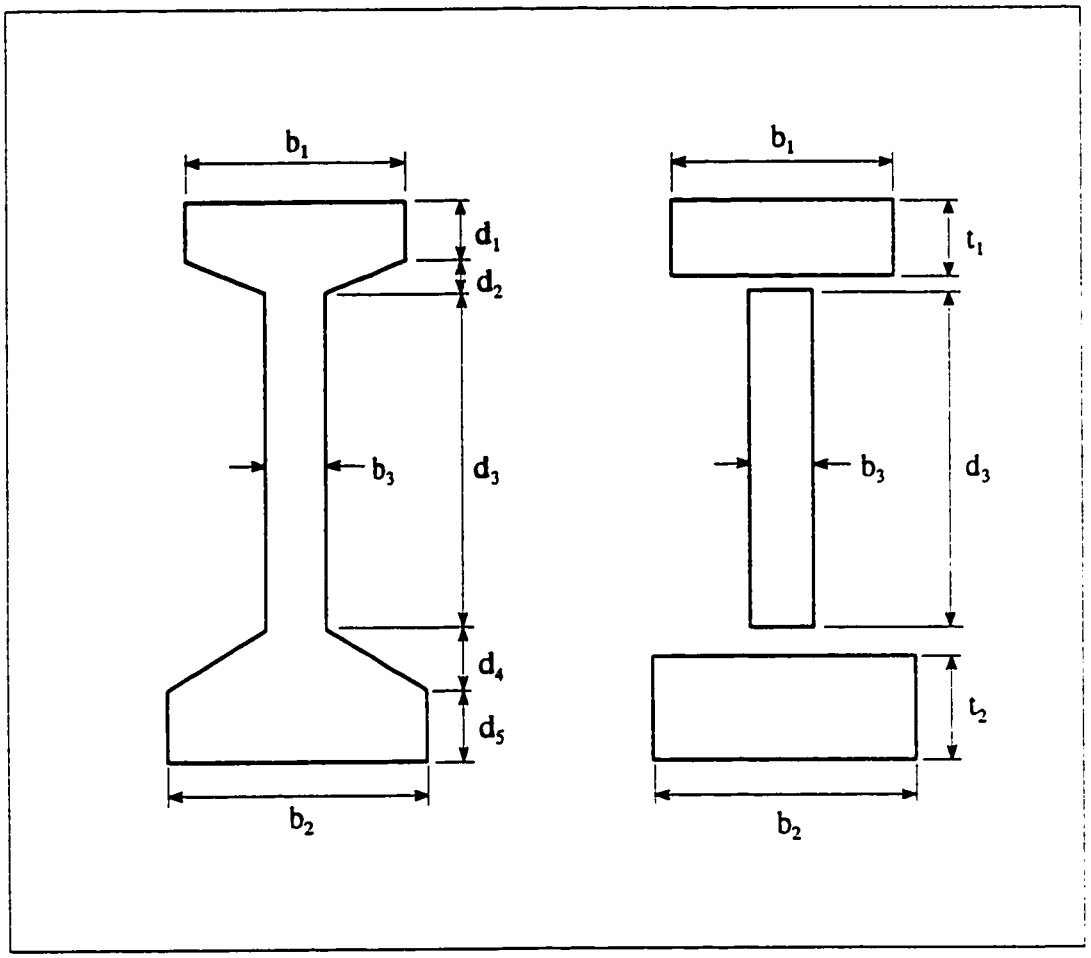

Figure 4.21 General I-girder section and discretization

4.5 CREEP AND SHRINKAGE EFFECTS IN CONTINUOUS BRIDGES

4.5.1 Creep Moments due to Prestressing and Dead Loads

One of the unique features of the design of slab-on-girder bridges is that positive moments develop over piers due to creep in the prestressed girders as well as due to the effect of live loads in remote spans. Positive moments due to creep under sustained loads, i.e. prestressing and dead loads, are partially counteracted by the negative moments resulting from differential shrinkage between the cast-in-place deck slab and the precast girders. The assessment of these positive moments is usually not readily possible because of uncertainties in creep analysis models and the many factors on which it depends (e.g. state of stress, relative humidity, temperature, volume to surface area ratio, concrete mix design, time). This has led to some suggestions for neglecting the structural effects of creep (and shrinkage) in this type of bridges, and just providing a nominal minimum amount of positive reinforcement between the girders if for no other reason than increasing the structural integrity [139,157]. These suggestions were also based on the observed good performance of structures for which the design utilized full continuity for superimposed dead loads and live loads, but neglected the structural consequences of time-dependent effects.

Several methods of creep analysis are proposed in the literature; they differ only in the assumed creep function, $\Phi(t,t_0)$, which describes the total strain (instantaneous elastic plus creep) at observation time (measured from casting of concrete, i.e. age t) caused by a unit sustained stress applied at age t_0. Among the methods proposed in the literature [158] are the effective modulus method, the rate of creep method, the rate of flow method, the improved Dischinger method and the Trost-Bažant method (the age-adjusted effective modulus method). All these methods are based on the assumption that creep varies linearly with stress, and they all obey the principle of superposition of strains (i.e. the total strain at time t, $\varepsilon_c(t)$, of a concrete subjected to varying stress is obtained by summing the strains caused by each stress increment (or decrement), $\Delta\sigma_c(t_0)$, applied at age t_0). The Trost-Bažant method, which was originated by Trost during the late sixties and later refined by

Bažant in the early seventies, is the most practical and widespread method for directly computing the strain under a varying stress. It has been adopted by the ACI Committee 209 [159] since 1982 to predict creep effects in structural concrete. Recently, Bažant *et al.* [160], and Gardner *et al.* [161] have proposed two different methods as possible alternatives to the current ACI method. However, their adoption by the ACI Committee 209 is still under consideration.

According to the Trost-Bažant method, the strain which occurs during a period t_0 to t due to a stress which varies in magnitude during the same period is given by

$$\varepsilon_c(t) = \sigma_c(t_0)\,\frac{1 + \varphi(t,t_0)}{E_c(t_0)} + \frac{\Delta\sigma_c(t)}{\overline{E}_c(t,t_0)} \tag{4.23}$$

where $\sigma_c(t_0)$ is a stress introduced at age t_0 and sustained during the period t_0 to t, $\varphi(t,t_0)$ is the creep coefficient, i.e. the ratio of creep to the instantaneous elastic strain, $E_c(t_0)$ is the elastic modulus of concrete at age t_0, $\Delta\sigma_c(t)$ is the final value at age t of a stress increment increasing gradually from magnitude zero at t_0, and $\overline{E}_c(t,t_0)$ is the age-adjusted effective modulus of concrete and is given by

$$\overline{E}_c(t,t_0) = \frac{E_c(t_0)}{1 + \chi(t,t_0)\,\varphi(t,t_0)} \tag{4.24}$$

where $\chi(t,t_0) = \chi$ is the aging coefficient, which generally varies in value between 0.6 and 0.9. This coefficient reduces the creep function to compensate for treating the stress increment as if it were introduced with its full magnitude at age t_0 and sustained to age t.

For illustration, reference is made to Fig. 4.22 which shows a continuous girder with n spans, initially assumed simply supported from age t_0 (see Fig. 4.22a), and subsequently made continuous at age t_1 (see Fig. 4.22b). Using the Trost-Bažant method, the moment $M_n(t)$ induced by creep at support n is given by

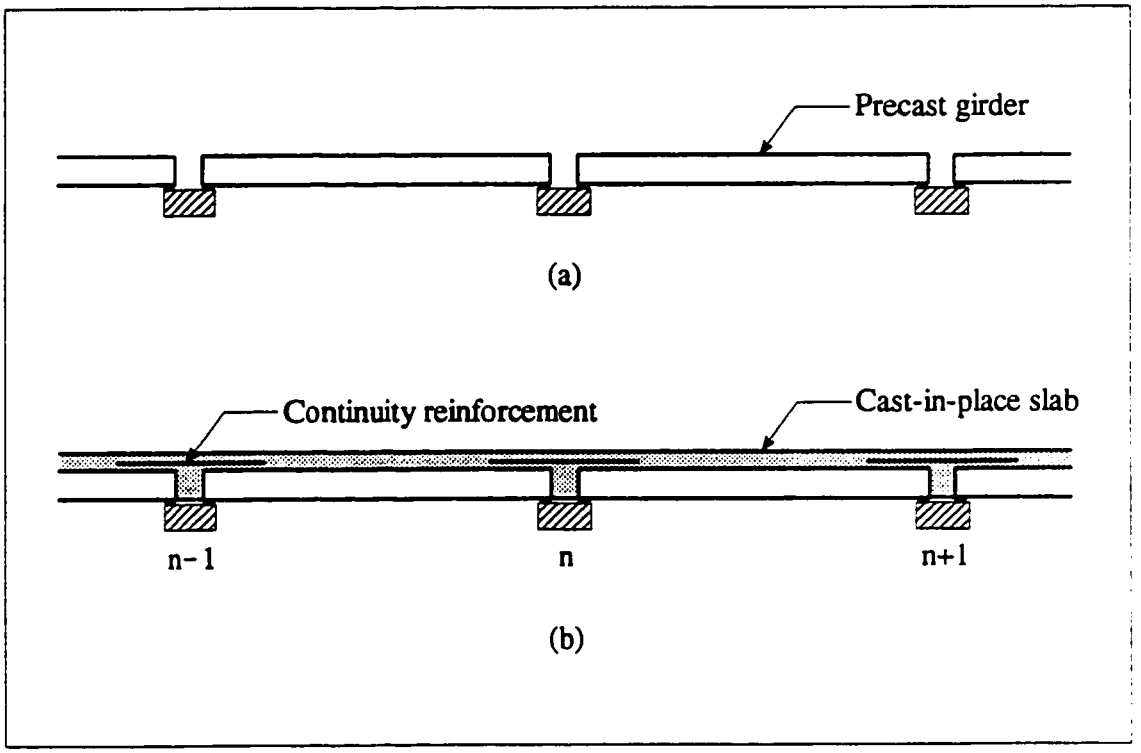

Figure 4.22 Continuous precast girder with n spans

$$M_n(t) = M_n \frac{\varphi(t,t_0) - \varphi(t_1,t_0)}{1 + \chi\, \varphi(t,t_1)} \tag{4.25}$$

where M_n is the elastic restraint moment at support n if the girder were continuous and monolithically cast in a single stage, and can be determined using any elastic analysis method such as the simple three-moment equation.

Assuming $t_1 = 28$ days and $t = \infty$, the following values can be obtained from the ACI Committee 209 report [159]: $\varphi(t,t_0) = 0.96\ \varphi_u$, $\varphi(t_1,t_0) = 0.42\ \varphi_u$ and therefore $\varphi(t,t_1) = 0.54\ \varphi_u$, where φ_u is the ultimate creep coefficient. In the absence of specific creep data for local aggregates and conditions, an average value of $2.35\ \gamma_c$ is suggested for φ_u, with γ_c being a correction factor that is the product of several multipliers depending upon the relative humidity, volume to surface area ratio, temperature, concrete mix design and age of loading. The aforementioned report [159] states that the normal range for φ_u is between 1.30 and 4.15.

Conservatively, φ_u may be taken as 4.50 [102]. Assuming $\chi = 0.8$ and substituting in Eq. (4.25), one obtains the final moment due to creep at support n as

$$M_n(t=\infty) \approx 0.80\, M_n \tag{4.26}$$

4.5.2 Shrinkage Moments

Shrinkage of the cast-in-place deck slab with respect to the precast girders induces negative restraint moments, M_{sh}, over the piers. The differential shrinkage moment is given by [162]

$$M_{sh} = \varepsilon_{sh}\, E_s\, A_s\, y_s \tag{4.27}$$

where ε_{sh} is the differential shrinkage strain = 100×10^{-6} [163], E_s is the elastic modulus of the slab concrete, A_s is the cross-sectional area of the slab, and y_s is the distance between the centroid of the slab to the centroid of the composite section. The restraint moments induced by shrinkage can also be determined using the three-moment equation. However, the presence of creep reduces shrinkage restraint moments. In the absence of accurate experimental data, the OHBDC [163] recommends the use of a 60% creep reduction factor. Therefore, the final moment, M_{csn}, at support n due to the combined effect of creep and shrinkage is

$$M_{csn} = 0.80\,(M_{pn} - M_{dn}) - 0.40\, M_{shn} \tag{4.28}$$

where M_{pn}, M_{dn}, M_{shn} are the restraint moments at support n due to prestressing, dead load and shrinkage, respectively. General formulas for these moments are derived in Ref. [162], and are given here for completeness.

$$M_{pn} = a\, \theta_p \frac{EI}{L} \tag{4.29a}$$

$$M_{dn} = b\, w_d\, L^2 \tag{4.29b}$$

$$M_{shn} = c\, M_{sh} \tag{4.29c}$$

where

$$\theta_p = \frac{P_e L (2e_c - e_e)}{6 EI} \tag{4.29d}$$

The coefficients a, b and c are given in Table 4.1 for two, three and four-span continuous girders. In Eqs (4.29a - d), I and L are first moment of inertia of the girder and its span length, respectively, E is the elastic modulus of the girder concrete, w_d is the dead load, P_e is the effective prestressing force, e_c and e_e are the tendon eccentricities with respect to the centre of gravity of the composite section at mid-span and support, respectively.

Table 4.1 Restraint moment coefficients in continuous girders

Section	2 - span girder			3 - span girder			4 - span girder		
	a	b	c	a	b	c	a	b	c
First support	3.0	0.125	1.5	2.4	0.1	1.2	2.57	0.107	1.286
Second support	—	—	—	2.4	0.1	1.2	1.72	0.071	0.857
Third support	—	—	—	—	—	—	2.57	0.107	1.286

4.6 ARCHING EFFECT IN BRIDGE DECK SLABS

4.6.1 Internal Arching Action

Until 1979, highway bridges in North America were designed according to the AASHTO specifications which required the deck slabs of slab-on-girder bridges to be designed for pure bending. Extensive laboratory and field testing of bridges in Canada [164,165] and the United States [166] has conclusively shown that these slabs were greatly over-designed, i.e. their load capacities were substantially greater than necessary for safety.

This very significant enhancement of the deck slab carrying capacity is reportedly caused by a major change in the way these slabs were believed to carry loads. It was found that the primary structural action by which deck slabs resist concentrated wheel loads is not flexure, as traditionally believed, but a complex internal membrane stress state referred to as internal arching. This action is caused by the cracking of the concrete in the positive moment region of the deck slab and the accompanying upward shift of the neutral axis in that portion of the slab. The action is sustained by in-plane compressive membrane forces which develop as a result of the lateral confinement provided by the surrounding concrete slab, diaphragms and supporting components acting compositely with the slab. Figure 4.23 illustrates this phenomenon.

The arching creates what can best be described as an internal compressive dome, the failure of which usually occurs as a result of over-straining around the perimeter of the wheel footprint. The resulting failure mode is that of punching shear (see Fig. 4.24), although the inclination of the fracture surface is much less than 45° due to the presence of large in-plane compressive forces associated with arching. The arching action, however, cannot resist the full wheel load. There remains a small flexural component for which a minimum amount of reinforcement is required. This reinforcement has two purposes: it provides for both local flexural resistance and global confinement required to develop arching effects.

4.6.2 Empirical Design Method for Deck Slabs

The findings of the above research were first incorporated as a formal design method for deck slabs in the OHBDC, first published in 1979. The method was later refined. The current edition of the OHBDC [94] permits deck slabs of slab-on-girder bridges which conform to certain conditions to be designed according to an empirical design method that takes account of internal arching in slabs. When this method is used, it is no longer necessary to calculate and design for the transverse moments.

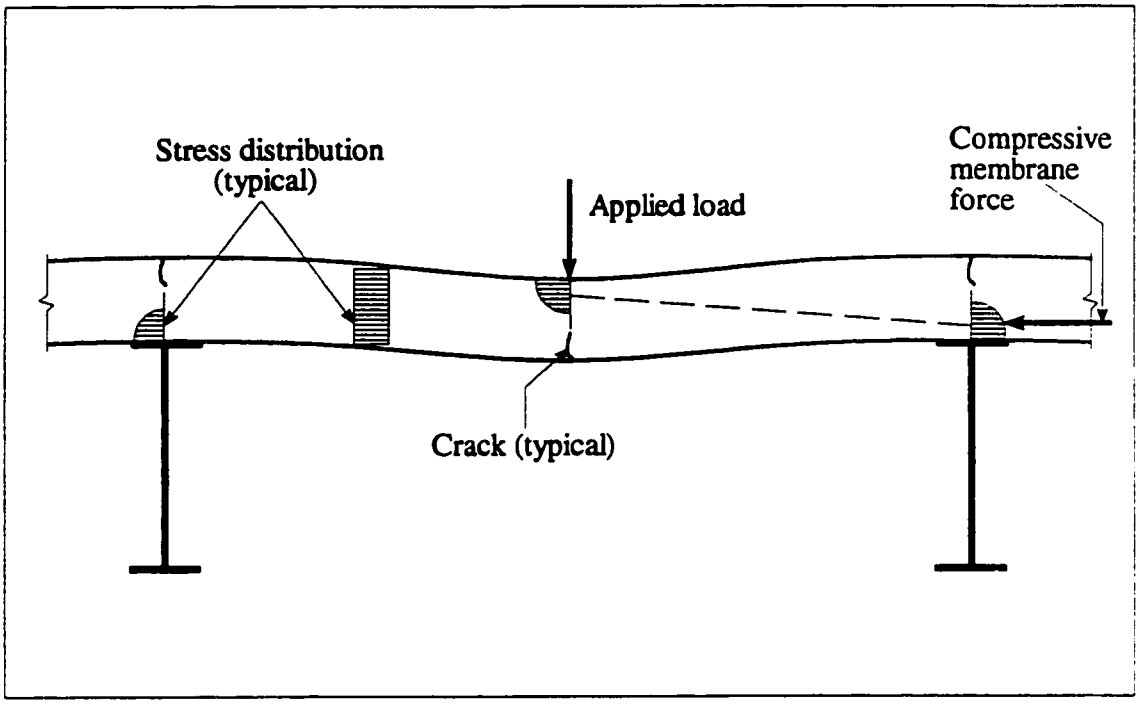

Figure 4.23 Compressive membrane action

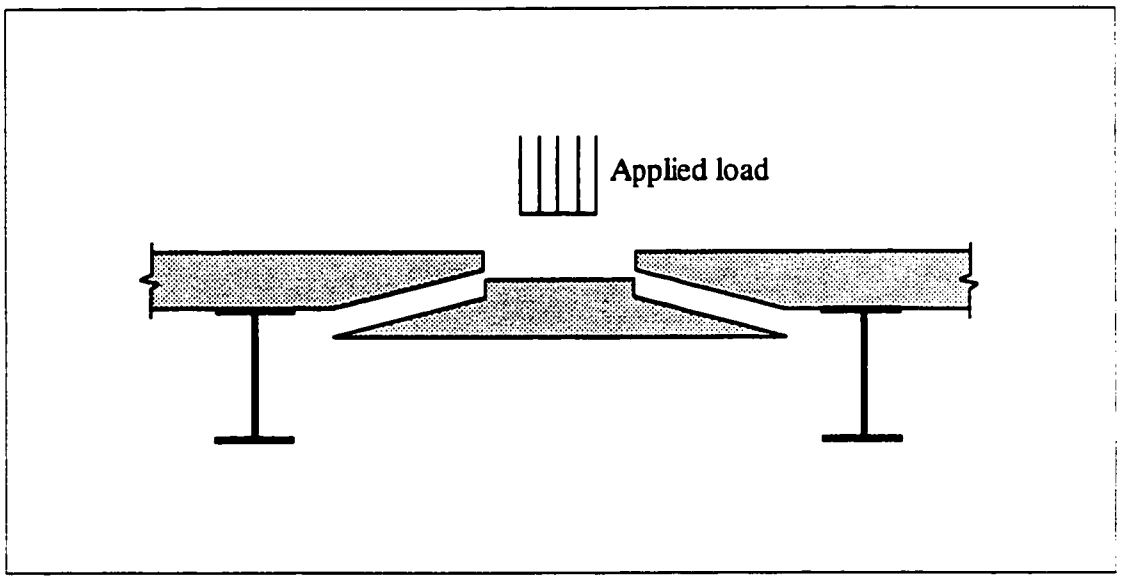

Figure 4.24 Punching shear failure mode

According to the empirical design method, the slab thickness should not be less than 225 mm, and the reinforcement should comprise two orthogonal meshes with a minimum reinforcement ratio, in each direction of each mesh, of 0.3% of the gross concrete cross-sectional area as shown in Fig. 4.25. The minimum thickness of 225 mm relates to extra cover to the reinforcement for protection against corrosion of the steel bars caused by the use of deicing salts during winter maintenance operations. Corrosion of embedded reinforcement is a primary cause of rapid and premature deterioration of highway bridges. The use of increased concrete cover is one effective means of guarding against corrosion of the steel bars. Figure 4.26, which is adopted from Ref. [167], illustrates the bases for specifying a minimum deck thickness of 225 mm.

According to the current OHBDC [94], the empirical design method is applicable only when the following conditions are satisfied:

1. There are at least three girders in the system.
2. The bridge has diaphragms at least at all supports. These must extend to the exterior girders.
3. The centre-to-centre spacing of girders does not exceed 3.7 m.
4. The slab extends at least 1.0 m beyond the centre line of the exterior girders, or has a curb of equivalent area of cross section.
5. The ratio of centre-to-centre spacing of girders to thickness of the slab does not exceed 15.0.
6. Spacing of the reinforcing bars in each face does not exceed 300 mm.

The method has been adopted by the new CHBDC. Moreover, it has been recently incorporated with some refinements in the AASHTO LRFD Bridge Design Specifications [151]. Recent tests have resulted in the elimination of condition 1 above from both the CHBDC and the AASHTO specifications as it was found that an adequate degree of arching action can develop even with only two girders in the system [168]. Based on recent experiments, the centre-to-centre spacing of girders in the AASHTO specifications has been

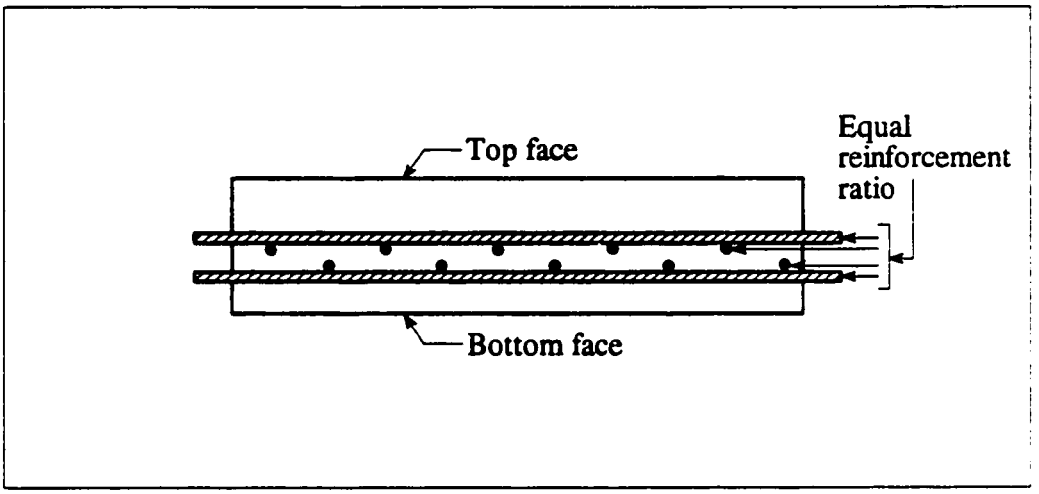

Figure 4.25 Deck slab reinforcement requirements (transverse section)

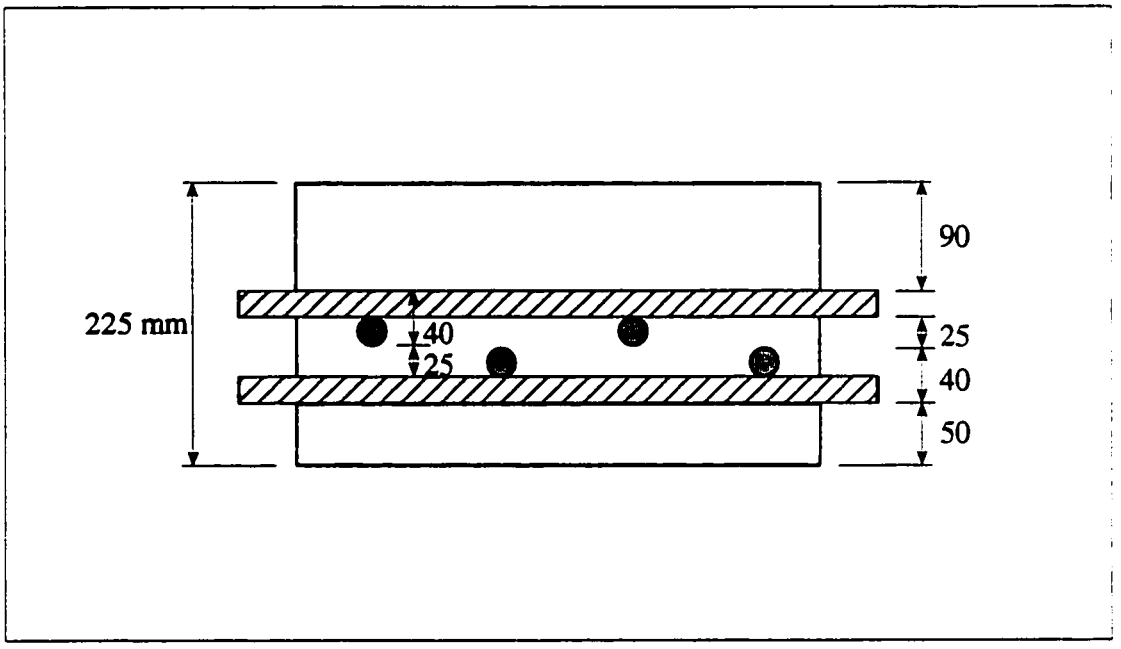

Figure 4.26 Tolerances for location of reinforcing steel bars in deck slabs

increased to a maximum of 4.1 m plus the width of the girder web. Also, the ratio in condition 5 above has been increased from 15.0 to 18.0. In addition, the overhang in condition 4 is taken to be at least 5.0 times the slab thickness, with this condition being satisfied if the overhang is at least 3.0 times the slab thickness and a curb is made composite with the overhang. It is worth mentioning that the minimum slab thickness in the AASHTO specifications is 175 mm.

Several studies have confirmed that the amount of steel reinforcement in deck slabs can be considerably reduced by taking into account the internal arching action. It is estimated that about $1 million worth of steel has been saved in Ontario each year for the past fifteen years or so by using the empirical method to design deck slabs [169]. This initial saving in material cost does not include the substantial long-term savings resulting from the increased durability of the deck slabs as a consequence of their reduced steel reinforcement. In addition, the empirical design method results in a simpler and cleaner reinforcement arrangement leading consequently to savings in time as well.

CHAPTER 5

FORMULATION OF THE OPTIMAL DESIGN PROBLEM

5.1 INTRODUCTION

In the previous chapter, it was explained that the analysis problem in structural engineering is concerned with determining the distribution of load effects in the various components of a structure. Final design of the structural components is based on such effects. Determining load effects implies calculation of these components' responses under some specified inputs. These inputs must include, in addition to the magnitude of the load, sizes of the various structural components and their configurations, i.e. the design of the structure must be known at the outset. Yet the determination of these sizes and configurations to meet performance requirements under the applied loads is the precise purpose of the design problem. The design of a structure, therefore, must be conducted in a trial-and-error manner. A preliminary design is estimated and then analysed. If it performs adequately, it is considered to be a feasible design. But if this trial design does not perform satisfactorily, then the designer, with the results of the analysis at hand, needs to change it and repeat the analysis until a feasible design is obtained. It follows, therefore, that design is an iterative process.

There usually exists an infinite number of feasible designs, and designers strive to find the best (optimal) one. In structural engineering, "best" generally implies cost effective and durable structures. Traditionally, the process of design has relied solely on the designer's experience, intuition and ingenuity. Although this process has worked well as evidenced by the existence of many fine structures, it has led to a less than rigorous approach to design. In addition, it has been quite labourious and time consuming, and has often led to conservative designs that were not the optimum. Scarcity of resources and the need for efficiency in

today's competitive world force the designer to evince much greater interest in computational design optimization techniques. These have matured over the past four decades [100], and can be of substantial aid to the designer not only in the creative process of finding the optimal design, but also in significantly reducing the amount of effort and time required to do so.

Design optimization techniques are based on computer-oriented mathematical programming algorithms that can transform the conventional design process discussed above into a more formal and systematic procedure. The designer must clearly and precisely identify a set of *design variables* that describe the design of the structure, an *objective function* that measures the relative merit of alternate feasible designs, and all *design constraints* on performance that the final design must satisfy [106,107]. The objective function and all of the constraints must be functions of the design variables. Once these have been identified, it is said that the optimal design problem has been formulated. The next step involves transcribing the above formulation of the specific problem into a well-defined standard mathematical model. This standard model is quite general, and can describe design optimization problems from different fields of engineering. General-purpose design optimization software packages utilize this model to solve the optimal design problem. The optimization process consists of cycling between two distinct phases defined as analysis and optimal design in an iterative fashion until the optimum is reached. The computer is most suitable to carry out the substantial amount of repetitive calculations involved, allowing the designer to concentrate more on the creative side of the design process.

In spite of the significant aid that computational design optimization techniques can provide to the designer, there has always been an obvious gap between the progress of the optimization theory and its application to the practice of structural engineering. It has been suggested that a major reason for this gap is the undisturbed priority of mathematical over structural aspects of optimization. Often the latter are confined to rather trivial examples intended to illustrate the successful application of a particular algorithm. This academic optimization trend is referred to as an "algorithm-seeks-problem" approach, as opposed to

the engineering need of a "problem-seeks-algorithm" approach [101]. This study is intended, in part, to fill a portion of the gap between the theory and practice of structural optimization.

This chapter describes the formulation of the optimal design problem of slab-on-girder bridges. First, the design variables, objective function and design constraints are identified and defined. Next, the standard design optimization mathematical model is described. Finally, a design optimization software package is introduced to solve the optimal design problem.

5.2 DESIGN VARIABLES

5.2.1 General

The design of a structure can be described by a set of quantities, some of which are viewed as variables during the optimization process and are called *design variables*. Other quantities defining the design that are not varied by the optimization algorithm are called *preassigned parameters*. The design variables, together with the preassigned parameters, will completely describe the design of a structure [106]. An important first step in the proper formulation of any optimal design problem is identification of the design variables. If proper variables are not selected, the formulation will be either incorrect or not possible at all. At the initial stage of problem formulation, it is sometimes desirable to designate more design variables than may be apparent from the statement of the problem. This gives an added flexibility in the formulation. Later, it is possible to assign a fixed value to any variable, i.e. transform it into a preassigned parameter, and thus eliminate it from the problem formulation. Another important point is that design variables should be independent of each other as far as possible. It is sometimes possible to have dependent design variables; however, the formulation will be unnecessarily complicated because of the additional constraints that have to be imposed in order to describe the relationships among dependent variables. One solution in such situations is to substitute for some of those variables in terms of the others, and thereby eliminating them from the problem and reducing the number of design variables as well as constraints [107].

5.2.2 Design Variables for Slab-on-Girder Bridges

A typical cross section of a slab-on-girder bridge is illustrated in Fig. 5.1. For standard precast I-girders, cross-sectional dimensions are known and become preassigned parameters instead of design variables. Five CPCI girders [156] are used for this study. These are commonly utilized in Canada for highway bridges with span lengths of up to about 50 m. The girders investigated are shown in Fig. 5.2, and their section properties are summarized in Table 5.1.

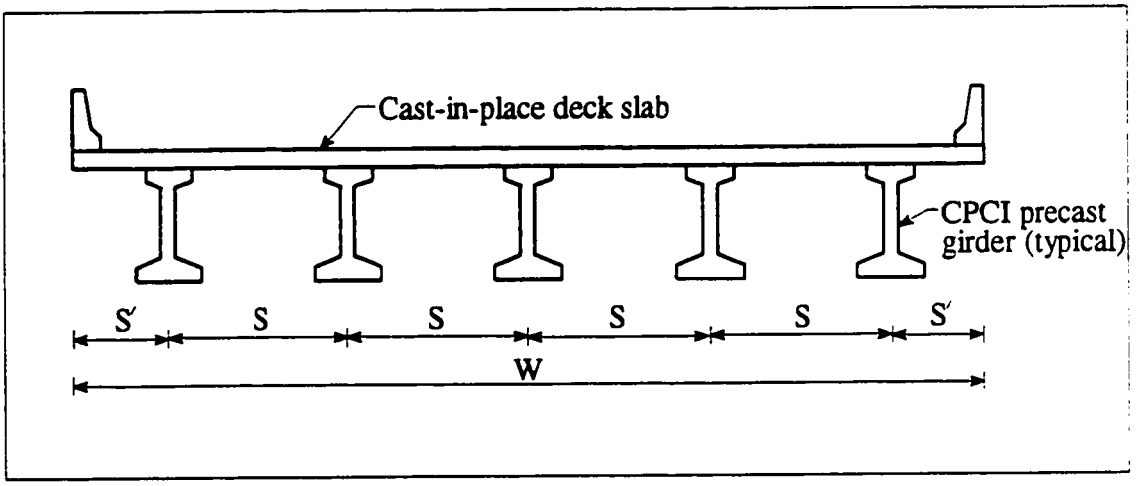

Figure 5.1 A typical cross section of a slab-on-girder bridge

Table 5.1 Section properties of the CPCI girder types investigated

Girder type	Area, A ($mm^2 \times 10^3$)	y_b (mm)	Moment of inertia, I ($mm^4 \times 10^6$)	Top section modulus, S_t ($mm^3 \times 10^3$)	Bot. section modulus, S_b ($mm^3 \times 10^3$)	Torsional constant, J ($mm^4 \times 10^4$)
1200	320	527	53 868	80 004	102 279	412 560
1400	414	636	102 583	134 191	161 409	595 829
1600	499	793	174 715	216 572	220 246	669 544
1900	544	940	268 418	279 464	285 696	703 294
2300	604	1135	431 793	370 763	380 303	748 294

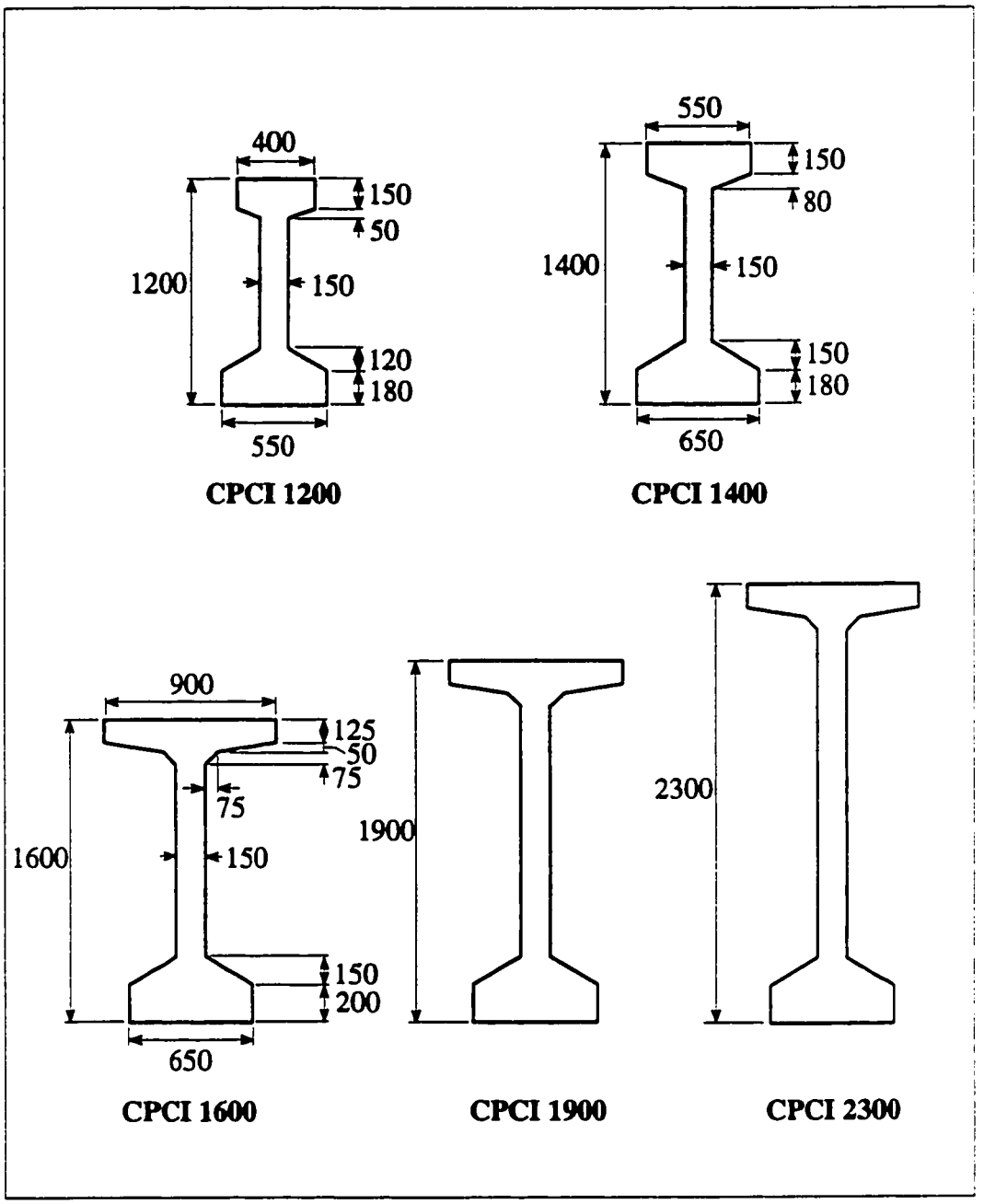

Figure 5.2 Standard CPCI girder types investigated

Design variables for the problem under consideration include the following:

- The prestressing force; alternatively, this could be taken as the required amount of prestressing flexural reinforcement, which is proportional to the prestressing force.
- Eccentricities at girder mid-span and at piers, which define the tendon profile as shown in Fig. 5.3. The tendons are assumed to be draped at the third-points of the span; this is in accordance with the current practice of pretensioning.
- The required amounts of non-prestressing flexural reinforcements in the slab and girders.
- Girder concrete compressive strength at 28 days.
- The deck slab thickness, since composite action of the cast-in-place slab and the precast girders is assumed.

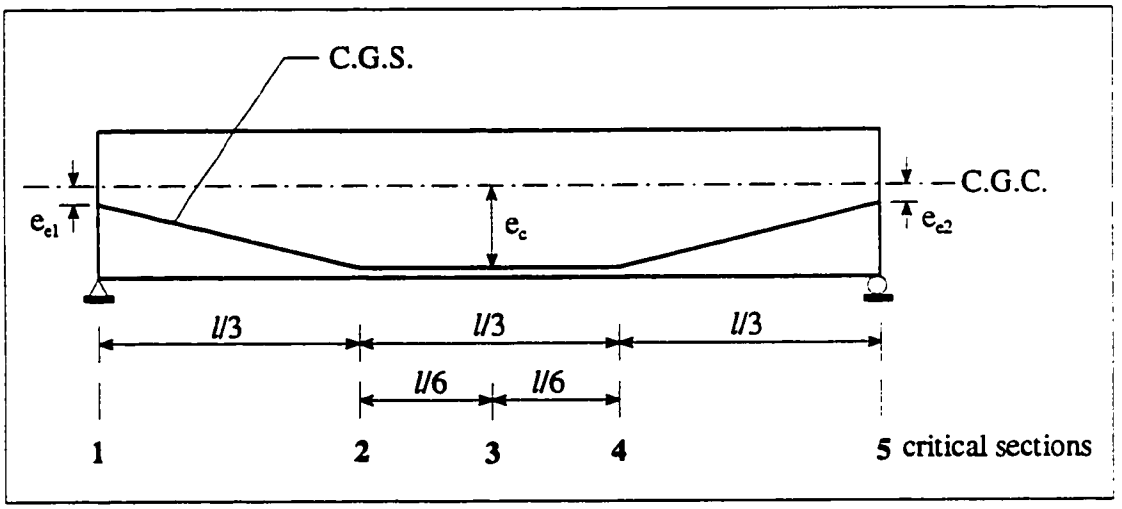

Figure 5.3 Tendon profile and locations of critical sections

5.3 OBJECTIVE FUNCTION

5.3.1 General

It has been explained in Sec. 5.1 that there usually exists an infinite number of feasible designs for a structure. In order to find the optimal one, it is necessary to form a function of

the design variables that can be used for comparison of feasible design alternatives. Such a function is called an *objective function* for the optimal design problem.

Selection of a proper objective function is an important decision in the design process. In general, the objective function should represent the most important single property of a design, but it may represent also a weighted sum of a number of properties. Care must be taken to optimize with respect to the objective function that most nearly reflects the true goals of the design problem. Weight is a very commonly used objective function due to the fact that it is readily quantified. In prestressed concrete design optimization, however, minimum weight may not be always the cheapest. Cost is of wider practical importance than weight, although it is often difficult to obtain sufficient data for the construction of a real cost function. A general cost function may include the cost of materials, fabrication, transportation, etc. In addition to the costs involved in the design and construction, other factors such as operating and maintenance costs, repair costs, etc., may be considered. However, it is not usually desirable to consider an objective function which is as general as possible. The result might be a "flat" function that is not sensitive to variations in the design variables, and the optimization process, practically, will not improve the design. Therefore, from a practical viewpoint, it is desirable to adopt such an objective function that is both sensitive to variations in the design variables and representative of the most important cost components [106].

Another approach is to consider both the initial cost of the structure as well as the failure costs which depend upon the probabilities of failure. Failure costs include such items as additional replacement costs, damage to property, casualties, business interruption and legal services. The assumption is that the failure cost is given by the damage cost associated with a particular failure multiplied by its probability of occurrence. It is, however, recognized that answering the moral question of what constitutes an appropriate failure damage cost is likely to be as difficult as estimating the probability of failure of a structure [106].

5.3.2 Cost Function

The most relevant objective function in the design of slab-on-girder bridges with a fixed number of spans is the minimum superstructure cost. This assumes that the cost of piers, abutments and approaches is relatively unaffected by changes in the number of girders. The bridge superstructure is assumed herein to consist solely of the deck slab and the girders. The objective (cost) function is thus taken as the material (concrete and steel) costs plus overhead and waste, in addition to the labour cost for both the deck slab and the girders. Additionally, transportation and erection costs for the precast girders are also included. Slab formwork cost may vary slightly with the change in the number of girders. For example, as the number of girders decreases, the actual slab formwork area increases; however, the labour cost of placing this formwork decreases in a way that may partially or fully compensate for the increase in material cost. Therefore, it was decided to exclude the slab formwork cost from the cost function. Furthermore, costs of some other items that are relevant to the superstructure such as wearing surfaces, traffic barriers and drains were not included in the cost function because their costs are not affected by the use of HPC. Therefore, these items, if considered, would just add a common cost to all designs, and would not influence the optimal number of girders.

For the present formulation, different superstructure feasible designs are compared for their relative initial cost effectiveness on a dollar-per-square-metre-of-deck basis, i.e. the objective function is defined as the minimum initial superstructure cost / deck area, or

$$\text{Cost} = [\, n_g C_g + C_c V_c + C_s (m_s + n_p (m_{sn} + m_{sp}) + m_p) \,] \;/\; WL \qquad (5.1)$$

where n_g is the number of girders, n_p is the number of positive moment connections at the piers, C_g is the cost of one girder, including cost of materials, production, transportation and erection, C_c is the cost of concrete in the slab per unit volume, C_s is the cost of non-prestressing steel per unit mass, V_c is the volume of concrete in the slab, m_s, m_{sn},m_{sp}, m_p are

the masses of non-prestressing steel in the slab, negative moment steel in the slab at each pier, positive moment connection steel at each pier, and positive moment steel in the girders, respectively, W is the width of the bridge, and L is the total length of the bridge.

5.3.3 Unit Cost Estimation

Computing a value for the cost function necessitates that unit costs for the materials, labour, etc. be established. Establishing these is more difficult a task than it would first appear. This is primarily due to the variability of the costs of these items within a region, as well as to the use of HPC as a new product. Because the quality and availability of the raw materials and labour needed to produce and place concrete can be quite variable, the cost of using this material may vary to a large extent even on a local basis. Moreover, with HPC being a new product, most precasters and contractors have little or no experience with its use. Therefore, they are somewhat uncertain as to what it would cost them to mix and place concrete with a compressive strength as high as 100 MPa.

Thus, it was necessary to estimate typical or average unit costs for the materials, labour, etc. in order to compute a value for the cost function. Because the girder concrete strength was taken as a design variable that can change at each iteration in the optimization process, it was necessary to have a continuous function for the concrete mix cost. In order to accomplish this end, several groups of current concrete cost data from local producers[1], and relative cost data from the literature [13,43,72,82,90] were compiled and normalized with respect to the cost of a 40-MPa concrete mix, which has been assumed to be $\$95/m^3$ including an overhead rate of 18%. Using regression analysis, the following relationship between the girder concrete strength and the concrete mix cost ratio was established:

---

[1] Private communications with Mr. Al Findlay, Contracts Administrator / Chief Estimator, Con-Force Structures Limited, Calgary and Mr. Chris Huizer, Technical Sales Representative, Burnco Rock Products Limited, Calgary, January 1997.

$$CMCR = 0.936 + \left(\frac{f_c'}{100}\right)^3 \tag{5.2}$$

in which CMCR is the concrete mix cost ratio and f_c' is the girder concrete compressive strength at 28 days. Figure 5.4 depicts a graphical representation of the above relationship. The concrete mix cost ratio can be obtained from Eq. (5.2) or from Fig. 5.4, for any level of girder concrete strength, and then multiplied by the cost of mixing 40-MPa concrete to get the cost of that particular girder concrete mix. In addition to the mix cost and overhead charges, labour and curing cost an additional \$34/m^3. Seven-wire, 15.2-mm-diameter prestressing strands cost \$1.78/m for material and labour including a wastage rate of 10% and an overhead rate of 18%. Epoxy-coated reinforcing steel bars cost \$1.68/kg for material and labour including a wastage rate of 5% and an overhead rate of 15%.

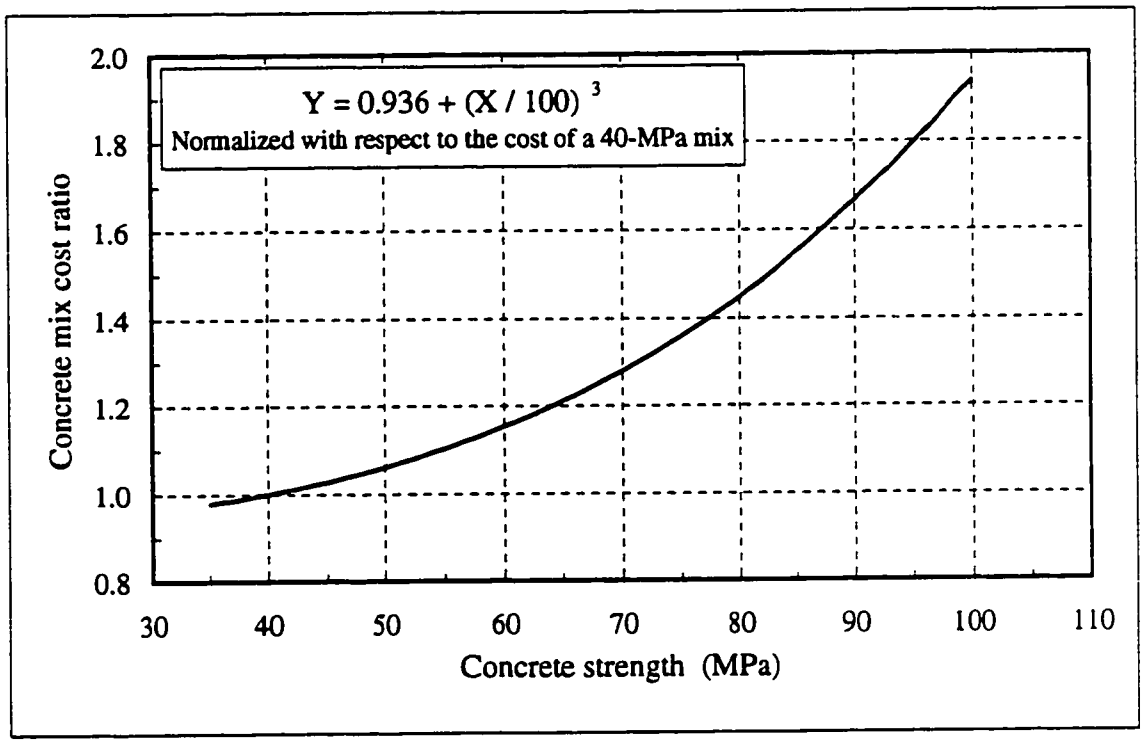

Figure 5.4 Concrete mix cost ratio vs. concrete strength

Estimating transportation and erection costs for the precast girders would be very difficult without a specific bridge project since these costs depend on the distance between the precasting plant and the construction site, and on the condition of the site among other factors. Transportation and erection costs, however, represent a major consideration in slab-on-girder bridge construction, and, therefore, they cannot be ignored just because sufficient cost data is difficult to obtain. One solution is to specify some type of average costs based on typical or representative bridge projects. This was the approach used in this study. In this approach, transportation and erection costs were considered to be the sum of two cost items. The first item is a fixed cost that is independent of the number of girders transported and erected. This cost represents the mobilization, setup and dismantling charges of the crane. The second cost item depends on the number of girders, and is a function of the girder span length and its mass. Mathematically, the overall transportation and erection costs for the precast girders may be represented by the following expression:

$$C_{te} = C_f + n_g [f(l_g) + f(m_g)] \tag{5.3}$$

where C_{te} is the transportation and erection costs, C_f is a fixed cost representing the mobilization, setup and dismantling charges of the crane, $f(l_g)$ is a transportation cost function of the girder span length, and $f(m_g)$ is an erection cost function of the girder mass. It was estimated that it would cost \$500/hour to mobilize, set up and dismantle a 100-tonne crane. Assuming that one workday (8 hours) is needed for setup and another for dismantling, the fixed cost portion of Eq. (5.3) would come to be \$8000. In order to establish the second cost item, a typical layout for a slab-on-girder bridge was assumed. It consists of two equal spans of 30 m in length each. This span length is slightly more than what is required to cross a typical three-lane urban roadway in order to allow for possible future road widening. The bridge has three traffic lanes with an overall width of 12 m. The slab is supported on seven girder lines spaced at 1.67 m. This relatively narrow girder spacing is in accordance with the spacings currently used in the design and construction of this type of bridges. The fourteen girders are CPCI Type 1600 which represents an intermediate cross

section among the CPCI girders. Information from a local precaster indicated that, on average, a girder of this cross section and length would cost about $6000 to transport and erect. This figure was used to obtain a value for C_{te} in Eq. (5.3). Values for f (l_g) and f (m_g) were estimated, based on cost data from the local precaster and from the literature [170], to obtain the pre-calculated value of C_{te}. It should be mentioned here that the cost data obtained from the literature, which is based on a study conducted during the late sixties, was adjusted for inflation. Using the transportation and erection general cost trends of the above study, while utilizing the estimated values of f (l_g) and f (m_g) for the representative bridge as checkpoints, it was possible to establish Figs 5.5 and 5.6. They relate the transportation cost per metre to the length of girder, and the erection cost per tonne to the mass of girder, respectively. Notice the sharp rise in cost per metre of transporting girders of span lengths exceeding 35 m. This is because steerable trailers with additional axles will be needed to transport these girders. Although the approach used here to estimate transportation and erection costs is approximate, it is sufficiently accurate for the purposes of this study. Some average cost data obtained from the local precaster for slab-on-girder bridges with layouts deviating from the one described above was compared to the costs obtained from Figs 5.5 and 5.6 for the same bridges; they came out to be relatively close.

5.4 DESIGN CONSTRAINTS

5.4.1 General

Any set of values for the design variables represents a design of the structure. Even if this design is inadequate in terms of its function or its behaviour, it can still be called a design. Clearly, some designs are useful and others are not. If a design meets all the requirements placed on it, then it is a feasible design. The restrictions that must be satisfied in order to produce a feasible design are called *design constraints*. Each design constraint must be influenced by one or more design variables. Only then is it meaningful and does it have influence on the optimal design [106,107].

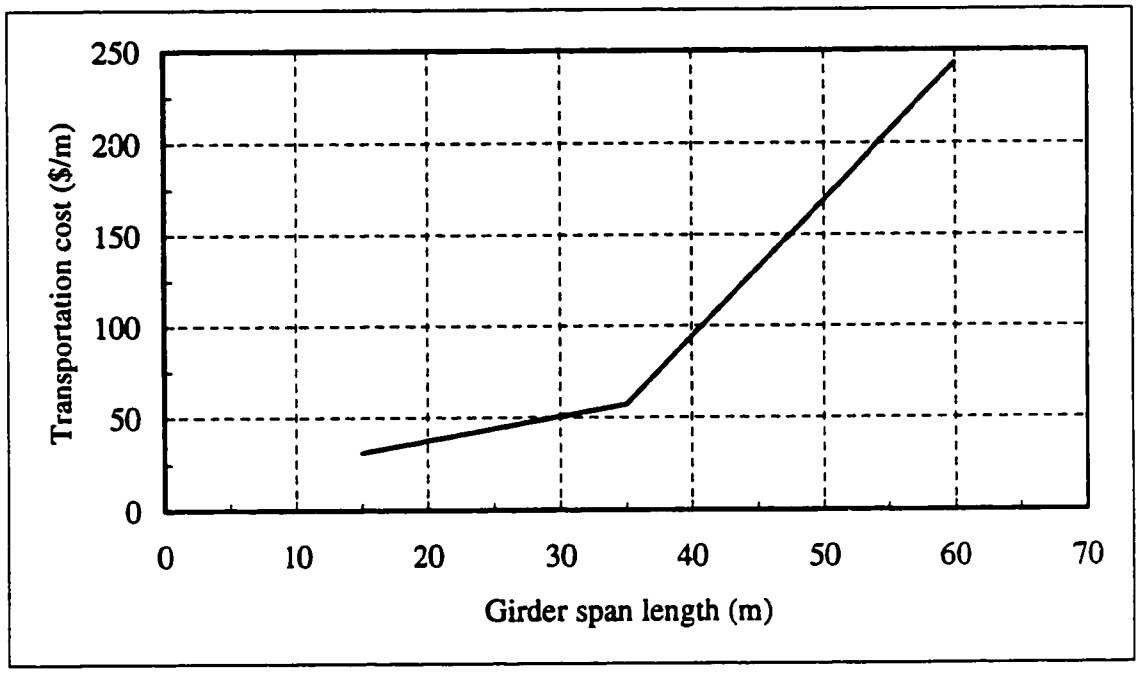

Figure 5.5 Cost per metre of transporting girders

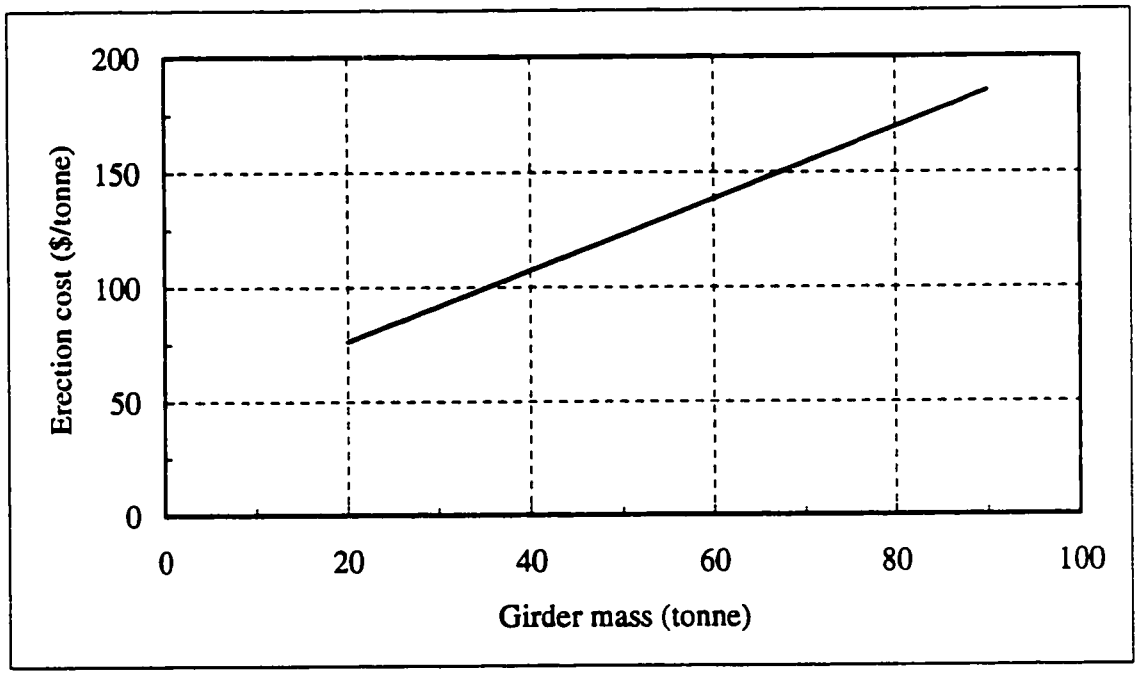

Figure 5.6 Cost per tonne of erecting girders

In structural engineering, constraints on a design may be classified into two kinds: functional constraints and practical constraints. The first kind concerns compliance of the design with both serviceability and ultimate limit state provisions. The second kind of constraints represents some practical limits imposed on some of the design variables. Design problems may have equality as well as inequality (≤ 0 form) constraints. An equality constraint may represent, for example, a desired ratio between the width of a cross section and its depth. An example of an inequality constraint is that calculated stress must be less than or equal to the allowable stress for the material. A feasible design must satisfy precisely all the equality constraints. There are, however, many feasible designs with respect to an inequality constraint. It is, therefore, easier to find feasible designs for a structure having only inequality constraints [107].

The concept of constraint activity is very important in design optimization. Loosely speaking, an active constraint corresponds to a critical design requirement, i.e. one whose presence determines where the optimum will be. An inequality constraint is said to be active at a design point if it is satisfied at equality, i.e. its value is zero or, numerically, a very small number. For a feasible design, an inequality constraint may or may not be active. However, all equality constraints are active for all feasible designs. An inequality constraint is said to be inactive at a design point if it is strictly satisfied, i.e. its value is negative. An inequality constraint is said to be violated at a design point if its value is positive. An equality constraint is violated at a design point if its value is not identically zero. Note that by these definitions, an equality constraint is either active or violated at any given design point [107].

For the present formulation, all design constraints are expressed as inequalities; there are no equality constraints. Furthermore, the constraints are formulated according to the OHBDC provisions [94] unless otherwise specified. Only the flexural constraints at transfer, during construction, at serviceability limit states and at ultimate limit states are considered, in addition to the practical constraints. Other constraints (e.g. shear and deflections) could be added. However, in general, they have marginal effect on the design. When designing bridges

with relatively long spans, which is one of the objectives of this study, the allowable stress requirements for flexure tend to provide designs that can readily conform to the strength requirements for shear; this is because shear loads increase approximately linearly with span lengths, but dead load moments tend to increase as the square of the span. In addition, the relatively high average prestressing force in bridge girders made with HPC contributes significantly to the shear strength of the girders. Therefore, it was decided not to consider shear loads in this formulation. It should be mentioned here that the OHBDC does not have any explicit criteria for limiting deflections in prestressed concrete bridges. Constraints other than those pertaining to flexure are left to be checked at the final design stage.

5.4.2 Functional Constraints

5.4.2.1 Stress Constraints at Transfer:

At the time of prestress transfer, concrete stresses at the top face of the girder due to its own weight must be within the allowable limits at all the critical sections shown in Fig. 5.3. (Tensile stresses are assumed positive and compressive stresses are assumed negative)

$$-\frac{P_i}{A}+\frac{P_i e}{S_t}-\frac{M_{dg}}{S_t}\le 0.2\sqrt{f'_{ci}} \tag{5.4}$$

where P_i is the initial prestressing force, A is the girder cross-sectional area, e is the tendon eccentricity, S_t is the girder cross section modulus with respect to the top surface, M_{dg} is the moment due to the girder's own weight and f'_{ci} is the girder concrete strength at transfer. At the bottom face of the girder

$$-\frac{P_i}{A}-\frac{P_i e}{S_b}+\frac{M_{dg}}{S_b}\ge -0.6 f'_{ci} \tag{5.5}$$

where S_b is the girder cross section modulus with respect to the bottom surface.

5.4.2.2 Stress Constraints During Construction:

For the usual case where the girder is not shored or temporarily supported during construction, the girder alone must carry its own weight plus the weight of the wet concrete of the cast-in-place deck slab. At this stage, which is some time after prestress transfer, the concrete strength will have reached f'_c while the prestressing force will lie between the initial force, P_i, and the final effective force, P_e. As a simplification, the prestressing force is conservatively taken as P_e [171]. The concrete stresses at this stage must satisfy the allowable limits at all critical sections. At the top face of the precast girder

$$-\frac{P_e}{A}+\frac{P_e e}{S_t}-\frac{M_{dg}+M_{ds}}{S_t}\geq -0.45f'_c \tag{5.6}$$

where M_{ds} is the moment caused by the dead load of the slab concrete. At the bottom face of the precast girder

$$-\frac{P_e}{A}-\frac{P_e e}{S_b}+\frac{M_{dg}+M_{ds}}{S_b}\geq -0.45f'_c \tag{5.7}$$

5.4.2.3 Stress Constraints at Serviceability Limit States:

- ***Stresses in Concrete***

The hardening of the cast-in-place concrete slab results in a composite section that will resist all future loads as a unit. It is assumed that the stresses on the girder due to prestress, its own weight and weight of the slab remain unchanged from those calculated during construction. The stresses due to the additional dead load and live load are assumed to be resisted by the composite section, with the final stresses being found by summing these two sets of stresses. This assumes that most prestress losses have occurred before the section becomes composite. The final concrete stresses must be within the allowable limits at all critical sections. At the top face of the composite section

$$\frac{M_{da}+M_l}{S_{tc}} \cdot \frac{E_{cs}}{E_{cg}} \geq -0.45f'_{cs} \tag{5.8}$$

where M_{da} is the moment caused by the additional dead load applied after the slab hardens, M_l is the live load moment, S_{tc} is the section modulus of the composite transformed section, E_{cs} is the elastic modulus of the cast-in-place slab concrete, E_{cg} is the elastic modulus of the precast girder concrete, and f'_{cs} is the slab concrete compressive strength at 28 days.

At the top face of the precast girder

$$-\frac{P_e}{A}+\frac{P_e e}{S_t}-\frac{M_{dg}+M_{ds}}{S_t}-\frac{M_{da}+M_l}{S_{ic}} \geq -0.45f'_c \tag{5.9}$$

where S_{ic} is the section modulus of the composite transformed section at the interface of the cast-in-place and precast concretes. At the bottom face of the precast girder

$$-\frac{P_e}{A}-\frac{P_e e}{S_b}+\frac{M_{dg}+M_{ds}}{S_b}+\frac{M_{da}+M_l}{S_{bc}} \leq 0.2\sqrt{f'_c} \tag{5.10}$$

where S_{bc} is the section modulus of the composite transformed section with respect to the bottom face of the composite girder.

It should be mentioned here that the live load used to calculate the moment M_l in Eqs (5.8) through (5.10) is based on the 1994 draft CHBDC specifications [172] rather than the OHBDC provisions [94] or the CAN/CSA-S6-88 Standard, Design of Highway Bridges [173]. The CHBDC, which still is to be published, is expected to be used by all Federal and Provincial government departments in Canada. The CHBDC loading is shown in Fig. 5.7. Dynamic load allowance (DLA) is the same as in the OHBDC for the axle loads. However, DLA is no longer applied to the uniformly distributed portion of the lane load. Modification factors for multi-lane loading in the CHBDC are identical to those in the OHBDC.

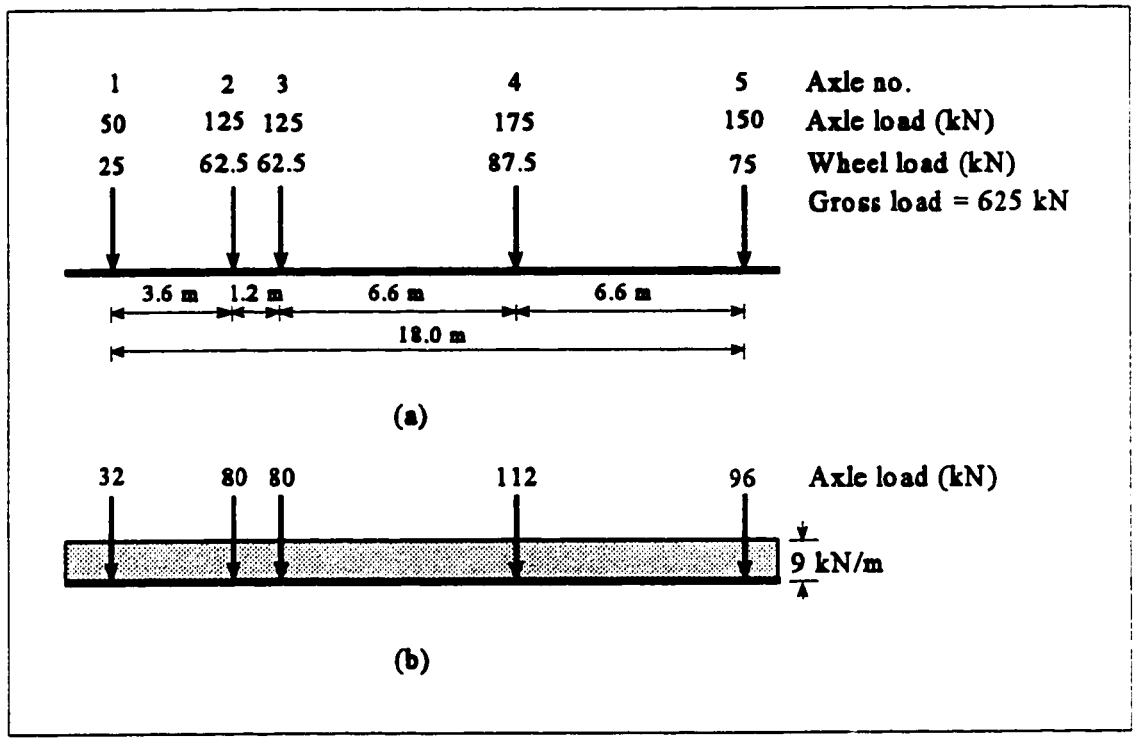

Figure 5.7 (a) The CHBDC truck load (1994 draft)
(b) The CHBDC lane load (1994 draft)

- ***Stresses in Reinforcing Steel***

According to the OHBDC [94], the area of the positive moment connection reinforcing steel bars over the piers shall be sufficient to limit the stress in the bars to 0.6 f_y (i.e. 240 MPa) at serviceability limit states, where f_y is the yield strength of the reinforcing bars and is taken as 400 MPa. Positive moments develop over piers in continuous slab-on-girder bridges due to creep in the prestressed girders as well as due to the effect of live loads in remote spans. In the previous chapter, it was found that the final moment at any support n, M_{csn}, due to the combined effect of creep and shrinkage is given by Eq. (4.28) which is repeated here for convenience

$$M_{csn} = 0.80\ (M_{pn} - M_{dn}) - 0.40\, M_{shn} \qquad (4.28)$$

Using the appropriate load factors, the serviceability limit state moment at support n, M_{SLSn}, can be written as

$$M_{SLSn} = 0.80\ [\,0.80\ (M_{pn} - M_{dn}) - 0.40\,M_{shn}\,] + 0.75\,M_{ln} \qquad (5.11)$$

where M_{ln} is the live load moment at support n. To satisfy the OHBDC provision [94], M_{SLSn} should not exceed the service moment at support n, M_{sn}, provided by the composite section and given as

$$M_{sn} = A_{spn}\,(0.6\,f_y)\ jd_s \qquad (5.12)$$

where, as shown in Fig. 5.8, A_{spn} is the area of positive moment steel at support n, jd_s is the moment arm with d_s being the effective depth of the composite section with respect to the reinforcing bars. From Fig. 5.8, it can be seen that

$$jd_s = d_s - \frac{kd_s}{3} \qquad (5.13)$$

where k, which locates the neutral axis, is given as [174]

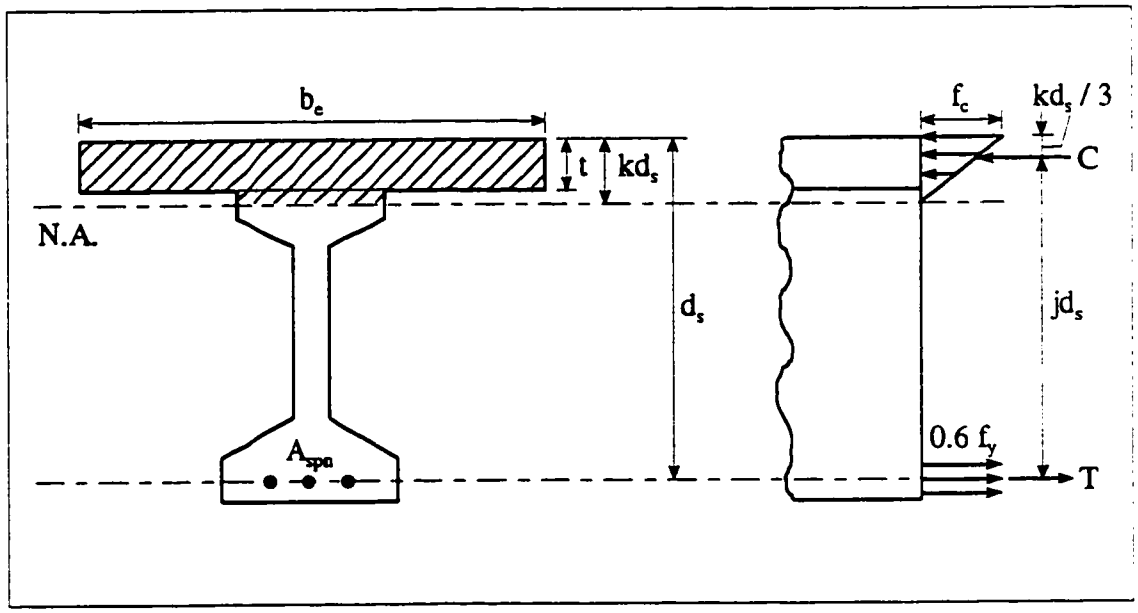

Figure 5.8 Notation for the constraint on the area of the positive moment connection steel at serviceability limit states

$$k = \frac{n_r \rho + \frac{1}{2}\left(\frac{t}{d_s}\right)^2}{n_r \rho + \frac{t}{d_s}} \qquad (5.14)$$

in which n_r is the modular ratio between the reinforcing steel and the girder concrete, ρ is the reinforcement ratio given as $A_{spn}/ b_e d_s$ with b_e being the effective flange width, and t is the thickness of the deck slab.

The final form of the constraint on the area of the positive moment connection steel can be written as

$$0.80\ [0.80\ (M_{pn} - M_{dn}) - 0.40\, M_{shn}] + 0.75\, M_{ln} \le A_{spn}(0.6 f_y)\left(d_s - \frac{k d_s}{3}\right) \qquad (5.15)$$

or simply

$$M_{SLSn} \le M_{sn} \qquad (5.16)$$

5.4.2.4 Constraints at Ultimate Limit States:

- ***Ultimate Positive Moment***

At ultimate limit states, a structural component should be designed so that the factored flexural resistance, M_r, is equal to or greater than the factored load moment, M_f, i.e.

$$M_r \ge M_f \qquad (5.17)$$

This constraint ensures the adequacy of positive moment reinforcement at the critical sections of the girders, i.e. at sections 2, 3 and 4 in Fig. 5.3.

Figure 5.9 illustrates the strain and stress distributions, and forces at ultimate limit states. According to CSA Standard A23.3-94, Design of Concrete Structures [175], the maximum strain in the concrete at the extreme compression fibre, ε_c, is -0.0035. In addition,

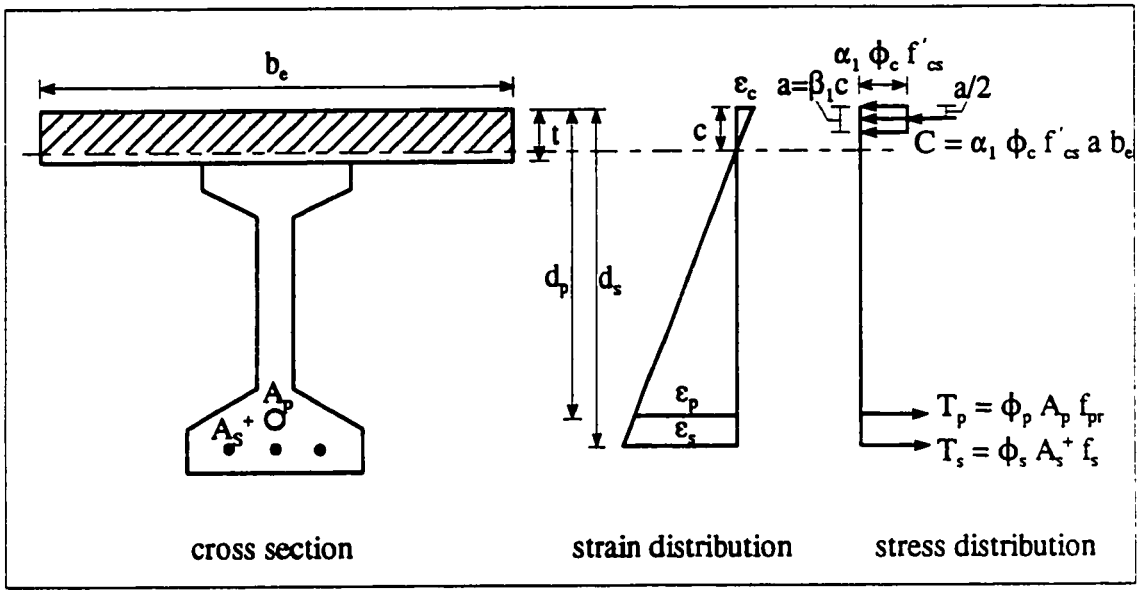

Figure 5.9 Strain and stress distributions, and forces at ultimate limit states

$$\alpha_1 = 0.85 - 0.0015 f'_c \geq 0.67 \tag{5.18}$$

and

$$\beta_1 = 0.97 - 0.0025 f'_c \geq 0.67 \tag{5.19}$$

Care should be taken to evaluate α_1 and β_1 with respect to the appropriate value of the concrete compressive strength, f'_c, depending on the location of the neutral axis as it is usually the case that the concrete strength of the cast-in-place slab is different from that of the precast girders

Force equilibrium leads to the following equation for the factored flexural resistance when the neutral axis is located within the flange (provided by the cast-in-place slab) which is the usual case for the typical configuration of slab-on-girder bridges [176,177]:

$$M_r = \phi_s A_s^+ f_s \left(d_s - \frac{a}{2} \right) + \phi_p A_p f_{pr} \left(d_p - \frac{a}{2} \right) \tag{5.20}$$

in which

$$a = \frac{\phi_s A_s^+ f_s + \phi_p A_p f_{pr}}{\alpha_1 \phi_c f'_{cs} b_e} \tag{5.21}$$

where ϕ_s, ϕ_p and ϕ_c are the material resistance factors for reinforcing bars, prestressing tendons and concrete, respectively. According to the OHBDC [94], these shall be taken as 0.90, 0.95 and 0.75, respectively. A_s^+ is the area of the positive moment reinforcing steel bars in the girder, A_p is the area of the prestressing tendons, f_s is the tensile stress in the reinforcing bars, f_{pr} is the stress in the prestressing tendons at factored flexural resistance, and d_p is the effective depth of the composite section with respect to the prestressing tendons. Minor modifications to Eqs (5.20) and (5.21) are necessary if the neutral axis is located below the flange.

Generally, the reinforcing steel stress can be taken as equal to the yield strength, f_y. However, care should be taken to verify that the steel has yielded at the ultimate condition. Provided that the effective stress in prestressing tendons, f_{pe} is not less than 60% of their yield strength, f_{py}, and the ratio c/d_p, where c is the depth of the neutral axis, is not greater than 0.5, the stress in the tendons, f_{pr}, may be found from the approximate equation

$$f_{pr} = f_{pu}\left[1 - k_p \frac{c}{d_p}\right] \tag{5.22}$$

in which

$$k_p = 2\left(1.04 - \frac{f_{py}}{f_{pu}}\right) \tag{5.23}$$

where f_{pu} is the ultimate strength of the tendons. Otherwise, f_{pr} should be determined by a more exact method based on strain compatibility [175].

Using the appropriate load factors for ultimate limit states, the factored load positive moment can be written as

$$M_f = 1.1\,M_{dg} + 1.2\,M_{ds} + 1.5\,M_{da} + 1.6\,M_l \qquad (5.24)$$

The first three of these load factors are according to the current OHBDC [94] and are expected to remain the same in the CHBDC. The fourth factor, associated with the live load moment, is expected to be in excess of 1.6 [172], compared to 1.4 in the OHBDC. It has been taken here as 1.6.

- ***Ultimate Negative Moment***

In continuous slab-on-girder bridges, most of the dead load moments are carried by the girders acting as simple beams. The negative moments over the piers are those due to live load and any additional dead load applied after continuity is achieved. The factored load negative moment can thus be written as

$$M_f = 1.5\,M_{da} + 1.6\,M_l \qquad (5.25)$$

This negative moment is resisted by longitudinal reinforcing bars embedded in the cast-in-place deck slab across the piers. It is usually the case that the depth of the compression block will be less than the thickness of the bottom flange of the precast girder [162]. For this reason, the factored flexural resistance, M_r, can be determined by assuming the girder to be a rectangular section with a width equal to the bottom flange width, b_f. This leads to the following equation for M_r over the pier under consideration:

$$M_r = \phi_s A_s^- f_y \left(d_s - \frac{a}{2} \right) \qquad (5.26)$$

in which

$$a = \frac{\phi_s A_s^- f_y}{\alpha_1 \phi_c f_c' b_f} \qquad (5.27)$$

where A_s^- is the area of the negative moment reinforcing steel over the pier under consideration. The final form of the constraint that ensures the adequacy of negative moment reinforcement over the piers can be represented by Eq. (5.17).

5.4.3 Practical Constraints

5.4.3.1 Constraint on the Maximum Eccentricity at and Near Girder Mid-span:

This constraint relates to the physical limitations of the girder cross section with regard to the placement of prestressing strands. Essentially it states that strands must fit inside the cross section with an adequate concrete cover. Thus, the design eccentricity, e_c, at and near mid-span must be less than or equal to a maximum practical value, e_{max}, i.e.

$$e_c \leq e_{max} \tag{5.28}$$

in which

$$e_{max} = y_b - (d_c)_{min} \tag{5.29}$$

where y_b is the distance from the centroid of the cross section to the extreme bottom fibre, and $(d_c)_{min}$ is the minimum feasible value of concrete cover measured from the bottom fibre to the centroid of the strands.

In order to accurately determine $(d_c)_{min}$, location of the strands must be known. Figure 5.10 illustrates the layout used in this study for strand placement at and near mid-span. Seven-wire, 15.2-mm-diameter strands are used rather than 12.7-mm-diameter strands because the former help to effectively utilize HPC as was previously discussed in Sec. 2.5.2.2. The centre-to-centre spacing between strands is 50 mm in both vertical and horizontal directions. Groups of eight strands are bundled at and near mid-span to touch one another in a vertical plane as shown in the figure; the clear distance between groups of bundled strands is taken as 25 mm. Strands are positioned in the bottom row first, and by moving to higher rows as required. This is to achieve maximum eccentricity. If the total number of strands required is large, strands may be placed within the web. However, in no case may strands be placed above the centroid of the girder cross section.

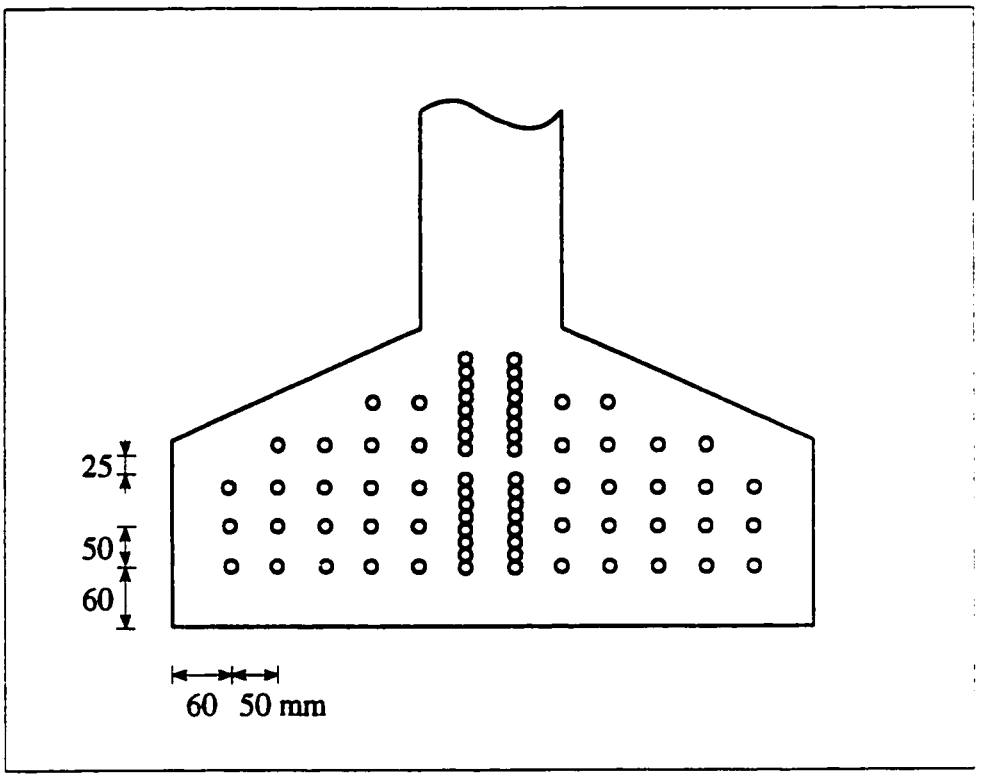

Figure 5.10 Layout used for strand placement at and near girder mid-span

5.4.3.2 Constraint on the Minimum Amount of Flexural Reinforcement:

It is desirable that girders contain sufficient flexural reinforcement at the critical sections to ensure that a reserve of strength exists after initial cracking. If the girders do not contain enough reinforcement, they may fail abruptly with rupturing of the steel immediately after cracking. The total amount of flexural reinforcement should be such that

$$M_r \geq 1.20\, M_{cr} \tag{5.30}$$

unless

$$M_r \geq 1.33\, M_f \tag{5.31}$$

where M_{cr} is the cracking moment of the composite section and is given as

$$M_{cr} = (M_{dg} + M_{ds}) + S_{bc}\left(\frac{P_e}{A} + \frac{P_e e}{S_b} + f_{cr} - \frac{M_{dg} + M_{ds}}{S_b}\right) \tag{5.32}$$

where f_{cr} is the cracking strength of concrete and is given as

$$f_{cr} = 0.5\sqrt{f'_c} \tag{5.33}$$

5.4.3.3 Constraint on the Maximum Area of Negative Continuity Reinforcement:

To ensure ductile behaviour, the amount of negative moment continuity reinforcement over the piers should be limited to 0.5 times the amount that would produce balanced strain conditions. In other words

$$\rho \leq 0.5\,\rho_b \tag{5.34}$$

in which

$$\rho_b = \alpha_1 \beta_1 \frac{\phi_c f'_c}{\phi_s f_y}\left(\frac{700}{700 + f_y}\right) \tag{5.35}$$

where ρ is the ratio of the continuity reinforcement given as $A_s^- / b_f d_s$ and ρ_b is the balanced reinforcement ratio.

5.4.3.4 Constraint on the Ratio of Girder Spacing to Slab Thickness:

According to the empirical design method for deck slabs allowed by the OHBDC [94], the ratio of centre-to-centre girder spacing, S, to the thickness of the slab, t, shall not exceed 15.0. This ratio has been increased to 18.0 in the AASHTO LRFD Bridge Design Specifications [151] as was discussed in Sec. 4.6.2. The latter ratio is used in this study because it allows a larger limit for this constraint. Thus,

$$\frac{S}{t} \leq 18.0 \tag{5.36}$$

5.4.3.5 Constraint on the Slab Overhang:

For dead load analysis, the OHBDC [94] allows the use of the beam analogy method for bridges having longitudinal girders and an overhanging deck slab provided that the overhang, S′, does not exceed 60% of the spacing between the girders, nor is it more than 1.80 m. This constraint can be written as

$$S' \leq \text{Minimum } (0.60S, 1.80\text{m}) \tag{5.37}$$

5.4.3.6 Other Constraints:

There are some practical constraints that represent explicit lower and upper bounds on some of the design variables. They represent the smallest and largest allowed practical values for these design variables. For example, the OHBDC [94] requires the deck slab of slab-on-girder bridges to have a minimum thickness of 225 mm, i.e.

$$t \geq 225 \text{ mm} \tag{5.38}$$

Such constraints are quite simple and easy to implement in numerical methods of optimization if they are treated in their original form without converting them to inequality constraints. This is discussed further in the next section.

5.5 STANDARD DESIGN OPTIMIZATION MATHEMATICAL MODEL

Once the optimal design problem has been formulated, i.e. the design variables, objective function and design constraints have been identified, the problem is transcribed into the following standard design optimization mathematical model: Find the set of n design variables contained in the vector {b} that will minimize the objective function

$$f(\{b\}) = f(b_1, b_2, ..., b_n) \tag{5.39}$$

subject to the constraints

$$h_i(\{b\}) = 0, \quad i = 1, ..., k \tag{5.40}$$

$$g_i(\{b\}) \leq 0, \quad i = 1, ..., m \tag{5.41}$$

$$b_i^l \leq b_i \leq b_i^u, \quad i = 1, ..., n \tag{5.42}$$

where k is the number of equality constraints, m is the number of inequality constraints, b_i^l and b_i^u are the lower and upper bounds on the ith design variable, respectively [107].

Although the objective (cost) function represented by Eq. (5.39) will always be minimized in this study, there is no loss of generality with the above mathematical model because maximization of $f(\{b\})$ can be transformed into minimization of $-f(\{b\})$. It should also be noted that "$\geq$ type" inequality constraints can be converted to the "$\leq$ type" inequalities represented by Eq. (5.41) by simply multiplying them by -1. Furthermore, it is possible to assign a fixed value to any design variable, i.e. transform it into a preassigned parameter, by setting both b_i^l and b_i^u in Eq. (5.42) to be equal to that value. It follows, therefore, that the above mathematical model is quite general, and can encompass all the possibilities encountered in design optimization problems from different fields of engineering.

In numerical calculations, it is desirable to normalize (non-dimensionalize) all the constraint functions. Consequently, all inequality constraints must be transformed to the form depicted by Eq. (5.41). This is because active and violated constraints are used in computing a desirable direction of design change during the optimization process, and usually one parameter, ε_1, is used for all constraints to decide if a certain "percent" violation of a constraint is acceptable; if all constraint violations are less than ε_1, the design is considered as feasible. Since different constraints may involve widely different orders of magnitude, it is not proper to use the same ε_1 for all the constraints unless they are normalized. This can be achieved by dividing the constraints by their respective allowable values [107]. For example, consider a stress constraint as

$$\sigma \le \sigma_a \quad \text{or} \quad \sigma - \sigma_a \le 0 \tag{5.43}$$

where σ is the calculated stress in a member and σ_a is an allowable stress. This constraint may be normalized as

$$r - 1.0 \le 0 \tag{5.44}$$

where $r = \sigma/\sigma_a$. Here, σ_a is assumed to be positive; otherwise, sense of the inequality will change. There are other constraints that may be written in the form

$$1.0 - r \le 0 \tag{5.45}$$

when normalized with respect to their nominal value. For example, the flexural resistance, M_r, of a member should exceed the applied factored moment, M_f, i.e. $M_r \ge M_f$. When this constraint is normalized and converted to the standard "≤ form", it is given as in Eq. (5.45) with $r = M_r/M_f$.

Both linear and nonlinear programming problems can be transformed into the form of Eqs (5.39) through (5.42). In this study, the optimal design problem of slab-on-girder bridges is highly nonlinear because both the cost function as well as most of the constraints are nonlinear functions of the design variables. Many numerical methods have been developed to solve nonlinear optimization problems. The methods start from an initial design provided by the designer which is iteratively improved until the optimum is reached. Many of these methods have been incorporated into general-purpose design optimization software packages. One such package is used in this study and is introduced in the following section to solve the nonlinear optimal design problem using the mathematical model described above.

5.6 DESIGN OPTIMIZATION SOFTWARE (IDESIGN)

5.6.1 User Interface

IDESIGN (*I*nteractive *DESIGN* Optimization of Engineering Systems) is a general-purpose design optimization software package that can solve the general nonlinear

programming problem [178,179,180]. IDESIGN is widely used in the United States [181] and elsewhere. It is written in structured, double precision FORTRAN 77, and consists of a main program and several standard subroutines that need not be changed by the user. In order to solve a design problem, the user must describe it by coding the following four FORTRAN subroutines:

USERMF: Minimization (cost) Function evaluation subroutine

USERCF: Constraint Functions evaluation subroutine

USERMG: Minimization (cost) function Gradient evaluation subroutine

USERCG: Constraint functions Gradients evaluation subroutine

A fifth subroutine, USEROU, may also be provided by the user to perform post-optimality analyses for the optimal solution and obtain more OUtput. Other subroutines specific to the design problem may be called through the above subroutines. All of the user-supplied subroutines must be compiled and linked to IDESIGN to create an executable code with IDESIGN controlling the flow. Figure 5.11 shows a conceptual layout of the design optimization procedure.

IDESIGN can be used in either an interactive or batch mode of computation. It has been designed to accommodate both beginner and experienced users. The beginner can respond to one menu at a time as guided by the on-line instructions. The expert can prepare an input data file and thus bypass intermediate menus. IDESIGN requires minimal input data for the problem; the user must provide the initial design, lower and upper bounds on design variables, problem parameters, and the parameter values to invoke various options available in the program [178,179,180]. A sample input data file is presented in Appendix A.

5.6.2 Gradient Evaluation Capabilities

Numerical design optimization methods utilize gradients of the cost and constraint functions during the optimization procedure. The following capabilities to evaluate gradients and / or check gradient expressions are available in the IDESIGN software package:

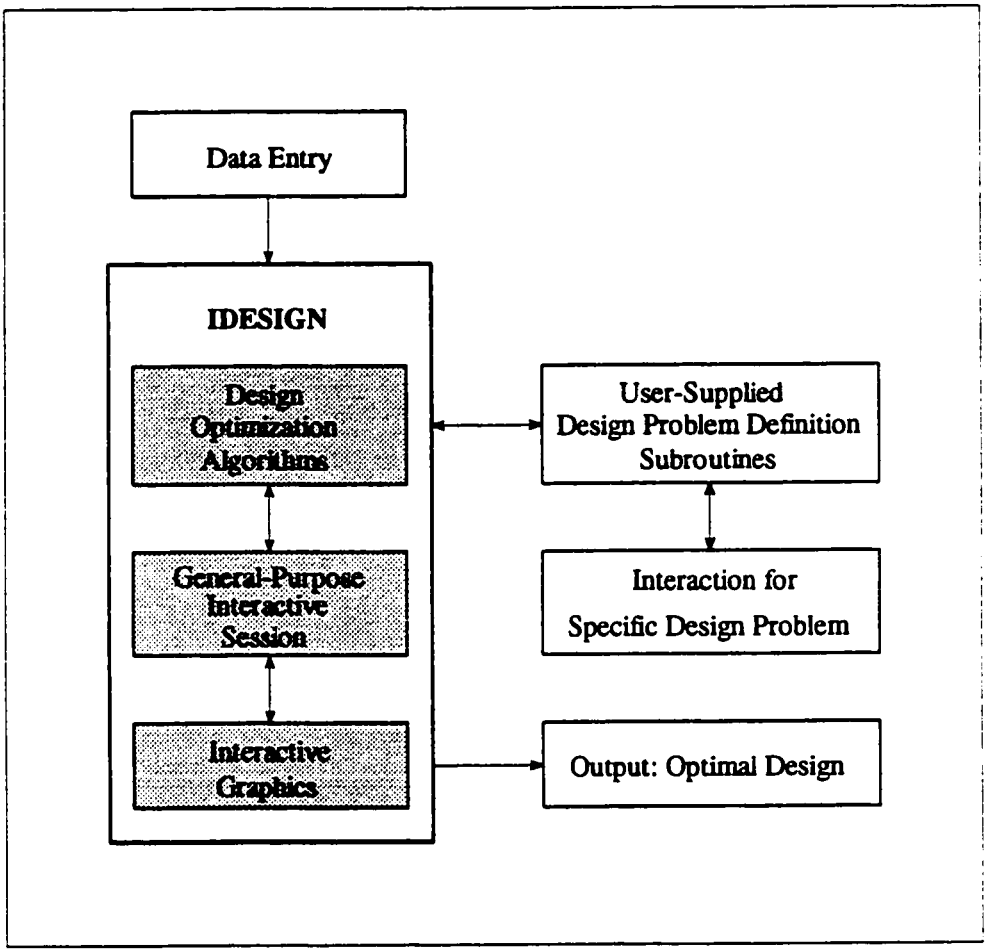

Figure 5.11 Conceptual layout of the design optimization procedure

1. If the user does not program gradient expressions in USERMG and USERCG subroutines, the program has an option to automatically calculate them. The finite difference method is employed using the specified value of δ (input data).
2. An option is available to determine the optimal value of δ for the finite difference gradient evaluation of cost and constraint functions.
3. If the user has programmed gradient expressions in USERMG and USERCG subroutines, an option is available to verify them, i.e. the gradient evaluation is checked using the finite difference approach. If the gradient expressions are in error, an option is available to either stop IDESIGN or continue its execution.

These options have proven to be extremely useful in practical applications [178,179,180]. The complexity of the problem under investigation herein makes it cumbersome to calculate the gradients analytically. Numerical evaluation of the gradients is commonly used and practically justified for such a problem with adequate accuracy being obtained. Therefore, it was decided to use the finite difference approach available in IDESIGN to calculate the gradients automatically based on an optimal value of δ.

5.6.3 Convergence Criteria

The central idea behind numerical methods of optimization is to search for the optimal point in an iterative manner generating a sequence of designs. The success of a method depends on the guarantee of convergence of the sequence to the optimal point. In IDESIGN, the following stopping criteria are used to signify convergence of the sequence [180]:

1. The maximum constraint violation should be less than a specified parameter, ε_1.
2. The length of the search direction vector (convergence parameter) should be less than a specified parameter, ε_2.
3. The percentage change in the cost function is less than a specified parameter, ε_3, for a specified number of consecutive iterations, I, and the design is feasible.

It is important to specify proper values for ε_1, ε_2, ε_3 and I; otherwise premature

convergence may occur, or IDESIGN may not be able to meet the convergence criteria. Values for these parameters should be selected after some preliminary analyses of the problem.

5.6.4 Levels of Output

Several levels of output can be obtained from IDESIGN. This is specified in the input data. The minimum output gives the optimal design, design variables and constraint activities along with histories of the cost function, maximum constraint violation and convergence parameter. More detailed information at each iteration can also be obtained. The detailed output is used primarily for debugging purposes. A sample minimum output data file is presented in Appendix B.

CHAPTER 6

ECONOMIC STUDIES

6.1 INTRODUCTION

The main objective of this chapter is to assess the potential economic benefits from the utilization of HPC for precast, prestressed concrete slab-on-girder bridges. To reach this objective, the information provided in Chapters 4 and 5 was used to develop an optimization system that can be utilized to perform economic studies on this type of bridges. The system can be used to analyse and design economical slab-on-girder bridges of typical configurations according to the OHBDC provisions taking into account practical considerations.

This chapter is organized into three main sections. The first states the assumptions made in developing the optimization system and presents a computer program developed to perform the analysis phase of the optimization process. The application and capabilities of the system are demonstrated in the second part of the chapter through a numerical design example. Finally, in the third part of this chapter, data from a series of economic studies is presented and discussed to evaluate the cost effectiveness of using concretes with strengths of up to about 100 MPa for precast, pretensioned slab-on-girder highway bridges.

6.2 ANALYSIS PROGRAM DEVELOPMENT

6.2.1 Assumptions

The following assumptions were made in developing the analysis program and the USER subroutines of IDESIGN. Some of these assumptions have been mentioned previously; they are stated here again for completeness.

1. Analysis and design conform to the OHBDC provisions [94] except where otherwise noted.
2. Flexure governs the design of girders. In general, constraints other than those pertaining to flexure (e.g. shear and deflections) have marginal effect on the design. These are left to be checked at the final design stage.
3. The 1994 draft CHBDC live load specifications shown in Fig. 5.7 [172]. These are expected to be used by all Federal and Provincial government departments in Canada once the new Code is published.
4. Unshored, composite construction. Interface surfaces between the cast-in-place slab and precast girders are intentionally roughened for proper shear transfer.
5. Tendon profile and locations of the critical sections are as shown in Fig. 5.3. The tendons are draped at the third-points of the span. The layout used for strand placement is as shown in Fig. 5.10; this is in accordance with the current practice of pretensioning.
6. A future wearing surface having a thickness of 75 mm will be placed on top of the concrete deck slab as shown in Fig. 6.1.
7. Each traffic barrier has a cross-sectional area of 0.3 m^2 in accordance with the OHBDC specifications [163]. This load is distributed equally among the girders.

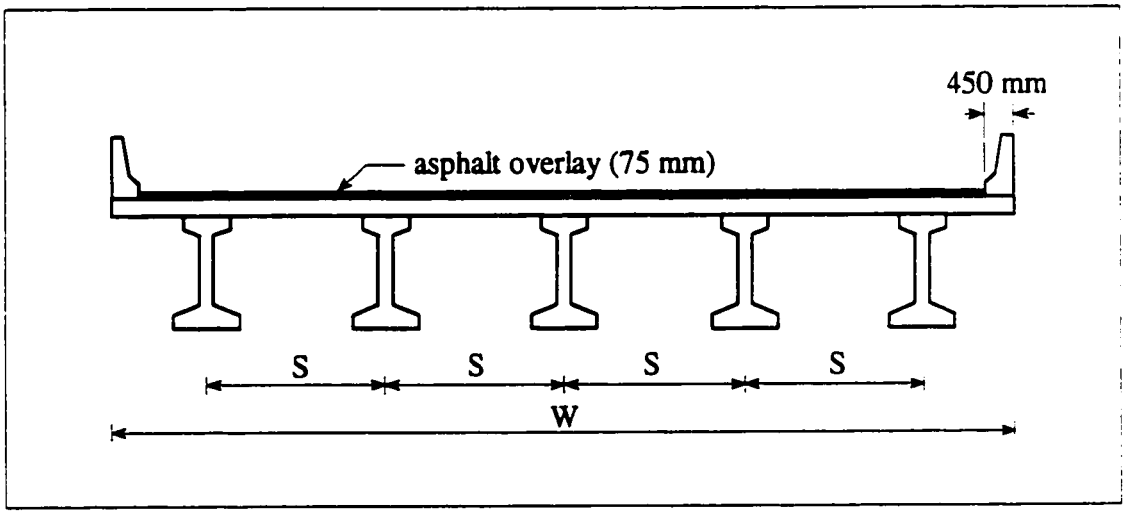

Figure 6.1 Cross section of a typical slab-on-girder bridge

8. Traffic lane width is 3.70 m [94].
9. There are no intermediate diaphragms in bridges. Conflicting opinions exist on the benefits gained from the addition of such diaphragms to slab-on-girder bridges. Some [182] believe that they improve the distribution of loads to the girders, while others [183,184] have shown that the addition of intermediate diaphragms to a bridge may not reduce the maximum moments in girders and may in some cases cause moderate increases. In any case, the OHBDC [94] states that for slab-on-girder bridges, the effect of intermediate diaphragms on the structural responses may be ignored.
10. Reinforcing steel bars are epoxy-coated. They have a yield strength of 400 MPa and an elastic modulus of 200,000 MPa.
11. Seven-wire, low relaxation, 15.2-mm-diameter prestressing strands having a tensile strength of 1860 MPa are used. The effective stress in strands is 0.60 of their tensile strength.
12. The effective prestressing force after losses is 0.80 of the prestressing force at the time of transfer.
13. Concrete compressive strength at transfer is 0.70 of the 28-day strength. This ratio has been previously used satisfactorily in some studies [89]. It is also in accordance with Canadian and American practices.
14. The elastic modulus, E_c, of concrete is given in accordance with CSA Standard A23.3-94 [175] as

$$E_c = (3300\sqrt{f'_c} + 6900)\left(\frac{\gamma_c}{2300}\right)^{1.5} \qquad (6.1)$$

where γ_c is the mass density of concrete. For reinforced concrete, γ_c is taken as 2450 kg/m^3, while for prestressed concrete, it is taken as 2500 kg/m^3.

15. Unit cost estimates for the materials, labour, etc., and for the transportation and erection charges are in accordance with Sec. 5.3.3.

6.2.2 Program BRIDGE

As was discussed in Chapter 4, dead load effects in the various components of a slab-on-girder bridge are often obtained using methods of statics such as the beam analogy method. Live load effects, on the other hand, are not so easily determined because of the wide variety of parameters (from the structure's geometry to its components' material properties) that influence exactly how live loads are distributed, especially in continuous bridges. Because of this, it was necessary to develop a live load analysis computer program that can be incorporated with IDESIGN into the optimization system. The program was called BRIDGE. It is written in structured, double precision FORTRAN 77 and is based on the general semicontinuum method described in Chapter 4. This method is highly efficient and fairly accurate compared to other refined methods of analysis, such as the finite element method which requires much larger computer power, and is prone to common errors of idealization and interpretation of results.

Program BRIDGE works in a batch mode of computation. The designer has to prepare an input data file describing the configuration or layout of the bridge under consideration, as well as the loading. Defining the configuration involves specifying the number of spans, span lengths, number of girder lines, number of traffic lanes, etc. When identifying the girder cross section for the bridge to be investigated, the designer has to input the section's dimensions. The program can then calculate the section's geometric properties. This makes it possible to easily describe and examine bridges with precast I-girders other than the CPCI sections used for this study. The 1994 draft CHBDC live load specifications [172], shown in Fig. 5.7, are built into BRIDGE. However, it is easy to specify any other design loading, such as AASHTO loading [151], by modifying the appropriate subroutines in BRIDGE. The program can handle a multitude of live load cases to determine whether truck loading or lane loading produces the maximum load effects at the critical sections depending on the span length of the bridge under consideration. Once the maximum load effects have been determined by BRIDGE, they are used by the USER subroutines to solve the optimal

design problem. Subsequent reanalyses are conducted by program BRIDGE during the iterative design process.

6.3 NUMERICAL DESIGN EXAMPLE

6.3.1 Problem Statement

To illustrate the application of optimal design procedures discussed in Chapter 5 and the analysis program presented in the previous section, and to test the validity of the optimization system, a typical slab-on-girder bridge is studied. It consists of two equal spans of 34 m in length each. This span length is somewhat more than what is required to cross a typical three-lane urban roadway in order to allow for possible future road widening. The bridge has three traffic lanes with an overall width of 12 m. The slab is supported on four girder lines spaced at 3.0 m. This spacing was chosen because it optimized the design of the exterior and interior girders. Exterior girders are generally required to have a load carrying capacity greater than or equal to the load carrying capacity of interior girders unless future widening of the bridge is virtually inconceivable [151]. Design is optimized by increasing the girder spacing until the service load stresses in the exterior girders are nearly equal to those in the interior ones. The eight girders are CPCI Type 1600 which represents an intermediate cross section among the CPCI girders. Strength of the deck slab concrete was fixed at 35 MPa. In this study, design of this bridge implies finding values for all of the design variables stated in Sec. 5.2.2.

6.3.2 Solution of the Optimal Design Problem

Appendix B gives the output data file generated by IDESIGN for the above problem. As shown, the optimal design process starts from an initial design provided by the designer which is iteratively improved until the optimum is reached. At the first iteration, an optimal value of δ for the finite difference gradient evaluation is determined as was explained in Sec. 5.6.2. At each iteration, values of the design variables, maximum constraint violation,

convergence parameter and cost function are given. The file also gives constraint activity at the optimal point indicating whether a constraint is active or not along with the constraint function values. Design variable activity is shown at the optimal point, and the final cost function value is also given.

For the problem under consideration, the following stopping criteria were used in IDESIGN to signify convergence of the solution:

1. The maximum constraint violation at the optimal point should be less than 1.0×10^{-3}.
2. The convergence parameter value should be less than 1.0×10^{-1}.
3. The percentage change in the cost function should be less than 1.0×10^{-3} for 5 consecutive iterations.

As was mentioned in Sec. 5.6.3, it is important to specify proper values for these parameters; otherwise premature convergence may occur, or IDESIGN may not be able to meet the convergence criteria. Values for these parameters were selected after some preliminary analyses of the problem.

The starting design estimate is highly infeasible with a maximum constraint violation of 526%. It takes 6 iterations to obtain a feasible (usable) design with a maximum constraint violation of 4.65×10^{-5}. Five more iterations are needed to reach the optimal design. Figures 6.2 through 6.4 display graphically the history of the iterative design process. Figure 6.2 shows a plot of maximum constraint violation versus the iteration number. Using this graph, one can locate feasible designs. For example, designs after iteration 5 are feasible, while designs at all previous iterations have some violation of constraints. Figure 6.3 shows the convergence parameter history. For this problem, the convergence parameter should be less than 1.0×10^{-1} at the optimum. It can be seen that the parameter is quite close to zero at the fifth iteration and beyond. The iterative process could have been terminated interactively in IDESIGN as soon as a feasible design was reached. It is interesting to note the sharp rise in the plot after the second iteration. This can be explained by considering the actual meaning of the convergence parameter. In IDESIGN, change in the value of a design variable between

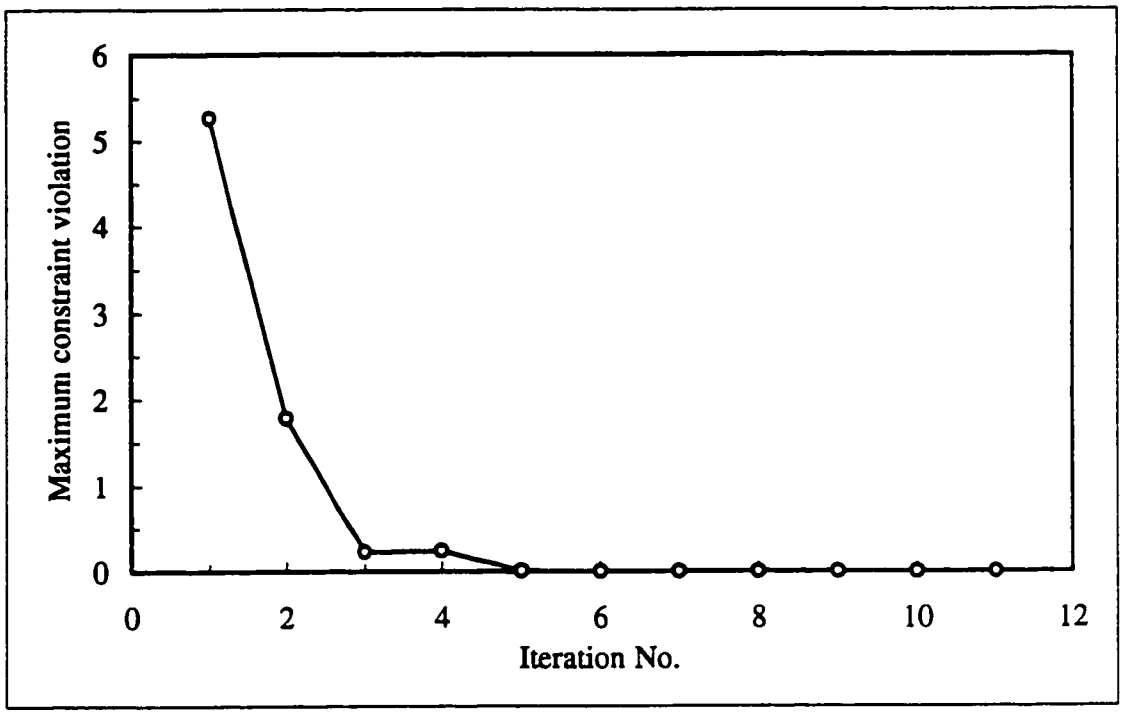

Figure 6.2 History of the maximum constraint violation for the design example

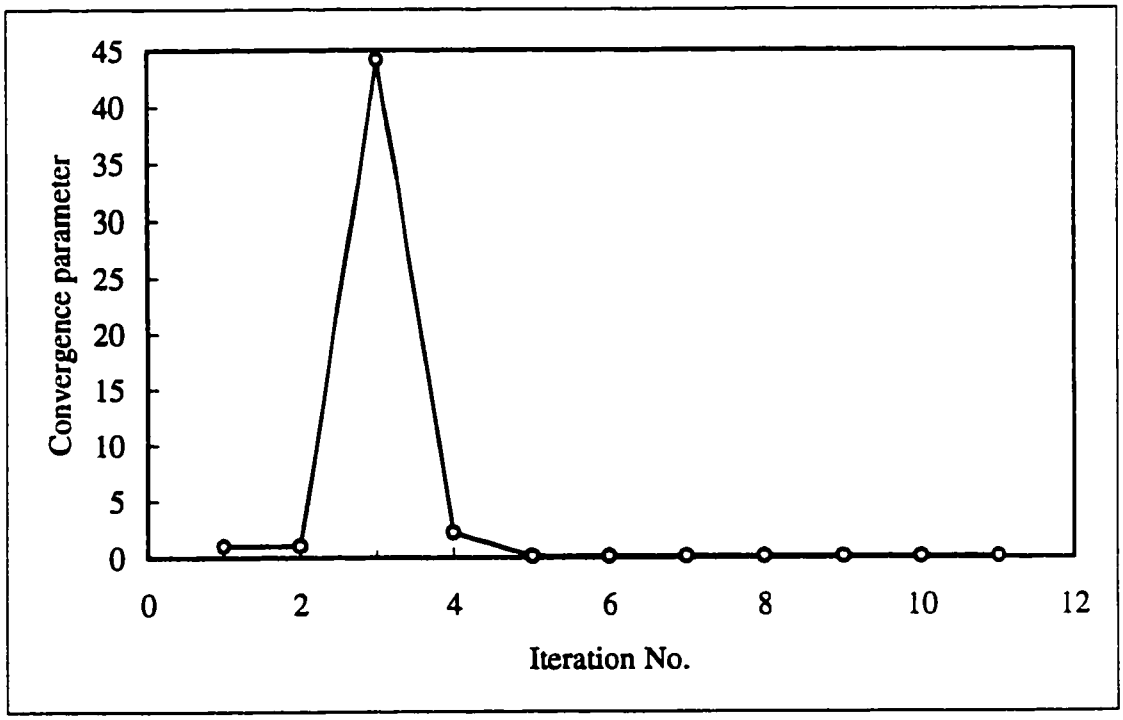

Figure 6.3 History of the convergence parameter for the design example

one iteration and another is associated with a search direction vector. As explained above, for the problem under consideration, one of the criteria used to signify convergence was for the length of this vector (called *convergence parameter*) to be less than 1.0×10^{-1} at the optimum. If design variables have small values, the direction vector will also have small components. The effect will be opposite if the design variables have large values. For this problem, the design variable with the largest value relative to the other variables is the girder concrete strength. A look at the change in the value of this design variable between the second and the third iterations (from 47 MPa to 58 MPa) reveals that it is associated with the longest search direction vector, i.e. the largest convergence parameter. Subsequent iterations are accompanied by shorter search direction vectors as indicated in the plot. Figure 6.4 shows the variation of the cost function as the iterations progress. It shows that there is a relatively large increase in the cost function value after the second iteration. This increase is primarily associated with a large increase in the girder concrete strength (from 47 MPa to 58 MPa) and, thus, its cost. After the fourth iteration, the change in the cost function value is negligible. For practical purposes, the iterative process could have been terminated at a feasible design.

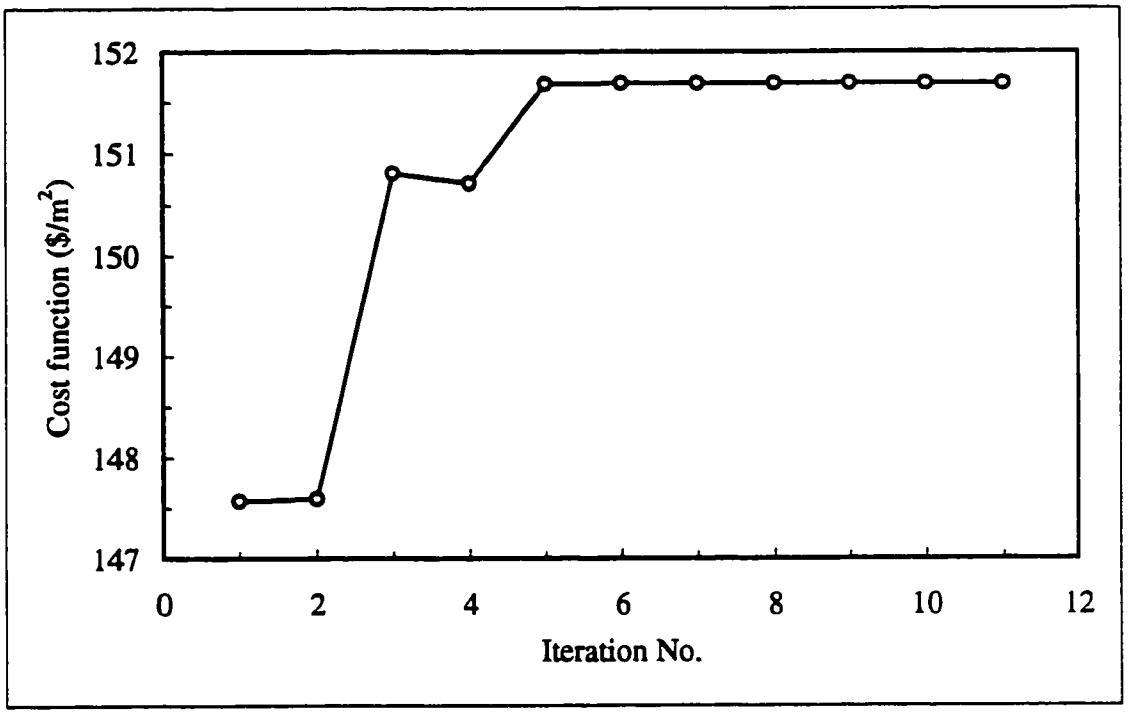

Figure 6.4 History of the cost function for the design example

Kirsch [185] has indicated that in many practical design problems, the object is to find an improved feasible design rather than the theoretical optimum. This is particularly useful in cases where the cost function is not sensitive to changes in the design variables near the optimum. He presented some methods intended to introduce improved feasible designs. These methods, however, require an initial feasible design which might be difficult to find *a priori*, especially for large-scale design problems.

At the optimal point, the following values for the design variables were obtained:

- The initial prestressing force, P_i, in each girder is 6.26 MN, i.e. P_e is 5.01 MN. This translates into 32 strands per girder.
- Tendon eccentricity, e_c, at and near girder mid-span is 699 mm, and eccentricities, e_{e1} and e_{e2}, over the piers are 423 mm each.
- Area of the positive moment connection reinforcing steel bars over each pier, A_{spn}, is 2513 mm^2.
- Area of the negative moment reinforcing steel bars over each pier, A_s^-, is 7100 mm^2.
- No positive moment reinforcing steel bars are needed in the girders, i.e. the girders are fully prestressed.
- Girder concrete compressive strength at 28 days, f_c', is 60.2 MPa.
- The deck slab thickness, t, is 225 mm.

Final value of the cost function at the optimal point is \$151.69/m^2.

It was noted that the active constraints (governing design criteria) at the optimal point are those represented by Eqs (5.5) and (5.10) which set the limits on compression at transfer and tension at serviceability limit states, respectively, at the bottom face of the girder. In addition, the constraint on the ultimate negative moment over the piers (Sec. 5.4.2.4) was also found to be active at the optimal point. Another active constraint was that on the maximum eccentricity at and near girder mid-span (Eq. 5.28). Moreover, the optimal deck slab thickness was found to always correspond to the minimum thickness permitted by the OHBDC (Eq. 5.38). Constraint activity will be investigated further in the next chapter.

6.3.3 Graphical Interpretation of the Solution

As a way of verifying the results of the optimization process and of gaining additional insight into the solution of the design example, graphical interpretation can be very useful. The graphical solution of the allowable stress conditions in prestressed concrete was first explored by Magnel [186], and later by Naaman [187] and Loov [188]. The approach used by Loov is utilized herein.

It is recalled that at the time of prestress transfer, the allowable stress condition at the top face of the girder can be written as

$$- \frac{P_i}{A} + \frac{P_i e}{S_t} - \frac{M_{dg}}{S_t} \leq 0.2\sqrt{f'_{ci}} \tag{5.4}$$

Defining k_b as the distance from the centroid of the girder cross section to the lower limit of the central kern area, or $k_b = S_t/A$, one can rewrite Eq. (5.4) as follows:

$$P_i (e - k_b) - M_{dg} \leq 0.2\sqrt{f'_{ci}}\, S_t \tag{6.2}$$

Assuming that the ratio P_e / P_i is R, the above equation can be rewritten as

$$e \leq k_b + \frac{1}{P_e}[R(M_{dg} + 0.2\sqrt{f'_{ci}}\, S_t)] \tag{6.3}$$

Similarly, if k_t is the distance from the centroid of the girder cross section to the upper limit of the central kern area, or $k_t = S_b / A$, one can rewrite the allowable stress condition at the bottom face of the girder at transfer (Eq. 5.5) as

$$e \leq \frac{1}{P_e}[R(M_{dg} + 0.6 f'_{ci} S_b)] - k_t \tag{6.4}$$

At serviceability limit states, the allowable stress condition at the top face of the girder (Eq. 5.9) can be rewritten as

$$e \geq k_b + \frac{1}{P_e}\left[(M_{dg} + M_{ds}) + (M_{da} + M_l)\frac{S_t}{S_{ic}} - 0.45 f'_c S_t\right] \quad (6.5)$$

and at the bottom face of the girder (Eq. 5.10)

$$e \geq \frac{1}{P_e}\left[(M_{dg} + M_{ds}) + (M_{da} + M_l)\frac{S_b}{S_{bc}} - 0.2\sqrt{f'_c} S_b\right] - k_t \quad (6.6)$$

The geometric properties of the girder cross section, i.e. S_t, S_b, A, and subsequently k_b and k_t are given. Also, the values of S_{ic} and S_{bc} associated with the transformed composite section can easily be calculated. The magnitudes of the applied moments, M_{dg}, M_{ds}, M_{da} and M_l can readily be determined. Moreover, girder concrete strength at transfer, f'_{ci}, and at 28 days, f'_c, are given for a particular design. The only unknown variables in Eqs (6.3) to (6.6) are e and P_e.

For the design example under consideration, the following information is known:

- $S_t = 0.2166$ m^3, $S_b = 0.2203$ m^3 and $A = 0.4994$ m^2. Subsequently, $k_b = 0.4337$ m and $k_t = 0.4410$ m.
- $S_{ic} = 1.1698$ m^3 and $S_{bc} = 0.3304$ m^3.
- At girder mid-span, $M_{dg} = 1.768$ MN·m, $M_{ds} = 2.341$ MN·m, $M_{da} = 0.642$ MN·m and $M_l = 2.279$ MN·m. The magnitude of M_l is obtained from program BRIDGE used aside from IDESIGN.
- $f'_c = 60.2$ MPa, obtained from the optimization process. Thus, $f'_{ci} = 42.2$ MPa.

To solve the problem graphically, one can plot the curves corresponding to Eqs (6.3) to (6.6) at equality as shown in Fig. 6.5. Each curve separates the plane into two parts, one where the inequality is satisfied and the other where it is not. If e (or in this case e_c) is plotted versus P_e, the curves will be hyperbola. However, if e_c is plotted versus $1/P_e$, then straight lines are obtained and the graphical representation is much simplified. When plotted as shown

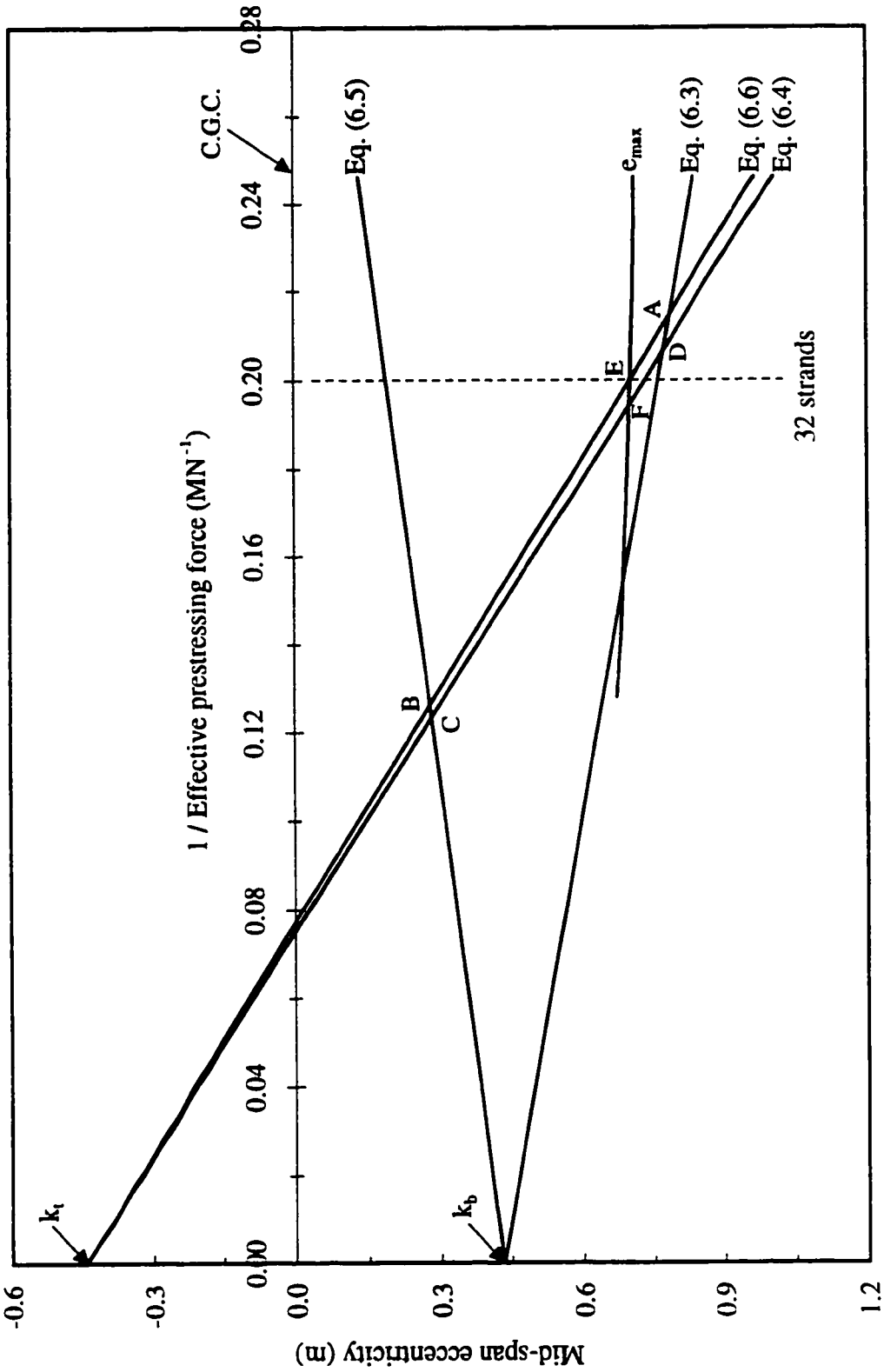

Figure 6.5 Graphical solution of the allowable stress inequality conditions

in the figure, the inequality equations delineate a feasible zone limited by the area ABCD. Essentially any point inside this zone has coordinates P_e and e_c which satisfy the four allowable stress inequality conditions, i.e. Eqs (6.3) through (6.6). The practical constraint on maximum eccentricity, e_{max} (Eq. 5.28) can also be represented at equality on the same graph as shown. In this particular case, the line representing e_{max} intersected the area ABCD producing a new reduced feasible zone limited by the area EBCF. Any point inside this new zone would have satisfactory and practically feasible values of P_e and e_c . The smallest (optimal) value for P_e is obtained at point E, i.e. at the intersection of the lines representing Eq. (6.6) and e_{max}. The coordinates of E can be read on Fig. 6.5 as e_c = 702 mm and $1/P_e$ = 0.20 MN^{-1} which leads to P_e = 5.00 MN; this corresponds to 32 strands. Thus, it can be seen that the graphical solution gives the same answer as that obtained from the optimization process.

6.4 ECONOMIC ANALYSIS

6.4.1 Investigation Layout

In order to achieve the main objective of this study, namely to assess the potential economic advantages from the utilization of HPC for precast, prestressed concrete slab-on-girder bridges, the developed optimization system was used to generate some 115 optimal superstructure designs for a bridge of a configuration typical or representative of most existing bridges of this type. The resulting designs were compared for their relative initial cost effectiveness on a dollar-per-square-metre-of-deck basis to determine the economic impact of using HPC for such bridges.

The representative bridge used for this study consisted of two equal spans. It had three traffic lanes with an overall width of 12 m. Strength of the cast-in-place deck slab was fixed at 35 MPa. There were three main parameters that were varied throughout the generated series of optimal designs due to their potentially significant impact on any economic analysis. These parameters were girder cross section, number of girder lines (or transverse

girder spacing) and girder span length. Each of these three parameters is now discussed in detail.

1. Girder Cross Section

As was mentioned in Sec. 5.2.2, five standard CPCI girder cross sections were used for this study. These are CPCI Type 1200, 1400, 1600, 1900 and 2300. They are commonly used in Canada for highway bridges with span lengths of up to about 50 m. It is outside the scope of this study to examine every I-girder cross section because the number of available girder sections is simply prohibitive. A recent study [125] has reported over 100 existing precast, pretensioned bridge girder sections in the United States. In Canada, several Provinces have developed their own girder sections. However, it has been shown that in some cases, the use of standard CPCI girders or standard AASHTO girders, for example, results in practically identical optimal solutions [102]. It is believed that the girder types used for this study constitute an adequate range over which it would be possible to generalize the conclusions obtained.

2. Number of Girder Lines (or Transverse Girder Spacing)

Although the fact that, for a given bridge width and span, it is most economical to use as few girder lines as possible has been known for quite some time [76,77], common practice in the design and construction of precast, prestressed concrete slab-on-girder bridges has been to place girders close to each other with transverse spacings rarely exceeding 2.5 m, but most often less than 2.0 m. As a result of the increase in girder capacity associated with the use of HPC, it has become possible to convince designers to use fewer girder lines for a given bridge width and span. In this study, spacings of the girders were varied as 3.0, 4.0 or 6.0 m. Similar to what was explained in Sec. 6.3.1, these spacings were chosen because they optimized the design of the exterior and interior girders when 4, 3 or 2 girder lines were used, respectively. Although the use of 2 girder lines spaced at 6.0 m for a 12-m wide slab-on-girder bridge is virtually unheard of in North America, there is at least one of a comparable width in Europe. It has been recently built in Spain [67]. The superstructure is simply supported and consists

of eight equal spans of 26.25 m each. It is 11.3-m wide, with 2 I-girder lines spaced at 6.5 m to support a 250-mm thick deck slab. This experimental bridge has no intermediate diaphragms; the 1738-mm deep, pretensioned girders are just braced over the piers using precast braces. One might argue that for the bridge layout in this study, a slab overhang cantilevering 3.0 m would be excessive. However, box-girder bridges with overhangs of 3.0 m and more have performed satisfactorily for many years; there is no apparent reason why slab-on-girder bridges with similar overhangs should not perform adequately.

It should be noted that while the 4.0-m girder spacing used in this study exceeded the 3.7-m maximum limit imposed by the OHBDC [94] when designing deck slabs according to the empirical design method, it was less than the equivalent limit in the AASHTO LRFD specifications [151] as was mentioned in Sec. 4.6.2. The latter limit was used in this case. For this spacing, the overhang was 2.0 m which would violate the constraint on the length of the slab overhang imposed by the OHBDC. As was explained in Sec 5.4.3.5, for dead load analysis, the OHBDC allows the use of the beam analogy method for bridges having longitudinal girders and an overhanging deck slab provided that the overhang does not exceed 60% of the spacing between the girders, nor is it more than 1.8 m (Eq. 5.37). However, the Code states that in a case where such condition is not met, "engineering judgement shall be exercised" as to whether the bridge being designed meets it sufficiently closely for the analysis method to be applicable. It was believed that the 0.2-m difference between the length of the overhang and the imposed limit could be reasonably overlooked in this case. Therefore, for the 4.0-m spacing, this constraint was eliminated from the optimization process.

As for the case of the 6.0-m girder spacing, the investigation of the feasibility of using only 2 girder lines was primarily intended to provide the incentive for designers to consider as few girder lines as possible, and to promote the need for further research in this case. Therefore, practical constraints that would have been violated if considered for the case of 2 girder lines were eliminated from the optimization process. These were the constraint on the length of the overhang discussed above and the constraint on the ratio of centre-to-centre

girder spacing to the thickness of the slab (Eq. 5.36). These constraints are mostly based on conservative empirical results, and in many cases the limits of their applicability could be extended if more extensive laboratory and field testing is carried out as was discussed in Sec. 4.6.2. In addition, the elimination of these constraints does not jeopardize the flexural strength of girders in any way. It should be noted that had the constraint represented by Eq. 5.36 not been eliminated, a 333-mm slab thickness would have been required for this case. Bypassing this constraint allowed for consistency in the design of the various bridge configurations investigated in this study by using a 225-mm thick slab for all of them. Sensitivity of the solutions obtained to different values for the slab thickness will be studied in the next chapter.

3. Girder Span Length

Although this study is directed toward bridges with girders having relatively long spans, it was necessary to adopt a range of span lengths that would be sufficient to generalize the conclusions obtained. The range adopted was from 20 m to 52 m. The incremental increase for the girder span length was taken as 2 m for all cases. This small increment allowed fairly accurate trends to be obtained and made it easier to identify maximum span lengths within an acceptable range.

It is recognized that shipping and handling lengths, girder masses, lateral stability of girders, and prestressing bed capacities that currently exist could limit the type of girders that can be produced. In addition, adequate design information for use with concretes of very high strength may not be available. However, these limitations were not used as a means to restrict potential applications of HPC in precast, prestressed concrete slab-on-girder bridges. The intent of this study was to look beyond current design and production capabilities.

6.4.2 Interpretation and Discussion of Results

6.4.2.1 Cost Effectiveness Studies:

Some 115 optimal design solutions were generated using the developed optimization

system in order to evaluate the cost effectiveness of using concretes with strengths of up to about 100 MPa for precast, prestressed concrete slab-on-girder highway bridges. For every transverse configuration, i.e. for every specified number of girder lines (referred to from now on, for simplicity, as just number of girders), girder span lengths were increased over the adopted range for the girder cross sections considered. For every case, complete design information was obtained. However, what is of interest for the purpose of studying the economic impact of using HPC for bridges is the optimal value of the girder concrete compressive strength, f'_c, along with the value of the cost function. These are tabulated for all of the cases investigated in Tables 6.1 through 6.3. Table 6.1 contains the optimal f'_c and the minimum superstructure cost / deck area for the different combinations of span length and girder cross section, for the 2-girder bridge. It should be mentioned that the CPCI Type 1200 girder was eliminated from this series because it was found that using 2 of these girders with a span length of just 22 m would require them to be manufactured with concrete of a strength of about 100 MPa from the outset. Tables 6.2 and 6.3 contains the results for the 3-girder bridge and the 4-girder bridge, respectively. It should be emphasized that the cost data contained in these tables excludes the costs of such items as slab formwork, wearing surfaces, traffic barriers and drains. As was explained in Chapter 5, this cost data is relative and not absolute. It was used in this study as a measure of comparison between the various designs. It should not be used, however, as estimates of the actual costs of bridge superstructures.

It can be noted that the optimal values of f'_c contained in Tables 6.1 through 6.3 are distributed in unequal intervals for the equal increments of span length used. For example, for the 2-girder bridge (Table 6.1), using CPCI Type 1400 girders spanning 20 m would require them to be manufactured with concrete of a strength of 52.8 MPa. To span 22 m, the concrete strength used should be 65.0 MPa; up by 12.2 MPa. However, for these girders to span 24 m, the strength required would be 77.9 MPa; up by 12.9 MPa from the value of f'_c for the previous span length. This trend of unequal concrete strength intervals continues for the rest of the equal span length increments. It is desirable to have equal increments of f'_c because

Table 6.1 Results of the optimal design solutions for the 2-girder bridge

Span length (m)	CPCI 1400		CPCI 1600		CPCI 1900		CPCI 2300	
	f'_c (MPa)	Cost ($/m²)	f'_c (MPa)	Cost ($/m²)	f'_c (MPa)	Cost ($/m²)	f'_c (MPa)	Cost ($/m²)
20	52.8	94						
22	65.0	95	48.2	99				
24	77.9	98	57.8	101	44.9	102		
26	91.5	102	67.9	104	52.8	105		
28	105.9	107	78.6	107	61.2	107	46.2	110
30	121.1	113	90.0	111	70.0	110	52.9	112
32			101.9	116	79.4	113	60.0	115
34					89.2	118	67.4	118
36					99.4	123	75.2	122
38					110.1	131	83.3	129
40							91.8	135
42							100.7	143

Table 6.2 Results of the optimal design solutions for the 3-girder bridge

Span length (m)	CPCI 1200		CPCI 1400		CPCI 1600		CPCI 1900		CPCI 2300	
	f'_c (MPa)	Cost ($/m²)	f'_c (MPa)	Cost ($/m²)	f'_c (MPa)	Cost ($/m²)	f'_c (MPa)	Cost ($/m²)	f'_c (MPa)	Cost ($/m²)
20	54.2	97								
22	66.7	100	44.3	105						
24	79.8	103	53.3	108						
26	93.4	108	62.0	111	46.5	118				
28	108.1	113	71.7	115	53.7	121				
30	123.5	121	81.9	119	61.3	125	48.0	127		
32			92.6	124	69.3	129	54.2	130	41.3	136
34			103.9	131	77.8	133	60.8	134	46.3	140
36			115.8	140	86.6	140	67.7	140	51.5	145
38			128.2	152	95.9	149	74.9	148	57.0	152
40					105.7	160	82.5	156	62.7	159
42					115.8	171	90.4	165	68.7	167
44							98.6	175	75.0	176
46							107.2	186	81.5	184
48									88.2	194
50									95.3	204
52									102.5	214

Table 6.3 Results of the optimal design solutions for the 4-girder bridge

Span length (m)	CPCI 1200		CPCI 1400		CPCI 1600		CPCI 1900		CPCI 2300	
	f'_c (MPa)	Cost ($/m²)	f'_c (MPa)	Cost ($/m²)	f'_c (MPa)	Cost ($/m²)	f'_c (MPa)	Cost ($/m²)	f'_c (MPa)	Cost ($/m²)
22	52.2	108								
24	61.2	112								
26	71.7	116	47.7	124						
28	83.0	121	55.2	128						
30	94.8	127	63.1	133	47.4	142				
32	107.4	134	71.4	137	53.7	147	42.0	151		
34	120.6	144	80.2	143	60.2	152	47.1	156		
36			89.3	151	67.1	159	52.5	163		
38			99.0	162	74.4	169	58.2	172	44.3	180
40			109.0	176	81.9	180	64.1	182	48.8	189
42			119.5	191	89.8	192	70.2	192	53.5	199
44					98.0	204	76.6	203	58.4	209
46					106.6	218	83.3	214	63.4	219
48							90.3	226	68.7	230
50							97.5	239	74.2	240
52									79.9	252

it would make it possible to interpret the results more readily. An increment of 10 MPa is reasonable within the range of strengths considered. The approach used to equalize the increments of f_c' was to plot the data contained in the tables for each of the three bridge configurations, and then to interpolate on the graphs to find the corresponding values of span length and cost function for every 10-MPa increment of girder concrete strength.

Figures 6.6 through 6.11 depict the results of the optimal design solutions contained in Tables 6.1 through 6.3. Figure 6.6, for example, is a plot of girder concrete strength versus span length for the various girder cross sections in the 2-girder bridge. A plot of the same values of girder concrete strength versus the corresponding minimum superstructure cost for the different girder sections in the 2-girder bridge is shown in Fig. 6.7. The results of the 3-girder bridge are plotted in Figs 6.8 and 6.9, and those of the 4-girder bridge are illustrated in Figs 6.10 and 6.11.

Before carrying on with the approach outlined above for equalizing the increments of f_c', it is worthwhile mentioning some observations regarding Figs 6.6 to 6.11. It can be noted that the plots of the relationship between the girder concrete strength and its span length for all bridge configurations (see Figs 6.6, 6.8 and 6.10) have the same general trends. It can be seen that, for a given transverse girder spacing (i.e. number of girders), increasing the girder concrete strength results in an increase in its span length. During the optimization process, span length was considered as a preassigned parameter while concrete strength was treated as a design variable. By examining constraint activity at the optimal points, it was found that these span lengths were actually the maximum achievable spans at the corresponding optimal values of f_c'. For example, for the 2-girder bridge (Table 6.1), the maximum achievable span of a CPCI Type 1400 girder made with 65.0-MPa concrete is 22 m. Increasing this girder's span length, for the same concrete strength, beyond 22 m would violate the active allowable stress constraints. It follows, therefore, that Figs 6.6, 6.8 and 6.10 can be used by designers at the preliminary design stage to determine the maximum achievable span length of a certain

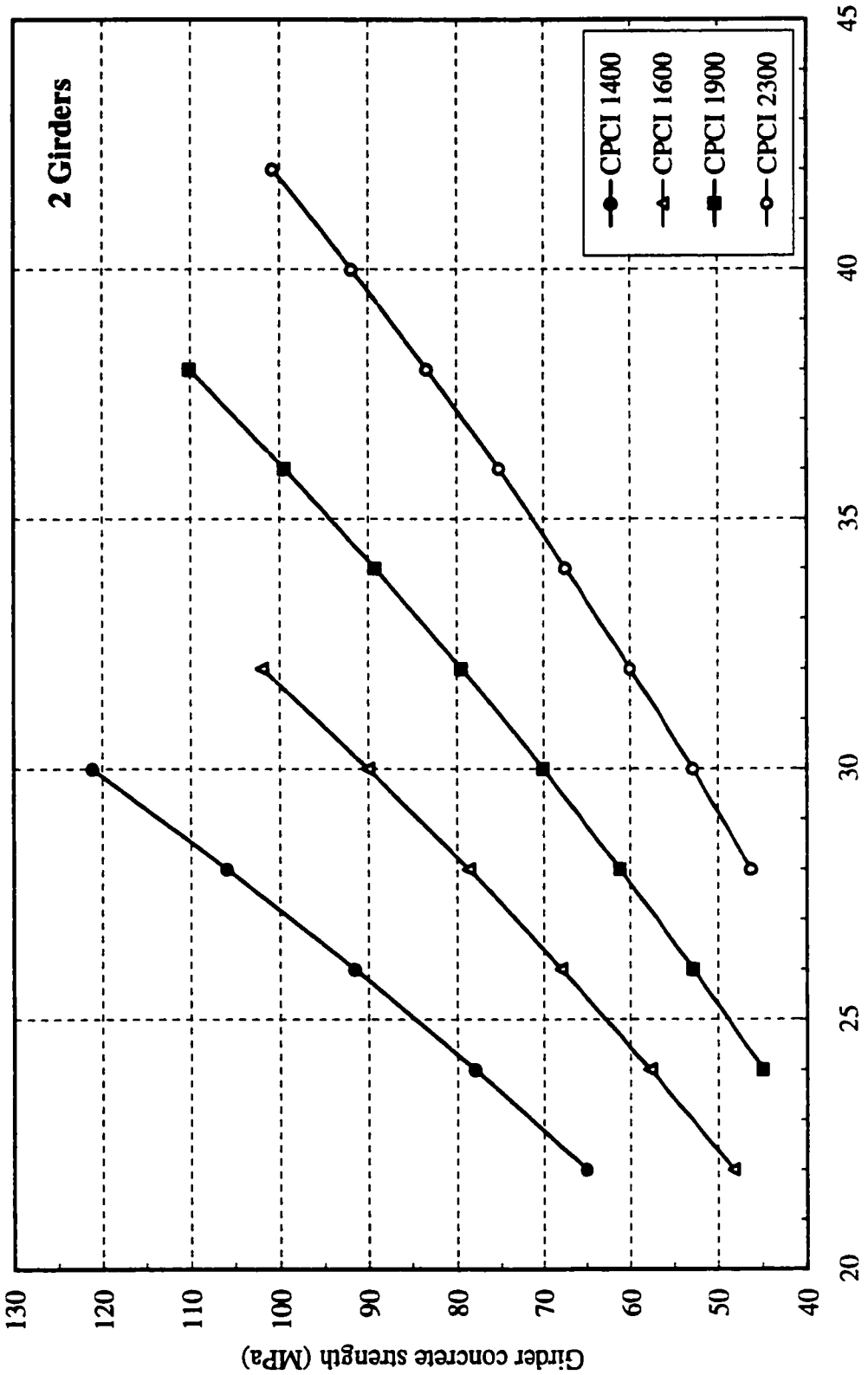

Figure 6.6 Girder concrete strength vs. span length for the 2-girder bridge

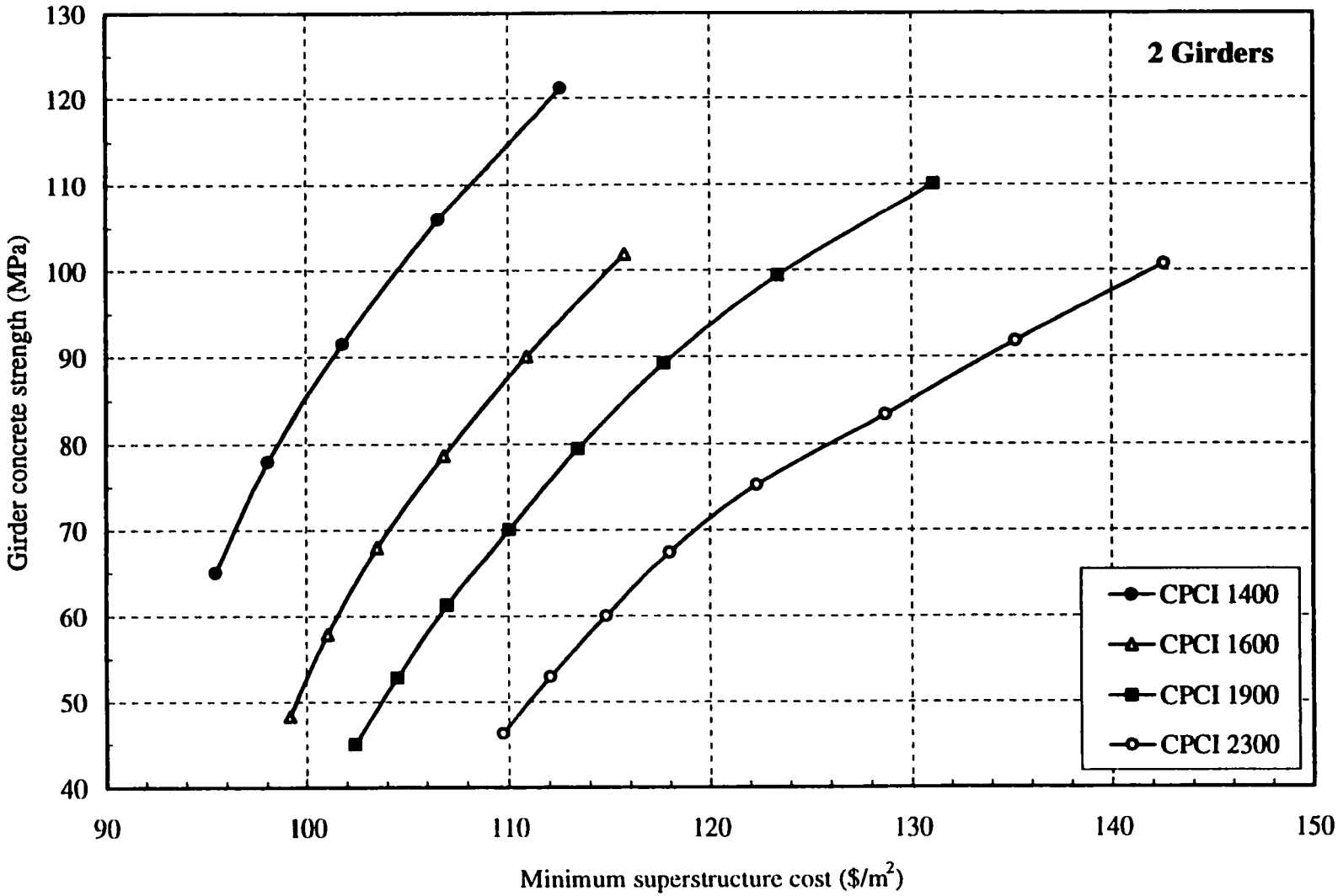

Figure 6.7 Girder concrete strength vs. minimum superstructure cost for the 2-girder bridge

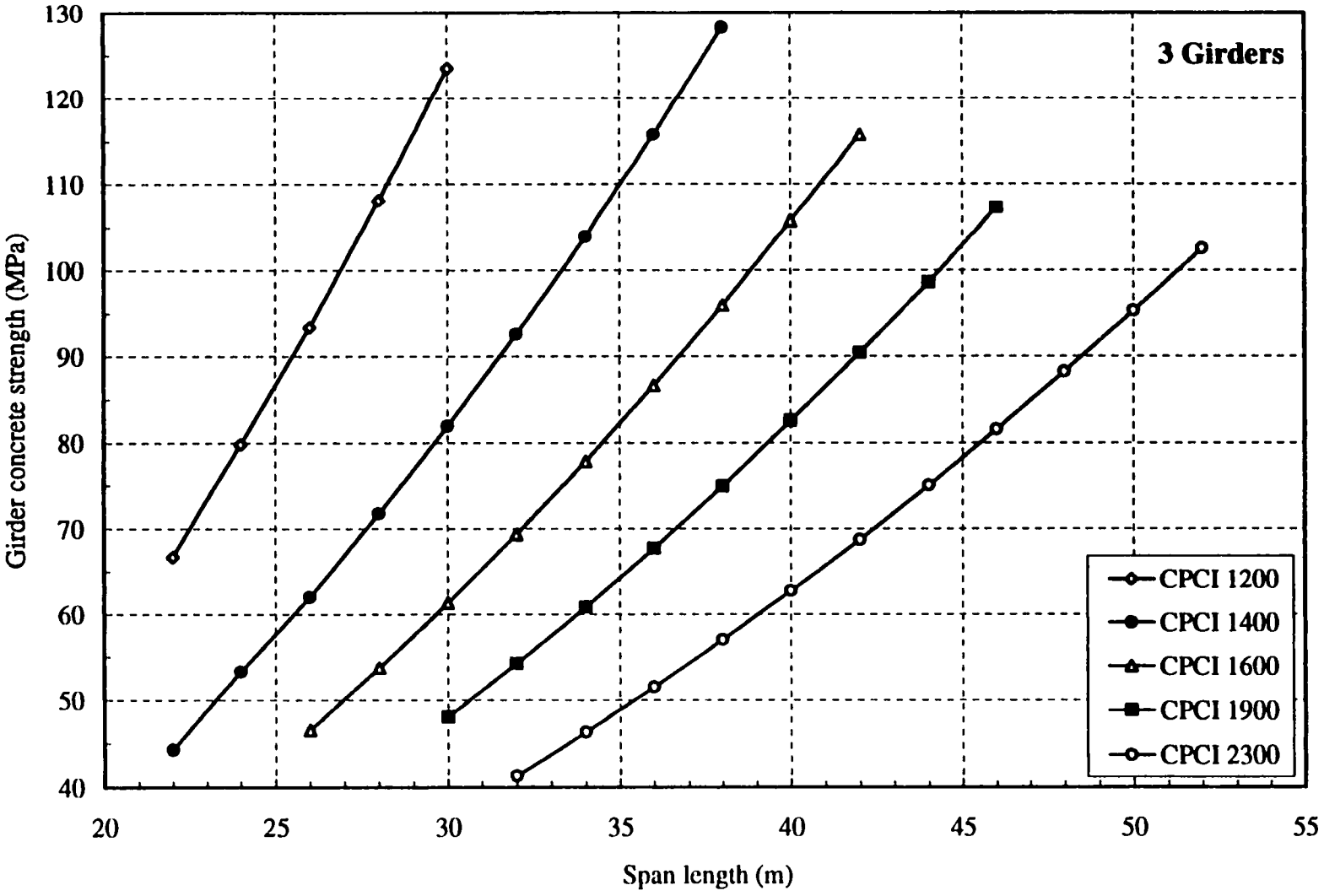

Figure 6.8 Girder concrete strength vs. span length for the 3-girder bridge

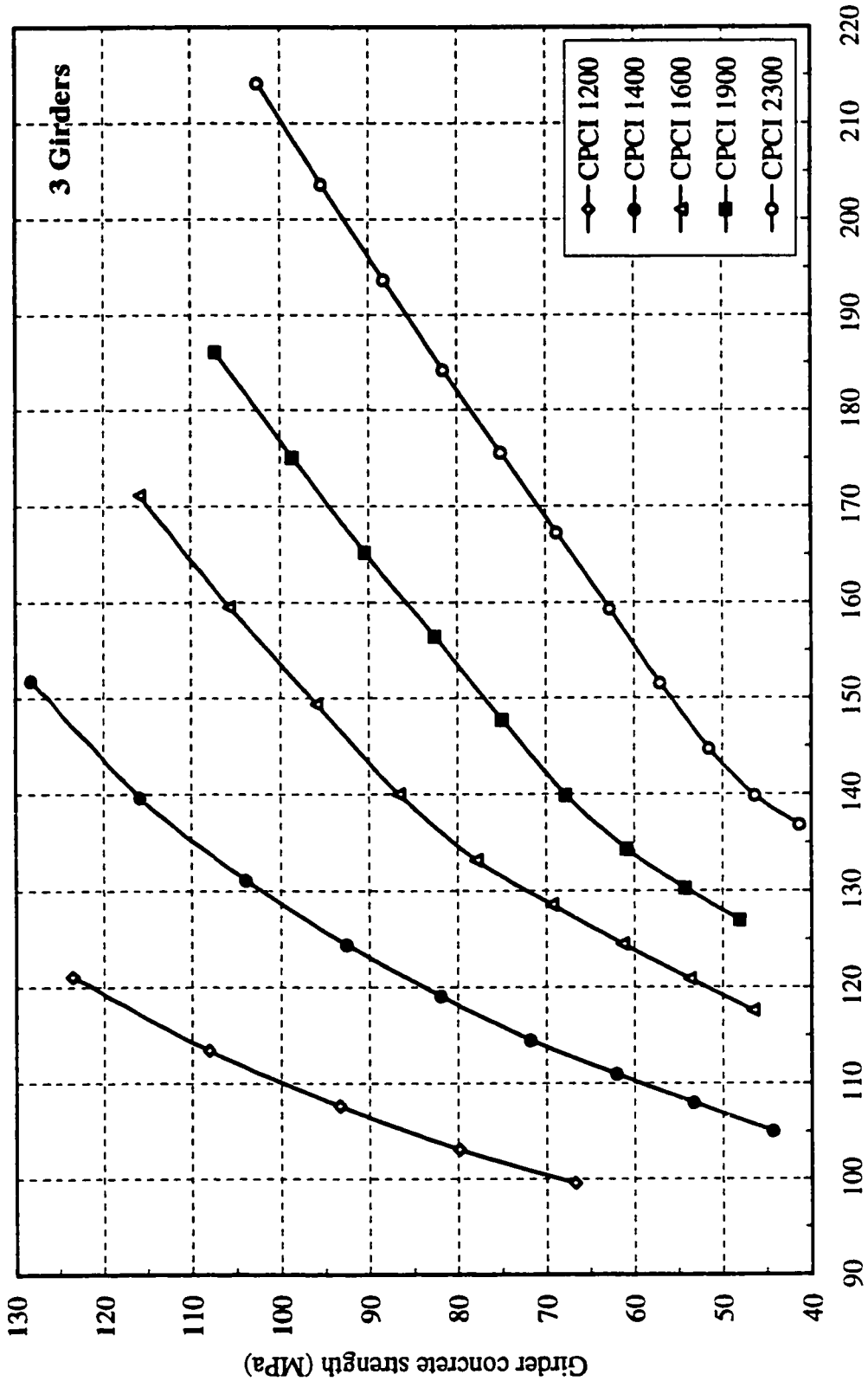

Figure 6.9 Girder concrete strength vs. minimum superstructure cost for the 3-girder bridge

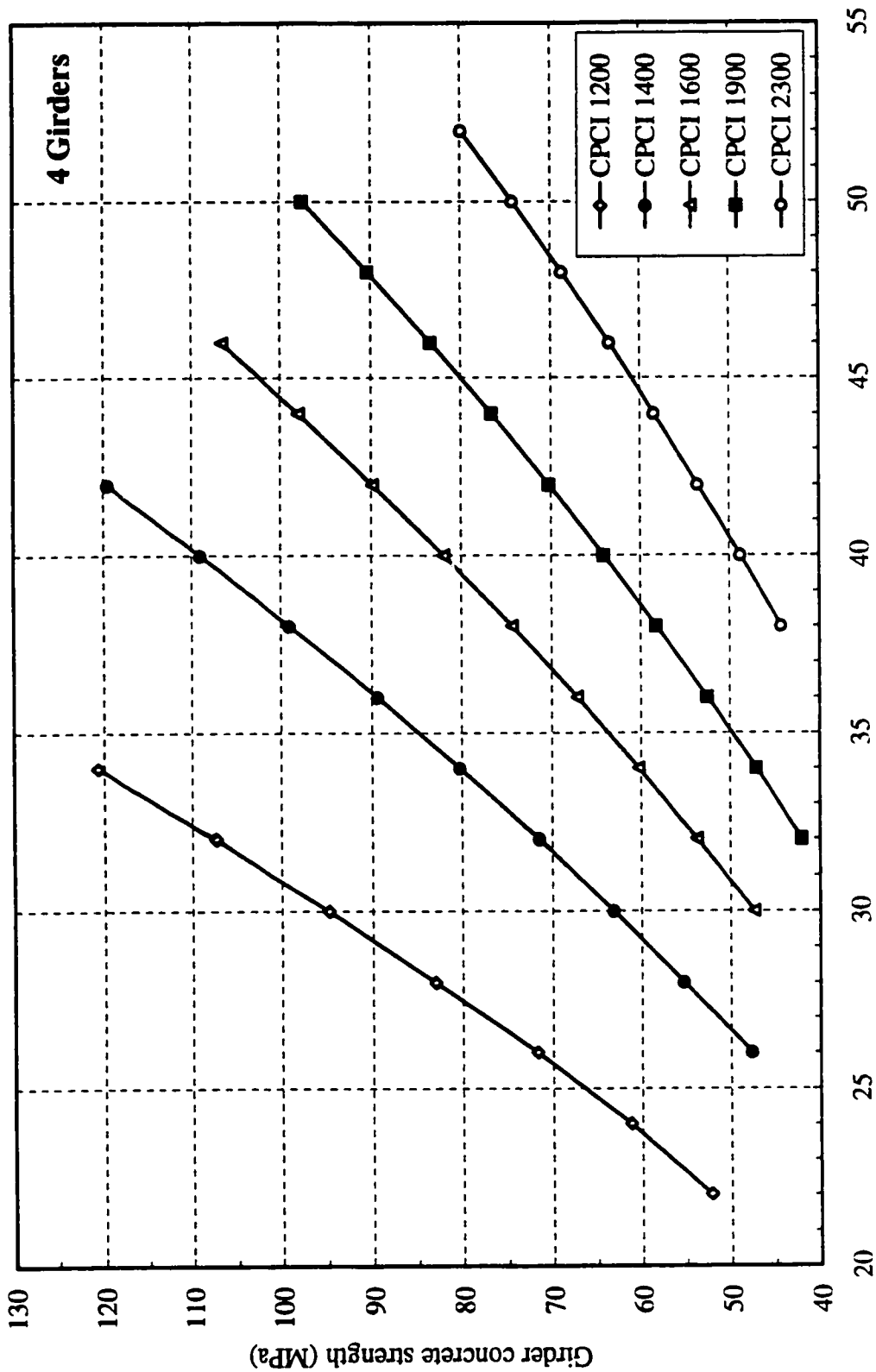

Figure 6.10 Girder concrete strength vs. span length for the 4-girder bridge

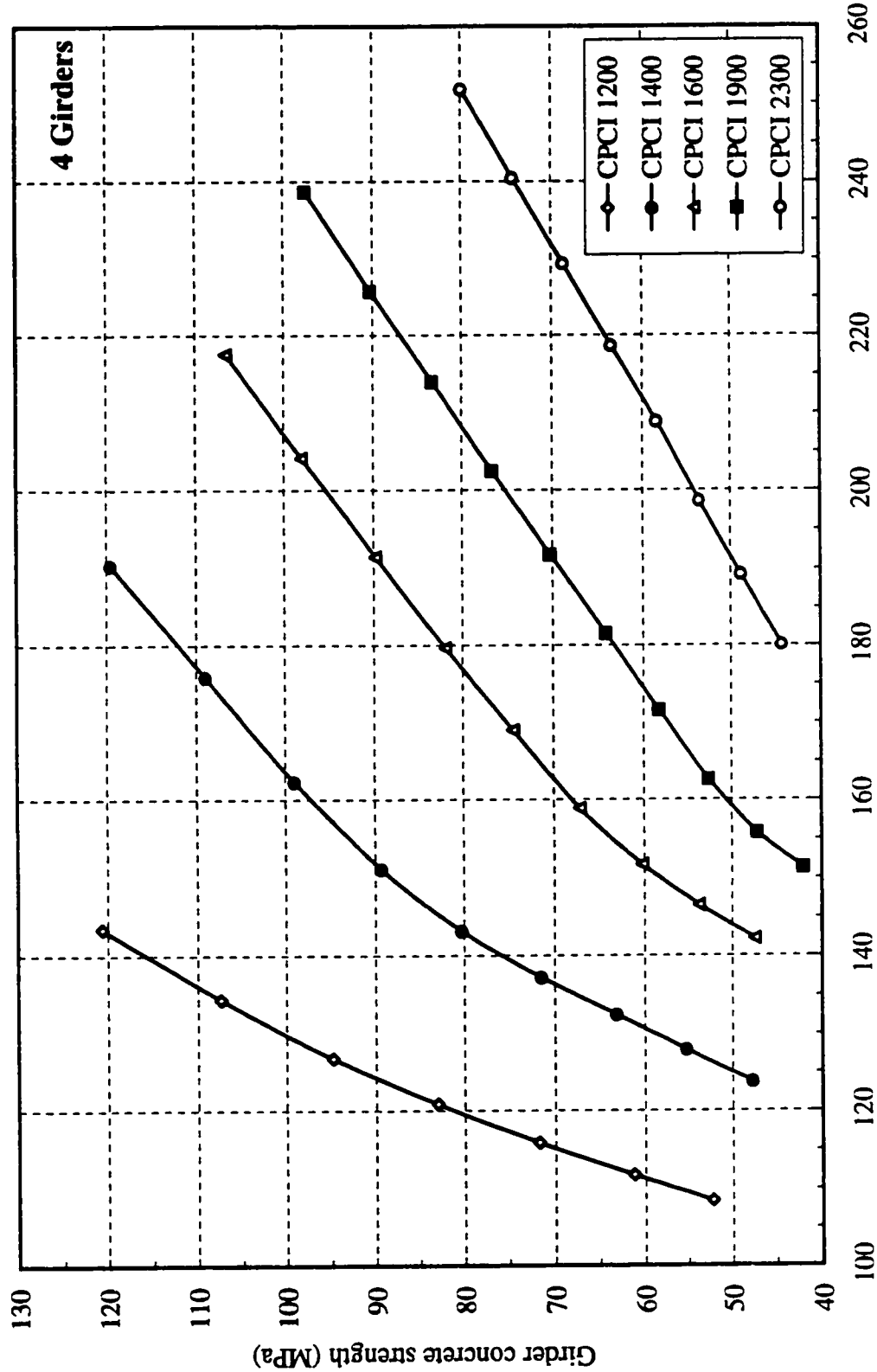

Figure 6.11 Girder concrete strength vs. minimum superstructure cost for the 4-girder bridge

CPCI girder made with concrete of a specified strength for a given bridge configuration. This will be discussed further in the next section.

Examining Figs 6.7, 6.9 and 6.11 which depict the relationship between girder concrete strength and the minimum superstructure cost for all bridge configurations reveals that these plots also have the same general trends. It can be seen that, for a given number of girders, increasing the girder concrete strength results in an increase in the superstructure cost because of the higher cost of concretes of higher strength. The shape of the curves mostly resembles the third-degree curve established previously in Chapter 5 (see Fig. 5.4) for the relationship between the girder concrete strength and the concrete mix cost ratio. In some cases, however, it can be noted that the plots take more of a straight line shape than a curved path. This is especially true for CPCI Type 2300 girders in the 3-girder bridge (see Fig. 6.9) and for both CPCI Type 1900 and Type 2300 girders in the 4-girder bridge (see Fig. 6.11). To determine the reasons behind this behaviour, the major cost components were compared for a CPCI Type 1400 girder and a CPCI Type 2300 girder, both in the 3-girder bridge. The plot corresponding to the former has a curved shape to it, while the major portion of the plot corresponding to the latter takes more of a straight line shape. The cost components considered for comparison were the cost of concrete as well as transportation and erection costs. It was felt that studying these two cost components more closely would reveal the reasons behind that behaviour. Figure 6.12 illustrates the variations of these cost components for a single girder over a range of span lengths for both girder sections. On the same figure also are plots of the sum of the two cost components for each girder cross section. It helps here to recall shapes of the plots established previously in Chapter 5 for transportation and erection costs of precast girders (see Figs 5.5 and 5.6). From Fig. 6.12, it can be noted that transportation and erection costs constitute the major portion of the total cost of a girder. Plots representing these costs are mostly straight lines. This is true for both girder sections. However, for the shallower girder section, the shape of the total cost plot follows primarily the curved path of the concrete cost plot as it goes to higher strengths. For the other section, the effect of the concrete cost plot is not that profound because this deeper section can span

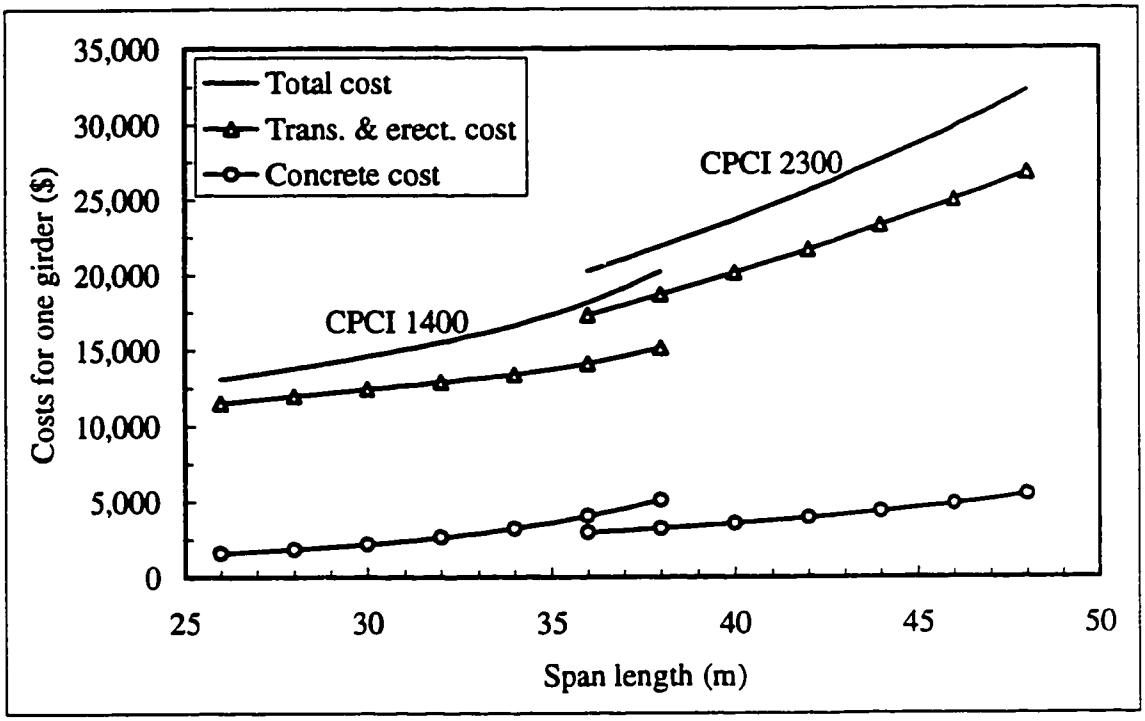

Figure 6.12 Cost components and the corresponding total cost of a single girder in the 3-girder bridge

longer lengths utilizing relatively lower concrete strengths than the shallower section. Because of this, the curvature of the plot for the former is flatter than that for the latter. When the flatter concrete cost curve is added to the mostly straight-line shaped transportation and erection cost curve, the resulting total cost plot is also mostly a straight line. It follows, therefore, that transportation and erection cost trends can dominate bridge superstructure costs in general. For longer and heavier precast girders, closer attention must be paid to the assessment of the costs associated with their shipping and handling. It is recalled here that estimates of girder transportation and erection charges used in this study are based on an average cost of $6000 per girder, as was mentioned in Sec. 5.3.3.

Attention is now drawn back to the approach outlined earlier for equalizing the increments of f'_c. Values of the span length corresponding to every 10-MPa increment of f'_c were interpolated on Figs 6.6, 6.8 and 6.10, and values of the minimum superstructure cost

corresponding to the same increments of f_c' were interpolated on Figs 6.7, 6.9 and 6.11 for all bridge configurations. The resulting data was plotted in Figs 6.13, 6.14 and 6.15 for the 2-girder bridge, 3-girder bridge and 4-girder bridge, respectively. It must be noted that in these figures and in some of the figures to follow, similar values for the cost function were obtained in some instances for the same span length using different girder cross sections. Therefore, the curves associated with these values tended to overlap when the data was plotted. Thus, on occasion it may be difficult to distinguish the resulting curves at some of the span lengths. Keeping this in mind, as the figures are examined, will lessen any possible confusion.

Figure 6.13 illustrates the variations in the minimum superstructure cost with span length for the various girder sections in the 2-girder bridge. Girder concrete strength associated with the first point on each curve is shown in the figure. Strengths corresponding to subsequent points on each curve are increased in 10-MPa increments. These curves show that, for a given girder spacing, the cost of a structure increases with the compressive strength as was mentioned earlier in this section. It can also be noted that in order to achieve longer span lengths, the use of concrete of higher strength becomes necessary. Based on these curves, it is possible to identify the most cost effective designs for various ranges of girder span length, assuming that there was no practical limit on the level of concrete strength that can be achieved. It is clear from the curves shown in Fig. 6.13 that for a girder span length of up to 28 m, it would be most economical to use CPCI Type 1400 cross section for the girders. Concrete having a compressive strength of about 106 MPa would be required for this cross section to achieve that span length. From 28 m to about 34.5 m, the most economical cross section for the girders in this bridge configuration would be CPCI Type 1900. For this cross section to reach a span length of 34.5 m, it must be manufactured with concrete of a strength close to 92 MPa. Beyond 34.5 m, the most cost effective design would use CPCI Type 2300 cross section for the girders. At a span length of 34.5 m, these girders would have to be made with a concrete of a strength of about 69 MPa. This strength increases with the increase in span length until it reaches 100 MPa at a span length close to 42 m.

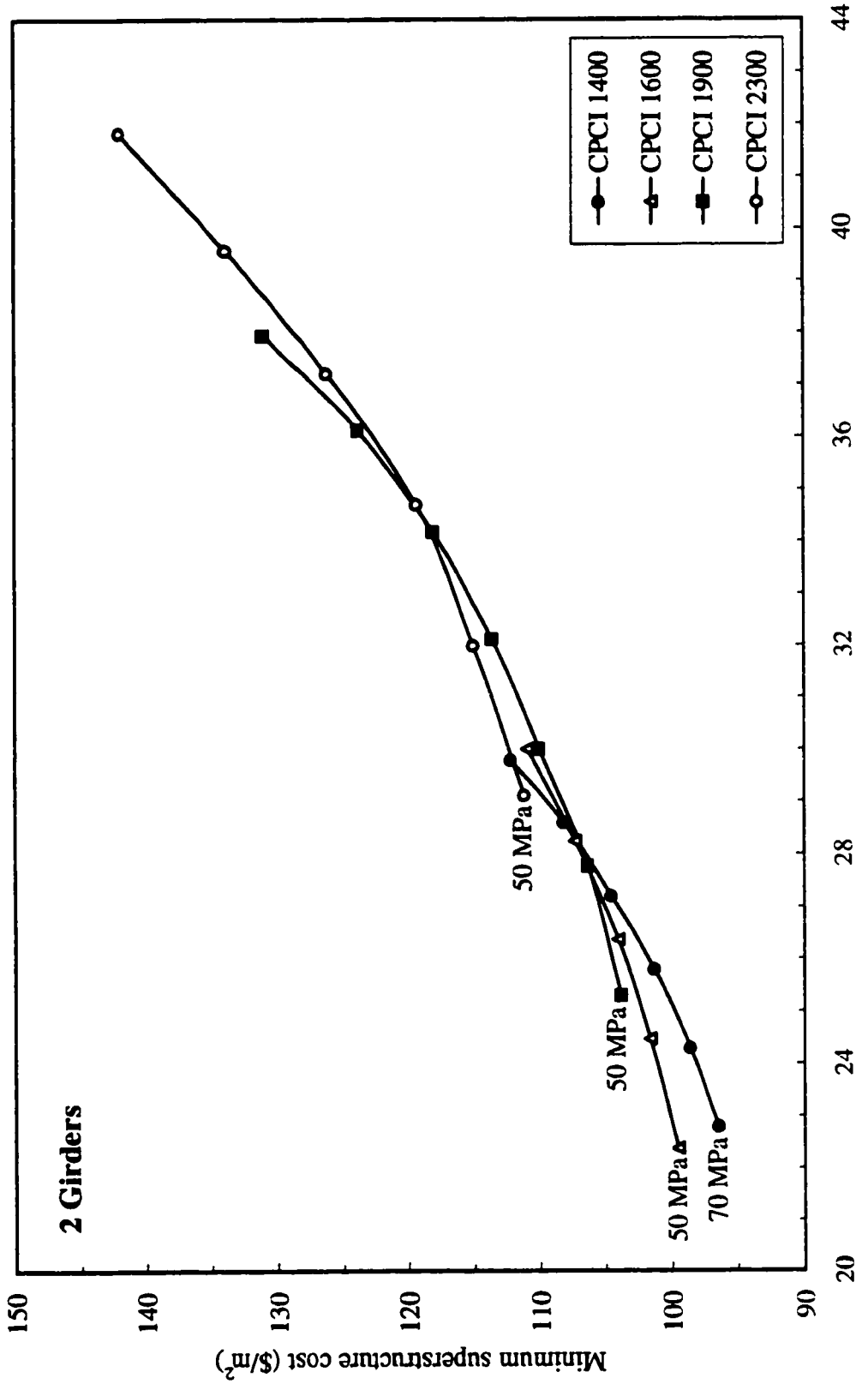

Figure 6.13 Minimum superstructure cost vs. span length for the 2-girder bridge

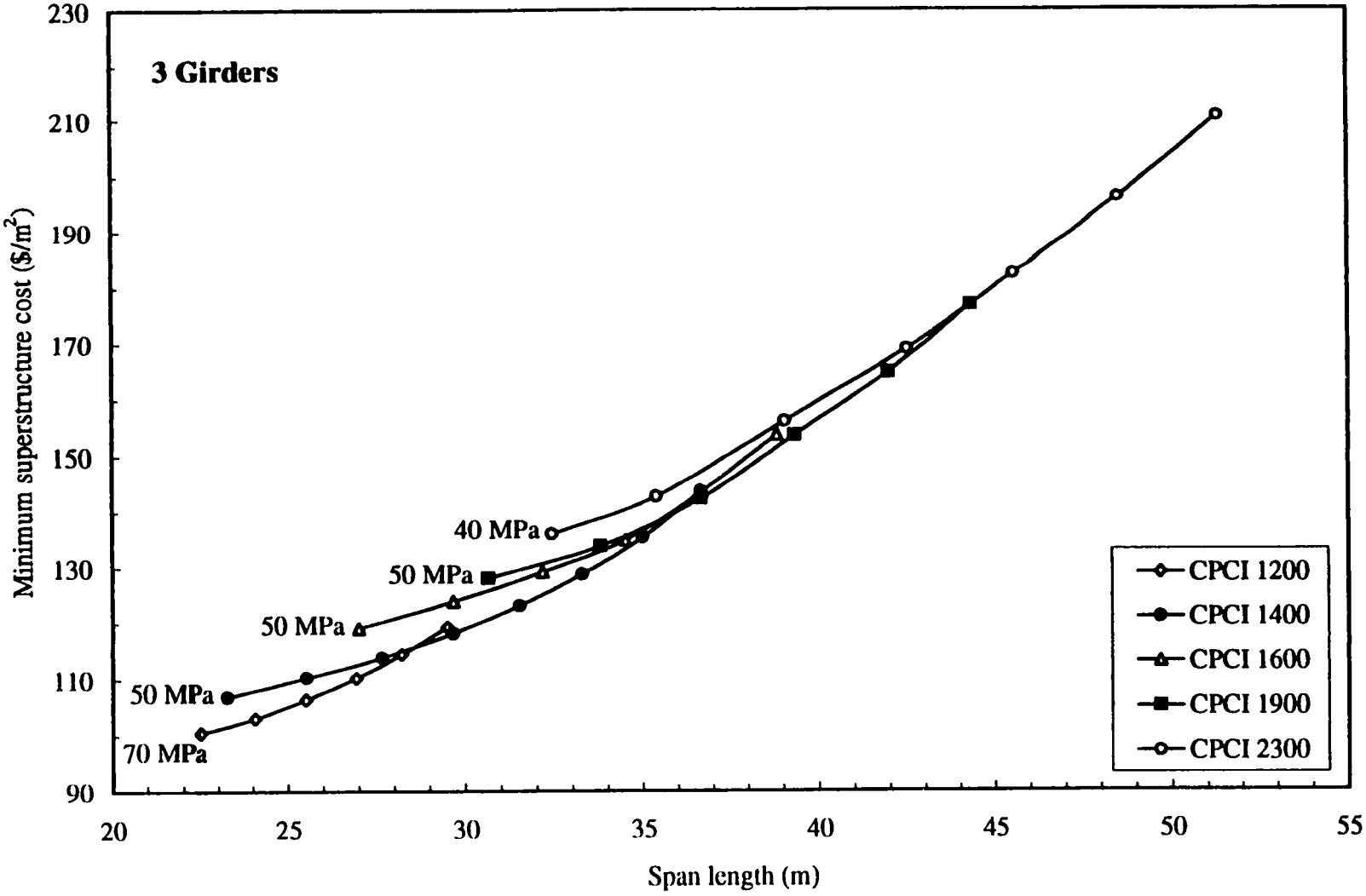

Figure 6.14 Minimum superstructure cost vs. span length for the 3-girder bridge

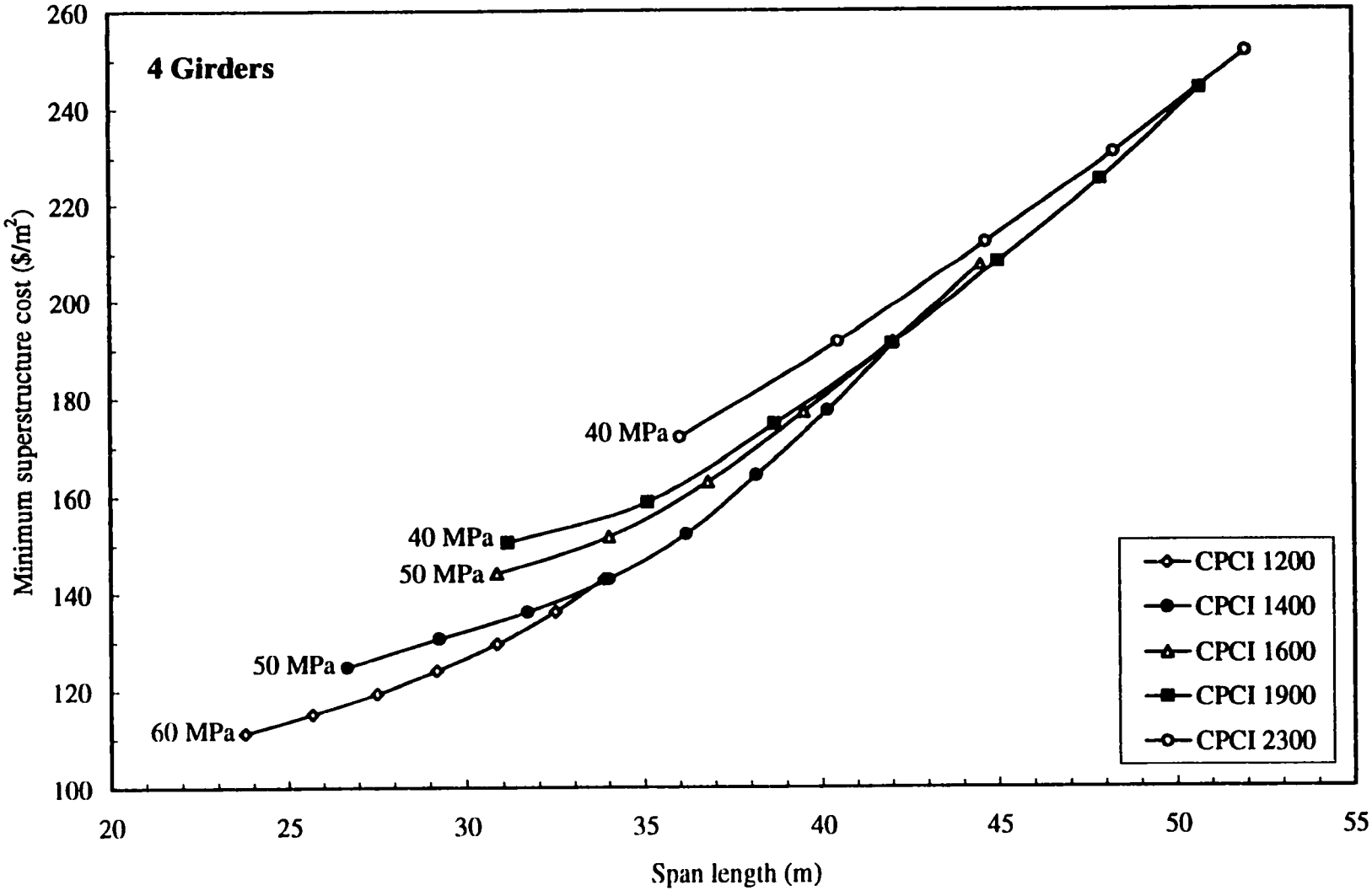

Figure 6.15 Minimum superstructure cost vs. span length for the 4-girder bridge

It is interesting to note in Fig. 6.13 that CPCI Type 1600 cross section never provides the most economical design at any span length, provided that there was no limit on the level of concrete strength that can be used to manufacture Type 1400 girders. This was true for all of the bridge configurations studied, as will be seen shortly. It was expected that Type 1600 would provide the most economical designs for a range of span lengths that is intermediate between spans associated with Type 1400 and those associated with Type 1900. To find out why the curves did not behave accordingly, the major cost components were compared for the different girder sections at a span length of 28 m, where the transition from Type 1400 to Type 1900 occurs. It was found that although the deeper Type 1600 cross section is structurally more efficient than the shallower Type 1400 section in the sense that it can reach this span length using a relatively lower concrete strength, the reduction in the material (i.e. concrete) cost is not sufficient enough to absorb the increase in the erection cost of the heavier Type 1600 section before Type 1900 takes over and becomes economically more competitive. Once again, the influence of girder erection costs on the overall cost of a bridge is clearly demonstrated.

The patterns exhibited in Fig. 6.13 for the 2-girder bridge were typical for all bridge configurations. Figures 6.14 and 6.15 illustrate the variations in the minimum superstructure cost with span length for the various girder cross sections in the 3-girder bridge and the 4-girder bridge, respectively. In a manner similar to that used above for the 2-girder bridge, it is possible to identify the most economical designs for various ranges of girder span length. It can be noted once again from the curves shown in Figs 6.14 and 6.15 that CPCI Type 1600 cross section never provides the most economical design at any span length, for the range of concrete strengths considered.

The data plotted separately in Figs 6.13 through 6.15 for the different bridge configurations was combined in Fig. 6.16 to show the cost effectiveness of the different layouts. Some data points have been eliminated so that the curves of one configuration do not intersect those of another in order to lessen any possible confusion. From the figure, it is clear

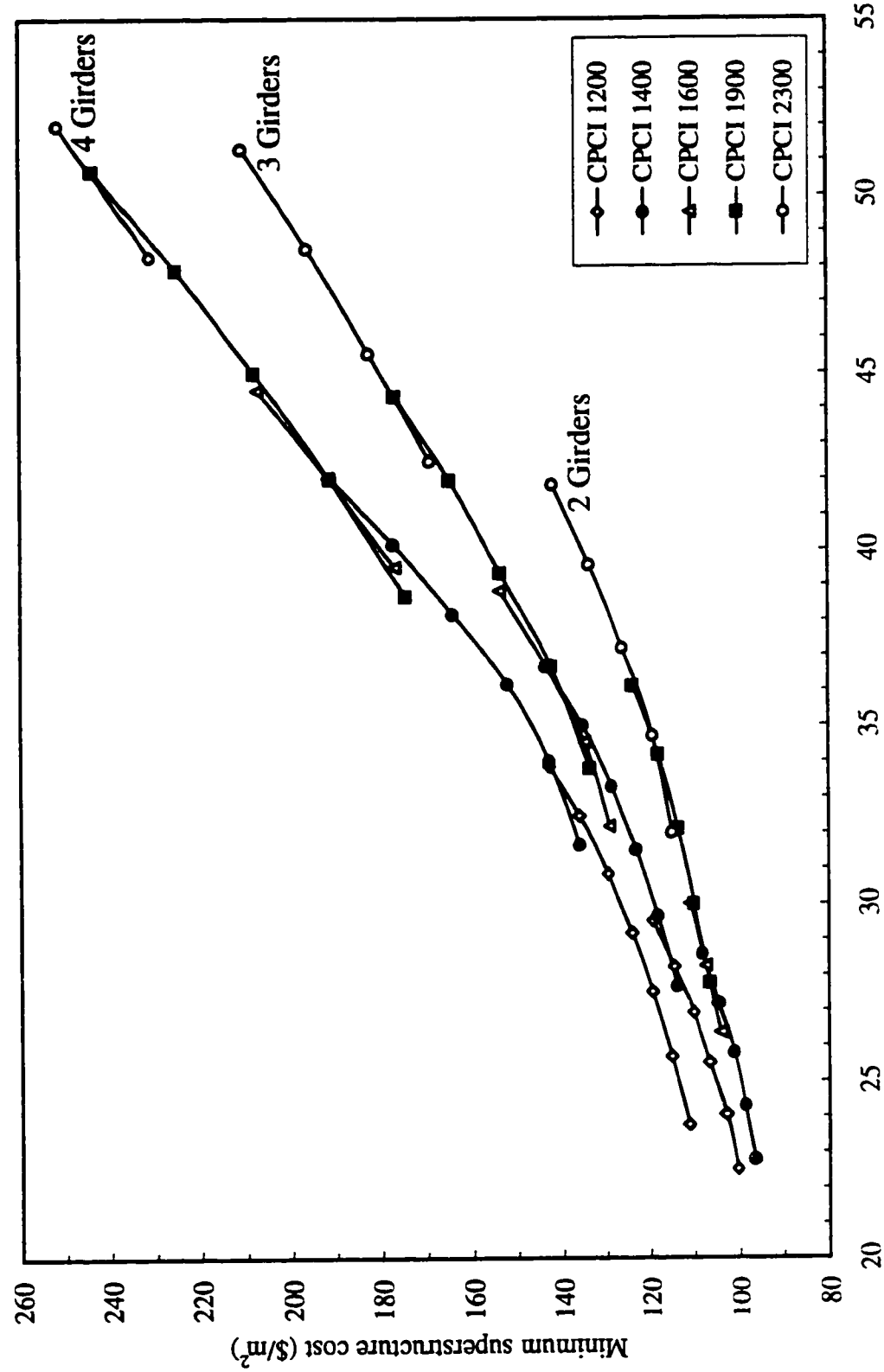

Figure 6.16 Minimum superstructure cost vs. span length for the various bridge configurations

that for a span length of up to about 42 m, it is most economical to use only 2 girders to carry the deck slab. Beyond 42 m, the use of 3 girders provides the most cost effective design. This is assuming that there was no constraints on the production of concretes with compressive strengths of up to about 100 MPa.

Current production capabilities in some precasting plants might preclude producing concretes of very high strength. In this case, Figs 6.13 to 6.15 can be used to establish minimum cost curves for certain maximum concrete strengths. These curves can be used for design purposes when girder concrete strength is specified. Two such curves are plotted in Fig. 6.17 for maximum available girder concrete strengths of 60 MPa and 80 MPa. To explain how these curves were plotted, consider, for example, the one corresponding to a maximum concrete strength of 80 MPa. Referring to Fig. 6.13 of the 2-girder bridge configuration, it can be seen that the most economical design would have to utilize 2 CPCI Type 1400 girders made with concrete of a strength not exceeding 80 MPa for spans up to 24.3 m. Beyond this span length, the most cost effective girders are Type 1600. Thus, there is a "jump" in the cost curve of Fig. 6.17 at 24.3 m. At 27.8 m, it can be seen from Fig. 6.13 that Type 1900 girders become more economical than Type 1600 girders even though the concrete strength of the latter has not reached 80 MPa. There is a smooth transition in the cost curve at 27.8 m from Type 1600 to Type 1900 cross sections. Using 2 Type 1900 girders proves to be most economical from 27.8 m to about 32 m where the maximum limit on concrete strength is reached. The cost curve jumps to the next most cost effective alternative which is 2 Type 2300 girders. These can span up to 37.2 m if manufactured with concrete of a strength not exceeding 80 MPa. Beyond 37.2 m, the most economical design would have to use 3 CPCI Type 1900 girders (see Fig. 6.14). There is a big jump in the cost curve associated with the increase in the number of girders, as shown in Fig. 6.17. Beyond 39.3 m, it would be no longer possible to use concrete strengths not exceeding 80 MPa to make the girders. Therefore, the cost curve jumps to the next most economical alternative which is 3 Type 2300 girders. These can be used for spans up to 45.6 m utilizing concrete strengths not exceeding 80 MPa. Beyond 45.6 m, the most cost effective design would have to utilize 4

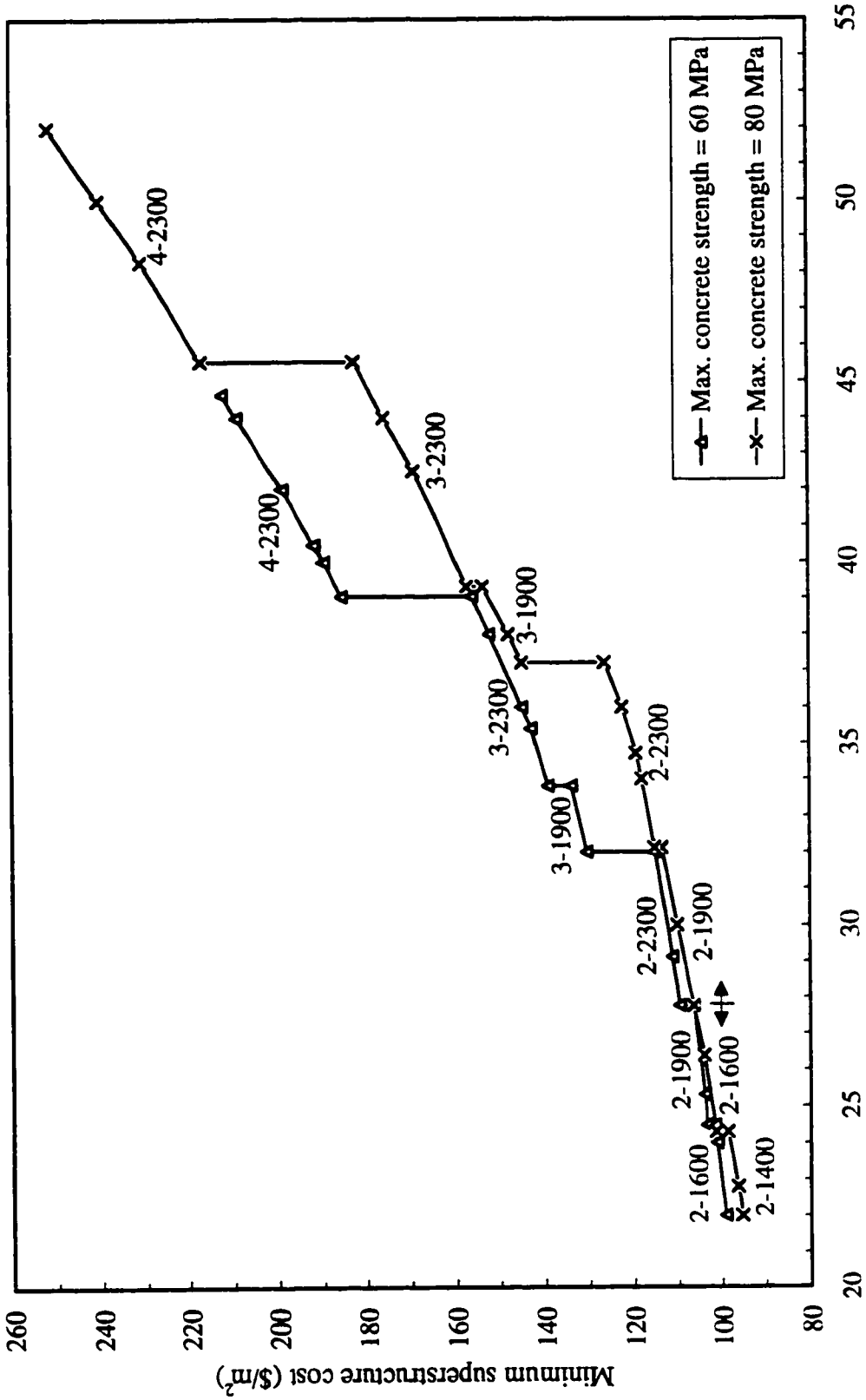

Figure 6.17 Cost curves for maximum girder concrete strengths of 60 MPa and 80 MPa

CPCI Type 2300 girders (see Fig. 6.15) if a maximum concrete strength of 80 MPa is to be used.

Figure 6.17 reveals that, in general, as a result of the increase in girder capacity, the increase in concrete cost associated with the use of concretes of higher strength can be fully offset by the reduced number of girders for a given span length. For example, using concrete with a compressive strength of 60 MPa for CPCI Type 1900 girders to span 33 m would require 3 girders at a total superstructure cost of $\$132/m^2$. Only 2 Type 2300 girders would be required if the concrete strength specified was increased to 80 MPa resulting in a total superstructure cost of $\$116/m^2$. Thus, a saving of about $\$16/m^2$ would be achieved. For this two-span bridge, the cost savings would have exceeded $12,600 or approximately 12% of the total superstructure cost. The economic advantage of using HPC becomes even more apparent for longer span lengths. Referring again to Fig. 6.17, it can be seen that a designer would have to utilize 4 Type 2300 girders made with 60-MPa concrete to span 44 m at a total superstructure cost of $\$209/m^2$. If 80-MPa concrete was used to manufacture the girders, then only 3 of them would be needed resulting in a total superstructure cost of $\$176/m^2$. This would translate into a saving of about $\$33/m^2$. For this bridge, the cost savings associated with the use of the higher-strength concrete would have been close to $35,000 or about 16% of the total superstructure cost.

Figure 6.17 reveals also that the use of a shallower girder cross section manufactured with a higher-strength concrete can be more economical than the use of a deeper section made with a lower-strength concrete. For example, for the range of spans from 27.8 m up to about 32 m, it is more economical to use 2 CPCI Type 1900 girders made with 80-MPa concrete than it is to use 2 Type 2300 girders made with 60-MPa concrete. While the saving in the superstructure cost associated with the use of the shallower section , in this case, did not exceed 3% within the range of spans considered, it is important to keep in mind that there will be other savings from the reduced substructure height. There are other ranges of span lengths in Fig. 6.17 where it can be seen that it is more cost effective to use shallower sections

with higher concrete strengths than it is to use deeper sections with lower concrete strengths.

Figure 6.18 shows the minimum cost curves for maximum available girder concrete strengths of 80 MPa and 100 MPa. The patterns exhibited in this figure are, in general, similar to those demonstrated in Fig. 6.17. It can be seen that as the number of girders decreases as a result of specifying concretes of higher strength, the total superstructure cost also decreases. The economic advantage of using shallower sections made with concretes of higher strength over using deeper sections made with concretes of lower strength is also illustrated. In addition, Fig. 6.18 shows another important conclusion, which concerns the diminishing benefits realized with the use of concretes of very high strength for relatively shorter span lengths. Consider, for example, the range of span lengths from 27.8 m up to about 32 m. It can be seen that, over this range, the cost curves for strengths of 80 MPa and 100 MPa completely overlap, which means that there is no benefit realized from the utilization of the 100-MPa concrete for the 2 CPCI Type 1900 girders at a given span length within the range considered. For these spans, one of the active constraints (governing design criteria) at the optimal point was that represented by Eq. (5.5) which sets the limit on compressive stresses at the bottom face of the girder at the time of prestress transfer. For a given span length, there is a point at which additional prestressing will cause tensile stresses at the top face of the girder regardless of the concrete strength, thus activating the constraint represented by Eq. (5.4). Although these tensile stresses would be offset at the service load condition, the dead load at prestress transfer is constant for a given girder span and cross section. As a result, there would be no beneficial effect realized for very high-strength concretes at these span lengths.

6.4.2.2 Analytical Studies:

It was shown in the previous section that, for a given transverse girder spacing, increasing the girder concrete compressive strength results in an increase in its span length. Increasing girder span lengths is highly beneficial because it results in a reduction in the

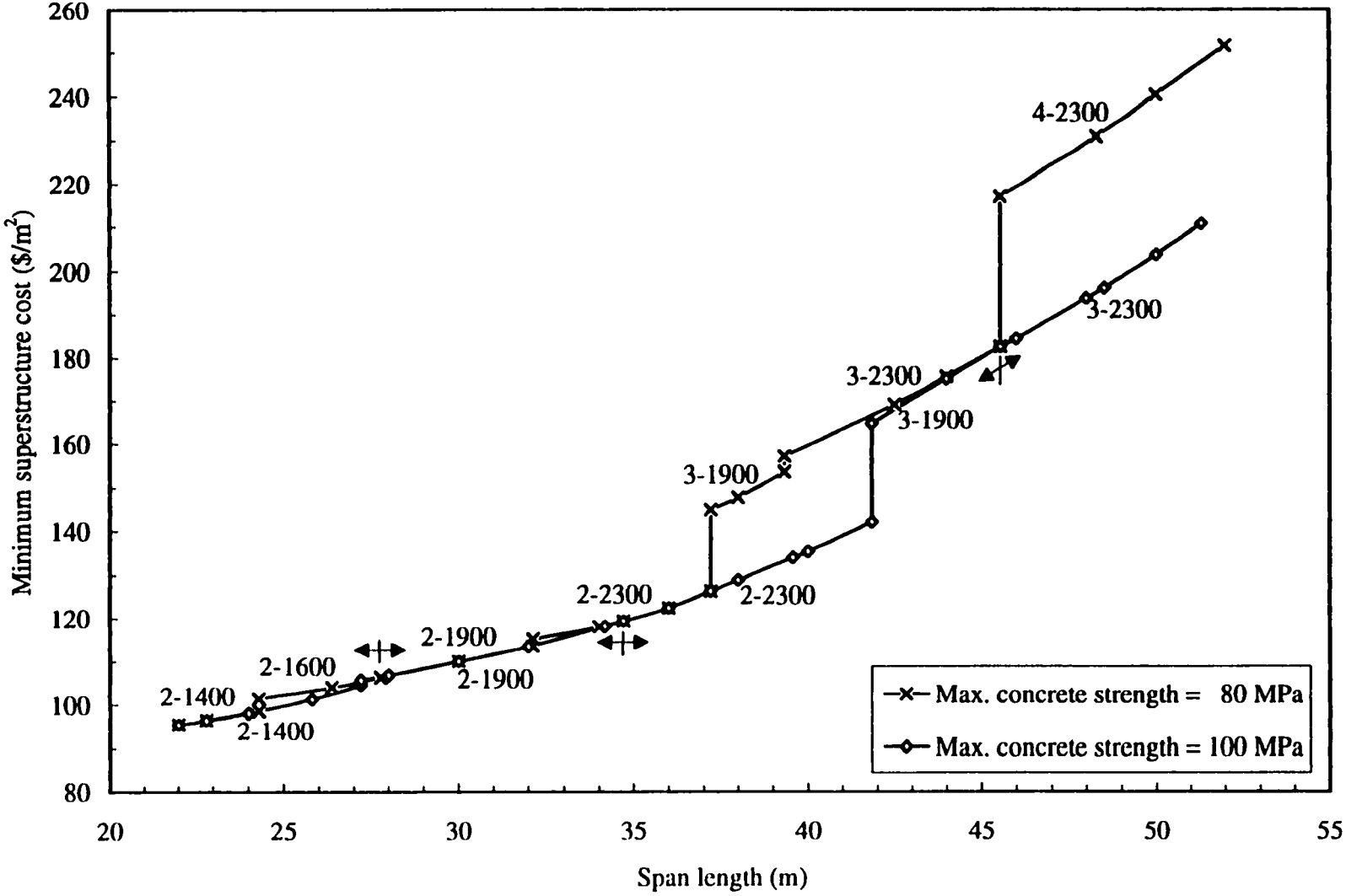

Figure 6.18 Cost curves for maximum girder concrete strengths of 80 MPa and 100 MPa

number of piers and foundations, which in turn reduces the cost of the substructure. If the bridge is crossing a roadway, a reduction in the number of piers and foundations would also ease traffic disruptions to the roadway underneath during construction of the bridge.

Table 6.4 contains the maximum achievable span lengths for the various girder cross sections in the different bridge configurations investigated, at different levels of girder concrete strength, along with the corresponding minimum superstructure costs. On average, an increase in concrete strength from 60 to 100 MPa resulted in a 30% increase in span capability for the five girder types considered in this study. Figures 6.19 through 6.23 illustrate graphically some of the information contained in the table for each of the girders. From the figures, it is clear that increases in concrete strength allow increases in span limits. These figures can be used as guidelines at the preliminary design stage.

Figure 6.24 depicts the relationship between girder concrete strength and maximum span length for the standard CPCI sections studied. The figure illustrates the results of the 3-girder bridge; however, the trends shown are typical of all bridge configurations. Judging from the slopes of the plots in this figure, one can conclude that the deeper girders with larger section moduli utilize the increased concrete strength more efficiently, i.e. the deeper girders have greater span increase capabilities. This fact was noted also in the previous section. It must be mentioned, however, that this study is not advocating the use of deeper sections. As was revealed earlier, the use of shallower sections made with HPC can be more economical than the use of deeper sections manufactured with normal-strength concrete.

Some previous studies in this area [e.g. 43,89] have indicated that continual increases in a girder's concrete strength does not guarantee an increase in its span length. In some cases, the maximum achievable span length levelled off at some level of concrete strength, i.e. there was no further increase in the maximum span when the strength was increased beyond this level. As was discussed previously in Sec. 2.5.2.2, this levelling off of the maximum span length occurs because additional prestressing cannot be fitted into the girder cross section

Table 6.4 Maximum span lengths vs. concrete strengths for the girders investigated, along with the corresponding minimum superstructure costs

Girder type	f'_c (MPa)	3.0-m spacing			4.0-m spacing			6.0-m spacing		
		Span (m)	Cost ($/m²)	Cost‡ ($/m²)	Span (m)	Cost ($/m²)	Cost‡ ($/m²)	Span (m)	Cost ($/m²)	Cost‡ ($/m²)
CPCI 1200	60	23.8	111	63	21.0	98	58	—§	—	—
	70	25.7	115	66	22.5	101	61	—	—	—
	80	27.5	119	70	24.1	103	63	—	—	—
	90	29.2	124	74	25.5	107	67	20.8	93	61
	100	30.8	130	80	26.9	110	70	22.0	95	63
CPCI 1400	60	29.3	131	71	25.5	110	63	21.2	95	59
	70	31.7	136	75	27.7	114	67	22.8	96	60
	80	34.0	143	80	29.7	118	70	24.3	99	64
	90	36.2	152	86	31.5	123	75	25.8	101	66
	100	38.2	164	92	33.3	129	80	27.2	105	70
CPCI 1600	60	34.0	152	77	29.7	124	68	24.5	102	62
	70	36.8	163	82	32.2	129	72	26.4	104	64
	80	39.5	177	88	34.5	135	76	28.2	107	66
	90	42.0	192	96	36.7	144	82	30.0	111	70
	100	44.5	207	103	38.8	154	87	31.6	115	74
CPCI 1900	60	38.7	175	81	33.8	134	71	27.8	106	62
	70	42.0	191	86	36.7	142	74	30.0	110	66
	80	45.0	208	94	39.3	154	80	32.1	114	69
	90	47.9	225	101	42.0	165	85	34.2	118	72
	100	50.7	243	110	44.3	177	91	36.1	124	77
CPCI 2300	60	44.7	212	86	39.1	156	74	32.0	115	65
	70	48.3	231	93	42.5	169	79	34.7	119	68
	80	52.0	252	101	45.6	182	84	37.2	126	72
	90	—	—	—	48.5	196	90	39.6	134	76
	100	—	—	—	51.3	211	98	41.8	142	80

‡ Minimum superstructure cost without transportation and erection charges.

§ Span lengths are not within the range investigated in this study.

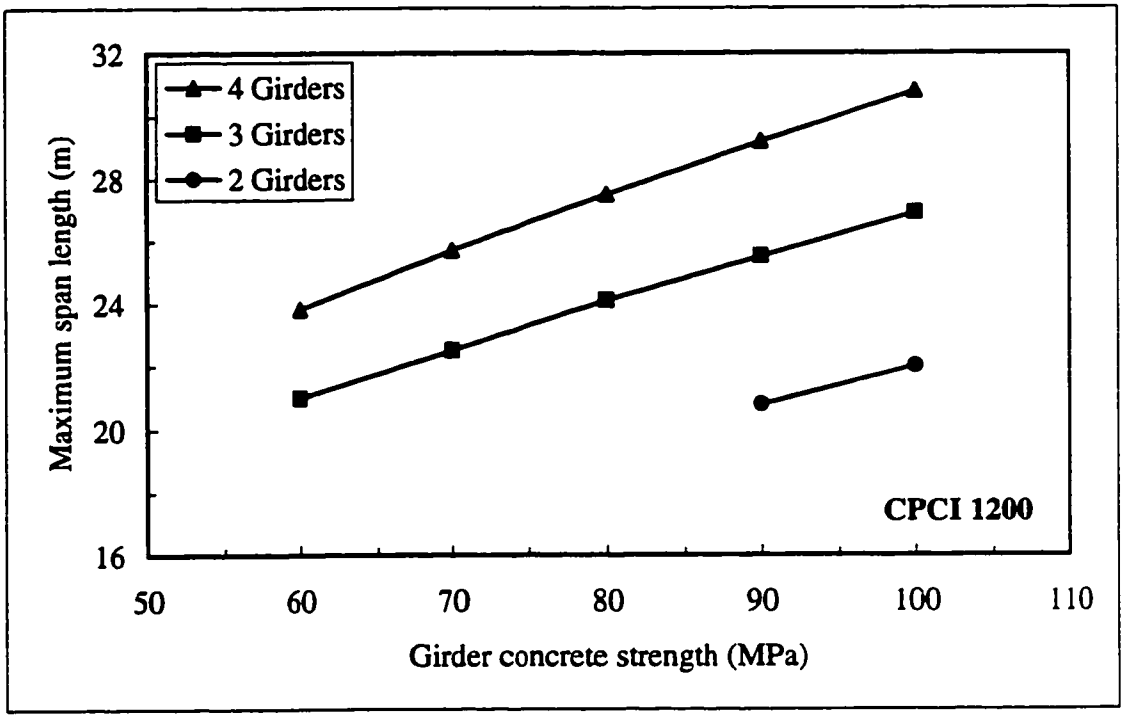

Figure 6.19 Maximum span vs. concrete strength for CPCI Type 1200 girders

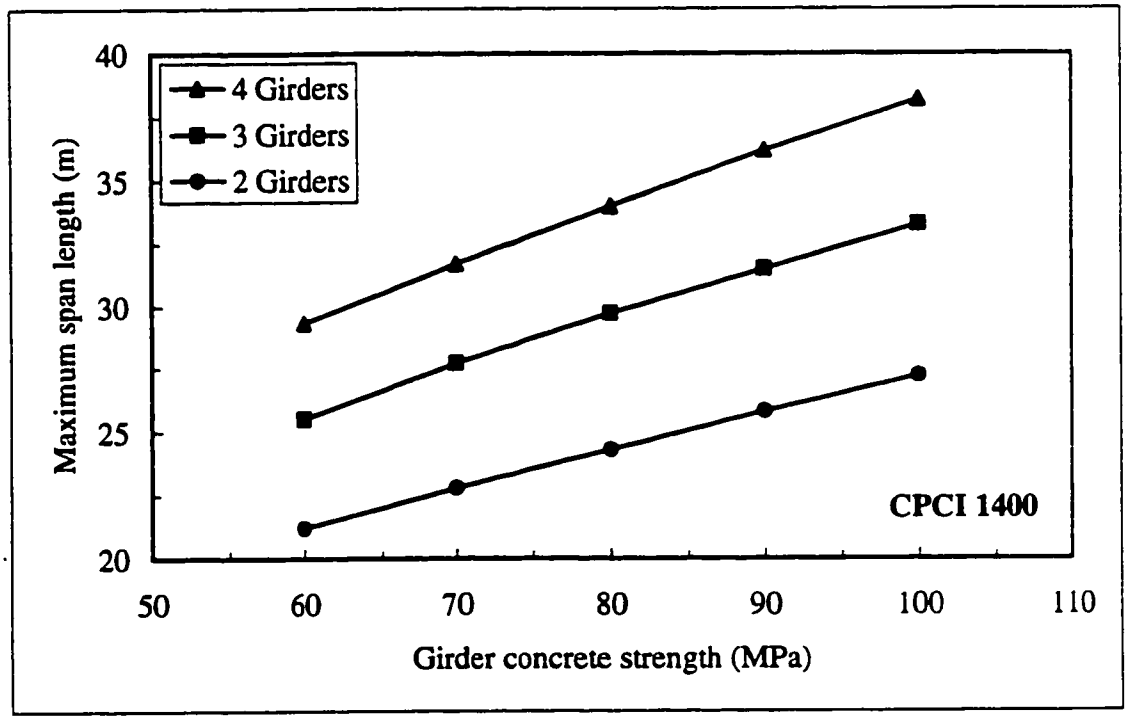

Figure 6.20 Maximum span vs. concrete strength for CPCI Type 1400 girders

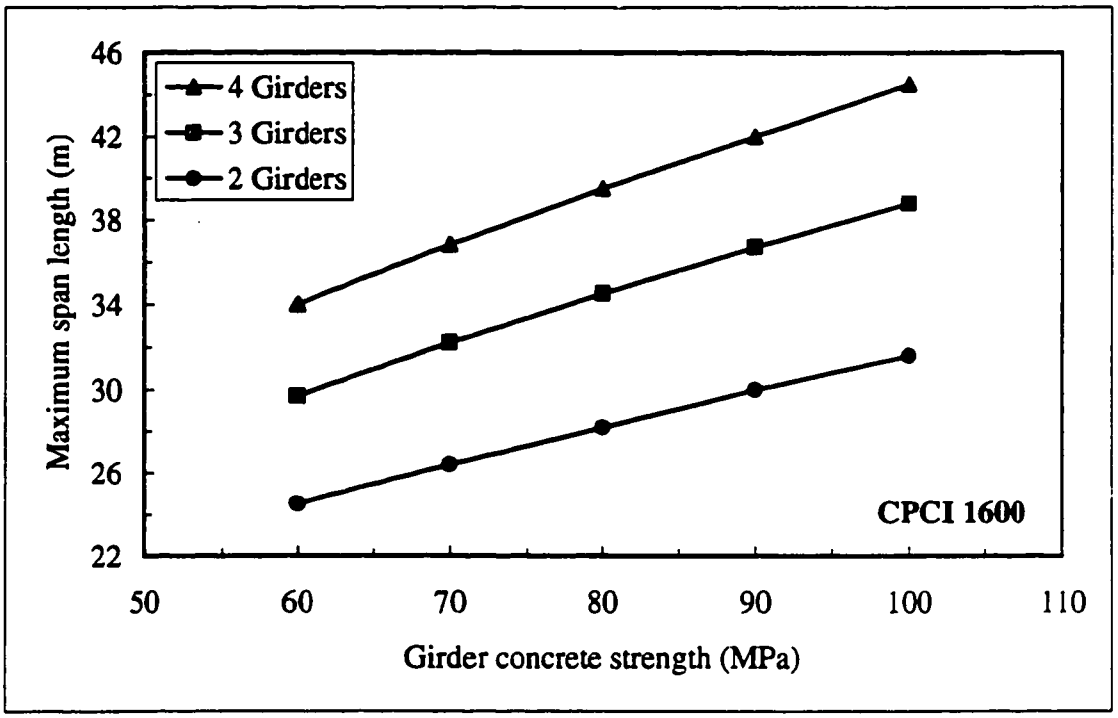

Figure 6.21 Maximum span vs. concrete strength for CPCI Type 1600 girders

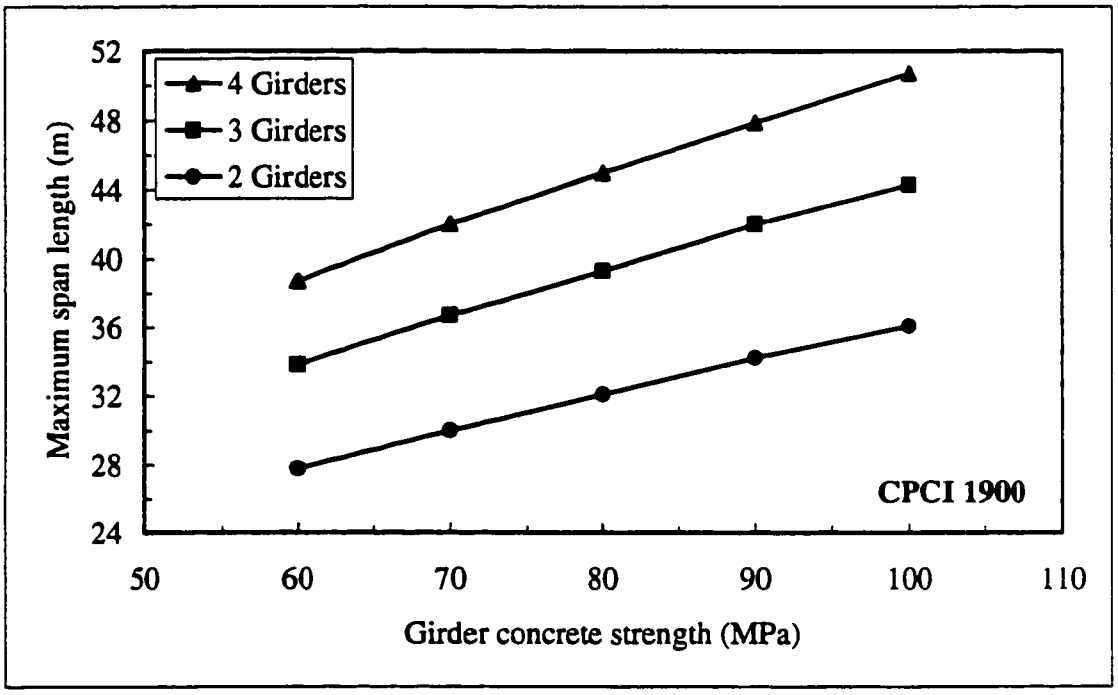

Figure 6.22 Maximum span vs. concrete strength for CPCI Type 1900 girders

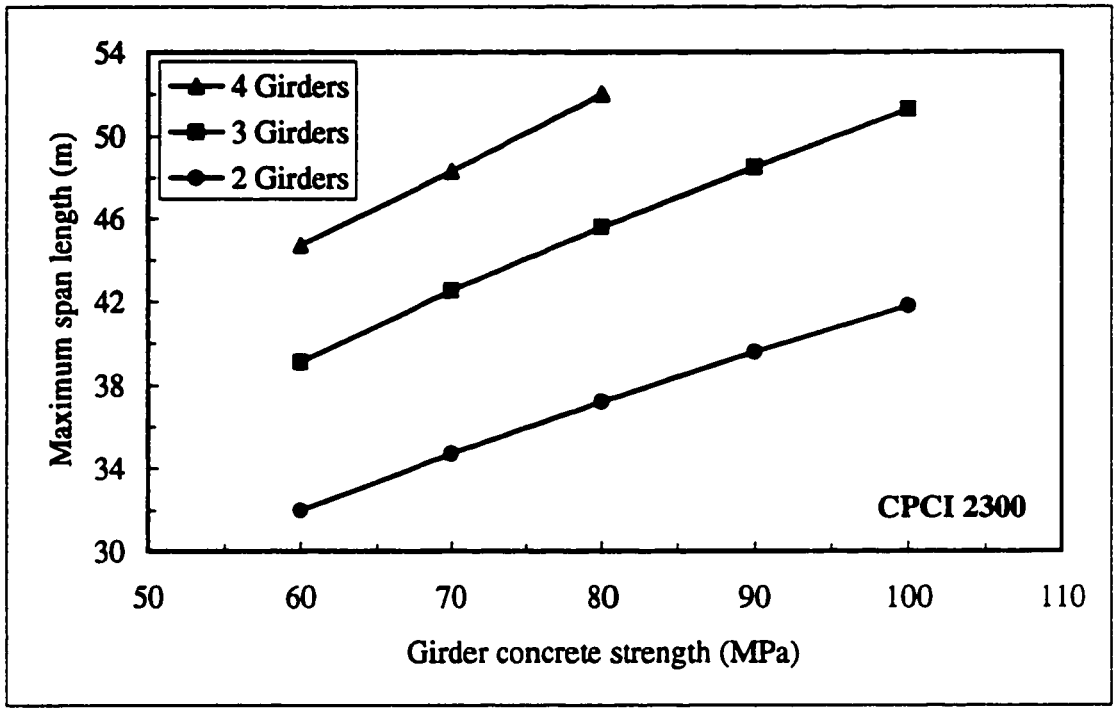

Figure 6.23 Maximum span vs. concrete strength for CPCI Type 2300 girders

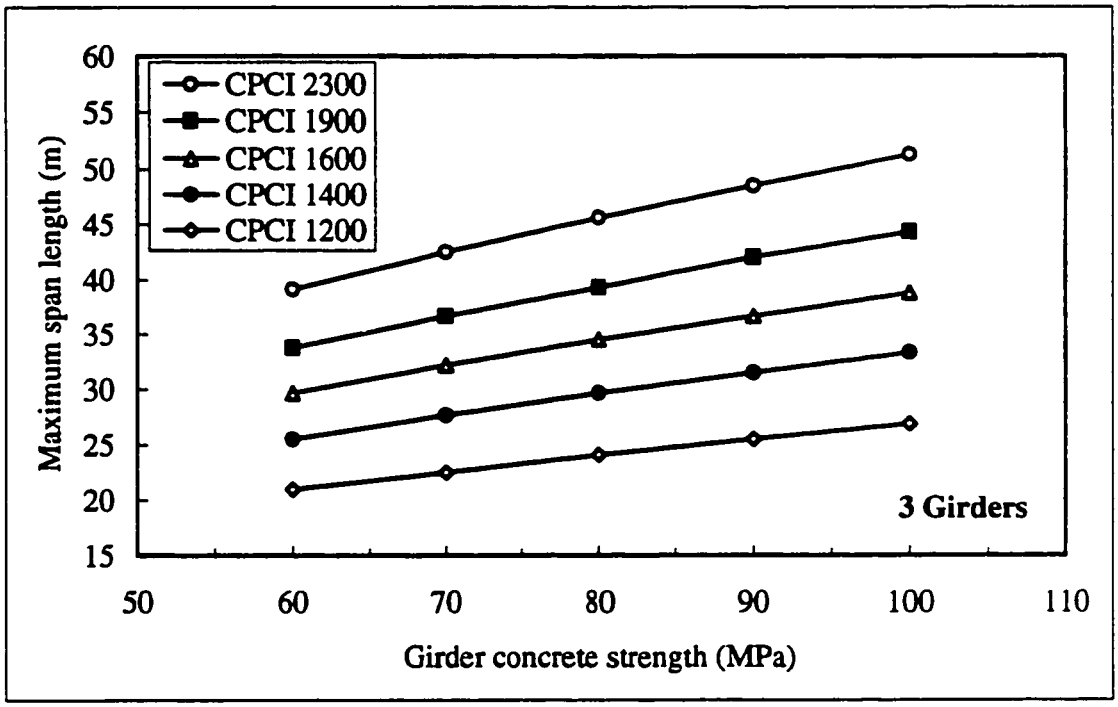

Figure 6.24 Maximum span vs. concrete strength for the standard CPCI sections studied

below its neutral axis at that level of concrete strength. As a result, HPC cannot be used efficiently. To effectively utilize HPC in this study, 15.2-mm-diameter strands were used instead of 12.7-mm-diameter strands which represent the norm in the current practice of pretensioning. It can be seen in Figs 6.19 to 6.23 that by allowing more prestressing force to be accommodated within the section at a larger eccentricity, the use of 15.2-mm-diameter strands has eliminated any levelling off of the maximum span lengths at very high-strength concretes. Thus, the increase in maximum span lengths would continue with each increase in girder concrete strength, limited only by practical considerations such as shipping and handling lengths, girder masses, lateral stability and / or prestressing bed capacities.

6.5 SUMMARY

In a relatively recent survey conducted by the PCI High-Strength Concrete Committee, the average 28-day concrete strength used in the American precast, prestressed concrete industry was found to be 41 MPa [34]. The maximum strength that producers felt they can reliably supply was 59 MPa. Strengths in the same order of magnitude represent the norm in the Canadian industry. These strengths are much less than those in the 100 MPa range that have been achieved for many buildings. One major reason for the reluctance within the precast industry to utilize concretes of such high strengths despite their potential advantages is the misconception that these advantages do not justify the higher costs of the material and of the increased quality control requirements associated with its production. The main objective of this chapter was to evaluate the cost effectiveness of using concretes with strengths of up to about 100 MPa for precast, pretensioned slab-on-girder bridges, and thereby provide the economic incentive for precasters to use HPC widely.

To reach the above objective, an optimization system was developed to perform a series of economic studies on slab-on-girder bridges. The application of the system was illustrated and its validity was tested on a representative bridge of a typical configuration. Based on the results of some 115 optimal superstructure designs generated by the developed

optimization system, one can conclude that the economic benefits from using concretes with strengths of up to 100 MPa for precast, prestressed slab-on-girder bridges are quite promising, particularly for longer girder span lengths. It was found that the increase in material cost associated with the use of these concretes can be fully offset by the reduced number of girders required for a given span length, as a result of the increase in girder capacity. Moreover, it was shown that it is more economical to use a shallower girder cross section manufactured with a higher-strength concrete than it is to use a deeper section made with a lower-strength concrete. This can be accompanied by additional savings from the reduced substructure height. Charts were developed that can be used to identify the most cost effective designs for various ranges of girder span length in a variety of bridge configurations, assuming that there was no practical limit on the level of concrete strength that can be achieved. For cases where there was a certain maximum concrete strength that can be obtained, other charts were developed that can be utilized to identify the most economical designs.

It was shown that the use of HPC makes it possible to reach span lengths previously unattainable with standard girder sections and concretes of normal strength. On average, an increase in girder concrete strength from 60 to 100 MPa resulted in a 30% increase in span capability for the five girder types considered. This results in a reduction in the substructure cost as a result of the reduced number of piers and foundations for multi-span bridges.

An additional important conclusion that was pointed out in this chapter was that at relatively shorter span lengths, the economical benefits realized with the use of concretes of very high strength (in the order of 100 MPa) may diminish. Thus, it would be more economical not to utilize such high strengths for relatively shorter spans unless it can be proven that the reduction in the life-cycle costs resulting from the increased durability of these concretes would more than offset the higher cost of the material.

CHAPTER 7

CONSTRAINT ACTIVITY AND SENSITIVITY ANALYSIS

7.1 INTRODUCTION

The concept of *constraint activity* is very important in design optimization. Loosely speaking, an active constraint corresponds to a critical design requirement, i.e. one whose presence determines where the optimum will be; this is why active constraints are often appropriately referred to as the governing design criteria. Another important topic in the area of optimal design that is often overlooked in the literature on structural optimization is the study of variations in the optimal solution as some of the original problem parameters are changed. Such a study is known as *post-optimality analysis* or *sensitivity analysis*.

This chapter is organized into two main sections. In the first, the governing design criteria of the optimal design problem of precast, prestressed concrete slab-on-girder highway bridges are identified and their significance studied. Sensitivities of the obtained optimal solutions with respect to the major assumptions made in developing the optimization system are then investigated in the second section.

7.2 CONSTRAINT ACTIVITY

7.2.1 Governing Design Criteria

All design constraints for the problem under consideration that the optimal design must satisfy were identified and defined in Sec. 5.4. Formally speaking, an inequality (≤ 0 form) constraint is said to be active at a design point if it is satisfied at equality, i.e. its value is zero or, numerically, a very small number. Constraint activity at the optimal point was

observed for all of the 115 optimal bridge designs generated by the developed optimization system. The following list outlines the governing design criteria:

1. Concrete allowable compressive stress at the time of prestress transfer at the bottom face of the girder, i.e. Eq. (5.5).
2. Concrete allowable tensile stress at serviceability limit states at the bottom face of the girder, i.e. Eq. (5.10).

3a. Concrete allowable tensile stress at transfer at the top face of the girder for the shorter span lengths, i.e. Eq. (5.4).

3b. Maximum eccentricity at and near girder mid-span for the longer span lengths, i.e. Eq. (5.28).

4. Negative moment over the piers at ultimate limit states (Sec. 5.4.2.4).
5. Minimum deck slab thickness, i.e. Eq. (5.38).

7.2.2 Discussion

It was mentioned in Sec. 6.4.2.1 that during the optimization process, girder span length was considered as a preassigned parameter while concrete strength was treated as a design variable. By examining constraint activity at the optimal points, it was found that the given span lengths were actually the maximum achievable spans at the corresponding optimal values of concrete compressive strength. In each case, the maximum length was found to correspond to the lesser of the two maximum lengths obtained from the constraints which set the limits on allowable compression at transfer and allowable tension at serviceability limit states, respectively, at the bottom face of the girder. Increasing a girder's span length, for the same concrete strength, beyond its given value would violate the active allowable stress constraints. It was noted that the constraint on ultimate flexural strength, i.e. on the positive moment reinforcement at and near girder mid-span at ultimate limit states was never active in any of the 115 optimal solutions obtained as it was satisfied by conformance to the allowable stress requirements. This can be explained by considering the nature of the loads applied when checking for allowable stresses and when designing for flexural strength.

Under allowable stress requirements, no load factors are applied, yet dead load contributes to a larger percentage of the total load as spans get longer. However, in the factored load design for flexural strength, live load receives a larger multiplier than dead load. Thus, as spans lengthen and dead load becomes a greater portion of the total unfactored load, flexural strength constraints tend to be satisfied by the constraints imposed by the allowable stress limits.

As indicated in the list that outlined the governing design criteria in the previous section, it was found that in addition to the constraints which set the limits on compression at transfer and tension at serviceability limit states at the bottom face of the girder being active, the constraint limiting the eccentricity at and near girder mid-span was also active for the longer span lengths. This was illustrated graphically for a 34-m span length in the numerical design example considered in Chapter 6 (see Fig. 6.5). It was shown that the line representing e_{max} intersected the feasible zone delineated by the allowable stress requirements, i.e. area ABCD, to produce a new reduced feasible zone. Any point inside that new zone had satisfactory and practically feasible values of P_e and e_c. The smallest (optimal) value for P_e was obtained at the intersection of the lines representing Eq. (6.6) and e_{max}. It should be mentioned here that this behaviour emphasizes the importance of the size of the girder's bottom flange discussed earlier in Chapters 2 and 3. A larger bottom flange that can accommodate more prestressing strands at a large eccentricity can be very effective in improving the efficiency of HPC bridge girders by allowing them to reach longer spans. For the shorter span lengths, it was noted that the constraint limiting the eccentricity at and near mid-span ceases to be active and, alternatively, the constraint which sets the limit on the allowable tension at transfer becomes active. This is illustrated graphically in Fig. 7.1 for the case of 4 CPCI Type 1200 girder lines having a span length of 22 m each. It can be readily seen that the line representing e_{max} did not intersect the feasible zone ABCD. In this case, the smallest value for P_e is obtained at point A, i.e. at the intersection of the lines representing Eqs (6.3) and (6.6). This implies that the optimal design does not necessarily require maximum tendon eccentricity.

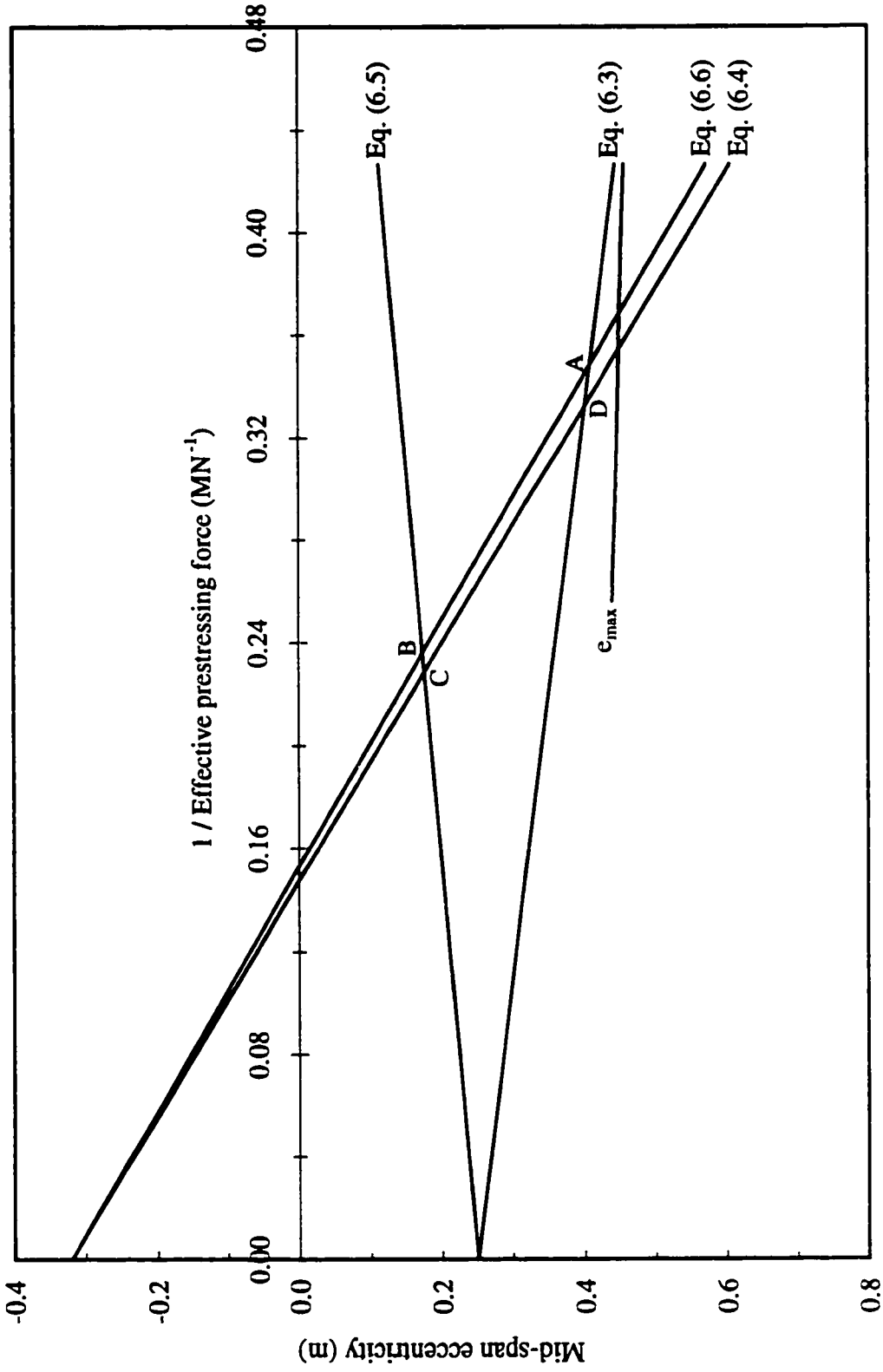

Figure 7.1 Graphical solution of the allowable stress requirements for the shorter span lengths

Another governing design criterion was found to be the constraint on negative moment over the piers at ultimate limit states. This negative moment is due to live load and any additional dead load applied after continuity is achieved, and is resisted by longitudinal reinforcing bars embedded in the cast-in-place deck slab across the piers. One reported potential problem with this type of construction is that cracks may develop near the top surface of the deck in the pier area due to this negative continuity moment [132]. Exposure of these cracks to deicing salts can promote deck deterioration. It should be noted, however, that the use of HPC, with its improved durability, accompanied by an adequate concrete cover for the deck slab can be an effective solution to this problem.

The last of the governing design criteria was that imposed by the OHBDC [94] on the deck slab thickness. It was noted that the optimal slab thickness always corresponds to the 225-mm minimum thickness permitted by the Code. As was explained in Sec. 4.6.2, this thickness relates to extra cover to the reinforcement for protection against possible corrosion of the steel bars in the deck.

All constraints that were inactive during the optimization process may be disregarded in the design of prestressed concrete slab-on-girder bridges. Of special interest here is the constraint on the area of the positive moment connection steel over the piers. As was explained in Sec. 4.5.1, positive moments develop over piers in continuous slab-on-girder bridges due to creep in the prestressed girders as well as due to the effect of live loads in remote spans. Positive moments due to creep under sustained loads, i.e. prestressing and dead loads, are partially counteracted by the negative moments resulting from differential shrinkage between the cast-in-place deck slab and the precast girders. The assessment of these positive moments is usually not readily possible because of uncertainties in creep analysis models and the many factors on which it depends. This has led to suggestions for neglecting the structural effects of creep (and shrinkage) in this type of bridges, and just providing a nominal minimum amount of positive reinforcement between the girders if for no other reason than increasing the structural integrity [139,157]. These suggestions were also based on the observed good

performance of structures for which the design utilized full continuity for superimposed dead loads and live loads, but neglected the structural consequences of time-dependent effects. It can be said that there may be some merit to such a notion since the constraint on the positive moment connection steel was never active in any of the 115 optimal design solutions obtained. With the use of HPC, which can decrease the effects of creep and shrinkage, there is certainly a stronger case for this notion. Further research is needed in this area.

7.3 SENSITIVITY ANALYSIS

7.3.1 General

The optimal solutions presented in this study were based on a set of assumptions that were made in developing the optimization system. These assumptions were listed in Sec. 6.2.1, and were generally consistent with current bridge design and construction practices. It is important, however, to test the validity and possible application of the optimal solutions obtained outside the range of values assumed. Sensitivity of the cost function with respect to the major assumptions made in this investigation is now studied. Unless otherwise noted, the same bridge superstructure configuration was used to carry out the sensitivity analyses. It consists of two equal spans of 30 m in length each with 3 CPCI Type 1400 girder lines. It was found that other bridge configurations yielded essentially the same general trends exhibited by the adopted configuration.

7.3.2 Discussion

- ***Live Load Factor***

It was mentioned in Sec. 5.4.2.4 that the live load factor applied to moments at ultimate limit states is expected to be in excess of 1.6 in the new CHBDC when it is published [172], compared to 1.4 in the current OHBDC [94]. In this study, the live load factor was taken as 1.6. The variation in cost for a range of factors from 1.4 to 1.7 was investigated. It was found that the cost function is insensitive to variations in the live load factor. This can

be attributed to the fact that the constraint on the positive moment reinforcement at and near girder mid-span at ultimate limit states was never active.

- ***Location of Tendon Deflection Points***

In this study, the prestressing tendons were assumed to be draped at the third-points of the girder span in accordance with the current practice of pretensioning. Figure 7.2 illustrates the effect of changes in the location of the deflection points. It should be noted that the vertical axis represents the ratio of "cost", which is the value of the cost function corresponding to a specified location, to "base cost", which is the value of the cost function corresponding to the "base" location; using such a ratio facilitates the comparisons more than if the absolute values of the cost function were utilized. From the figure, it can be seen that hardly any differences in cost occur when this parameter is varied as shown.

- ***The Ratio*** $R = P_e / P_i$

Figure 7.3 illustrates the effect of changing the ratio, R, of the effective prestressing force after losses to the prestressing force at transfer. It is recalled that the ratio adopted in this study was 0.80 corresponding to 20% prestress losses. It can be seen in the figure that varying R over a range of possible practical values resulted in marginal differences in cost. For example, assuming 25% losses resulted in about 1.5% difference in cost. In addition, assuming 15% losses made a difference of less than 1% in the cost of the superstructure.

- ***The Ratio*** $R_f = f'_{ci} / f'_c$

Marginal differences in cost were also observed when the ratio, R_f, of the girder concrete compressive strength at transfer to the 28-day strength was varied over a range of possible practical values, as shown in Fig. 7.4. The base cost in this case corresponded to R_f equals 0.70.

- ***Deck Slab Concrete Strength and Thickness***

It is recalled that all of the 115 optimal bridge designs generated by the optimization

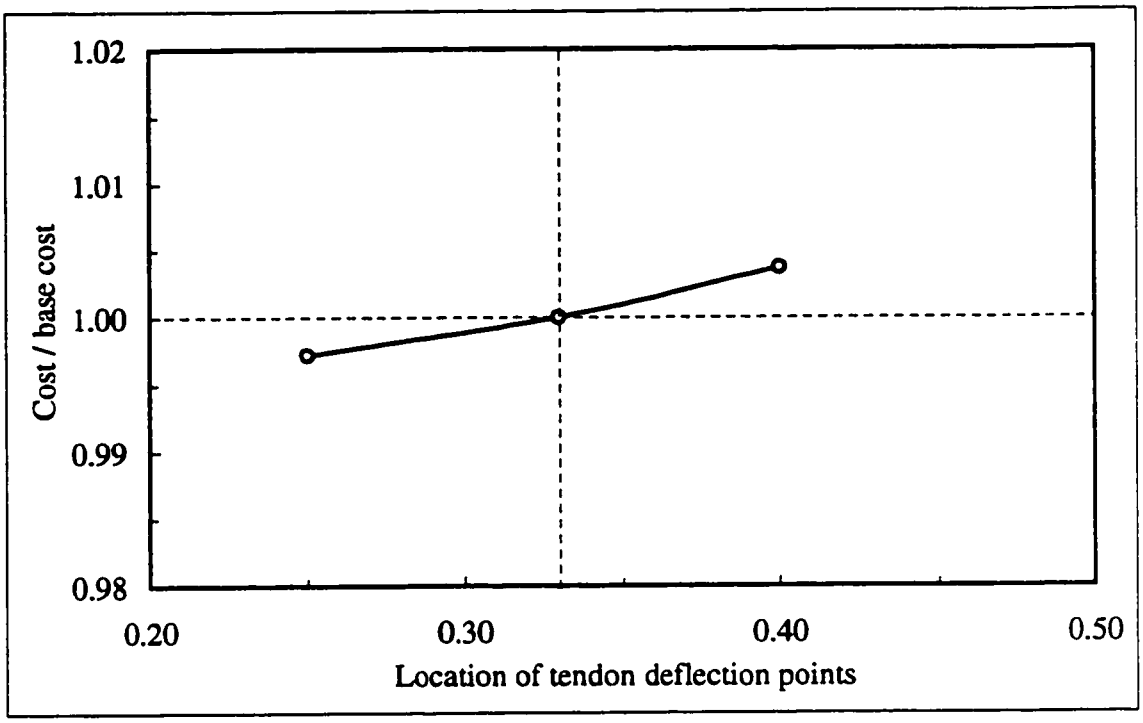

Figure 7.2 Effect of different locations of tendon deflection points on cost

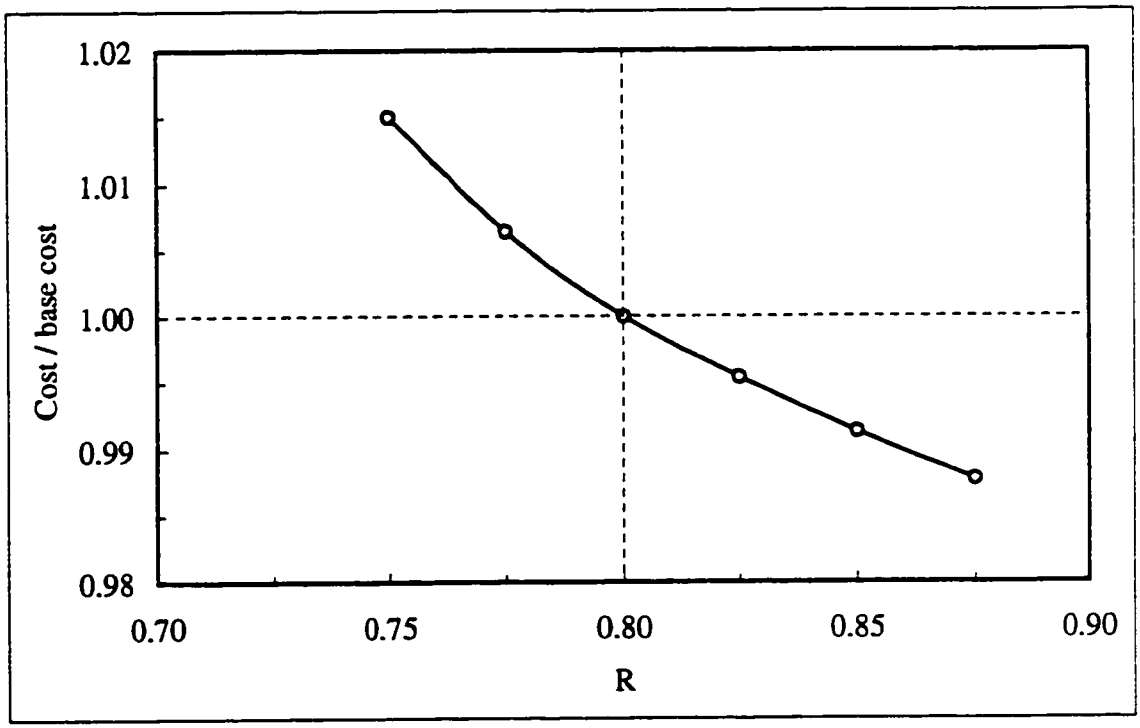

Figure 7.3 Effect of $R = P_e / P_i$ on cost

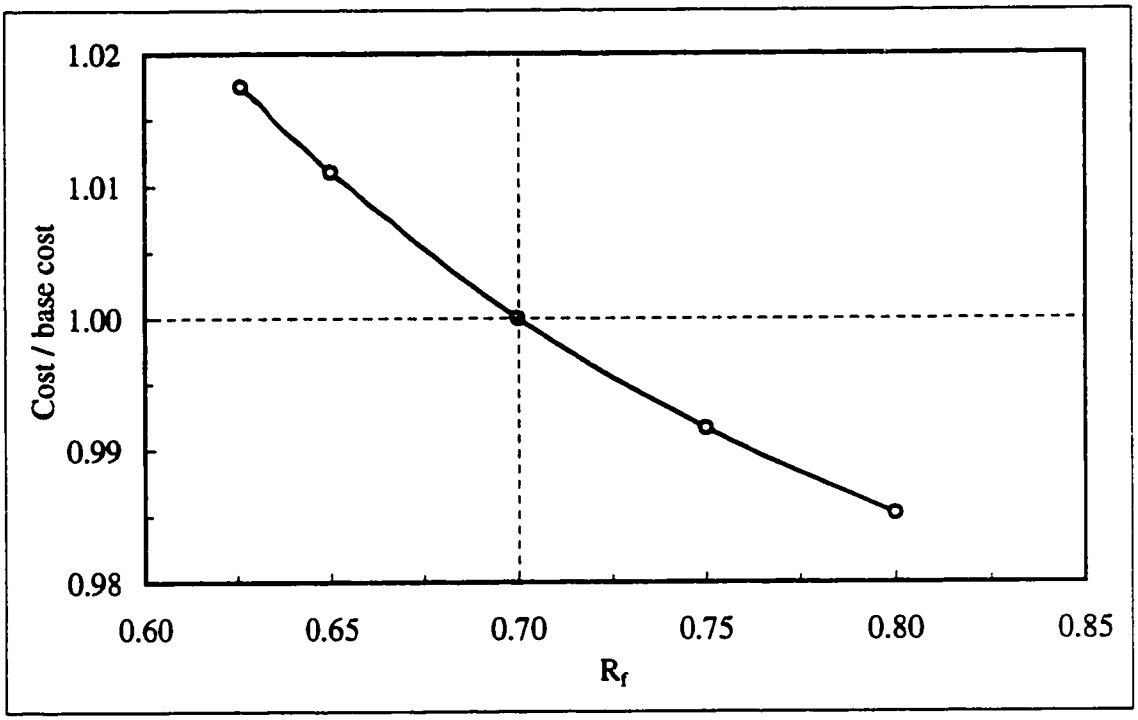

Figure 7.4 Effect of $R_f = f'_{ci} / f'_c$ on cost

system utilized 35-MPa concrete for the cast-in-place deck slab. It is also recalled that the optimal slab thickness was found to always correspond to the 225-mm minimum thickness permitted by the OHBDC [94]. To study the effect of changing the slab concrete strength and its thickness on the cost, Fig. 7.5 was established. It illustrates the variation in cost over a range of concrete strengths from 35 to 50 MPa for two different slab thicknesses of 200 mm and 225 mm. It can be seen that, in both cases, the use of concretes of higher strengths for the bridge deck did not provide any economic advantage due to the practical limitations on the minimum thickness of a slab. The increased durability of these concretes, however, may provide a serviceability benefit for the deck that is worth the additional cost of using them.

- ***Transportation and Erection Costs***

Although it would be difficult to estimate precast girder transportation and erection costs without a specific bridge project, it is crucial in a study of this kind to pay closer attention to the assessment of these costs especially for longer and heavier girders. This is because, as was indicated in the previous chapter, the cost associated with the girders'

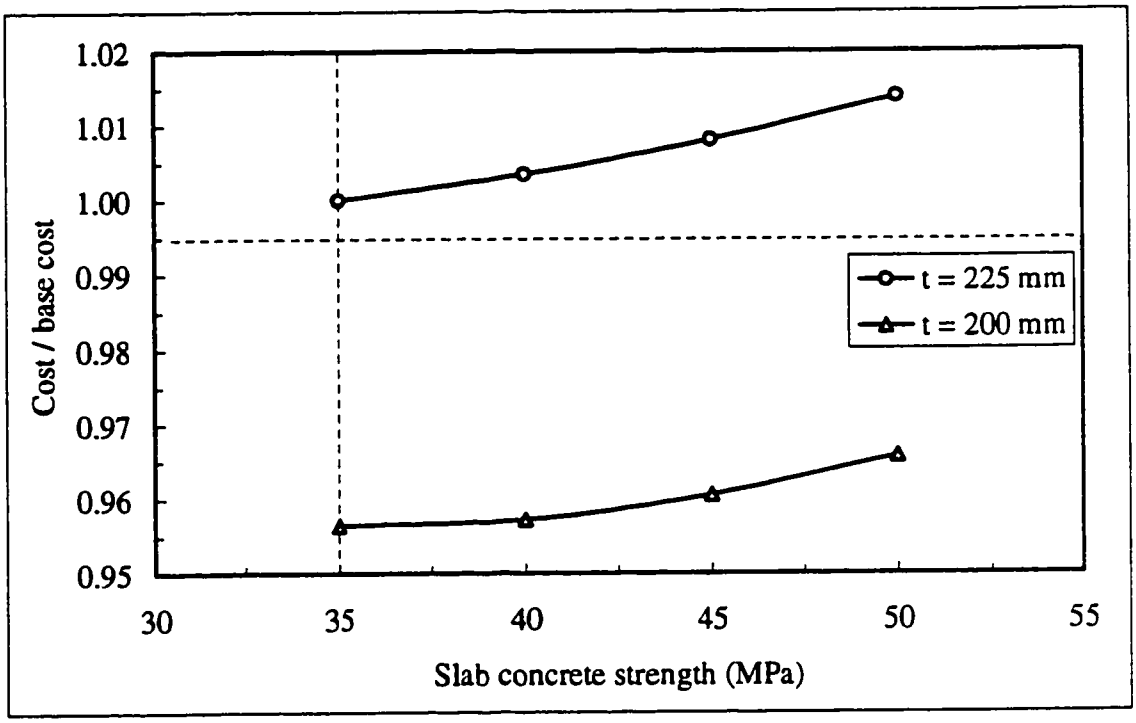

Figure 7.5 Effect of the deck slab concrete strength and its thickness on cost

shipping and handling tends to dominate slab-on-girder bridge construction costs in general. To show the effect of varying these costs on the total superstructure cost, Fig. 7.6 was established. Three bridge configurations were examined: a 2-girder bridge, a 3-girder bridge and a 4-girder bridge. For all configurations, CPCI Type 1900 girders having a span length of 36 m were used for the superstructure. Two levels of transportation and erection costs were considered. The first level was based on the average values used originally in developing the optimization system, i.e. $500/hour for mobilization, setup and dismantling of the crane, and $6000 for shipping and handling a girder. This first level is referred to here, for comparison purposes, as low transportation and erection costs. The other level was based on $750/hour for mobilization, setup and dismantling of the crane, and $12,000 for shipping and handling a girder. This level is referred to as high transportation and erection costs. It should be mentioned that adopting these new values necessitated modifying Figs 5.5 and 5.6 to reflect the changes in these cost items. The importance of having as close an estimate as possible for transportation and erection costs is obvious from Fig. 7.6. It is clear that as the number of girders increases for a given bridge project, the increase in the superstructure cost

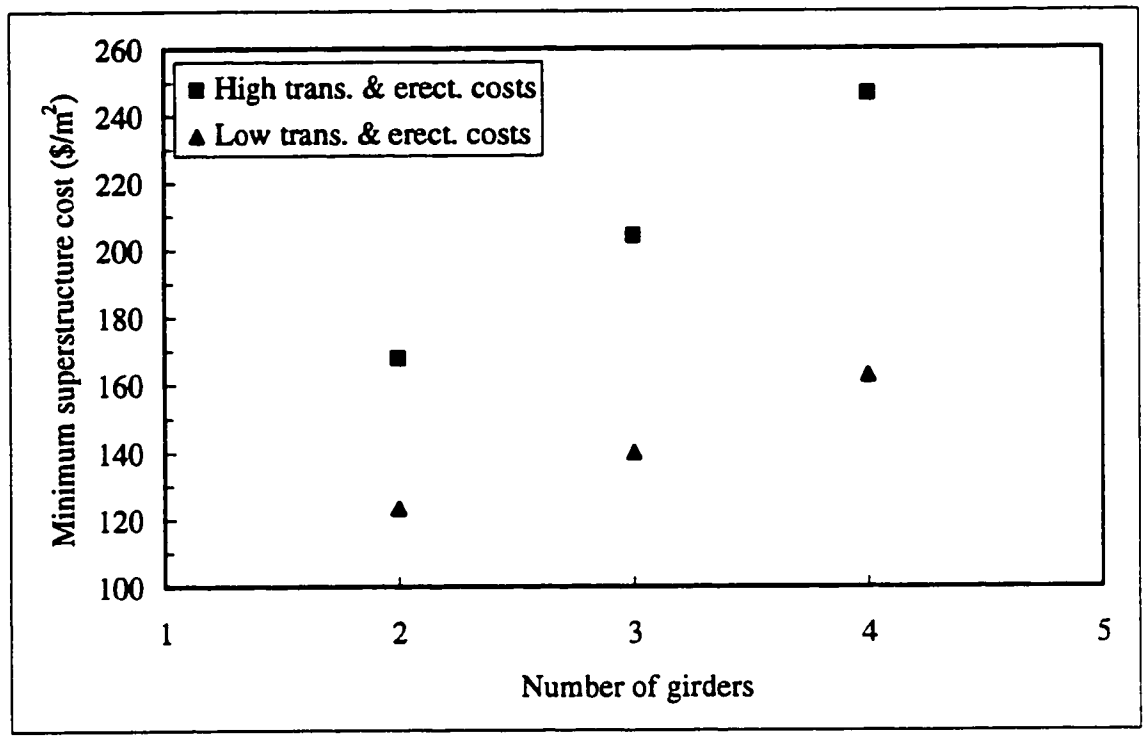

Figure 7.6 Effect of transportation and erection costs on the total superstructure cost

associated with high transportation and erection costs becomes higher than that associated with low transportation and erection costs.

CHAPTER 8

CONCLUSIONS AND RECOMMENDATIONS

8.1 INTRODUCTION

This chapter gives an overall summary of the motive behind this study, and the methodology used to achieve the stated objective of the investigation. The conclusions drawn from the study are outlined. Then, some recommendations for further research are listed.

8.2 SUMMARY

For several years, the most common application of HPC has been in the building industry. Concrete strengths of 100 MPa and more have been frequently used in the lower columns of high-rise buildings where conventional concrete would make those unacceptably large. In comparison, strengths of about 60 MPa have been considered the maximum achievable in the precast, prestressed concrete industry; this appears to be very timid especially considering that several research studies have indicated that the potential advantages from the utilization of HPC with its increased strength and improved durability for precast, prestressed concrete highway bridges are quite promising. In spite of this, there is still some disagreement in the precast industry that HPC is beneficial. This can be attributed to the fact that the benefits of the material are not fully understood within the industry due, in part, to the lack of research in this area. More significantly, the misconception that those advantages do not justify the higher cost of the material and the increased quality control requirements associated with its production, and the higher initial costs that have been reported lately for some HPC bridges seem to deter most designers and precast concrete producers from exploiting the material. The use of HPC in bridges in unlikely to advance

quickly without a clear economic incentive for precasters to utilize the material widely. To help provide such an incentive, this study was conducted.

The overall objective of this study was to assess the potential economic benefits from the utilization of concretes with compressive strengths of up to about 100 MPa for continuous, precast, pretensioned slab-on-girder highway bridges. These were chosen because they represent the most common type of precast, prestressed concrete bridges constructed in North America. To reach the above objective, refined computer-oriented structural analysis methods combined with modern computational design optimization techniques were used to develop an optimization system that was utilized to perform economic studies on the type of bridges investigated.

The intent of this study was to look beyond current precast, prestressed concrete production capabilities, and bridge analysis, design and construction methods. Although current practice was considered as the basis for the assumptions made in developing the optimization system, it was not used as a means to restrict potential applications of HPC in precast, prestressed slab-on-girder bridges. The findings of the study were based on a bridge of a configuration typical or representative of the majority of existing bridges of this type. It was outside the scope of this study to consider every possible variation in bridge geometry or layout. The results obtained, however, are general enough to apply for all slab-on-girder bridges.

8.3 CONCLUSIONS

Based on the findings of this study, the following conclusions are drawn:

1. Apart from the main objective of this research, namely to assess the potential economic benefits from the utilization of HPC for precast, prestressed concrete slab-on-girder bridges, this study was intended to fill a portion of the gap that exists

between the progress of the optimization theory, and its application to the practice of structural engineering in general and bridge engineering in particular. It has been demonstrated that computational structural analysis methods and design optimization techniques can be combined, and effectively applied to everyday design problems; thus, providing substantial aid to the designer not only in the creative process of finding the optimal design, but also in significantly reducing the amount of effort and time required to do so.

2. The use of HPC for standard precast, prestressed girders allows them to reach span lengths previously unattainable with the utilization of concretes of normal strength. On average, an increase in girder concrete strength from 60 to 100 MPa resulted in a 30% increase in span capability for the five girder types considered. When span lengths increase, the number of piers and foundations can be reduced for multi-span bridges, reducing in turn the cost of the substructure. If the bridge is crossing an existing roadway, a reduction in the number of piers and foundations would also ease traffic disruptions on the roadway underneath during construction of the bridge.

3. The use of 15.2-mm-diameter prestressing strands eliminates any levelling off of the maximum span lengths at very high-strength concretes by allowing more prestressing force to be accommodated within the girder cross section at a larger eccentricity. Thus, the increase in maximum span lengths continues with each increase in girder concrete strength, limited only by practical considerations such as shipping and handling lengths, girder masses, lateral stability and/or prestressing bed capacities.

4. With HPC being a new product, most precasters and contractors have little or no experience with its use. Therefore, they are somewhat uncertain as to what it would cost them to mix concrete with a compressive strength as high as 100 MPa. An equation and a chart were established that can be used to estimate the cost of a concrete mix having a compressive strength of up to 100 MPa. They are based on

several groups of current concrete cost data from local producers and relative cost data from the literature, and can prove valuable to precasters and contractors.

5. Although the basic material cost per cubic metre for concretes of higher strengths is obviously increased, primarily due to increased mix constituent and quality control costs, this can normally be fully offset by the reduced quantities of concrete required in the form of fewer girders for a given span length as a result of the proportionate increase in girder capacity. Consequently, for a given span length, it is more economical to use a fewer number of girders made with HPC than it is to use a larger number of them manufactured with normal-strength concrete. This implies that it is most economical to place girders at the largest practical transverse spacing. This economic advantage of using HPC becomes more apparent for longer span lengths. Referring to Fig. 6.17, it can be seen that, for example, using 3 CPCI Type 2300 girders made with 80-MPa concrete to span 44 m is more economical than using 4 of them made with 60-MPa concrete to span the same length. The cost saving, in this case, was about 16% of the total superstructure cost.

6. Despite the fact that a deeper girder with a larger section modulus utilizes the increased concrete strength more efficiently, i.e. the deeper girder has greater span increase capabilities, the use of a shallower girder cross section manufactured with a higher-strength concrete to span a given length can be more economical than the use of a deeper section made with a lower-strength concrete. For example, it is more economical to use 2 CPCI Type 1900 girders made with 80-MPa concrete than it is to use 2 Type 2300 girders made with 60-MPa concrete for any span length in the range from 27.8 m up to about 32 m (see Fig. 6.17). Although the saving in the superstructure cost associated with the use of the shallower section, in this case, did not exceed 3% within the range of spans considered, it is important to keep in mind that there will be additional savings from the reduced substructure height.

7. At relatively shorter span lengths, the economical benefits realized with the use of concretes of very high strength may diminish. For example, it was found that over the range of span lengths from 27.8 m up to about 32 m, the cost curves for strengths of 80 MPa and 100 MPa completely overlap (see Fig. 6.18), which means that there is no advantage realized from the utilization of the 100-MPa concrete at any span length within the range considered. Thus, it would be more economical not to use such a very high strength for relatively shorter spans unless it can be proven that the reduction in the life-cycle costs resulting from the increased durability of this concrete would more than offset the higher cost of the material.

8. Although it would be very difficult to estimate precast girder transportation and erection costs without a specific bridge project, it is crucial in a study of this kind to pay closer attention to the assessment of these costs especially for longer and heavier girders. This is because the cost associated with the girders' shipping and handling tends to dominate slab-on-girder bridge construction costs in general.

9. One point that is relevant to the series of girders considered in this investigation is that CPCI Type 1600 cross section never provides the most economical design at any given span length, provided that there was no limit on the level of concrete strength that can be used to manufacture Type 1400 girders. This was true for all of the bridge configurations studied (see Figs 6.13, 6.14 and 6.15). Although the deeper Type 1600 cross section is structurally more efficient than the shallower Type 1400 section in the sense that it can reach longer span lengths using relatively lower concrete strengths, the reduction in the material (i.e. concrete) cost is not sufficient enough to absorb the increase in the erection cost of the heavier Type 1600 section before Type 1900 takes over and becomes economically more competitive.

10. The use of HPC for the bridge deck slab does not provide any economic advantage. This is due to the practical limitations on the minimum thickness of a slab. The

increased durability of HPC may provide a serviceability benefit for the deck that is worth the additional cost of using the material.

11. For all of the 115 optimal bridge designs generated by the optimization system, the allowable stress inequality conditions governed the flexural design; specifically, the constraints which set the limits on compression at transfer and tension at serviceability limit states were active for all optimal designs. Additionally, the constraint which sets the limit on tension at transfer was active for the shorter span lengths. It was found that the constraint on the positive moment reinforcement at and near girder mid-span at ultimate limit states was never active; therefore, this constraint may be disregarded in the design of prestressed concrete slab-on-girder bridges.

12. It has been found that the constraint on the area of the positive moment connection steel over the piers was never active in any of the optimal design solutions obtained. Thus, there may be some merit to the notion of neglecting the structural effects of creep and shrinkage in continuous, precast, prestressed concrete slab-on-girder bridges, and just providing a nominal minimum amount of positive reinforcement between girders if for no other reason than increasing the structural integrity. Such notion is primarily based on the observed good performance of structures for which the design utilized full continuity for superimposed dead loads and live loads, but neglected the structural consequences of time-dependent effects. With the use of HPC, which can decrease the effects of creep and shrinkage, there is certainly a stronger case for that notion.

13. Sensitivity analyses of the obtained results with respect to the major assumptions made in developing the optimization system suggest that the findings of this study are applicable to a wide range of practical values surrounding those assumed. For example, marginal differences in the value of the cost function were obtained when the ratio of the effective prestressing force to the prestressing force at transfer, and

the ratio of the concrete compressive strength at transfer to the 28-day strength were varied over a range of possible practical values.

8.4 RECOMMENDATIONS FOR FURTHER RESEARCH

The following recommendations are suggested for future work in this area:

1. Precast, prestressed I-girders made of HPC tend to be longer and more slender than those fabricated with normal-strength concrete. As the cross sectional areas reduce and masses decrease, there is the possibility of increased vulnerability to lateral stability problems. Ways of improving the stability of long I-girders have been suggested in the literature as was discussed in Sec. 2.5.2.4. Additional research studies and field tests may be needed to ascertain shipping and handling requirements for the longer HPC I-girders.

2. Analytical and experimental studies are needed to test the notion of neglecting the structural consequences of time-dependent effects in continuous, precast, prestressed concrete slab-on-girder bridges. Long-term field measurements are also required in order to assess the accuracy of the research results.

3. It has been seen in this study that had some of the constraints imposed by the OHBDC empirical design method for deck slabs been adhered to exactly, many of the bridge configurations investigated would have not been possible. These constraints are mostly based on conservative empirical results, and in many cases the limits of their applicability could be extended if more extensive laboratory and field testing were conducted. Thus, further research is needed on the internal arching action of deck slabs.

4. Sufficient data for specific cases have been presented in this study which point the way

for further research on slab-on-girder bridges. The developed optimization system represents a powerful tool for the analysis and design of this type of bridges; a tool that can be expanded to include various other bridge configurations, different types of girder cross sections and different live load specifications.

5. The methodology used in this study to formulate the optimal design problem of precast, prestressed concrete slab-on-girder bridges can be used to study the potential economic benefits from the utilization of HPC for other types of highway bridges, such as box-girder bridges.

REFERENCES

1. Paxson, Glenn S., "Standardization of Prestressed Concrete Highway Bridge Members," *PCI Journal*, Vol. 7, No. 1, February 1962, pp. 13-19.

2. Taly, Narendra, *Design of Modern Highway Bridges*, The McGraw-Hill Companies Inc., New York, 1998.

3. Dunker, Kenneth F. and Basile G. Rabbat, "Performance of Prestressed Concrete Highway Bridges in the United States - The First 40 Years," *PCI Journal*, Vol. 37, No. 3, May-June 1992, pp. 48-64.

4. Kulka, Felix and T. Y. Lin, "Comparative Studies of Medium Span Box Girder Bridges with Other Precast Systems," *International Conference on Short and Medium Span Bridges*, Proceedings, Volume 1, Toronto, August 8-12, 1982, pp. 81-94.

5. Stanfill-McMillan, Kim and Cherilyn A. Hatfield, "Performance of Steel, Concrete, Prestressed Concrete, and Timber Bridges," *Developments in Short and Medium Span Bridge Engineering '94*, Papers presented at the Fourth International Conference on Short and Medium Span Bridges, Halifax, August 8-11, 1994, Mufti, Aftab A., Baidar Bakht and Leslie G. Jaeger (Editors), pp. 341-354.

6. Gustaferro, Armand, Marc A. Hillier and Jack R. Janney, "Performance of Prestressed Concrete on the Illinois Tollway After 25 Years of Service," *PCI Journal*, Vol. 28, No. 1, January-February 1983, pp. 50-67. Reader Comments: *PCI Journal*, Vol. 28, No. 5, September-October 1983, pp. 157-159.

7. Pessiki, Stephen, Mark Kaczinski and Herbert H. Wescott, "Evaluation of Effective Prestress Force in 28-Year-Old Prestressed Concrete Bridge Beams," *PCI Journal*, Vol. 41, No. 6, November-December 1996, pp. 78-89.

8. Ahmad, S. H., "Short Term Mechanical Properties," *High Performance Concrete: Properties and Applications*, Shah, S. P. and S. H. Ahmad (Editors), McGraw-Hill, Inc., 1994, pp. 27-64.

9. Loov, Robert E., "Reinforced Concrete at the Turn of the Century," *Concrete International*, Vol. 13, No. 12, December 1991, pp. 67-73.

10. Towles, Thomas T., "Advantages in the Use of High Strength Concretes," *ACI Journal*, Proceedings Vol. 28, No. 9, May 1932, pp. 607-612. Discussion: *ACI Journal*, Proceedings Vol. 29, No. 3, November 1932, pp. 149-152.

11. Hollister, S. C., "Urgent Need for Research in High-Strength Concrete," *ACI Journal*, Proceedings Vol. 73, No. 3, March 1976, pp. 136-137.

12. Loov, Robert E., "A General Stress-Strain Curve for Concrete; Implications for High Strength Concrete Columns," *Proceedings of the 1991 Annual Conference of the Canadian Society for Civil Engineering*, Vol. II, Vancouver, May 29-31, 1991, pp. 302-311.

13. ACI Committee 363, "State-of-the-Art Report on High-Strength Concrete," *ACI Manual of Concrete Practice*, Part 1, American Concrete Institute, Farmington Hills, Michigan, 1997.

14. Mindess, S., "Materials Selection, Proportioning and Quality Control," *High Performance Concrete: Properties and Applications*, Shah, S. P. and S. H. Ahmad (Editors), McGraw-Hill, Inc., 1994, pp. 1-25.

15. Richard, P. and M. H. Cheyrezy, "Reactive Powder Concretes with High Ductility and 200-800 MPa Compressive Strength," *Concrete Technology: Past, Present, and Future*, ACI Special Publication SP-144, Mehta, P. Kumar (Editor), 1994, pp. 507-518.

16. Richard, Pierre, "Reactive Powder Concrete: A New Ultra-High-Strength Cementitious Material," *Fourth International Symposium on the Utilization of High Strength/High Performance Concrete*, Proceedings-Volume 3, Paris, France, May 29-31, 1996, de Larrard, F. and R. Lacroix (Editors), pp. 1343-1349.

17. Bonneau, Oliver, Claude Poulin, Jerome Dugat, Pierre Richard and Pierre-Claude Aitcin, "Reactive Powder Concretes: From Theory to Practice," *Concrete International*, Vol. 18, No. 4, April 1996, pp. 47-49.

18. Aitcin, Pierre Claude and Pierre Richard, "The Pedestrian / Bikeway Bridge of Sherbrooke," *Fourth International Symposium on the Utilization of High Strength/High Performance Concrete*, Proceedings-Volume 3, Paris, France, May 29-31, 1996, de Larrard, F. and R. Lacroix (Editors), pp. 1399-1406.

19. O'Neil, Edward Francis, Christophe Evian Dauriac and Scott Keith Gilliland, "Development of Reactive Powder Concrete (RPC) Products in the United States Construction Market," *High-Strength Concrete: An International Perspective*, ACI Special Publication SP-167, Bickley, John A. (Editor), 1996, pp. 249-261.

20. Dowd, William M. and Edward F. O'Neil, "Development of Reactive Powder Concrete (RPC) Precast Products for the USA Market," *Fourth International Symposium on the Utilization of High Strength/High Performance Concrete*,

Proceedings-Volume 3, Paris, France, May 29-31, 1996, de Larrard, F. and R. Lacroix (Editors), pp. 1391-1398.

21. Aïtcin, Pierre-Claude and Adam Neville, "High-Performance Concrete Demystified," *Concrete International*, Vol. 15, No. 1, January 1993, pp. 21-26.

22. Zia, Paul, Michael L. Leming and Shuaib H. Ahmad, *High Performance Concretes, A State-of-the-Art Report*, Report No. SHRP-C/FR-91-103, Strategic Highway Research Program, National Research Council, Washington, D. C., January 1991.

23. Goodspeed, Charles H., Suneel Vanikar and Raymond A. Cook, " High-Performance Concrete Defined for Highway Structures," *Concrete International*, Vol. 18, No. 2, February 1996, pp. 62-67.

24. Russell, Henry G., "High-Performance Concrete - From Buildings to Bridges," *Concrete International*, Vol. 19, No. 8, August 1997, pp. 62-63.

25. Nagataki, Shigeyoshi, "High-Strength Concrete in Japan: History and Progress," *High-Strength Concrete: An International Perspective*, ACI Special Publication SP-167, Bickley, John A. (Editor), 1996, pp. 1-25.

26. Helland, Steinar, "Application of High-Strength Concrete in Norway," *High-Strength Concrete: An International Perspective*, ACI Special Publication SP-167, Bickley, John A. (Editor), 1996, pp. 27-53.

27. Godfrey, K. A., Jr., "Concrete Strength Record Jumps 36%," *Civil Engineering*, ASCE, Vol. 57, No. 10, October 1987, pp. 84-88.

28. Randall, Vaughn and Kenneth Foot, "High-Strength Concrete for Pacific First Center," *Concrete International*, Vol. 11, No. 4, April 1989, pp. 14-16.

29. Moreno, Jaime, "225 W. Wacker Drive," *Concrete International*, Vol. 12, No. 1, January 1990, pp. 35-39.

30. Aïtcin, Pierre-Claude, Pierre Laplante and Claude Bedard, "Development and Experimental Use of a 90 MPa (13,000 psi) Field Concrete," *High-Strength Concrete*, ACI Special Publication SP-87, Russell, Henry G. (Editor), 1985, pp. 51-70.

31. Miao, Buquan and Pierre-Claude Aïtcin, "Five Years' Monitoring of the Behavior of HPC Structural Columns," *High-Strength Concrete: An International Perspective*, ACI Special Publication SP-167, Bickley, John A. (Editor), 1996, pp. 193-210.

32. Ryell, J. and S. Fasullo, "The Characteristics of Commercial High Strength Concrete in the Toronto Area," *1993 CSCE/CPCA Structural Concrete Conference*, Proceedings, Toronto, May 19-21, 1993, pp. 277-293.

33. Russell, Henry G., "Structural Design Considerations and Applications," *High performance Concrete: Properties and Applications*, Shah, S. P. and S. H. Ahmad (Editors), McGraw-Hill, Inc., 1994, pp. 313-340.

34. Dolan, Charles W. and Robert W. LaFraugh, "High Strength Concrete in the Precast Concrete Industry," *PCI Journal*, Vol. 38, No. 3, May-June 1993, pp. 16-19.

35. Mitchell, Denis, Pierre-Claude Aïtcin and John A. Bickley, "High-Performance Concrete Bridges: The Canadian Experience," *PCI/FHWA International Symposium on High Performance Concrete*, New Orleans, Louisiana, October 20-22, 1997, Johal, L. S. (Paul) (Editor), pp. 355-367.

36. Mills, Donald, Kenneth T. Chow and Scott L. Marshall, "Design - Construction of Esker Overhead," *PCI Journal*, Vol. 36, No.5, September-October 1991, pp. 44-51.

37. *High-Performance Concrete in Québec: The Portneuf Experimental Bridge*, a booklet prepared by the Direction des communications of the ministère des Transports du Québec, 1993, 12 pp.

38. Aïtcin, P. C., G. Ballivy, D. Mitchell, M. Pigeon and L. G. Coulombe, "The Use of High Performance Air Entrained Concrete for the Construction of the Portneuf Bridge," *High Performance Concrete in Severe Environments*, ACI Special Publication SP-140, Zia, Paul (Editor), 1993, pp. 53-72.

39. Lachemi, Mohamed, Axel-Pierre Bois, Buquan Miao, Michel Lessard and Pierre-Claude Aïtcin, "First Year Monitoring of the First Air-Entrained High-Performance Bridge in North America," *ACI Structural Journal*, Vol. 93, No. 4, July-August 1996, pp. 379-386.

40. Jagasia, Hari K., "Design and Construction of High Performance Concrete Bridges on 407 Express Toll Route," *PCI/FHWA International Symposium on High Performance Concrete*, New Orleans, Louisiana, October 20-22, 1997, Johal, L. S. (Paul) (Editor), pp. 533-542.

41. Langley, W. S., R. Gilmour and E. Tromposch, "The Northumberland Strait Bridge Project," *Advances in Concrete Technology*, ACI Spacial Publication SP-154, Malhotra, V. M. (Editor), 1995, pp. 543-564.

42. Dunaszegi, Laszlo, "High Performance Concrete a Key Component in the Design of the Confederation Bridge," *Concrete Canada*; Newsletter of the High-Performance Concrete Network of Centres of Excellence, Vol. 1, No. 3, December 1996, pp. 1-2.

43. Durning, Timothy A. and Kenneth B. Rear, "Braker Lane Bridge - High Strength Concrete in Prestressed Bridge Girders," *PCI Journal*, Vol. 38, No. 3, May-June 1993, pp. 46-51.

44. Ralls, Mary Lou and Ramon Carrasquillo, "Texas High-Strength Concrete Bridge Project," *Public Roads*, Vol. 57, No. 4, Spring 1994, pp. 1-7.

45. Ralls, Mary Lou, "High-Performance Concrete U-Beam Bridge: From Research to Construction," *Fourth International Bridge Engineering Conference*, Volume 2, San Francisco, August 28-30, 1995, pp. 207-212.

46. Ralls, M. L., R. L. Carrasquillo and N. H. Burns, "Texas High Performance Concrete Bridges," *Fourth International Symposium on the Utilization of High Strength/High Performance Concrete*, Proceedings-Volume 3, Paris, France, May 29-31, 1996, de Larrard, F. and R. Lacroix (Editors), pp. 1475-1482.

47. Huo, Xiaoming and Maher K. Tadros, "Application of High Performance Concrete in Giles Road Bridge, Nebraska," *PCI/FHWA International Symposium on High Performance Concrete*, New Orleans, Louisiana, October 20-22, 1997, Johal, L. S. (Paul) (Editor), pp. 646-656.

48. Juliano, Michelle L. and Christopher M. Waszczuk, "Application of High Performance Concrete in Two Bridges in New Hampshire," *PCI/FHWA International Symposium on High Performance Concrete*, New Orleans, Louisiana, October 20-22, 1997, Johal, L. S. (Paul) (Editor), pp. 475-487.

49. Lwin, M. Myint, Alan W. Bruesch and Charles F. Evans, "High-Performance Concrete for a Floating Bridge," *Fourth International Bridge Engineering Conference*, Volume 1, San Francisco, August 28-30, 1995, pp. 155-162.

50. Azimi, Azam and Paul Zia, "Research and Utilization of High Performance Concrete in North Carolina," *PCI/FHWA International Symposium on High Performance Concrete*, New Orleans, Louisiana, October 20-22, 1997, Johal, L. S. (Paul) (Editor), pp. 635-645.

51. Ozyildirim, Celik and Jose Gomez, "Virginia's Bridge Structures with High Performance Concrete," *PCI/FHWA International Symposium on High Performance Concrete*, New Orleans, Louisiana, October 20-22, 1997, Johal, L. S. (Paul) (Editor), pp. 681-690.

52. Malier, Yves and Lucien Pliskin, "Bridge at Joigny: High-Strength-Concrete Experimental Bridge," *Transportation Research Record*, No. 1275, 1990, pp. 19-22.

53. Malier, Yves, Didier Brazillier and Stéphane Roi, "The Bridge of Joigny," *Concrete International*, Vol. 13, No. 5, May 1991, pp. 40-42.

54. Malier, Y. and F. de Larrard, "French Bridges in High-Performance Concrete," *Utilization of High Strength Concrete*, Symposium Proceedings - Volume 1, Lillehammer, Norway, June 20-24, 1993, Holand, Ivar and Erik Sellevold (Editors), pp. 534-544.

55. Moussard, Michel M. and Serge J. Montens, "Roize River Experimental Bridge" *Utilization of High Strength Concrete*, Symposium Proceedings - Volume 1, Lillehammer, Norway, June 20-24, 1993, Holand, Ivar and Erik Sellevold (Editors), pp. 562-569.

56. Pham, Xuan Thao and Yves Rialland, "An Urban Bridge: The Viaduct Over the Rhône River, in Lyon, France," *Fourth International Symposium on the Utilization of High Strength/High Performance Concrete*, Proceedings-Volume 3, Paris, France, May 29-31, 1996, de Larrard, F. and R. Lacroix (Editors), pp. 1437-1446.

57. Brazillier, D., P. Bar, A. L. Milan, F. de Larrard and S. Roi, "Innovative Design of Small Highway Bridges in H.P.C.," *Fourth International Symposium on the Utilization of High Strength/High Performance Concrete*, Proceedings-Volume 3, Paris, France, May 29-31, 1996, de Larrard, F. and R. Lacroix (Editors), pp. 1447-1456.

58. Brazillier, D., A. Roi, D. Hagolle, Jean Claude Ferté and Pierre Simonin, "New Developments in Standard Bridge Design Using H.P.C. (B80)," *New Technologies in Structural Engineering*, International Conference, Volume 1, Lisbon, Portugal, July 2-5, 1997, Santos, S. Pompeu and António M. Baptista (Editors), pp. 131-138.

59. Fergestad, Stein, Elljarn A. Jordet, Knut H. Nielsen and Trond Walstad, "An Evaluation of the Economical and Technical Potential of High Strength Concrete in Long Span Concrete Bridge Construction," *Utilization of High Strength Concrete*, Symposium Proceedings, Stavanger, Norway, June 15-18, 1987, Holand, Ivar, Steinar Helland, Bernt Jakobsen and Rolf Lenschow (Editors), pp. 597-607.

60. Sindre, Hallvard and Odd Georg Larsen, "The New Varodd Bridge, Norway, a Large Concrete Bridge Currently Under Construction by the Balanced Cantilever Method" *Utilization of High Strength Concrete*, Symposium Proceedings - Volume 1, Lillehammer, Norway, June 20-24, 1993, Holand, Ivar and Erik Sellevold (Editors),

pp. 527-533.

61. Melby, Karl, Elljarn A. Jordet and Carl Hansvold "Long Span Bridges in Norway Constructed in High-Strength LWA-Concrete" *Utilization of High Strength Concrete*, Symposium Proceedings - Volume 1, Lillehammer, Norway, June 20-24, 1993, Holand, Ivar and Erik Sellevold (Editors), pp. 545-553.

62. Sandvik Malvin, "Utilization of High Strength LWA-Concrete in Norway," *Utilization of High Strength Concrete*, Symposium Proceedings - Volume 1, Lillehammer, Norway, June 20-24, 1993, Holand, Ivar and Erik Sellevold (Editors), pp. 590-598.

63. Nagataki, Shigeyoshi and Etsuo Sakai, "Applications in Japan and South East Asia," *High Performance Concrete: Properties and Applications*, Shah, S. P. and S. H. Ahmad (Editors), McGraw-Hill, Inc., 1994, pp. 375-397.

64. Mitsui, K., T. Yonezawa, M. Kojima, M. Tezuka and M. Kinoshita, "Design and Construction of Prestressed Concrete Bridge Using 100 MPa High-Strength Concrete," *Fourth International Symposium on the Utilization of High Strength/High Performance Concrete*, Proceedings-Volume 3, Paris, France, May 29-31, 1996, de Larrard, F. and R. Lacroix (Editors), pp. 1493-1502.

65. De Vries, J., N. Kaptijn and H. Ouwerkerk, "High-Strength Concrete in Civil Bridge Engineering Practice in the Netherlands," *Fourth International Symposium on the Utilization of High Strength/High Performance Concrete*, Proceedings-Volume 3, Paris, France, May 29-31, 1996, de Larrard, F. and R. Lacroix (Editors), pp. 1427-1436.

66. Larsen, Erik Stoklund and Mette Geiker, "Two High Performance Concrete Bridges," *Structural Engineering International*, Journal of the International Association for Bridge and Structural Engineering, Vol. 5, No. 4, November 1995, p. 231.

67. Delgado, J. M., C. S. Oteo and F. Hue, "The Guadalete River: The First Spanish Experience on High-Strength Precast Concrete," *Fourth International Symposium on the Utilization of High Strength/High Performance Concrete*, Proceedings-Volume 3, Paris, France, May 29-31, 1996, de Larrard, F. and R. Lacroix (Editors), pp. 1417-1426.

68. Reddi, S. A., "Use of HSC / HPC for Road Bridges in India," *PCI/FHWA International Symposium on High Performance Concrete*, New Orleans, Louisiana, October 20-22, 1997, Johal, L. S. (Paul) (Editor), pp. 72-83.

69. Li, Shu-T'ien and Hsin-Hsiu Kuo, "High-Quality High-Strength Concrete--Its

Significant Attributes, Mix Design, and Application to Bridge Members and Piles: Part II Application to Bridge Members and Piles," *Concrete Bridge Design*, ACI Publication SP-26, Volume 2, 1971, pp. 1145-1173.

70. Carpenter, J. E., "Applications of High Strength Concrete for Highway Bridges," *Public Roads*, Vol. 44, No. 2, September 1980, pp. 76-83.

71. Jobse, Harold J. and Saad E. Moustafa, "Applications of High Strength Concrete for Highway Bridges," *PCI Journal*, Vol. 29, No. 3, May-June 1984, pp. 44-73.

72. Ahmad, Shuaib H. and S. P. Shah, "Structural Properties of High Strength Concrete and its Implications for Precast Prestressed Concrete," *PCI Journal*, Vol. 30, No. 6, November-December 1985, pp. 92-119. Reader Comments: *PCI Journal*, Vol. 32, No. 1, January-February 1987, pp. 130-132.

73. Castrodale, Reid W., M. E. Kreger and Ned H. Burns, *A Study of Pretensioned High Strength Concrete Girders in Composite Highway Bridges - Design Considerations*, Report No. FHWA/TX-88+381-4F, Center for Transportation Research, The University of Texas at Austin, January 1988.

74. Zia, Paul, John J. Schemmel and Thomas E. Tallman, *Structural Applications of High Strength Concrete*, Report No. FHWA/NC/89-006, Center for Transportation Engineering Studies, North Carolina State University, June 1989.

75. Taerwe, Luc, "High Strength Concrete for Prestressed Concrete Girders," *IABSE Symposium Leningrad 1991: Bridges: Interaction between Construction Technology and Design*, IABSE Reports, Volume 64, pp. 355-360.

76. Scott, Norman L., "Suggestions for Reducing Costs in Prestressed Concrete Bridges," *Highway Research Record*, No. 34, 1963, pp. 117-129.

77. Jacques, Francis J., "Study of Long Span Prestressed Concrete Bridge Girders," *PCI Journal*, Vol. 16, No. 2, March-April 1971, pp. 24-42.

78. Rabbat, B. G., T. Takayanagi and H. G. Russell, *Optimized Sections for Major Prestressed Concrete Bridge Girders*, Report No. FHWA/RD-82/005, Federal Highway Administration, U.S. Department of Transportation, February 1982.

79. Rabbat, Basile G. and Henry G. Russell, "Optimized Sections for Precast Prestressed Bridge Girders," *PCI Journal*, Vol. 27, No. 4, July-August 1982, pp. 88-104.

80. Rabbat, Basile G. and Henry G. Russell, "Optimized Sections for Pretensioned Concrete Bridge Girders in the United States," *International Conference on Short*

and Medium Span Bridges, Proceedings, Volume 2, Toronto, August 8-12, 1982, pp. 97-111.

81. Rabbat, Basile G. and Henry G. Russell, "Proposed Replacement of AASHTO Girders with New Optimized Sections," *Transportation Research Record*, No. 950, 1984, pp. 85-92.

82. Adelman, Douglas and Thomas E. Cousins, "Evaluation of the Use of High Strength Concrete Bridge Girders in Louisiana," *PCI Journal*, Vol. 35, No. 5, September-October 1990, pp. 70-78. Reader Comments: *PCI Journal*, Vol. 36, No. 3, May-June 1991, p. 78.

83. Weerasekera, Ilisha Ruwan Abeyratne, *Transfer and Flexural Bond in Pretensioned Prestressed Concrete*, Ph.D. Thesis, Department of Civil Engineering, The University of Calgary, June 1991.

84. Mitchell, Denis, William D. Cook, Arshad A. Khan and Thomas Tham, "Influence of High Strength Concrete on Transfer and Development Length of Pretensioning Strand," *PCI Journal*, Vol. 38, No. 3, May-June 1993, pp. 52-66.

85. Dilger, Walter H. and Changqing Wang, "Shrinkage and Creep of High-Performance Concrete (HPC) - A Critical Review," *Adam Neville Symposium on Concrete Technology*, Malhotra, V. M. (Editor), Las Vegas, June 12, 1995, pp. 59-84.

86. Roller, John J., Henry G. Russell, Robert N. Bruce and Barney T. Martin, "Long-Term Performance of Prestressed, Pretensioned High Strength Concrete Bridge Girders," *PCI Journal*, Vol. 40, No. 6, November-December 1995, pp. 48-59.

87. Shilstone, J. M., Sr. and J. M. Shilstone, Jr., "High Performance Concrete Mixtures for Durability," *High Performance Concrete in Severe Environments*, ACI Special Publication SP-140, Zia, Paul (Editor), 1993, pp. 281-305.

88. Gjørv, O. E., "Durability," *High Performance Concrete: Properties and Applications*, Shah, S. P. and S. H. Ahmad (Editors), McGraw-Hill, Inc., 1994, pp. 139-160.

89. Russell, Bruce W., "Impact of High Strength Concrete on the Design and Construction of Pretensioned Girder Bridges," *PCI Journal*, Vol. 39, No. 4, July-August 1994, pp. 76-89. Reader Comments: *PCI Journal*, Vol. 40, No. 1, January-February 1995, pp. 104-105.

90. Russell, Henry G., Jeffery S. Volz and Robert N. Bruce, "Applications and Limitations of High-Strength Concrete in Prestressed Bridge Girders," *Fourth International Bridge Engineering Conference*, Volume 2, San Francisco, August

28-30, 1995, pp. 169-180.

91. Deatherage, J. Harold, Edwin G. Burdette and Chong Key Chew, "Development Length and Lateral Spacing Requirements of Prestressing Strand for Prestressed Concrete Bridge Girders," *PCI Journal*, Vol. 39, No. 1, January-February 1994, pp. 70-83.

92. Russell, Bruce W. and Ned H. Burns, "Measured Transfer Lengths of 0.5 and 0.6 in. Strands in Pretensioned Concrete," *PCI Journal*, Vol. 41, No. 5, September-October 1996, pp. 44-65.

93. Russell, Bruce W. and Ned H. Burns, "Measurement of Transfer Lengths on Pretensioned Concrete Elements," *Journal of Structural Engineering*, ASCE, Vol. 123, No. 5, May 1997, pp. 541-549.

94. *Ontario Highway Bridge Design Code* (3rd edition), Ministry of Transportation, Ontario, 1992.

95. Mast, Robert F., "Lateral Stability of Long Prestressed Concrete Beams - Part 1," *PCI Journal*, Vol. 34, No. 1, January-February 1989, pp. 34-53. Reader Comments: *PCI Journal*, Vol. 34, No. 6, November-December 1989, p. 143.

96. Imper, Richard R. and George Laszlo, "Handling and Shipping of Long Span Bridge Beams," *PCI Journal*, Vol. 32, No. 6, November-December 1987, pp. 86-101. Reader Comments: *PCI Journal*, Vol. 34, No. 1, January-February 1989, pp. 164-168.

97. Mast, Robert F., "Lateral Stability of Long Prestressed Concrete Beams - Part 2," *PCI Journal*, Vol. 38, No. 1, January-February 1993, pp. 70-88. Reader Comments: *PCI Journal*, Vol. 39, No. 1, January-February 1994, pp. 96-100.

98. Mast, Robert F., "Lateral Stability Test to Destruction of a 149 ft Prestressed Concrete I-Beam," *PCI Journal*, Vol. 39, No. 4, July-August 1994, pp. 54-62.

99. Marshall, S. L. and R. E. Pelkey, "Production, Transportation, and Installation of Spliced Prestressed Concrete 'I' Girders for the Annacis Channel East Bridge," *Concrete in Transportation*, ACI Special Publication SP-93, Morgan, D. R. (Editor), 1986, pp. 737-767.

100. Arora, Jasbir S., "Computational Design Optimization: A Review and Future Directions," *Structural Safety*, Vol. 7, 1990, pp. 131-148.

101. Cohn, M. Z. and A. S. Dinovitzer, "Application of Structural Optimization,"

Journal of Structural Engineering, ASCE, Vol. 120, No. 2, February 1994, pp. 617-650.

102. Lounis, Z. and M. Z. Cohn, "Optimization of Precast Prestressed Concrete Bridge Girder Systems," *PCI Journal*, Vol. 38, No. 4, July-August 1993, pp. 60-78.

103. Cohn, M. Z. and Z. Lounis, "Optimal Design of Structural Concrete Bridge Systems," *Journal of Structural Engineering*, ASCE, Vol. 120, No. 9, September 1994, pp. 2653-2674.

104. Bonasia, Joseph J., "Design of Prestressed Concrete Beams by Computer," *Transactions of the American Society of Civil Engineers*, Vol. 126, Part II, 1961, pp. 901-928.

105. Naaman, Antoine, "Computer Program for Selection and Design of Simple Span Prestressed Concrete Highway Girders," *PCI Journal*, Vol. 17, No. 1, January-February 1972, pp. 73-81. Reader's Comment: *PCI Journal*, Vol. 17, No. 3, May-June 1972, pp. 75-78.

106. Kirsch, Uri, *Optimum Structural Design: Concepts, Methods, and Applications*, McGraw-Hill, Inc., New York, 1981.

107. Arora, Jasbir S., *Introduction to Optimum Design*, McGraw-Hill, Inc., New York, 1989.

108. Kirsch, Uri, "Optimum Design of Prestressed Beams," *Computers & Structures*, Vol. 2, No. 4, September 1972, pp. 573-583.

109. Kirsch, Uri, "Optimized Prestressing by Linear Programming," *International Journal for Numerical Methods in Engineering*, Vol. 7, No. 2, 1973, pp. 125-136.

110. Kirsch, Uri, "A Bounding Procedure for Synthesis of Prestressed Systems," *Computers & Structures*, Vol. 20, No. 5, 1985, pp. 885-895.

111. Morris, David, "Prestressed Concrete Design by Linear Programming," *Journal of the Structural Division*, ASCE, Vol. 104, No. ST3, March 1978, pp. 439-452.

112. Fereig, Sami M., "Preliminary design of standard CPCI prestressed bridge girders by linear programming," *Canadian Journal of Civil Engineering*, Vo. 12, No. 1, March 1985, pp. 213-225.

113. Fereig, S. M., "An Application of Linear Programming to Bridge Design with Standard Prestressed Girders," *Computers & Structures*, Vol. 50, No. 4, February 17,

1994, pp. 455-469.

114. Fereig, Sami M., "Economic Preliminary Design of Bridges with Prestressed I-Girders," *Journal of Bridge Engineering*, ASCE, Vol. 1, No. 1, February 1996, pp. 18-25.

115. Goble, G. G. and W. S. Lapay, "Optimum Design of Prestressed Beams," *ACI Journal*, Proceedings Vol. 68, No. 9, September 1971, pp. 712-718.

116. Bandyopadhyay, N. and M. P. Kapoor, "Optimal Design of Prestressed Concrete Bridge-Girder Section," *Journal of Structural Engineering* (Roorkee, India), Vol. 3, No. 4, January 1976, pp. 179-191.

117. Desayi, Prakash and Syed Abid Ali, "Optimum Design of Prestressed Concrete Girders," *Journal of Structural Engineering* (Roorkee, India), Vol. 3, No. 4, January 1976, pp. 192-200.

118. Cohn, M. Z. and A. J. MacRae, "Optimization of Structural Concrete Beams," *Journal of Structural Engineering*, ASCE, Vol. 110, No. 7, July 1984, pp. 1573-1588.

119. Cohn, M. Z. and A. J. MacRae, "Prestressing Optimization and Its Implications for Design," *PCI Journal*, Vol. 29, No. 4, July-August 1984, pp. 68-83.

120. Francis, R., "Optimal Design of Prestressed Concrete Continuous Beams," *Inelasticity and Non-Linearity in Structural Concrete*, Solid Mechanics Division, University of Waterloo, Study No. 8, Cohn, M. Z. (Editor), pp. 441-469.

121. Cohn, M. Z. and Z. Lounis, "Optimum Limit Design of Continuous Prestressed Concrete Beams," *Journal of Structural Engineering*, ASCE, Vol. 119, No. 12, December 1993, pp. 3551-3570.

122. Torres, G. Guzman Barron, J. F. Brotchie and C. A. Cornell, "A Program for the Optimum Design of Prestressed Concrete Highway Bridges," *PCI Journal*, Vol. 11, No. 3, June 1966, pp. 63-71.

123. Aguilar, Rodolfo J., Kambiz Movassaghi and John A. Brewer, "Computerized Optimization of Bridge Structures," *Computers & Structures*, Vol. 3, No. 3, May 1973, pp. 429-442.

124. Anderson, Arthur R., "Systems Concepts for Precast and Prestressed Concrete Bridge Construction," *Systems Building for Bridges*, Special Report 132, Highway Research Board, Washington, D. C., 1972, pp. 9-21.

125. Meir, Joseffa V., Michael R. Cicciarelli, Julio A. Ramirez and Robert H. Lee, "Alternatives to the Current AASHTO Standard Bridge Sections," *PCI Journal*, Vol. 42, No. 1, January-February 1997, pp. 56-66.

126. Csagoly, Paul F. and William N. Nickas, "Florida Bulb-Tee and Double-Tee Beams," *Concrete International*, Vol. 9, No. 11, November 1987, pp. 18-23.

127. Garcia, Antonio M., "Florida's Long Span Bridges: New Forms, New Horizons," *PCI Journal*, Vol. 38, No. 4, July-August 1993, pp. 34-49.

128. Burke, Martin P., Jr., "Bridge Aesthetics: World View," *Journal of Structural Engineering*, ASCE, Vol. 121, No. 8, August 1995, pp. 1252-1257.

129. Maestro, Manuel Burón, David Fernández-Ordóñez Hernández and Cándido Ovejero Sánchez,, "Aesthetics in the Design of Precast Prestressed Bridges," *Concrete International*, Vol. 17, No. 8, August 1995, pp. 39-44.

130. Menn, Christian, "The place of Aesthetics in Bridge Design," *Structural Engineering International*, Journal of the International Association for Bridge and Structural Engineering, Vol. 6, No. 2, May 1996, pp. 93-95.

131. Geren, K. Lynn, Ahmad M. Abdel-Karim and Maher K. Tadros, "Precast/ Prestressed Concrete Bridge I-Girders: The Next Generation," *Concrete International*, Vol. 14, No. 6, June 1992, pp. 25-28.

132. Geren, K. Lynn and Maher K. Tadros, "The NU Precast/Prestressed Concrete Bridge I-Girder Series," *PCI Journal*, Vol. 39, No. 3, May-June 1994, pp. 26-39.

133. Ralls, Mary Lou, Luis Ybanez and John J. Panak, "The New Texas U-Beam Bridges: An Aesthetic and Economical Design Solution," *PCI Journal*, Vol. 38, No. 5, September- October 1993, pp. 20-29. Reader Comments: *PCI Journal*, Vol. 39, No. 2, March-April 1994, pp. 122-124.

134. Bardow, Alexander K., Rita L. Seraderian and Michael P. Culmo, "Design, Fabrication and Construction of the New England Bulb-Tee Girder," *PCI Journal*, Vol. 42, No. 6, November-December 1997, pp. 30-40.

135. Kaar, Paul H., Ladislav B. Kriz and Eivind Hognestad, *Precast-Prestressed Concrete Bridges, 1. Pilot Tests of Continuous Girders*, Research and Development Laboratories, Development Department, Bulletin D34, Portland Cement Association, Skokie, Illinois, January 1960, 21 pp.

136. Hambly, E. C. and B. A. Nicholson, "Prestressed Beam Integral Bridges," *The*

Structural Engineer, Vol. 68, No. 23, 4 December 1990, pp. 474-481.

137. Hambly, E. C., "Integral Bridges," *Proceedings. Institution of Civil Engineers; Transportation*, Vol. 123, February 1997, pp. 30-38.

138. Russell, Henry G. and Lee J. Gerken, "Jointless Bridges - the Knowns and the Unknowns," *Concrete International*, Vol. 16, No. 4, April 1994, pp. 44-48.

139. Castrodale, Reid W., *Design of Continuous Highway Bridges with Precast, Prestressed Concrete Girders*, Portland Cement Association, Skokie, Illinois, December 1994, 17 pp.

140. Abdel-Karim, Ahmad M. and Maher K. Tadros, "Design and Construction of Spliced I-Girder Bridges," *PCI Journal*, Vol. 37, No. 4, July-August 1992, pp. 114-122.

141. Tadros, Maher K., Joseph A. Ficenec, Amin Einea and Steve Holdsworth, "A New Technique to Create Continuity in Prestressed Concrete Members," *PCI Journal*, Vol. 38, No. 5, September-October 1993, pp. 30-37.

142. Saleh, Mohsen A., Amin Einea and Maher K. Tadros, "Creating Continuity in Precast Girder Bridges," *Concrete International*, Vol. 17, No. 8, August 1995, pp. 27-32.

143. *Standard Specifications for Highway Bridges* (15th edition), American Association of State Highway and Transportation Officials, Washington, D.C., 1992.

144. Jaeger, Leslie G. and Baidar Bakht, "The Grillage Analogy in Bridge Analysis," *Canadian Journal of Civil Engineering*, Vol. 9, No. 2, June 1982, pp. 224-235.

145. Cusens, A. R. and R. P. Pama, *Bridge Deck Analysis*, John Wiley & Sons, Ltd., London, UK, 1975.

146. Jaeger, Leslie Gordon, "The Analysis of Grid Frameworks of Negligible Torsional Stiffness by Means of Basic Functions," *Proceedings. Institution of Civil Engineers*, Vol. 6, April 1957, pp. 735-750.

147. Jaeger, L. G. and B. Bakht, *A General Method for the Analysis of Slab-on-Girder Bridge Decks*, Report No. SRR-84-09, Ontario Ministry of Transportation and Communications, September 1984.

148. Jaeger, Leslie G. and Baidar Bakht, "Bridge Analysis by the Semicontinuum Method," *Canadian Journal of Civil Engineering*, Vol. 12, No. 3, September 1985, pp. 573-582.

149. Jaeger, Leslie G. and Baidar Bakht, *Bridge Analysis by Microcomputer*, McGraw-Hill, Inc., New York, 1989.

150. Jaeger, Leslie G., Baidar Bakht and Ahmed Aly, "Revisiting Simplified Analysis of Multi-Span Girder Bridges," *Proceedings of the 1996 Annual Conference of the Canadian Society for Civil Engineering*, Volume IIa, Edmonton, May 29-June 1, 1996, Rogowsky, David M. (Editor), pp. 431-442.

151. *AASHTO LRFD Bridge Design Specifications* (1st edition), American Association of State Highway and Transportation Officials, Washington, D.C., 1994.

152. Bakht, Baidar, Ahmed Aly and David S. Smith, "Semi-Continuum versus Grillage Methods of Analysis," *Canadian Journal of Civil Engineering*, Vol. 24, No. 1, February 1997, pp. 157-160.

153. Jaeger, Leslie G. and Baidar Bakht, "The Use of Harmonics in the Semi-Continuum Analysis of Bridges," *Proceedings of the 1985 Annual Conference of the Canadian Society for Civil Engineering*, Vol. IIB, Saskatoon, May 27-31, 1985, pp. 83-97.

154. Bakht, Baidar and Leslie G. Jaeger, *Bridge Analysis Simplified*, McGraw-Hill, Inc., New York, 1985.

155. Eby, Clifford C., John M. Kulicki, Celal N. Kostem and Martin A. Zellin, *The Evaluation of St. Venant Torsional Constants for Prestressed Concrete I-Beams*, Fritz Engineering Laboratory Report No. 400.12, Department of Civil Engineering, Lehigh University, September 1973.

156. *Design Manual: Precast and Prestressed Concrete* (3rd edition), Canadian Prestressed Concrete Institute, Ottawa, 1996.

157. Clark, L. A. and I. Sugie, "Serviceability Limit State Aspects of Continuous Bridges Using Precast Concrete Beams," *The Structural Engineer*, Vol. 75, No. 11, 3 June 1997, pp. 185-190.

158. Neville, A. M., W. H. Dilger and J. J. Brooks, *Creep of Plain and Structural Concrete*, Construction Press, London, UK, 1983.

159. ACI Committee 209, "Prediction of Creep, Shrinkage, and Temperature Effects in Concrete Structures," *ACI Manual of Concrete Practice*, Part 1, American Concrete Institute, Farmington Hills, Michigan, 1997.

160. Bažant, Zdeněk P., Liisa Panula, Joong-Koo Kim and Yunping Xi, "Improved Prediction Model for Time-Dependent Deformations of Concrete: Part 6 - Simplified

Code-Type Formulation," *Materials and Structures*, Vol. 25, No. 148, May 1992, pp. 219-223.

161. Gardner, N. J. and J. W. Zhao, "Creep and Shrinkage Revisited," *ACI Materials Journal*, Vol. 90, No. 3, May-June 1993, pp. 236-246. Discussion: *ACI Materials Journal*, Vol. 91, No. 2, March-April 1994, pp. 204, 216.

162. Freyermuth, Clifford L., "Design of Continuous Highway Bridges with Precast, Prestressed Concrete Girders," *PCI Journal*, Vol. 14, No. 2, April 1969, pp. 14-39.

163. *Ontario Highway Bridge Design Code* (2nd edition), Ministry of Transportation and Communications, Ontario, 1983.

164. Hewitt, Brian E. and Barrington deV. Batchelor, "Punching Shear Strength of Restrained Slabs," *Journal of the Structural Division*, ASCE, Vol. 101, No. ST9, September 1975, pp. 1837-1853.

165. Csagoly, P., M. Holowka and R. Dorton, "The True Behavior of Thin Concrete Bridge Slabs," *Transportation Research Record*, No. 664, 1978, pp. 171-179.

166. Beal, David B., "Load Capacity of Concrete Bridge Decks," *Journal of the Structural Division*, ASCE, Vol. 108, No. ST4, April 1982, pp. 814-832.

167. Manning, D., "A Rational Approach to Corrosion Protection of the Concrete Components of Highway Bridges," *Concrete Durability; Katharine and Bryant Mather International Conference*, ACI Special Publication SP-100, Volume 2, Scanlon, John M. (Editor), 1987, pp. 1527-1547.

168. Bakht, Baidar, "Revisiting Arching in Deck Slabs," *Canadian Journal of Civil Engineering*, Vol. 23, No. 4, August 1996, pp. 973-981.

169. Bakht, Baidar and Aftab A. Mufti, "FRC Deck Slabs without Tensile Reinforcement," *Concrete International*, Vol. 18, No. 2, February 1996, pp. 50-55.

170. Lin, T. Y. and Ben C. Gerwick, Jr., "Design of Long-Span Concrete Bridges with Special Reference to Prestressing, Precasting, Erection, Structural Behavior, and Economics," *Concrete Bridge Design*, ACI Special Publication SP-23, 1969, pp. 693-704.

171. Collins, Michael P. and Denis Mitchell, *Prestressed Concrete Structures*, Prentice-Hall, Inc., New Jersey, 1991.

172. Dorton, Roger A., "Development of Canadian Bridge Codes," *Developments in*

Short and Medium Span Bridge Engineering '94, Papers presented at the Fourth International Conference on Short and Medium Span Bridges, Halifax, August 8-11, 1994, Mufti, Aftab A., Baidar Bakht and Leslie G. Jaeger (Editors), pp. 1-12.

173. *Design of Highway Bridges*, CAN/CSA-S6-88, Canadian Standards Association, Toronto, June 1988.

174. Winter, George and Arthur H. Nilson, *Design of Concrete Structures* (8th edition), McGraw-Hill, Inc., New York, 1972.

175. *Design of Concrete Structures*, CSA Standard A23.3-94, Canadian Standards Association, Toronto, December 1994.

176. Lin, T. Y. and Ned H. Burns, *Design of Prestressed Concrete Structures* (3rd edition), John Wiley & Sons, Inc., New York, 1981.

177. Xanthakos, Petros P., *Theory and Design of Bridges*, John Wiley & Sons, Inc., New York, 1994.

178. Arora, J. S. and C. H. Tseng, "Interactive Design Optimization," *Engineering Optimization*, Vol. 13, No. 3, June 1988, pp. 173-188.

179. Arora, Jasbir S., "Interactive Design Optimization of Structural Systems," *Discretization Methods and Structural Optimization-Procedures and Applications*, Proceedings of a GAMM-Seminar, October 5-7, 1988, Siegen, FRG. Eschenauer, H.A. and G. Thierauf (Editors), Springer-Verlag, Berlin, 1989, pp. 10-16.

180. Arora, Jasbir S., *IDESIGN User's Manual, Version 3.5.2*, Technical Report No. ODL-89.7, Optimal Design Laboratory, College of Engineering, The University of Iowa, June 1989.

181. Kikuchi, Noboru and Kazuto Horimatsu, "Practical Shape Optimization for Mechanical Structures," *Advances in Design Optimization*, Adeli, Hojjat (Editor), Chapman & Hall, London, UK, 1994, pp. 400-450.

182. Libby, James R. and Norman D. Perkins, *Modern Prestressed Concrete Highway Bridge Superstructures: Design Principles and Construction Methods*, Grantville Publishing Company, California, 1976.

183. Sithichaikasem, S. and W. L. Gamble, *Effects of Diaphragms in Bridges with Prestressed Concrete I-Section Girders*, Report No. UILU-ENG-72-2003, Department of Civil Engineering, The University of Illinois, Urbana, February 1972.

184. Wong, A. Y. C. and W. L. Gamble, *Effects of Diaphragms in Continuous Slab and Girder Highway Bridges*, Report No. UILU-ENG-73-2006, Department of Civil Engineering, The University of Illinois, Urbana, May 1973.

185. Kirsch, U., "Feasibility and Optimality in Structural Design," *Computers and Structures*, Vol. 41, No. 6, 1991, pp. 1349-1356.

186. Magnel, Gustave, *Prestressed Concrete* (3rd edition), Concrete Publications Limited, London, UK, 1954.

187. Naaman, Antoine E., *Prestressed Concrete Analysis and Design*, McGraw-Hill, Inc., New York, 1982.

188. Loov, Robert E., *Behaviour and Design of Prestressed Concrete Members*, ENCI 637 Course Notes, Department of Civil Engineering, The University of Calgary, September 1994.

APPENDIX A

IDESIGN INPUT DATA FILE

This appendix contains the input data file required by IDESIGN to solve the numerical design example of Sec. 6.3.

```
    BRIDGE NO.  1:   4 - CPCI 1600   L = 34 m
 11     0    48    50     0    -1    11     0     2     5
1.0000D-03  1.0000D-01  1.0000D-05  1.0000D-03
  1     5.5000D+00     1.0000D+00     2.0700D+01
  2     5.0000D-01     2.0000D-01     7.3300D-01
  3     4.0000D-01    -7.0000D-01     6.0000D-01
  4     4.0000D-01    -7.0000D-01     6.0000D-01
  5     2.0000D-03     1.0000D-10     1.0000D-01
  6     9.0000D-03     1.0000D-10     1.0000D-01
  7     2.2500D-01     2.2500D-01     5.0000D-01
  8     3.0000D+00     3.0000D+00     3.0000D+00
  9     1.5000D+00     1.5000D+00     1.5000D+00
 10     0.0000D+00     0.0000D+00     1.0000D-01
 11     4.7000D+01     4.0000D+01     2.0000D+02
```

APPENDIX B

IDESIGN OUTPUT DATA FILE

This appendix contains the output data file generated by IDESIGN for the numerical design example of Sec. 6.3.

```
**************************************************
        WELCOME TO PROGRAM IDESIGN3.5
  INTERACTIVE DESIGN OPTIMIZATION OF ENGINEERING
  SYSTEMS TO SOLVE THE PROBLEM:  MINIMIZE  F(B)
  SUBJECT TO  HI(B) = 0, AND  GI(B) <= 0
  REPORT ANY PROBLEMS TO PROFESSOR J.S.ARORA
**************************************************

INPUT DATA IS ECHOED
     BRIDGE NO.  1:   4 - CPCI 1600   L = 34 m
  11    0   48   50    0   -1   11    0    2    5
 1.0000D-03  1.0000D-01  1.0000D-05  1.0000D-03
   1      5.5000D+00      1.0000D+00      2.0700D+01
   2      5.0000D-01      2.0000D-01      7.3300D-01
   3      4.0000D-01     -7.0000D-01      6.0000D-01
   4      4.0000D-01     -7.0000D-01      6.0000D-01
   5      2.0000D-03      1.0000D-10      1.0000D-01
   6      9.0000D-03      1.0000D-10      1.0000D-01
   7      2.2500D-01      2.2500D-01      5.0000D-01
   8      3.0000D+00      3.0000D+00      3.0000D+00
   9      1.5000D+00      1.5000D+00      1.5000D+00
  10      0.0000D+00      0.0000D+00      1.0000D-01
  11      4.7000D+01      4.0000D+01      2.0000D+02


  ****************************************************************
  *          BRIDGE NO.  1:   4 - CPCI 1600   L = 34 m           *
  ****************************************************************

        NUMBER OF DESIGN VARIABLES        =       11
        NUMBER OF EQUALITY CONSTRAINTS    =        0
        NUMBER OF INEQUALITY CONSTRAINTS  =       48
        MAXIMUM NUMBER OF ITERATIONS      =       50
        PREVIOUS ITERATIONS RUN           =        0
        PRINTING CODE                     =       -1
        GRADIENT CALCULATION INDICATOR    =       11
        PROBLEM TYPE (2=LP, 0,1=NLP)      =        0
        ALGORITHM INDICATOR               =        2
        NO. OF CONSECUTIVE ITER. FOR ACT  =        5
        TOL. IN CONSTR. VIOL. AT OPT.     =  1.0000D-03
        CONVERGENCE PARAMETER VALUE       =  1.0000D-01
        DEL FOR F. D. GRAD. CALCULATION   =  1.0000D-05
        ACCEPTABLE CHANGE IN COST FUNC.   =  1.0000D-03

:::::::   STARTING DESIGN AND ITS LIMITS  :::::::
**************************************************

   NO.         DESIGN       LOWER LIM       UPPER LIM
------------------------------------------------------
    1      5.5000D+00      1.0000D+00      2.0700D+01
    2      5.0000D-01      2.0000D-01      7.3300D-01
    3      4.0000D-01     -7.0000D-01      6.0000D-01
    4      4.0000D-01     -7.0000D-01      6.0000D-01
    5      2.0000D-03      1.0000D-10      1.0000D-01
    6      9.0000D-03      1.0000D-10      1.0000D-01
    7      2.2500D-01      2.2500D-01      5.0000D-01
    8      3.0000D+00      3.0000D+00      3.0000D+00
    9      1.5000D+00      1.5000D+00      1.5000D+00
   10      0.0000D+00      0.0000D+00      1.0000D-01
   11      4.7000D+01      4.0000D+01      2.0000D+02
```

```
 REQUIRED DIMENSION OF ARRAY A=       5212

 ***** IDESIGN IS CHECKING YOUR GRADIENT EXPRESSIONS *****


 INITIAL DESIGN VARIABLE
  1  5.5000D+00    2  5.0000D-01    3  4.0000D-01    4  4.0000D-01    5  2.0000D-03
  6  9.0000D-03    7  2.2500D-01    8  3.0000D+00    9  1.5000D+00   10  0.0000D+00
 11  4.7000D+01

 COST FUNCTION
     1.4757D+02

 CONSTRAINT VALUE
  1 -1.7457D+00    2  6.3962D-02    3 -9.6764D-01    4 -2.0557D-01    5 -9.6764D-01
  6 -1.3254D+01    7 -1.0000D+00    8 -5.8572D+00    9 -1.7099D-01   10 -2.6635D-01
 11 -8.9517D-01   12 -1.5724D-01   13  3.8697D+00   14 -1.2100D+00   15 -6.6479D+00
 16 -2.1617D-01   17 -1.6668D-01   18 -9.9318D-01   19 -5.9560D-02   20  5.2632D+00
 21 -1.2062D+00   22 -5.8572D+00   23 -1.7099D-01   24 -2.6635D-01   25 -8.9517D-01
 26 -2.0187D-01   27  1.2164D+00   28 -1.1241D+00   29 -1.7457D+00   30  6.3962D-02
 31 -9.6764D-01   32 -2.0557D-01   33 -1.0741D+00   34 -1.9581D+01   35 -7.9515D-01
 36 -2.9401D-01   37 -2.7147D+00   38  2.0398D-01   39 -2.4470D-01   40 -6.3254D-01
 41 -1.8901D-01   42 -1.3193D-01   43 -5.1143D-01   44 -5.9335D-01   45 -6.6397D-01
 46 -5.9335D-01   47 -2.5926D-01   48 -1.6667D-01

 ************************************************************************
 1.IDESIGN WILL FIRST CALCULATE THE BEST DELTA FOR GRADIENT EXPRESSIONS.
 2.??? IN THE TABLES MEAN GRADIENT EVALUATION IS NOT VERIFIED.
    ( GIVEN DEL WILL BE REDUCED BY A FACTOR OF 10 FIVE TIMES. )
 ************************************************************************

------------------------------------------------------------------------------
 DELTA FOR FINITE DIFFERENCE(DEL)
      1.0000D-05

------------------------------------------------------------------------------
 DELTA FOR FINITE DIFFERENCE(DEL)
      1.0000D-06

  IDESIGN CHECK FOR THE FINITE DIFFERENCE GRAD. CALCULATIONS IS OK.

  OPTIMUM DELTA FOR IDESIGN GRADIENT CALCULATIONS.
 DEL= 1.0000D-05

  ***** END OF GRADIENT CALCULATIONS *****

  DESIGN VARIABLES AT ITERATION =      1  (RQP ALGORITHM USED)
   1  5.5000D+00    2  5.0000D-01    3  4.0000D-01    4  4.0000D-01    5  2.0000D-03
   6  9.0000D-03    7  2.2500D-01    8  3.0000D+00    9  1.5000D+00   10  0.0000D+00
  11  4.7000D+01

         MAX VIO     CONV PARM          COST
      5.2632D+00    1.0000D+00    1.4757D+02

  DESIGN VARIABLES AT ITERATION =      2  (RQP ALGORITHM USED)
   1  5.5284D+00    2  7.3300D-01    3  3.6241D-01    4  3.6241D-01    5  2.3375D-03
   6  9.0000D-03    7  2.2500D-01    8  3.0000D+00    9  1.5000D+00   10  0.0000D+00
  11  4.7002D+01

         MAX VIO     CONV PARM          COST
      1.7801D+00    1.0000D+00    1.4759D+02

  DESIGN VARIABLES AT ITERATION =      3  (RQP ALGORITHM USED)
```

```
 1  6.1358D+00    2  7.0822D-01    3  3.6241D-01    4  3.6241D-01    5  2.5125D-03
 6  9.0000D-03    7  2.2500D-01    8  3.0000D+00    9  1.5000D+00   10  0.0000D+00
11  5.7966D+01

       MAX VIO     CONV PARM          COST
    2.2400D-01    4.4149D+01    1.5081D+02

DESIGN VARIABLES AT ITERATION =      4  (RQP ALGORITHM USED)
 1  6.1358D+00    2  7.0822D-01    3  3.6241D-01    4  3.6241D-01    5  2.5125D-03
 6  6.7500D-03    7  2.2500D-01    8  3.0000D+00    9  1.5000D+00   10  0.0000D+00
11  5.7966D+01

       MAX VIO     CONV PARM          COST
    2.2399D-01    2.1897D+00    1.5071D+02

DESIGN VARIABLES AT ITERATION =      5  (RQP ALGORITHM USED)
 1  6.2376D+00    2  7.0364D-01    3  3.7864D-01    4  3.7864D-01    5  2.5125D-03
 6  7.0996D-03    7  2.2500D-01    8  3.0000D+00    9  1.5000D+00   10  0.0000D+00
11  6.0156D+01

       MAX VIO     CONV PARM          COST
    5.2815D-03    1.1738D-01    1.5168D+02

DESIGN VARIABLES AT ITERATION =      6  (RQP ALGORITHM USED)
 1  6.2486D+00    2  7.0196D-01    3  3.9508D-01    4  3.9508D-01    5  2.5125D-03
 6  7.0996D-03    7  2.2500D-01    8  3.0000D+00    9  1.5000D+00   10  0.0000D+00
11  6.0222D+01

***** DESIGN AT THIS ITERATION IS USABLE *****

       MAX VIO     CONV PARM          COST
    4.6509D-05    1.1739D-01    1.5169D+02

DESIGN VARIABLES AT ITERATION =      7  (RQP ALGORITHM USED)
 1  6.2542D+00    2  7.0095D-01    3  4.0703D-01    4  4.0703D-01    5  2.5125D-03
 6  7.0996D-03    7  2.2500D-01    8  3.0000D+00    9  1.5000D+00   10  0.0000D+00
11  6.0222D+01

***** DESIGN AT THIS ITERATION IS USABLE *****

       MAX VIO     CONV PARM          COST
    3.6247D-05    1.1739D-01    1.5169D+02

DESIGN VARIABLES AT ITERATION =      8  (RQP ALGORITHM USED)
 1  6.2567D+00    2  7.0049D-01    3  4.1202D-01    4  4.1202D-01    5  2.5125D-03
 6  7.0996D-03    7  2.2500D-01    8  3.0000D+00    9  1.5000D+00   10  0.0000D+00
11  6.0222D+01

***** DESIGN AT THIS ITERATION IS USABLE *****

       MAX VIO     CONV PARM          COST
    3.4430D-05    1.1738D-01    1.5169D+02

DESIGN VARIABLES AT ITERATION =      9  (RQP ALGORITHM USED)
 1  6.2592D+00    2  7.0004D-01    3  4.1635D-01    4  4.1635D-01    5  2.5125D-03
 6  7.0996D-03    7  2.2500D-01    8  3.0000D+00    9  1.5000D+00   10  0.0000D+00
11  6.0222D+01

***** DESIGN AT THIS ITERATION IS USABLE *****

       MAX VIO     CONV PARM          COST
    3.2742D-05    1.1738D-01    1.5169D+02
```

```
DESIGN VARIABLES AT ITERATION =    10  (RQP ALGORITHM USED)
 1  6.2616D+00   2  6.9959D-01   3  4.2009D-01   4  4.2009D-01   5  2.5125D-03
 6  7.0996D-03   7  2.2500D-01   8  3.0000D+00   9  1.5000D+00  10  0.0000D+00
11  6.0222D+01

***** DESIGN AT THIS ITERATION IS USABLE *****

       MAX VIO     CONV PARM         COST
    3.1274D-05   1.1738D-01   1.5169D+02

DESIGN VARIABLES AT ITERATION =    11  (RQP ALGORITHM USED)
 1  6.2642D+00   2  6.9913D-01   3  4.2330D-01   4  4.2330D-01   5  2.5125D-03
 6  7.0996D-03   7  2.2500D-01   8  3.0000D+00   9  1.5000D+00  10  0.0000D+00
11  6.0222D+01

***** DESIGN AT THIS ITERATION IS USABLE *****

       MAX VIO     CONV PARM         COST
    3.0132D-05   1.1738D-01   1.5169D+02

***** CONVERGENCE CRITERIA SATISFIED *****

  I     MAX. VIO.     CONV. PARM          COST
-----------------------------------------------
 11   3.01316D-05   1.17384D-01   1.51693D+02
-----------------------------------------------

********************
*  HISTORY TABLE   *
********************
ITER       MAX VIO     CONV PARM         COST
-----------------------------------------------
  1   5.2632D+00   1.0000D+00   1.4757D+02
  2   1.7801D+00   1.0000D+00   1.4759D+02
  3   2.2400D-01   4.4149D+01   1.5081D+02
  4   2.2399D-01   2.1897D+00   1.5071D+02
  5   5.2815D-03   1.1738D-01   1.5168D+02
  6   4.6509D-05   1.1739D-01   1.5169D+02
  7   3.6247D-05   1.1739D-01   1.5169D+02
  8   3.4430D-05   1.1738D-01   1.5169D+02
  9   3.2742D-05   1.1738D-01   1.5169D+02
 10   3.1274D-05   1.1738D-01   1.5169D+02
 11   3.0132D-05   1.1738D-01   1.5169D+02

CONSTRAINT ACTIVITY
 NO.   ACTIVE          VALUE      LAGR. MULT.
   1           -1.23127D+00      0.00000D+00
   2      YES  -2.80633D-02      1.10413D-02
   3           -9.91135D-01      0.00000D+00
   4           -2.74287D-01      0.00000D+00
   5           -9.91135D-01      0.00000D+00
   6           -1.36715D+01      0.00000D+00
   7           -1.00000D+00      0.00000D+00
   8           -6.75416D-01      0.00000D+00
   9      YES  -2.01591D-06      1.00594D+01
  10           -6.04359D-01      0.00000D+00
  11           -6.54612D-01      0.00000D+00
  12           -5.10498D-01      0.00000D+00
  13           -1.22868D+00      0.00000D+00
  14           -1.20489D+00      0.00000D+00
  15           -1.37390D+00      0.00000D+00
  16      YES  -3.52637D-02      0.00000D+00
  17           -5.26573D-01      0.00000D+00
```

```
 18            -7.31101D-01     0.00000D+00
 19            -4.34440D-01     0.00000D+00
 20      YES    3.01316D-05     7.62516D-01
 21            -1.20112D+00     0.00000D+00
 22            -6.75416D-01     0.00000D+00
 23      YES   -2.01591D-06     0.00000D+00
 24            -6.04359D-01     0.00000D+00
 25            -6.54612D-01     0.00000D+00
 26            -5.48900D-01     0.00000D+00
 27            -3.60250D+00     0.00000D+00
 28            -1.12106D+00     0.00000D+00
 29            -1.23127D+00     0.00000D+00
 30      YES   -2.80633D-02     1.10413D-02
 31            -9.91135D-01     0.00000D+00
 32            -2.74287D-01     0.00000D+00
 33            -1.08249D+00     0.00000D+00
 34            -1.93184D+01     0.00000D+00
 35            -8.00587D-01     0.00000D+00
 36      YES   -4.03774D-03     0.00000D+00
 37            -1.65164D+00     0.00000D+00
 38      YES    1.01807D-13     1.10925D-01
 39      YES    9.01973D-09     3.18911D-01
 40            -7.58503D-01     0.00000D+00
 41            -5.18544D-01     0.00000D+00
 42            -4.45935D-01     0.00000D+00
 43            -9.31216D-01     0.00000D+00
 44            -4.05425D-01     0.00000D+00
 45            -4.46583D-01     0.00000D+00
 46            -4.05425D-01     0.00000D+00
 47            -2.59259D-01     0.00000D+00
 48            -1.66667D-01     0.00000D+00

DESIGN VARIABLE ACTIVITY
 NO.   ACTIVE        DESIGN         LOWER         UPPER   LAGR. MULT.
   1             6.26419D+00  1.00000D+00  2.07000D+01  0.00000D+00
   2    UPPER    6.99126D-01  2.00000D-01  7.33000D-01  3.76760D+01
   3             4.23304D-01 -7.00000D-01  6.00000D-01  0.00000D+00
   4             4.23304D-01 -7.00000D-01  6.00000D-01  0.00000D+00
   5             2.51250D-03  1.00000D-10  1.00000D-01  0.00000D+00
   6             7.09956D-03  1.00000D-10  1.00000D-01  0.00000D+00
   7    LOWER    2.25000D-01  2.25000D-01  5.00000D-01  1.29232D+01
   8    LOWER    3.00000D+00  3.00000D+00  3.00000D+00  0.00000D+00
   9    LOWER    1.50000D+00  1.50000D+00  1.50000D+00  2.19776D+03
  10    LOWER    0.00000D+00  0.00000D+00  1.00000D-01  0.00000D+00
  11             6.02224D+01  4.00000D+01  2.00000D+02  0.00000D+00

COST FUNCTION AT OPTIMUM =    1.516930D+02

************************************************
 COST REDUCTION HAVE MET CONVERGENCE CRITERIA
************************************************

NO. OF CALLS FOR COST FUNCTION EVALUATION (USERMF) ..................... =  169
NO. OF CALLS FOR EVALUATION OF COST FUNCTION GRADIENT  (USERMG) ..... =    0
NO. OF CALLS FOR CONSTRAINT FUNCTION EVALUATION (USERCF) ............. =  169
NO. OF CALLS FOR EVALUATION OF CONSTRAINT FUNCTION GRADIENTS (USERCG) =    0
NO. OF TOTAL GRADIENT EVALUATIONS ..................................... =   96
```

IMAGE EVALUATION
TEST TARGET (QA-3)

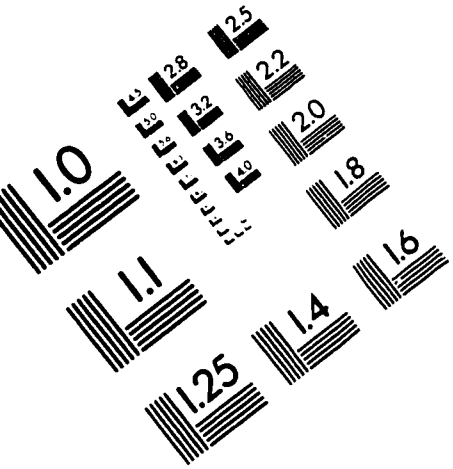

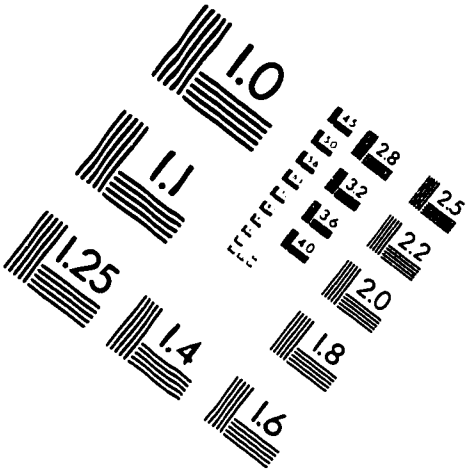

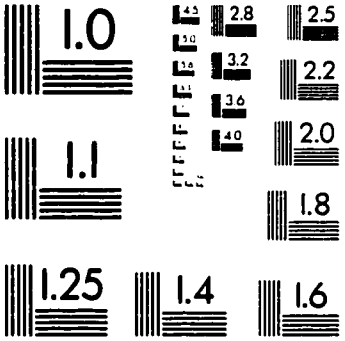

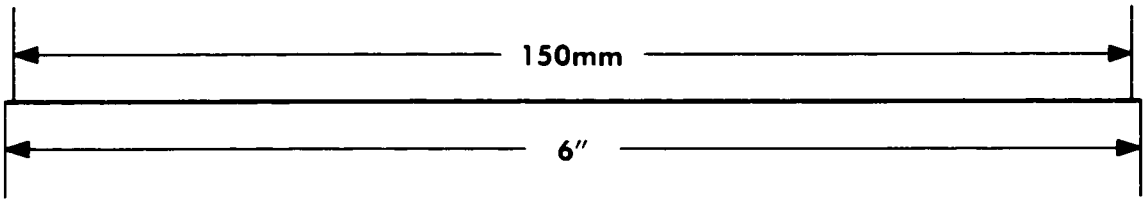

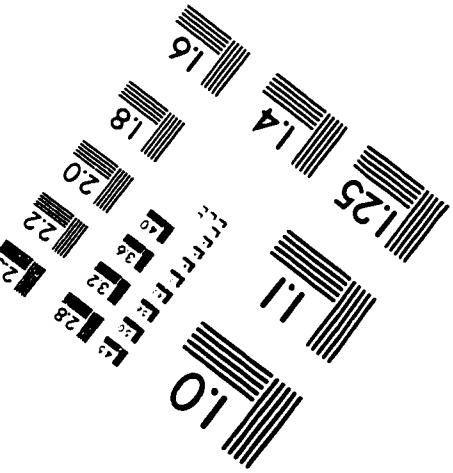

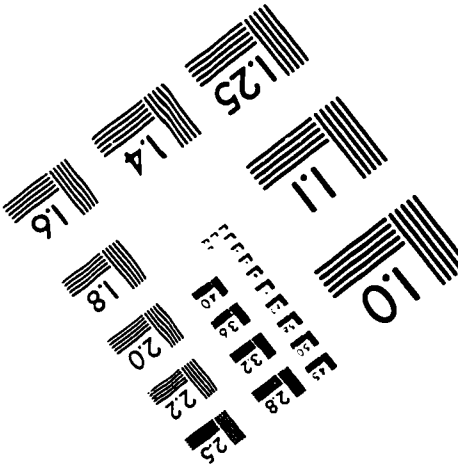

APPLIED IMAGE, Inc
1653 East Main Street
Rochester, NY 14609 USA
Phone: 716/482-0300
Fax: 716/288-5989